Glued-laminated bamboo

analysis of bamboo applied in laminated beams

Voermans, J.

Award date:
2006

Glued-Laminated Bamboo: Analysis of Bamboo Applied in Laminated Beams

Analytical and Experimental Study

Master of Science Thesis

Eindhoven, October 2006

Ing. J. Voermans

Supervisory Committee:

Prof. Dr. Ir. A.J.M. Jorissen

Dr. Ir. J.J.A. Janssen

Dr. Ir. S.P.G. Moonen

TU/e technische universiteit eindhoven

Eindhoven University of Technology

Department of Architecture, Building and Planning

Unit SDCT

Version:
Corrected version of September 2006

Report:
A-2006.14
O-2006.12

“Engineers participate in the activities which make the resources of nature available in a form beneficial to man and provide systems which will perform optimally and economically”

L. M. K. Boelter (1957)

Abstract

In construction, the use of bamboo in its original cylindrical form is shifting towards the use as engineered material: bamboo is modified in such a way that user defined forms and shapes are possible which can be standardized.
This study was focused on the development of a model for glued-laminated bamboo beams loaded in bending based on the properties of the individual laminations. The model was based on experimental and analytical investigations.

In laminated beams loaded in bending, the outermost laminations at the tension and compression side are subjected to nearly a uniform tension and compression force, respectively. Therefore, the properties of laminations loaded in tension and compression were determined by experimental tests. The results showed that bamboo under tension behaved proportionally and failed in a brittle way, while bamboo under compression exhibited a large yield capacity.
Since the length of beams exceeds the length of laminations, these have to be connected by end joints. The influence of both scarf- and finger-joints on the tensile strength and stiffness of laminations was studied by experimental tests. Additionally, an analytical model was elaborated which predicted the load-bearing capacity of the joints. The most important results showed that by lengthening the laminations by means of scarf-joints with a slope of 1 in 10, a joint efficiency of 93% could be achieved. The used adhesive melamine-urea formaldehyde was found to be suitable for scarf-jointing bamboo laminations.
Since nodes have a negative influence on stiffness and strength, the influence of nodes on the tensile strength of laminations was studied by experimental methods. Additionally, analytical analyses in combination with numerical simulations were carried out to predict the probability of failure initiated by nodes. It was found that failure of single- and triple-layer laminations loaded in tension was always initiated by a node.
The bond quality of face joints was studied based on two types of commercial adhesives commonly used in the manufacturing of glued-laminated timber: melamine-urea-formaldehyde and resorcinol-phenol. The results indicated that melamine-urea-formaldehyde could successfully be applied to bamboo.
Finally, an empirical model was established linking the properties of the individual laminations to those of the beams. This model was based on full-scale tests on glued-laminated bamboo beams loaded in four-point bending. It was found that the bending strength of a glued-laminated bamboo beam was directed by the tensile strength of the outermost lamination where failure was initiated either by a node or a joint. It was possible to link the tensile strength of the individual laminations to the bending strength of the beams by the laminating factor.

Regarding applications were strength is determining above stiffness, glued-laminated bamboo is a very promising material compared to engineered timber products.

Preface

The study presented in this report is elaborated within the framework of a graduation project at the Department of Architecture, Building and Planning, Eindhoven University of Technology. The study leads to a Master of Science degree.

In the past many research on the use of bamboo was carried out at the TU/e under supervision of Dr. ir. J.J.A. Janssen. This resulted in four PhD-theses, which were positively welcomed in bamboo growing countries. The work of Mr. Janssen and the other PhD-students was mainly focused on developing, improving and analysis of bamboo structures for lower income groups in developing countries. This work contributed considerably to the ISO standards 22156 and 22157 on bamboo as a building material.
Currently, Mr. Janssen has retired and his work is partly continued by Prof. Dr. Ir. A.J.M. Jorissen, professor in timber engineering. Nowadays, in construction, the use of bamboo in its original cylindrical form is shifting towards the use as engineered material: bamboo is modified in such a way that user defined forms and shapes are possible which can be standardized. This study can bee seen as the first under supervision of Mr. Jorissen towards the use of laminated bamboo as engineering material.

I feel very proud being the first person in the world who produced full-scale laminated beams of a marvelous material: bamboo. Since the results are promising, I hope this study will be continued in a PhD-study. At long last I hope this study gives way to the development of a glued-laminated bamboo industry in developing countries. The usage of laminated bamboo in construction will lead to a more sustainable building practice and ultimately contributes to a better life on earth.

This report is written for people in the field of structural engineering and material sciences. The review of literature presented in chapter 2 can also be read by everyone who is interested in bamboo and in using bamboo as a building material.

Jurgen Voermans

Eindhoven, September 2006

Acknowledgements

First of all, I wish to express my gratitude to the members of my committee: Prof. Dr. Ir. A.J.M. Jorissen, the chairman of my committee, for his academic and critical view during the sessions; Dr. Ir. S.P.G. Moonen, who enabled me to see things from a broad perspective; and finally, a special word of thanks is due to Dr. Ir. J.J.A. Janssen, a highly experienced and internationally esteemed expert within the field of building with bamboo and one of the first pioneers in that field, for his voluntary support. His contacts in the world of bamboo have made this project possible and his quick replies to my countless emails were of great support to me.

I wish to express my gratitude to the Nemaho in Doetinchem. This research would not have been possible without their support on preparing the finger-jointed laminations and the supply of their adhesives. I have to thank the company BOERBOOM HOUT B.V., for its efforts on working the laminations just in time, which enabled me to lengthen the laminations by means of scarf-joints.

I would like to show my appreciation to the members of the Pieter Van Musschenbroek Laboratory for helping me carrying out the experiments. Special thanks to ir. H.M. Lamers, T.J. van de Loo and ing. H.L.M Wijen, who were always very loyal and helpful.

I would also like to thank Dr. ir. A.J.M. Leijten, of the Delft University of Technology, for sending me the paper on fracture mechanics. A million thanks goes to Dr. ir. M.H. Jansen of the department of Mathematics and Computer Science of the Technische Universiteit Eindhoven for supporting me on the analysis of the influence of nodes on tensile strength by writing a program in MATLAB 6.1. Without his support the accomplished results would not have been possible in the given time scheme. Furthermore, I want to thank Dr. Wan Tarmeze Wan Ariffin of the Forest Research Institute Malysia for sending me a copy of the thesis of Nareswoho Nugroho.

Last but not least, I would like to thank my dear friends Pim van der Male and Liesbeth Vries. Pim for his constructive comments on the manuscript of this report and for supporting me during some hard moments, Lies for her constructive comments on the manuscript of the preliminary study.

Table of Contents

Symbols

Symbols are explained where they first appear in the text. For clarity, a list is also given here. The symbols used in the appendices are not included.

Latin upper case letters

A	= cross-sectional area, reduced cross-sectional area, sheared area	[mm^2]
A_{fj}	= joint area of finger-joint	[mm^2]
A_i	= area of internodes	[mm^2]
A_n	= area of nodes	[mm^2]
A_{sj}	= joint area of scarf-joint	[mm^2]
$E_{c,0}$	= modulus of elasticity in compression parallel to the grain	[N/mm^2]
E_m	= modulus of elasticity in bending	[N/mm^2]
$E_{t;0}$	= modulus of elasticity in tension parallel to the grain	[N/mm^2]
$E_{t;i;0}$	= modulus of elasticity in tension parallel to the grain of the internode	[N/mm^2]
$E_{t;j;0}$	= stiffness of the jointed area	[N/mm^2]
$E_{t;n;0}$	= modulus of elasticity in tension parallel to the grain of the node	[N/mm^2]
$F_2 - F_1$	= increment of loading on the straight portion of the load deformation curve	[N]
F	= final dimension, load	[mm]/[N]
F_c	= resultant compressive force	[N]
F_{max}	= maximum load	[N]
F_t	= resultant tensile force	[N]
I	= initial dimension, moment of inertia	[mm]/[mm^4]
L_2	= slope length	[mm]
MC	= moisture content	[%]
M_u	= ultimate bending moment	[Nmm]
P	= pitch	[mm]
RD	= relative density	[-]
S_r	= shrinkage	[%]
V	= green volume, volume determined at the moisture content of the test specimen	[mm^3]
V_1	= volume of member 1	[mm^3]
V_2	= volume of member 2	[mm^3]
W	= width of lamination, width of the beam, section modulus	[mm]/[mm^3]

Latin lower case letters

a	= distance between a loading position and the nearest support	[mm]
f	= mean strength value	[N/mm^2]
$f_{c;0}$	= compressive strength parallel to the grain	[N/mm^2]
f_k	= characteristic strength value	[N/mm^2]
f_m	= bending strength	[N/mm^2]

$f_{m;k}$	=characteristic bending strength	[N/mm^2]
$f_{m;beam}$	= bending strength of the beam	[N/mm^2]
$f_{t;0}$	= tensile strength parallel to the grain	[N/mm^2]
$f_{t;0;k}$	= characteristic tensile strength parallel to the grain	[N/mm^2]
$f_{t;i;0}$	= tensile strength of the internode	[N/mm^2]
$f_{t;j;0}$	= tensile strength parallel to the grain of jointed lamination	[N/mm^2]
$f_{t;j;0;k}$	= characteristic tensile strength parallel to the grain of jointed lamination	[N/mm^2]
$f_{t;lam;0}$	= tensile strength of the lamination	[N/mm^2]
$f_{t;n;0}$	= tensile strength of the node	[N/mm^2]
f_v	= shear strength	[N/mm^2]
h	= height of lamination, height of beam	[mm]
k	= percentage of nodes coinciding related to the total cross-section	[%]
$l_{glueline}$	= length of one glue line	[mm]
$l_{max;delam}$	= maximum delamination length of one glue line in the test specimen	[mm]
$l_{tot;delam}$	= delamination length of all glue lines in the test specimen	[mm]
$l_{tot;glueline}$	= entire length of glue lines on the two end-grain surfaces of each test specimen	[mm]
l_1	= gauge length	[mm]
m	= oven-dry mass, mass before drying, size parameter	[g]/[-]
m_0	= mass after drying	[g]
n	= ratio A_i / A_n	[-]
$t_{5/n-1}$	= Student's t value to calculate the 5th percentile	[-]
v	= coefficient of variation	[%]
$w_2 - w_1$	= increment of deformation corresponding to $F_2 - F_1$	[mm]
y	= coordinate of the element of area dA related to the neutral axis	[mm]
y_i	= vertical distance from the neutral axis to the centroid of the i^{th} surface S_i	[mm]

Greek lower case letters

δ	= deflection in the middle of the span	[mm]
$\varepsilon_2 - \varepsilon_1$	= increment of strain corresponding to $F_2 - F_1$	[-]
ε_{A-A}	= strain in section A-A	[-]
$\varepsilon_{A-A;i}$	= strain in internode in section A-A	[-]
$\varepsilon_{A-A;n}$	= strain in node in section A-A	[-]
$\varepsilon_{m;ten;u}$	= strain at ultimate bending stress at the tension side of the beam	[-]
$\varepsilon_{t;u}$	= strain at ultimate tensile stress	[-]
$\lambda_{lam;1}$	= laminating factor based on ordinary beam theory	[-]
$\lambda_{lam;2}$	= "real" laminating factor based on "real" strains	[-]
ρ_0	= density at the moisture content of the test specimen	[kg/m^3]
ρ_w	= density of water	[kg/m^3]
σ_1	= strength of member 1	[N/mm^2]
σ_2	= strength of member 2	[N/mm^2]

$\sigma_{A\text{-}A;i}$ = stress in internode [N/mm^2]

$\sigma_{A\text{-}A;n}$ = stress in node [N/mm^2]

1 Introduction

1.1 Motivation

Bamboo is a very promising sustainable building material. It grows in a large part of the world in abundance, contains favorable physical and mechanical properties, and matures fast. In a well managed plantation, the rotation cycle can be one year which is extremely short compared to that of most commercial timber species.
Bamboo is widely used in bamboo growing countries for structural applications. However, since it is used in its original form (culms) the utilization is limited by the dimensions and cross-section given by nature. To benefit the possibilities these restrictions have to be cancelled out by developing efficient manufacturing processes. These processes lead to engineered bamboo products which can be standardized. Additionally, the mechanical properties are more uniform which lead to higher strength and stiffness values.

Several studies (e.g., Ahmad, 2000; Amino, 2002; 2003; 2004; 2005; Lee et al., 1997; Nugroho, 2000; Nugroho and Ando, 2000; 2001; Wan Tarmeze, 2005) have been carried out on the use of bamboo as raw material for industrialized products for structural applications. Especially the study of Wan Tarmeze (2005) is of interest. This study consisted of a numerical analysis of laminated bamboo strip lumber which is equal to glued-laminated bamboo. However, to the author's knowledge, there is no experimental study reported on the application of bamboo in laminated beams taking into account the influence of joints.

1.2 Objective and Value

This study was focused on the development of a model for glued-laminated bamboo beams loaded in bending based on the properties of the individual laminations. This model was based on experimental and analytical investigations. Considering the similarities between wood and bamboo a close relationship with glued-laminated timber was considered with respect to manufacturing aspects and the bending behavior of the beams.

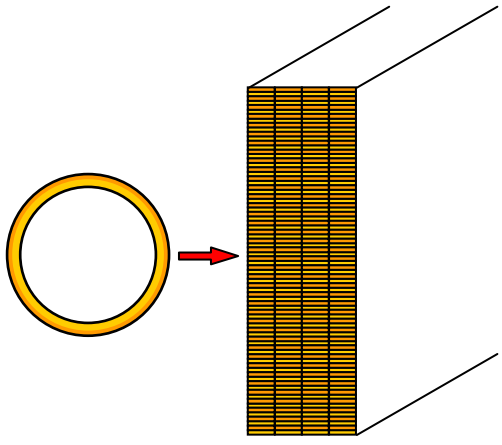

Figure 1.1: Laminated beam assembled out of laminated bamboo laminations

The results of this study may be used to open many markets for glued-laminated bamboo; not only local markets in areas where it is used already for building purposes but also in other parts of the world. The usage in western countries like the Netherlands is aimed at. This might be possible after having a reliable model for predicting the strength and stiffness of glued-laminated bamboo beams. Since the strength of bamboo exceeds the strength of most wood species, especially the soft wood species used in the Netherlands, there is a high potential for the usage where strength is determining above stiffness.

1.3 Outline

This report is divided into ten chapters. Chapter 2 concerns a literature review. Attention is given to various aspects of bamboo which are relevant to the scope of this study, e.g. physical and mechanical properties. The most important (recent) PhD studies on glued structural products of bamboo are discussed. Furthermore, it also includes information on the behavior of glued-laminated timber. The accompanying appendices A and B, tabulates the properties of several bamboo species and analyses the relations between properties, respectively.

Chapter 3 deals with manufacturing aspects of glued-laminated bamboo. Subsequently attention is given to the processing of strips into laminations, the processing of laminations into beams and the orientation of strips. The accompanying appendix C provides an analysis on vertical and horizontal laminated bamboo.

The experiments are described in the chapters 4 through 9. Each chapter gives attention to the used materials after which the method is explained. Subsequently, the results are presented and discussed. Finally the conclusions are summarized. The experimental and statistical results are presented by appendix H.

The behavior of laminated bamboo loaded in tension and compression is discussed in chapter 4 and 7, respectively. In appendix D an analysis is carried out on the configuration of the radius of the used tension test specimen.

Chapter 5 gives attention to the influence of both scarf- and finger-joints on the tensile strength and stiffness of laminations. An analytical model is elaborated in appendix E and F which attempts to predict the load-bearing capacity of the scarf- and finger-joint, respectively.

Chapter 6 presents the results of experimental, analytical and numerical research on the influence of nodes on the tensile strength. In appendix G the probability of failure initiated by nodes is predicted.

Chapter 8 treats the bond quality based on two types of commercial adhesives commonly used in the manufacturing of glued-laminated timber: melamine-urea-formaldehyde and resorcinol-phenol.

Chapter 9 describes the bending behavior of glued-laminated bamboo beams. An empirical model is proposed to link the properties of the individual laminations to those of the beams.

Finally, in the last chapter the overall conclusions are presented, together with recommendations for further research on glued-laminated bamboo.

2 Review of Literature

2.1 Introduction

Bamboo is a plant used for a wide range of purposes. In bamboo growing countries, bamboo is used as building material for many ages: in China 2000 years ago houses were made of bamboo (Wang and Guo, 2003). Today it is used for scaffolding, concrete formwork and housing materials. Important information on the use of bamboo as building material for these applications can be found in Janssen (1981; 1991; 1995; 2000), Arce-Villalobos (1993) and Jayanetti and Follet (1998). Bamboo is also widely used in the daily life of people for: baskets, vegetable, raw material for making paper, musical instruments and handicrafts (Dransfield and Widjaja, 1995).
In construction, the use of bamboo in its original cylindrical form is shifting towards the use as engineered material: bamboo is modified in such a way that user defined forms and shapes are possible which can be standardized. A good example is the use of bamboo based panels in construction. Panels are discussed in Ganapathy et al. (1999) and Qisheng, et al. (2001).

This chapter reviews important literature on bamboo. Paragraph 2.2 discusses general aspects towards bamboo. Successively attention is given to bamboo as plant, anatomical structure, chemical composition, physical properties, mechanical properties and variations in mechanical properties. Paragraph 2.3 discusses preservation in relation to bamboo on the basis of natural durability, factors reducing bamboo quality and preservation methods. Paragraph 2.4 discusses the most important (recent) PhD studies on glued structural products of bamboo. The studies are briefly described, the results are summarized and some critical remarks are made. Finally, paragraph 2.5 discusses the behavior of glued-laminated timber. The background to the current design rules for glued-laminated timber according to European Committee for Standardization (1999) is discussed. In addition to this attention is given to the most recent vision on the laminating effect by Serrano (1997; 2000) on the basis of fracture mechanics.

2.2 Bamboo in General

2.2.1 Bamboo as Plant

Botanical Classification

Most botanists agree in classifying bamboos in the grass family (Gramineae). The number of up till now described bamboo species varies greatly. According to Chunwarin (1975) there are 1250 species and 50 genera, according to Dunkelberg (1985) there are 500 different species with partial some hundred subspecies, according to Dransfield and Widjaja (1995) there are 1030 species and 77 genera and according to Janssen (1995) there are about 600 different species of bamboo in the world. The difference in estimating the number of bamboo species can be explained by the fact that sometimes the same name is given to different species and that there might be repetitive description

under different names. Also, bamboo classification is far from complete and research is still continuing so there will inevitably be changes in the scientific names.

According to Dunkelberg (1985) the lignifying cell structure of the bamboo tissue and its technological properties are very similar to the those of wood. Bamboo is therefore considered to a high extent as similar to wood. The term bamboo describes all tree or bush like grasses having a durable woody or branched stem.

Distribution of Bamboos over the World

Bamboos are distributed in the tropical, subtropical and temperate regions of all continents except Europe and western Asia, from lowlands up to 4000 m altitude. Most bamboos are found at low to medium elevations in the tropics (Dransfield and Widjaja, 1995). The distribution of bamboo over the world is shown in Figure 2.1. In Table 2.1 the approximate number of bamboo genera and species in the world is represented by region according to Dransfield and Widjaja (1995).

Table 2.1: Approximate number of bamboo genera and species in the world by region

Region	Genera	Species
Asia (tropical and subtropical)	24	270
Asia (temperate)	20	320
Africa	3	3
Madagascar	6	20
Australia	2	3
Pacific	2	4
America (tropical)	20	410
Total	77	1030

Source: Dransfield and Widjaja (1995)

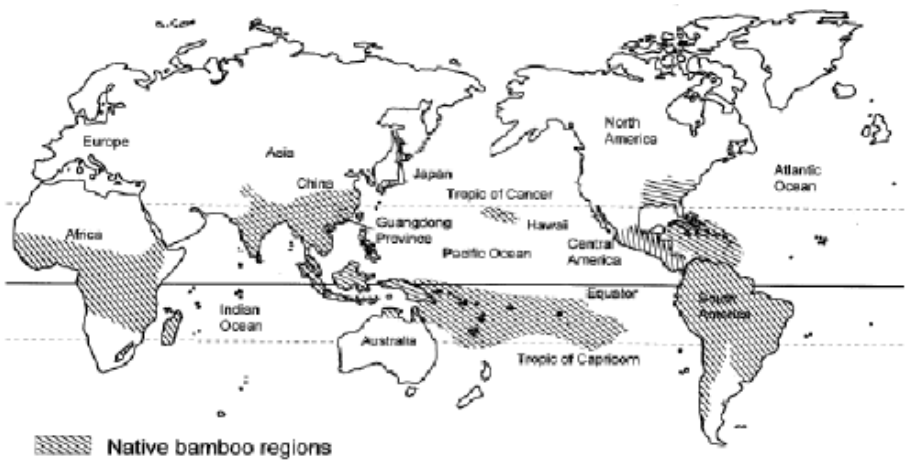

Figure 2.1: Distribution of bamboo over the world

Source: website Food and agriculture organization of the United Nations (December 2005),

http://www.fao.org/docrep/007/j1974e/J1974E35-7.gif

In recent years bamboo plants are introduced into Europe and North America. An example of this development is the introduction of Moso Bamboo in South Carolina and some Southeastern states in the U.S. (Ahmad, 2000).

Morphology

Bamboo can be divided into two parts, the rhizomes[1] and the culms[2]. The culm can be divided into nodes and internodes. Figure 2.2 shows the structure of bamboo.

Concerning the rhizomes, bamboo can be divided into two main types according to the basic form of the rhizome. One can distinguish the running type (leptomorph or monopodial bamboos) and the clump type (pachymorph or sympodial bamboos). In the running type bamboo culms are evenly distributed over the area, and in the clump type bamboo grows in clumps of about 50 or 100 culms. The running type of bamboo is found in subtropical and temperate regions. The clump type is found in the tropical regions (Chunwarin, 1975; Janssen, 1995).

According to Liese (1987: p. 190): “Bamboos are the fastest growing plants on earth. They reach their full height of 15-30 m within a period of 2 to 4 months by growth rates of about 20 cm up to 100 cm per day. The diameter of the culm can be 10-15 cm”. The internode length increases from the base towards the middle part of the culm and then decreases further upwards. The relation between the internode length and the culm height can be described by a parabolic graph. “The average length of internodes for most species is about 35 cm, but it may reach as much as 150 cm (as in *Schizostachum lima*)” (Dransfield and Widjaja, 1995: p.33). The features of the growth of bamboo together with those of timber are reflected in Table 2.2.

Bamboo culms will take 2 to 6 years to mature. It’s is important to know when a culm has grown to maturity. This can be estimated from the color of the culm but depends on the botanical species. In general, the surface of young bamboo culm is green, that of middle-aged is yellow-green and the matured one is yellow or bronze. The best period for harvesting is the dry season because then the culms have a lower moisture content which positively affects the chance of attack by fungi (Janssen, 1995; Liese, 1987).

[1] The rootstock
[2] The aerial axis emerging from buds of the subterranean system

a. Bamboo plant

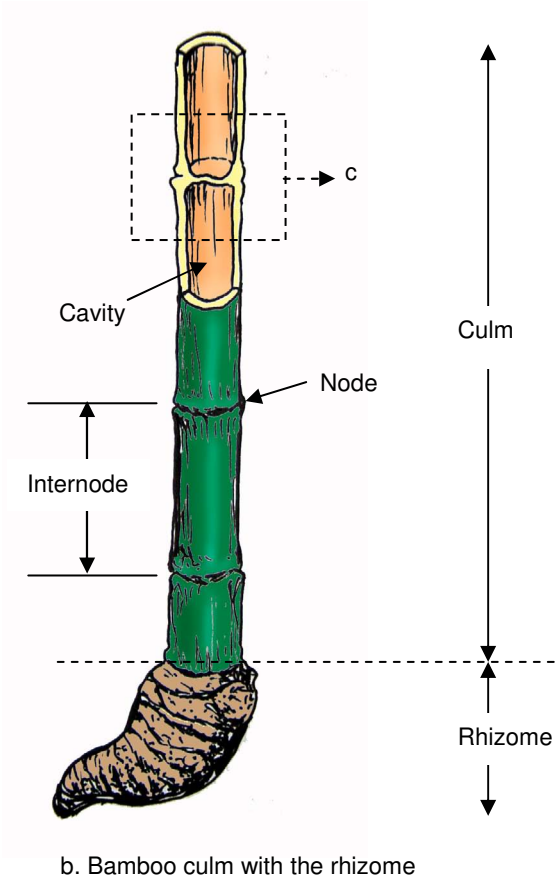

b. Bamboo culm with the rhizome

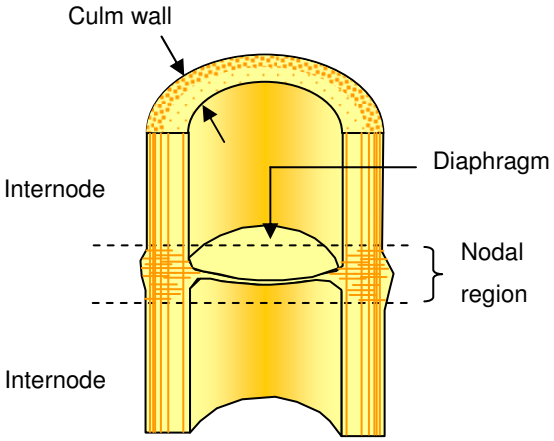

c. Half-split bamboo culm with node

Figure 2.2: Structure of bamboo

Source: Wan Tarmeze (2005)

Table 2.2: Main differences between the growth of bamboo and timber

Growth item	Bamboo	Timber
Height growth	Height growth completes within 2-4 months.	Height growth during the whole lifetime of the tree, the speed of growth declines with aging.
Diameter growth	In the process of height growth of young bamboo, the diameter of the culm and the thickness of the culm wall increase slightly.	The growth of diameter is realized by cambium.
	After the completion of height growth the diameter of the culm and the thickness of the culm wall does not increase.	Diameter growth during the whole lifetime of the tree.

Source: Qisheng et al. (2001)

Like in trees, bamboos carry leaves by branches. At each node a branch bud occur which are arranged on alternate sides of the culm. In some species they are found from the lowermost node upwards and in others from the midculm node upwards. (Dransfield and Widjaja, 1995; Dunkelberg, 1985).

Flowering of most bamboo species happens once in their lifespan. It occurs irregular at intervals of 30 to 40 years ore more. Flowering of a species means that all plants of the same species begin to flower irrespective of their age. Even when plants are located of hundreds of kilometers away from each other this phenomenon occurs. After flowering, plants will die within a few weeks. There is no explanation for the sudden and quite unpredictable simultaneous flowering of one bamboo species (Liese, 1987; Qisheng et al., 2001). For plantations this can be a big problem. It is recommended to cultivate at least two species of bamboo so there is always one that can be harvested.

2.2.2 Anatomical Structure

The anatomical composition of bamboo has been studied by Liese (1987; 1992; 1998). In general the total culm contains at about 50% parenchyma, 40% fibers and 10% conducting tissue (vessels and sieve tubes). Parenchyma and conducting cells are more frequent in the inner part of the culm, fibers more frequently in the outer part. In the internode the cells are axially oriented whereas the direction of the cell elements in the nodes is arranged perpendicular to the internode to provide the transverse interconnections. The amount of fibers increases from bottom to top while parenchyma content decreases. Vascular bundles are embedded in the parenchyma cells and, depending on the species, they are accompanied by fiber bundles. Figure 2.3 shows the anatomical structure of bamboo.

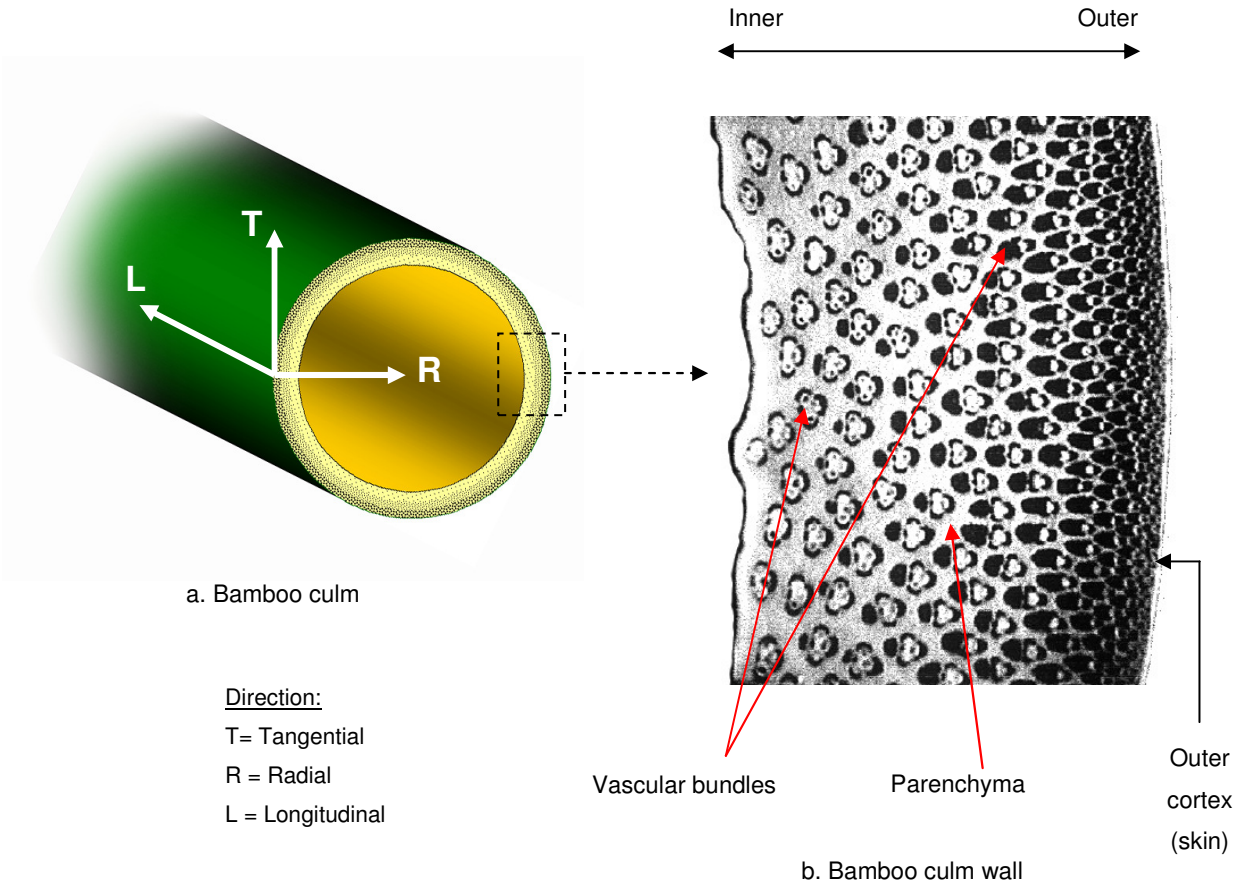

Figure 2.3: Anatomical structure

Source: Wan Tarmeze (2005)

2.2.3 Chemical Composition

The most important chemical constituents of bamboo are similar to those found in softwoods and hardwoods, however their quantities are different (Chunwarin, 1975). According to Dransfield and Widjaja (1995) major constituents of bamboo are cellulose, hemicellulose and lignin; the minor components include resins, tannins, waxes, and inorganic salts.

The anisotropic behavior of bamboo and wood can be explained by the behavior of cellulose. Cellulose is simultaneously a lattice chain and a lattice layer. It is very strong and stiff in the direction of the chain and weak in the direction of the layer.

2.2.4 Physical Properties

Relative Density

"Relative density (specific gravity) is defined as the ratio of the mass of a quantity of a substance to the mass of equal volume of water at 4℃. Because the mass and the dimensions of wood and bamboo change with their moisture content, it is necessary to express the specific gravity at specified

conditions of moisture content" (Chunwarin, 1975: p. 22). The following formula is valid for the relative density:

$$RD = \frac{\frac{m}{V} \cdot 10^6}{\rho_w} \qquad \text{eq.2.1}$$

where:

RD = relative density [-]
m = oven-dry mass [g]
V = green volume [mm^3]
ρ_w = density of water [kg/m^3]

The basic physical properties of several bamboo species are represented by Table A.1 of appendix A. The relative density of the bamboo species which are represented in this table varies between 0.73 and 0.91 for dry condition. This can be compared to that of hardwood.
The relative density of wood-based materials reflects the amount of fibers present in the material. Since the mechanical properties depend on the amount of fibers, the relative density is a criterion for the suitability of these materials for their use in structural applications. The relative density of bamboo varies with the age of the culm and the position along the culm height. The relative density of nodes is usually lower than that of internodes and the outermost portion of the wall has the highest relative density.

Moisture Content

The moisture content of bamboo is determined by the weight of water in the culm, expressed as a percentage of the dry weight of the culm. The moisture content is important since it affects physical and mechanical properties and also durability. The moisture content of mature culms of fresh bamboo ranges from 50-99% and of immature culms from 80-150%. For dried bamboo it varies between 12-18%. The moisture content increases from bottom to top, and from 1-3 years; it decreases in culms older than 3 years. It is much higher in the rainy season than in the dry season (Dransfield and Widjaja, 1995). The following formula defines the moisture content:

$$MC = \frac{m - m_0}{m_0} \cdot 100 \qquad \text{eq.2.2}$$

where:

MC = moisture content [%]
m = mass before drying [g]
m_0 = mass after drying [g]

Equilibrium Moisture Content

Equilibrium moisture content is defined as the moisture content that is in equilibrium with the relative humidity and temperature of the surrounding air (Ahmad, 2000). Like wood, bamboo in service is exposed to long-term (seasonal) and short-term (daily) variation in surrounding relative humidity and temperature, resulting in slight changes in the material. These usually gradual and short-term

fluctuations tend to influence only the surface. Moisture content changes can be reduced, but not prevented, by protective coatings. The objective of wood and bamboo drying is to bring the material moisture content close to the level which the finished product will have in service (Forest Products Laboratory, 1999).

Dimensional Stability

Dimensional stability has to do with the change of the dimensions of a product due to shrinking and swelling. Shrinking and swelling of a hygroscopic material are caused by changes in moisture content. When bamboo loses moisture it will shrink, when the opposite happens it will swell. Shrinking and swelling do affect the performance of a product because it can cause splitting. Like wood, the shrinking behavior of bamboo is different in different directions: one can distinguish the longitudinal (L), radial (R) or tangential (T) direction as is illustrated in Figure 2.3.

The following formula is valid for the shrinkage:

$$S_r = \frac{I - F}{I} \cdot 100 \qquad \text{eq.2.3}$$

where:

S_r = shrinkage [%]
I = initial dimension [mm]
F = final dimension [mm]

Compared to wood, shrinkage of bamboo is more in the radial direction than in the tangential direction; this is contradictory to wood. Furthermore, dimensional stability of bamboo is worse compared to wood. Bamboo starts shrinking right from green condition, even when the moisture content is about 100 to 150 percent which is unlike wood where shrinking starts below the fiber saturation point[3]. According to Kumar et al. (1994) shrinkage in fresh culms begins linearly, becomes negative or almost zero as moisture content falls between 100 and 70 percent and this continues until fiber saturation point is reached. Below this point, shrinkage again follows a linearly trend.

With respect to the information on the fiber saturation point, in combination to the shrinkage behavior, published research does not correspond to each other. According to Kumar et al. (1994) this point is around 20-22%, while according to Gnanaharan (1993) the term fiber saturation point is not applicable to bamboo.

It is a fact that at 20-22% the cell wall of bamboo is saturated with bound water, so the fiber saturation point is applicable on bamboo. However, bamboo shrinks and swells above the fiber saturation point which does not agree to the definition defined in Forest Products Laboratory (1999)[4].

[3] The fiber saturation point can be considered as that moisture content below which physical and mechanical properties of wood begin to change as a function of moisture content (Forest Products Laboratory, 1999). The fiber saturation point of wood is reached when the cell wall is saturated with bound water. The fiber saturation point of most softwoods averages about 30 % moisture content.

[4] Ibidem

2.2.5 Mechanical Properties

The mechanical properties for bamboo cited in the literature refer usually to the whole culm and not to split bamboo. The following parameters are commonly cited for bamboo (Dransfield and Widjaja, 1995):

- Modulus of elasticity in bending. This value indicates the ratio between the bending stress in the material and the relative deformation caused by this bending stress. The modulus of elasticity is directly related to the amount of fibers, thus in a culm the value of this parameter decreases from the outside to the inside along the culm wall thickness.
- Modulus of rupture (= ultimate bending stress). This value indicates the stress necessary to bring failure of the tested material when loaded in bending.
- Stress at proportional limit. No information is found on the definition of this value. It is assumed that below this value a linear relation exists between the bending stress and the relative deformations.
- Compression strength parallel to grain (= ultimate compression stress). This value indicates the stress necessary to bring failure of the tested material when loaded in compression. Sometimes the compression stress perpendicular to grain is also given.
- Shear strength. This value indicates the stress necessary to bring failure of the tested material when loaded in shear: sliding of surfaces over each other parallel to the direction of the grain.

In Table A.2 of appendix A some mechanical properties of several bamboo species are represented. It has to be remarked that comparison of results is questionable. In the past several methods were used to determine mechanical properties, due to this, results are affected by e.g. form and size of the specimen, testing speed and short or long-term loading. Nowadays there are standards for the determination of physical and mechanical properties so differences due to the testing method and the dimensions of the test specimen are reduced. There are two standards available:

- Bamboo - Structural design (ISO 22156:2004);
- Bamboo - Determination of physical and mechanical properties (ISO 22157-1:2004).

2.2.6 Variations in Mechanical Properties

Besides the fact that it is important to know the mechanical properties of the material in order to predict the mechanical behavior of a structure, it is also important to know which variables affect these properties and in what way. Mechanical properties of bamboo are affected mainly by a mix of biological, anatomical and physical variables:

- species and age;
- green or conditioned (with respect to the moisture content; green bamboo is freshly cut, moisture content = 50 to 100% and conditioned bamboo is dried until the moisture content is in equilibrium with the relative humidity and temperature of the surrounding air);
- density;
- position along the culm height;
- position along the culm wall thickness;

- node or internode.

The relations between some of these variables and several mechanical properties are analyzed on the basis of the researches summarized in Janssen (1991). This analysis can be found in appendix B. The following conclusions can be drawn:

- With respect to age, the mechanical properties increase up to a certain age after which they decrease. For the analyzed research appears that this optimum is 7-8 years for all properties.
- The moisture content correlates negatively with the mechanical properties: an increase of the moisture content results in a decrease of the mechanical properties.
- Density correlates positively with the mechanical properties: an increase of the density results in an increase of the mechanical properties.
- Position along the culm height correlates positively with the mechanical properties. Position along the culm height correlates also positively with density which can be explained by the fact that the number of vascular bundles which are mixed up with the fibers increases along the height of the culm.
- The relation between the vascular bundles and the density is linear so it is allowed to use the density as an estimator for the mechanical properties since these properties are primarily depending on the amount of fibers in the same way.

Furthermore, besides the fact that the mechanical properties vary along the culm heigth, they vary also along the culm wall thickness. This can be explained by the fact that the distribution of fibers along the culm wall thickness is not uniform; fibers are more frequently in the outer part. This is illustrated by the research of Li et al. (1994).
One culm was cut longitudinally into several beams, with the width of each beam being about 15 mm. Each beam was separated into several strips to determine experimentally the tensile and bending strength and the density. The tensile strength was determined with specimens of size 120 x 12 x h mm, with h the thickness of the specimen. The bending strength was measured in a three-point bending test with a span of 40 mm. Figure 2.4 shows the changing trends of the determined properties of bamboo along the radial direction. It can be seen that the tensile and bending strength are rather high: this has to do with the polylamellate wall structures of the fibers which lead to an extremely high tensile strength.

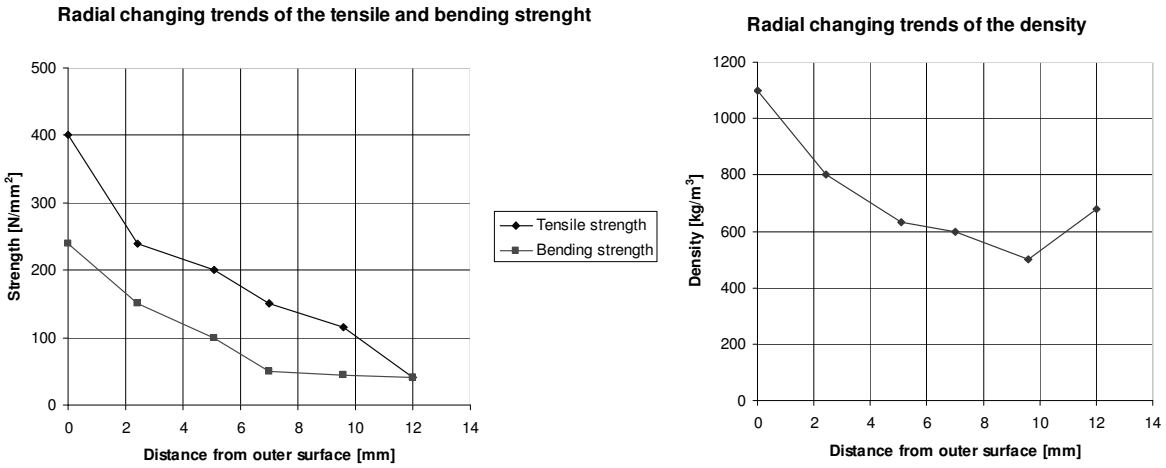

Figure 2.4: Left: radial changing trends of tensile and bending strength along the culm wall thickness; right: radial changing trend of density along the culm wall thickness

Source: Li et al. (1994)

Nodes have a negative influence on stiffness and strength. This has to do with fibers which are shorter and distorted vascular bundles (Liese, 1998), shown in Figure 2.5. It can be seen that vascular bundles in the outermost layer of the culm bend outwards. The vascular bundles in the inner part of the culm bend to reach the diaphragm.

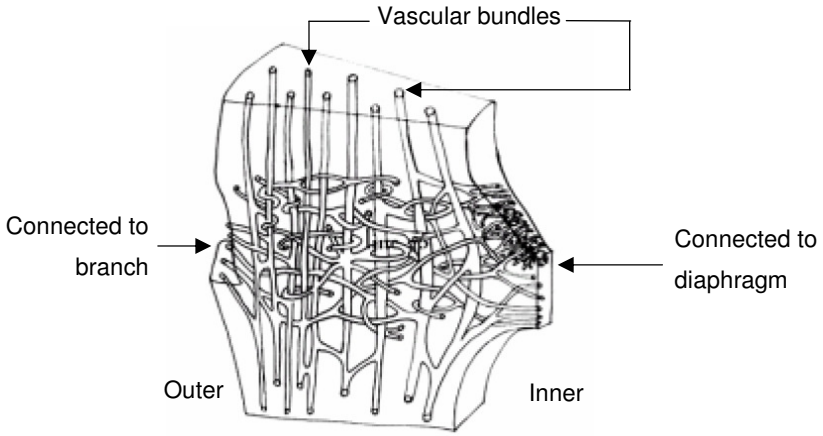

Figure 2.5: Vascular bundles within the node

Source: Wan Tarmeze (2005)

2.3 Preservation

Though literature on bamboo preservation is limited, good information can be found in Jayanetti and Follet (1998), Liese (1998), Janssen (2000) and Liese and Kumar (2003).

2.3.1 Natural Durability

The main problem in using bamboo in construction is the low natural durability of the material, which has to do with a lack of natural chemicals which are present in most woods: a bamboo culm does not

develop “heartwood” with ageing through deposits of toxic substances that increase durability. Hence, natural resistance is not influenced by age.

Natural resistance of bamboo depends on the type of attacking mechanisms and environmental conditions like soil contact, access of moisture, temperature and use. Untreated bamboo has roughly the following service life (Janssen, 2000):

- 1-3 years in open air and in ground contact;
- 4-6 years under cover and free from contact with the soil;
- 10-15 years under very good storage/use conditions.

Outside the humid tropics, well designed bamboo structures can last for a considerable time.

2.3.2 Factors Reducing Bamboo Quality

Factors reducing bamboo quality can be divided in abiotic and biotic factors. For example, cracks and splits occurring in full culms due to internal stresses caused by shrinking and swelling are abiotic factors which lead to deterioration by fungi.

There are many biotic factors cited in the literature: fungi (like moulds, blue-stain fungi, white- and brown-rot fungi and soft-rot fungi) and insects (like borers and termites). These invading organisms occur mostly through the cross-ends, and, to a lesser degree, at the leaf-scars and branch cuts at the nodes of full culms. However, some insects are also able to enter directly into the culm. The attack by fungi and insects is to some extend related to the presence of starch in the parenchyma. The amount of starch is related to the season. Therefore, culms should be cut during/after the rainy season when the starch content is at its lowest.

Bamboo with a moisture content above fiber saturation point (15-20%), is liable to be attacked by fungi, in comparison to about 28-30% for timber. Besides moisture, fungal activities need oxygen for their respiration and a temperature which is in the tropics in a suitable range.

2.3.3 Preservation Methods

The service life can be improved by preservation and falls into two categories: traditional and chemical. These are both active methods. Traditional treatments such as curing, smoking, soaking and seasoning and lime washing are used but the influence of these methods is not known.

Chemical treatments are carried out to protect bamboo against insects. The anatomical structure of the bamboo culm makes it difficult to preserve the material with chemicals which makes bamboo more resistant to chemical penetration than wood. This is caused by the vessels which are not more than 10% of the cross-section and access to these vessels gets reduced after the culm is harvested. Additionally, horizontal movement of preservative from the vessels into the neighboring tissue of parenchyma and fibers is a slow process due to the lack of radial pathways. Furthermore, radial penetration to the outer culm wall is resisted by the skin with its epidermis and waxy composition.

To introduce chemicals into the bamboo two methods are available. The modified Boucherie process passes a preservative under pressure resulting in pressing the preservative through the culm vessels till it comes out at the other end of the culm. This process can be seen in Figure 2.6. The dip diffusion method soaks the culm in the preservative so that a slow penetration process takes place. This

method is only suitable for split or sawn bamboo since whole culms will not allow the preservative to penetrate. By preservation the price of bamboo increases with 30% and its service life increases to 15 years in the open air and 25 years under cover.

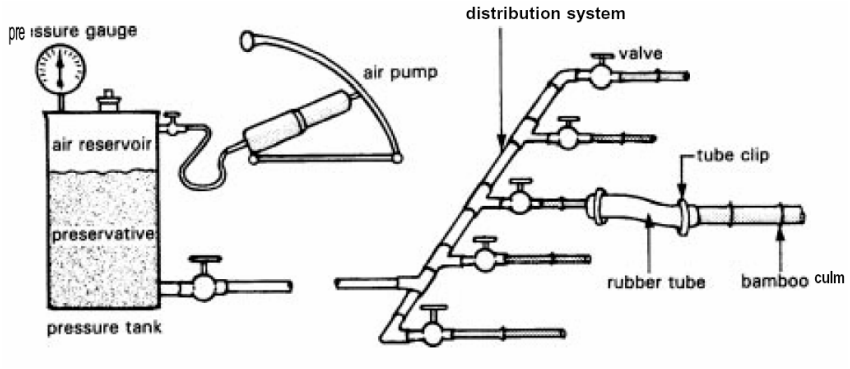

Figure 2.6: Modified Boucherie process

Source: Jayanetti and Follet (1998)

Besides traditional or chemical preservation, modification might be possible. Modification reported for wood consists of changing the basic chemical nature of the material. Modification falls into two categories: chemical and thermal modification. Both methods are mainly focused on improving the durability of wood by blocking hydroxyl groups. The hygroscopity is reduced and hence the dimensional stability and resistance to micro-organims will improve. However, modification can also change properties in a negative way, so one has to be cautious. Since the chemical composition of wood is the same as bamboo, modification should be suitable for bamboo too. This is an interesting subject which needs a closer investigation.

2.4 Earlier Work on Glued Structural Products of Bamboo

2.4.1 Analysis of Calcutta Bamboo for Structural Composite Materials

The study of Ahmad (2000) was focused on the suitability of Calcutta bamboo (*Dendrocalamus strictus*) for the use as raw material for glued structural products. The primary objective of the study was to determine the properties of bamboo and its interaction with adhesives. The properties investigated were relative density, dimensional stability, equilibrium moisture content, bending strength and stiffness, tensile strength, pH, buffer capacity, wettability and the adhesive penetration. In addition to this a prototype bamboo parallel strip lumber was manufactured and tested for its physical and mechanical properties. The study used mainly statistical techniques to ground the conclusion that Calcutta bamboo is technically a suitable raw material for structural composite products.

2.4.2 Mechanical Performance Evaluation of Bamboo-Timber Composite Beams

The study of Amino (2002; 2003; 2004; 2005) was focused on utilizing precocious wood species like poplar, eucalyptus, balsa etc. in building industry by combining bamboo with these species. The reason for the use of precocious wood lies in the fact that these species are abundant available in the warm regions. However, these species are not used in today's building industry because the

mechanical properties are poor. By reinforcing these species with bamboo the mechanical properties will increase, shown in Figure 2.7.

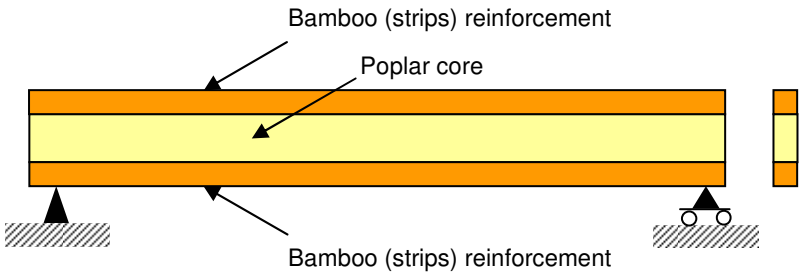

Figure 2.7: Principle of bamboo-timber composite beams

In this study a sandwich beam was assembled out of precocious wood and strips of bamboo. These strips were used as reinforcing flanges by gluing them on the surfaces of the precocious wood. The bamboo species used was Moso bamboo (*Phyllostachys pubescens*). The following properties were experimentally studied:

- bonding feasibility;
- bending capacity for static loading;
- bending capacity for long-term loading (creep behavior);
- local bearing capacity at supporting points.

The bonding feasibility of bamboo strips was studied by shear tests on adhesive joints. Two commercial adhesives were used: phenol-resorcinol formaldehyde and epoxy resin. The results are discussed in paragraph 3.4.2 and 8.1.

The bending capacity for static loading was investigated by four point bending tests. The average modulus of elasticity improved by a factor 1.3 compared to that of poplar. This improvement corresponded well with the predicted value by the laminated theory. The bending strength corresponded well with the predicted value by a model extending its plastic area across the section as well as the deflection.

The creep behavior was improved by the bamboo reinforcement. The estimated creep limit was 22.1% of the maximal static bending strength which means that if the load is lower than this level, the beams will not fail by creep. When the beams are loaded by the creep limit load the increase of the deflection can be estimated as about 14% of the initial deflection.

Local bearing capacity at supporting points was studied by compression tests perpendicular to the grain. The bamboo reinforcement flanges improved the compression strength perpendicular to the grain. By applying a bamboo layer of 5 mm (total height was 30 mm) on the surface of the poplar, the test specimens gained about 41% in the elastic modulus and about 33% in the elastic limit strength.

It has to be noticed that the properties of the individual components, bamboo and poplar, needed in the theoretically models, were taken from literature and were not determined experimentally which is doubtful when used in a comparison.

2.4.3 Development of Processing Methods for Bamboo Composite Materials and its Structural Performance

The study of Nugroho (2000) consisted out of four different experiments. In all the experiments, the bamboo species used was Moso bamboo (*Phyllostachys pubescens*). The first experiment was conducted to determine the suitability of zephyr strand for structural composite board manufacture. Zephyr is a sheet material of fibrous net like structures, shown in Figure 2.8.

Figure 2.8: Bamboo zephyr strand from moso bamboo. From the left to the right side: bamboo culm, bamboo zephyr strands with diameter of 9.5 mm, 4.7 mm, 2.8 mm and 1.5 mm, respectively

Source: Nugroho (2000)

The process involves the progressive crushing of materials through several sets of rollers until a continuous fibrous sheet is obtained. Several mechanical and physical properties were determined. It was concluded that bamboo zephyr board exhibits superior strength properties compared to commercial timber products.

In the second experiment the possibility of producing bamboo binder less board was investigated. This type of board is manufactured without any adhesive: the lignin takes over the function of the adhesive. Under influence of hot pressing modified bamboo fibers are formed into boards. Boards with a density of 800 kg/m^3 exceeded the minimum requirements for particleboard according to the Japanse Standard (JIS A-5908). It was concluded that there are possibilities to produce binder-less boards using bamboo.

The third experiment explored the technical feasibility of using bamboo zephyr mat with pre hot pressing treatment for the manufacture of laminated bamboo lumber. It was found that by orientating the glue line to the vertical direction the ultimate strength maximizes. The bending properties had similar values to LVL produced with Lauan veneer.

In the fourth experiment, the study was focused on the bending properties of bamboo reinforced composite beam made of particleboard, OSB and ordinary wood web with laminated bamboo mat as reinforcing flanges. These flanges were processed from bamboo zephyr with hot press treatment. It was found that the bending properties, modulus of elasticity in bending and modulus of rupture improved significantly.

2.4.4 Numerical Analysis of Laminated Bamboo Strip Lumber (LBSL)

The study of Wan Tarmeze (2005) was focused on the use of laminated bamboo strip lumber (LBSL) to broaden the use of bamboo for modern construction. The main objective of the study was to determine the bending properties of various configured LBSL beams by numerical simulation.

To model the culm wall a two layers model was used which was found to be suitable (see also paragraph 3.4.1). For the stress strain relationship an elastic-plastic model with softening was used. This model produced load-deflection graphs that resemble those produced by experimental bending tests on bamboo strips loaded in bending. By means of these two models the following aspects were investigated:

- The effect of strip orientation on the bending behavior of LBSL beams.
- The variations in bending properties of LBSL beams.
- The effects of the presence of nodes on the bending properties of LBSL beams.

Wide and narrow strips were distinguished, see also paragraph 3.2. For the use of wide strips inner-outer configuration is recommended which means that all the strips in the bottom half of the beam are strips oriented with their inner layer on top and all the strips in the upper half are strips orientated with their outer layer on top. For the use of narrow strips random orientation is recommended. Since random orientation could make the beam asymmetrical about a vertical axis the beam tends to twist and bend side way during bending. This behavior is not desired and to prevent this, the beam could be cut into two equal lengths after which one of the beams could be turned trough 180° about a vertical axis and finally both beams could be glued together.
It was found that the average bending properties of LBSL beams assembled out of narrow strips were not significantly affected by size due to the random orientation. For LBSL beams assembled out of wide strips this does not apply. Since these beams were set up by a standardized strip orientation, the bending properties were negatively affected by size.
Regarding nodes, it was found that they reduce the stiffness and strength of the beams. It is proposed to scatter them uniformly through the beams.

Some critical comments have to be made. The used model with softening can be used to simulate the behavior of a single strip loaded in bending. However, a LBSL beam assembled out of multiple strips makes that the outermost strips at the tension and compression side are subjected to nearly a uniform tension and compression force, respectively. It is questionable if the used model resembles this situation.
The difference between narrow and wide strips is relative: this means that the conclusions drawn for beams assembled out of narrow strips also apply to beams assembled out of wide strips depending on the dimensions of the strips related to the dimension of the beams.
Furthermore, it is not possible to glue the strips in such a way that the positions of nodes are uniformly scattered, see also chapter 6.

2.5 Behavior of Glued-Laminated Timber

2.5.1 Background to the Regulations in CEN

The bending strength of a glued-laminated timber beam is often directed by the tensile strength of the outermost lamination where failure can be initiated by a knot or a finger-joint, this because wood under compression has a large yield capacity. According to European Committee for Standardization (1999), these strength properties are related to each other by an empirical relationship, which is based on tests and analytical investigations. This relationship indicates that for standard lamination qualities the characteristic bending strength of glued-laminated timber beams is 40 to 90% higher than the characteristic tensile strength of the laminations. This can be explained by the laminating effect which is defined as the increase in strength of lumber laminations when bonded in a glued-laminated timber beam compared with their strength when tested by standard test procedures. The laminating factor can be determined by:

$$\lambda_{lam;1} = \frac{f_{m;beam}}{f_{t;lam;0}} \qquad \text{eq.2.4}$$

where:

$\lambda_{lam;1}$ = laminating factor based on ordinary beam theory [-]

$f_{m;beam}$ = bending strength of the beam (computed by ordinary beam theory) [N/mm^2]

$f_{t;lam;0}$ = tensile strength of the lamination [N/mm^2]

In summary this laminating effect can be explained by three physical factors: an effect of testing procedure (1), a reinforcement of defects (2) and an effect of dispersion (3). These effects are explained by Serrano (1997; 2000):

1) “A single lamination tested in pure tension by applying a centric force may bend laterally owing knots and unsymmetrical placed anomalies. This is due to the stiffness not being constant across the cross section of the lamination. If the same lamination were contained in a glued-laminated timber beam exposed to bending, the rest of the beam would prevent such lateral bending.
2) A lamination that contains knots or other zones of low stiffness will be reinforced by adjacent laminations when it is contained in a glued-laminated timber beam. This is due to the fact that the stiffer and stronger laminations take up a larger part of the tensile stresses.
3) In a glued-laminated timber beam, the defects are smeared out, resulting in a material more homogenous than solid wood. The probability of a defect having serious influence on the strength of the beam is less than it is in a single lamination”.

2.5.2 Influence of Lamination Thickness

It was shown by Serrano (1997; 2000) on the basis of both linear and non linear fracture mechanics that the thickness of laminations also affects the laminating effect. This was done by studying the behavior of a beam after failure at the outer lamination at the tension side. It was assumed that a crack is formed at the failed section in the glue line between the outer and second lamination. The

condition for that crack being stable, which is a condition for redistribution of stresses, was investigated. A crack is stable when it only will propagate when the load is increased. This implies that the initial failure of the finger-joint does not lead to a total collapse of the beam. It was found that a stable crack propagation along the outer lamination can take place, but only for small lamination thicknesses, typically less than 10 mm.

This phenomenon may explain the high bending strength of laminated-veneer-lumber (despite the butt-joints) which can be seen as glued-laminated timber on a micro scale.

3 Manufacturing Aspects of Glued-Laminated Bamboo

3.1 Introduction

Since bamboo is used in its original form (culms) the utilization is limited by the dimensions and cross-section given by nature. To benefit the possibilities these restrictions have to be cancelled out by developing efficient manufacturing processes. To process bamboo into glued-laminated bamboo two developments are thought of: assembling laminations out of strips and assembling beams out of these laminations. Thus the laminations are also laminated. To assemble beams immediately out of strips is not possible since the curing time of the adhesive can become critical due to the thickness of the strips, which is very thin: 5 mm.

This chapter presents how bamboo can be processed into glued-laminated bamboo using existing wood-technology. Since bamboo and wood are up to a high extent similar, existing techniques for wood are the techniques for this study to start with. Paragraph 3.2 discusses how laminations can be assembled out of strips. Paragraph 3.3 deals with the processing of laminations into beams on the basis of grading, end jointing, face bonding and finishing. Paragraph 3.4 discusses the orientation of strips. Successively attention is given to the influence of the non-uniform distribution of fibers along the culm wall thickness, bondability and nodes.

3.2 Processing of Strips into Laminations

Research institutes and manufacturers in China, India, Japan and Malaysia, respectively Fustar Company, Indian Plywood Industries Research & Training Institute (IPIRTI), Kagoshima Institute of Industrial Technology (KIT) and Forest Research Institute Malaysia (FRIM) are focused on developing and manufacturing bamboo floors and other products like furniture. For these purposes bamboo is processed into strips after which they can be assembled into laminations in the case of bamboo floor board.

One can distinguish two types of strips: narrow strips and wide strips. The narrow strips are obtained by conventional methods. Wide strips are obtained by experimental methods. The conventional method uses matured bamboo culms with a diameter of over 100 mm. The culms are cut into required lengths using cross cutting machines up to the length of the bamboo where the outer diameter is 100 mm. The culm wall should be thicker than 7 mm. Suitable species which exhibits those features are represented by Table A.3. Bamboo culms cut into required lengths are split into strips of about 20 mm wide in splitting and shaping machines. Bamboo strips are shaped to a rectangular cross-section with a thickness between 5 to 6 mm in a 4 side planing machine. Species which exhibits a large diameter with thick culm walls can produce strips of up to 35 mm wide (Wan Tarmeze, 2005). After boiling the strips with preservatives, which is done to remove starch and thereby improve the durability, and drying the strips in an oven at a temperature of 70 – 80° C, the strips can be assembled into laminations by gluing them together using urea formaldehyde resin under influence of hot pressing in

a special press at 105° C and with a specific vertical pressure of 1 N/mm^2 and 0.25 N/mm^2 side pressure for horizontal laminates.

The experimental method is discussed by Amino (2002; 2003). This method is developed by Kagoshima Institute of Industrial Technology (KIT) in Japan. This method enables to transform a half-cut bamboo culm into wide flat strips about 6 mm thick and 120 mm wide by radio frequency heating and pressure application. This is shown in Figure 3.1. After this process these strips can also be assembled into laminations.

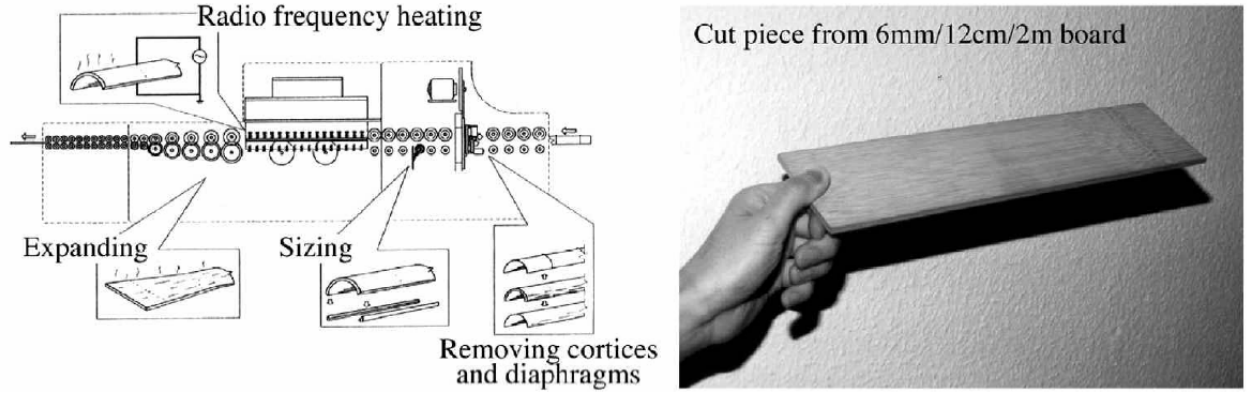

Figure 3.1: Bamboo Flat Board Production System

Source: Amino (2003)

The narrow strips can be obtained by using simple hand tools, so strips can be produced by using different manufacturing systems with different levels of investment for equipment. So, this means that the proposed structural members both by developing countries as developed countries can be produced since manual treatments as well as mechanization are possible.

It is obvious that the use of wide-strips has advantages compared to narrow-strips: for the same volume of glued-laminated bamboo a lesser number of strips is needed. Furthermore, the mechanical properties are better since the flattening process requires only a slight removal of the outer skin which contains the best mechanical properties. However this method is promising, laminations manufactured by this method are not used in this research since it is very difficult to obtain these laminations and the costs are high. The manufacturing process of both laminations assembled out of narrow and wide strips is schematically shown in Figure 3.2.

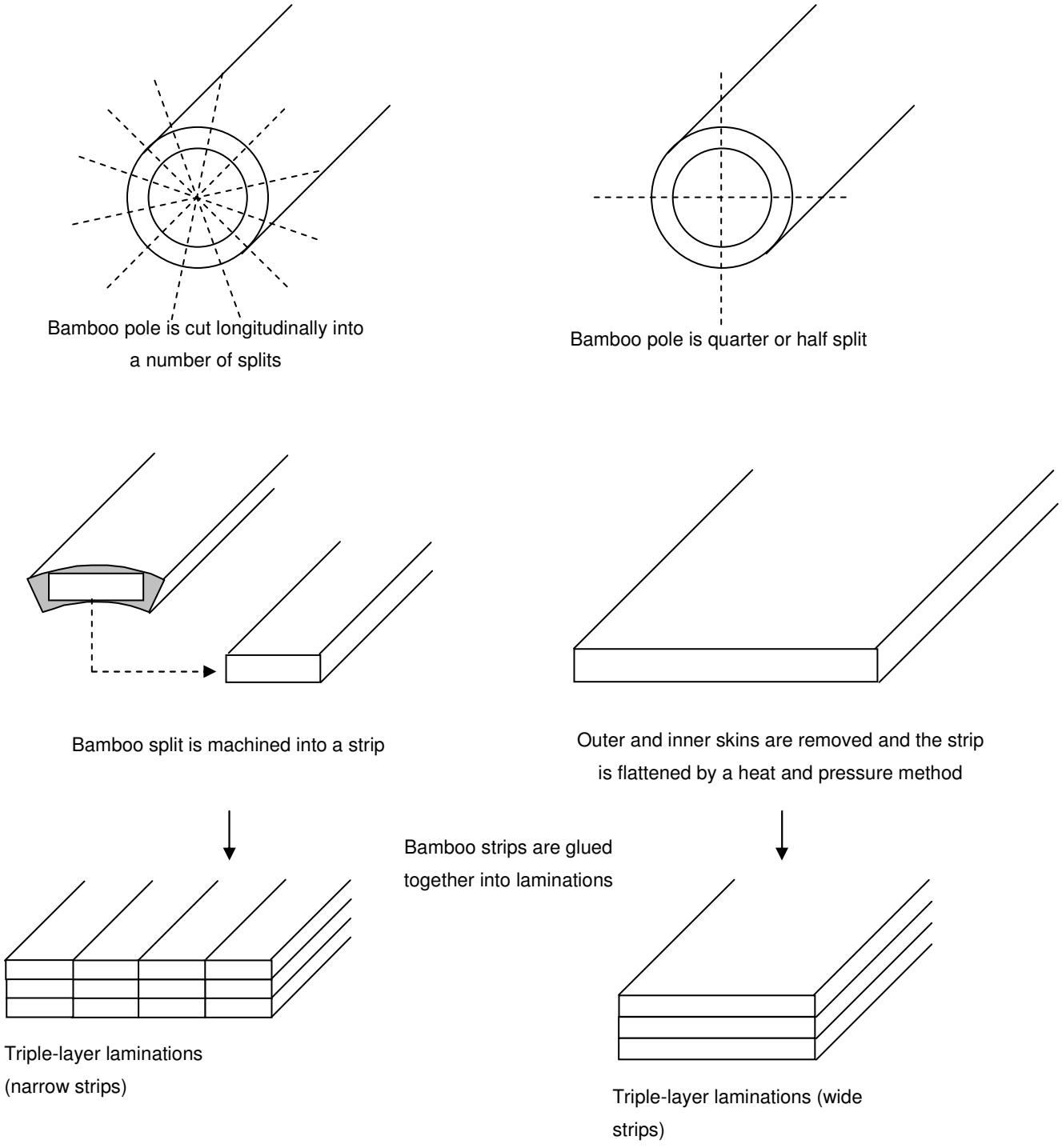

Figure 3.2: Manufacturing processes of (a) laminations assembled out of narrow-strips and (b) laminations assembled out of wide-strips

Source: Wan Tarmeze (2005)

3.3 Processing of Laminations into Beams

Beams can be assembled out of laminations by using existing wood-technology. This can be divided into four major parts:

- grading;
- end jointing;
- face bonding;
- finishing.

3.3.1 Grading

Grading of laminations can be done with E-rating. Since mechanical properties correlates linear with density, which follows from the analysis carried out in appendix B, it is also possible to relate mechanical properties to each other. The strength can be estimated from the stiffness on the basis of which the laminations can be graded into a specific grade. This makes it possible to provide a more economical use of the material since the grade can be varied by matching the lamination quality to the level of stress like in combined glued-laminated timber.

The application of several strength classes and the number of classes depends on the spreading of the properties. When there is a large spreading, it pays to distinguish several classes. When there is a small spreading, it does not have to be necessary to make a division in several classes.

3.3.2 End Jointing

Laminations have to be end jointed by means of scarf-joints or finger-joints. In this research both types of joints are studied. Attention to this subject is given in chapter 5.

3.3.3 Face Bonding

To obtain full-depth beams, the laminations are glued parallel to each other. In this research adhesives used for wood are applied. The adhesive cures under influence of pressure applied by a clamping system. Pressure can be applied by a mechanical ore a hydraulically system.

3.3.4 Finishing

To finish the beams the wide faces have to be planed to remove the adhesive that has squeezed out between adjacent laminations.

3.4 Orientation of Strips

3.4.1 Influence of Non-Uniform Distribution of Fibers Along the Culm Wall Thickness

Due to fact that the distribution of fibers and herewith the mechanical properties vary along the culm wall thickness, as is shown in paragraph 2.2.6, strips can not be regarded as homogeneous. Based on this fact, the orientation of strips would affect the mechanical behavior of a laminated beam assembled out of strips.

Strips can be regarded as layers of materials with different physical and mechanical properties. The actual distribution of the modulus of elasticity along the culm wall can be modeled in various ways. The distribution can be successfully modeled by a two layer model shown in Figure 3.3, as was proved by Wan Tarmeze (2005). The model consists out of two layers with different stiffness properties. It is reasonable to assume that the ratio between the modulus of elasticity of the inside and outside layer is two. Furthermore, the thickness of both layers can be assumed to be equal.

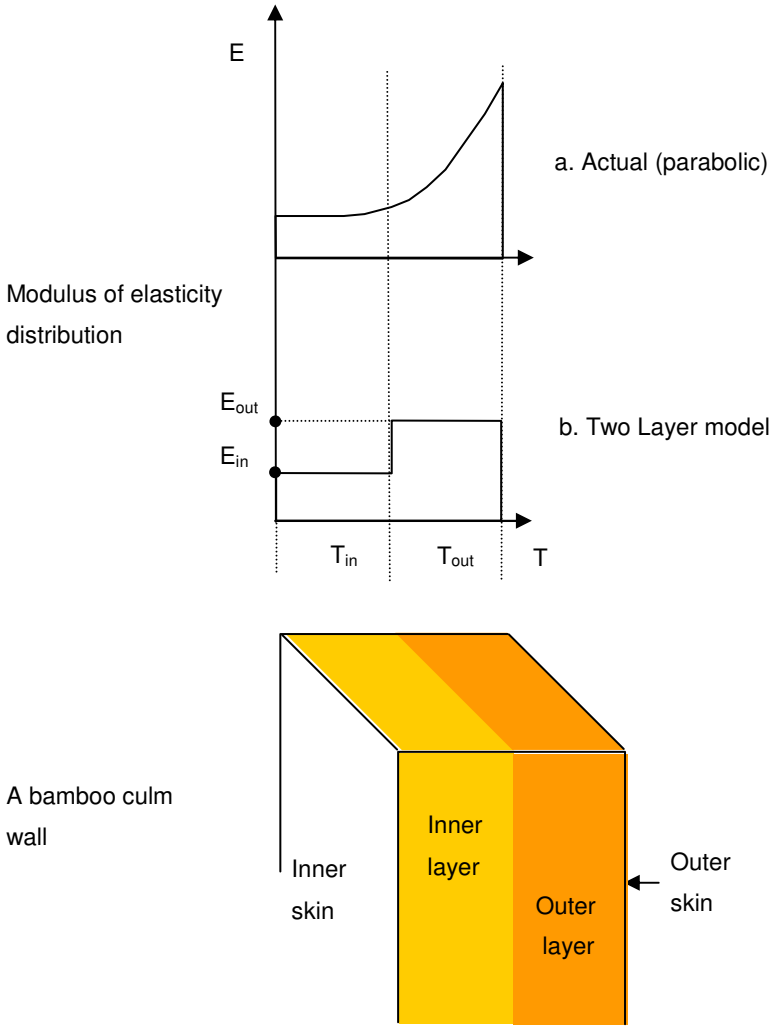

Figure 3.3: Modulus of elasticity distribution in bamboo culm wall

Source: Wan Tarmeze (2005)

Based on this model the influence of the orientation of strips on the mechanical behavior of a laminated beam assembled out of strips can be investigated. Strips can be orientated vertical or horizontal. In appendix C vertical and horizontal laminated bamboo is compared to each other by an analytical analysis using a two layer model as well. On the basis of that analysis it can be stated that strip orientation, vertical or horizontal, has no significant influence on the effective modulus of elasticity when a beam is assembled out of more than 12 strips on top of each other. Since beams assembled out of less than 12 strips will find no significant structural application it is clear that in practice, strip orientation, vertical or horizontal, is no issue.

Furthermore the orientation of strips in relation to each other plays no significant role either. Strips can be arranged with their inner layer on top, with their outer layer on top, combinations of these or randomly. It was found by Wan Tarmeze (2005) on the basis of numerical simulations that the orientation of strips in relation to each other plays little or no role in determining the bending properties since the properties converges when the number of strips increases. This is logical because a beam behaves itself homogeneous when the strips, which are not homogeneous, are distributed uniformly over the cross-section. Thus the orientation of strips can be done randomly.

3.4.2 Influence of Bondability

Amino (2002; 2003) found a relationship between the bond strength and the orientation of strips in relation to each other. Strips glued outer layer to outer layer gave lower values than other combinations, tough differences were small (9.81 N/mm^2 outer//outer combination compared to 11.13 N/mm^2 inner//inner combination for *Phyllostachys pubescens* glued with phenol-resorcinol formaldehyde). Furthermore a decrease of the strength was found for the highest density specimens of some combinations. The results may suggest a difficulty of bonding high-density bamboos. This is in agreement with wood as mentioned in Forest Products Laboratory (1999: p. 9-7). However, the number of specimens was not sufficient to recognize the tendency and more research is necessary on this subject.

Notice that when the influence of bondability has to be taking into account, strips should be glued outer layer to inner layer which is a compromise between strips glued outer layer to outer layer and strips glued inner layer to inner layer which is both not possible when more than two strip are involved. The profit of this is negligible thus with respect to bondability the orientation of strips can also be done randomly.

3.4.3 Influence of Nodes

Regarding nodes, strips can be randomly assembled into laminations. Hence it is possible that there is a cross-section where nodes are not counteracted by internodes. Attention to this subject is given in chapter 6.

4 Laminated Bamboo Loaded in Tension

4.1 Introduction

In laminated beams, the outermost laminations at the tension and compression side are subjected to nearly a uniform tension and compression force, respectively. It is believed that the bending strength of a glued-laminated bamboo beam is directed by the tensile strength of its outermost lamination, this because bamboo under compression has a large yield capacity. To predict the strength of beams assembled out of laminations based on the properties of the individual laminations these have to be studied.

The tensile strength of bamboo along with the modulus of elasticity in tension is not often determined in research and hence not often cited in literature. The reason for this might be that, since the tensile strength is rather high, this strength cannot be utilized in practice. When culms are used in construction (e.g. in a truss), bamboo will fail by shear before its full tensile stress is developed, since pure tension is difficult to realize (Ahmad, 2000). Furthermore, joints can not transmit such a high force (Janssen, 1981). The most reliable estimate of the tensile strength and modulus of elasticity are found in static bending tests. However, for laminations subjected to tension, the tensile strength is a fundamental criterion.
A nice discussion on the evolving of tension tests can be found in Arce-Villalobos (1993). The tensile strength is usually determined by test specimens made of split bamboo. Interesting is the review on a research carried out by Duff. The species involved was *Phyllostachys pubescens*. Strips tested were taken from culms and were reinforced at the extremes to avoid damage by the grips. This was done by gluing some extra material in the support region. The exact shape of the test specimens was not reported. A maximum tensile strength is reported in the outer layer of 342 N/mm^2 and a minimum for the inner layer of 54 N/mm^2. The modulus of elasticity varied consistently. The tensile strength of the nodes was 80% of that of the internodes.
Nugroho (2000) found a mean tensile strength of 132 N/mm^2 (standard deviation = 21 N/mm^2) for *Phyllostachys pubescens* determined by node and internode test specimens. The mean modulus of elasticity determined by test specimens subjected to bending was 10970 N/mm^2 (standard deviation = 1650 N/mm^2).
But there is no information available on the tensile strength and modulus of elasticity of laminated bamboo.

The purpose of this part of the research reported here is to study the behavior of laminated bamboo loaded in tension, and to determine the tensile strength and modulus of elasticity in tension. Paragraph 4.2.1 gives attention to the used materials. The used laminations and test specimens are described. Paragraph 4.2.2 discusses the experimental test methods and the statistical tests used to investigate differences between samples. Paragraph 4.3 outlines the results after which they are discussed. Finally, paragraph 4.4 summarizes the conclusions.

4.2 Experimental

4.2.1 Materials

Laminations

In this research laminations of three different batches were used. These were purchased from different manufacturers in Asia. Batch A and B were directly obtained from the manufacturer Fustar Bamboo and Lumber Co., Ltd Facsimile. Batch C was obtained from an importer in the Netherlands named MOSO International BV. These laminations are commonly used in laminated bamboo flooring. Table 4.1 summarizes some important information on these batches. The used species was *Phyllostachys pubescens*, one of the most potential species of China, with respect to availability, dimensions and structural properties.

Table 4.1: Information on batches

Batch	Botanical name	Local name	Locality site	Age of the culms	Used adhesive	Manufacturer
[-]	[-]	[-]	[-]	[yr]	[-]	[-]
A / **B**	*Phyllostachys pubescens*	Mao Zhu (Mao bamboo)	Zhejiang Province, China	4	Urea formaldehyde	Fustar Bamboo and Lumber Co., Ltd Facsimile
C	*Phyllostachys pubescens*	Mao Zhu (Mao bamboo)	Zhejiang, Fujian, Anhui and Jiangxi Province, China	4-5	Urea formaldehyde	Several

To study the tensile strength and modulus of elasticity in tension, triple-layer laminations of batch A and C were used. These are assembled out of three strips on top of each other and four strips side by side. By assembling the laminations in such a way shown in Figure 4.1, warping of the laminations due to shrinking and swelling is prevented. Furthermore, the variation in hardness at the top side is small which is important in laminated bamboo flooring.

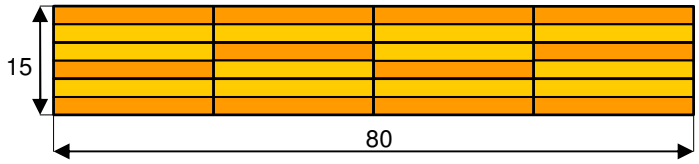

Note: dark color: outer part culm wall; light color: inner part culm wall

Figure 4.1: Composition three-layer laminations

Test Specimens: Tension Test on Triple-Layer Laminations

Test specimens were based on those used for wood according to EN 408 (European Committee for Standardization, 1995a). According to this code, the test specimen shall be of full structural cross section, and of sufficient length to provide a test length clear of the testing machine grips of at least nine times the larger cross-sectional dimension. These recommendations were adopted, with the exception of the application of a full structural cross section: the cross section within the gauge length

was reduced so that the section of failure could be kept under control, which enabled to calculate the stresses accurately. This was achieved by using a milling-machine shown in Figure 4.2.

Figure 4.2: Reduction of the cross-section by using a milling-machine

The geometry of the test specimens is shown in Figure 4.3. The total length of the test specimens was 1000 and 950 mm for those of sample A and C, respectively.

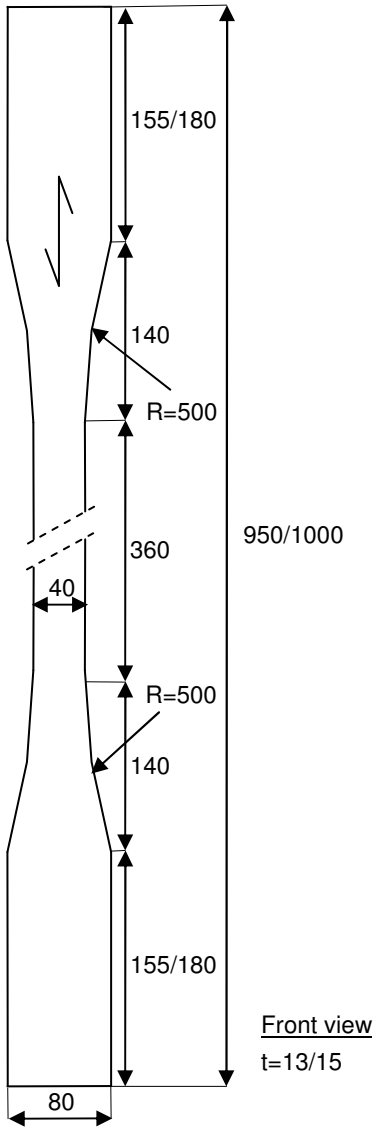

Note: dimensions in mm

Figure 4.3: Geometry tension test specimen

Table 4.2 provides an overview of the number of test specimens and their denomination.

Table 4.2: Number of test specimens and their denomination

Test	Sample	Specimen code	Number
Tension test on triple-layer laminations	A	A(Phyll.Pub)-TT-I-01 to 12	12
	C	C(Phyll.Pub)-TT-I-01 to 15	15

Test Specimens: Moisture Content and Density

Moisture content and density were determined by using two test pieces taken from each tension test specimen. These were based on ISO 22157-1:2004 (International Standard Organization, 2004). The test pieces were approximately 15 mm in thickness, 25 mm in width and 20 mm in height.

4.2.2 Method

Tension Test on Triple-Layer Laminations

The tensile strength determined by the tension test has to be representative for a lamination applied in a glued-laminated beam. Uncentered defects such as nodes or areas of unsymmetrical density (due to the non-uniform distribution of fibers along the culm wall thickness) can induce lateral bending stresses that, when combined with applied tensile stresses, reduce the measured tensile strength. In a glued-laminated beam subjected to bending, the rest of the beam would prevent such lateral bending. The tensile stress obtained with a free tension test is lower than that in a glued-laminated beam. For this reason the test was performed under clamped conditions, so that the conditions resemble those of a lamination in a glued-laminated beam. This principle is depicted in Figure 4.4 for the imaginary situation of a bamboo strip tested in tension. The modulus of elasticity of the outer part is higher than that of the inner part of the culm wall. When tested in a free tension test a bending moment would occur; in a test under clamped conditions this moment is prevented by the clamps.

The tension test was carried out in accordance with EN 408 (European Committee for Standardization, 1995a) by a universal testing machine Schenck (250 kN). The charge of the test specimens was electrically acquired through the load cell installed between the test specimens and the cross-head. For all tests reported in this report it was decided to chose a constant cross-head movement so adjusted that the maximum load was reached within 300 ± 120 s. This interval is specified for determining the short-term strength of wood. For the tension test, the maximum load was reached within the prescribed time by using a constant cross-head movement of 1.5 mm/min. The test setup is shown in Figure 4.5 (left).

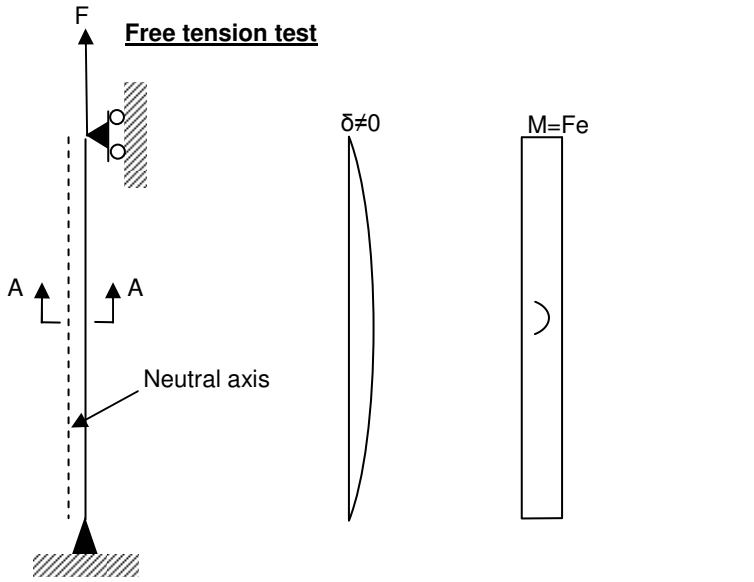

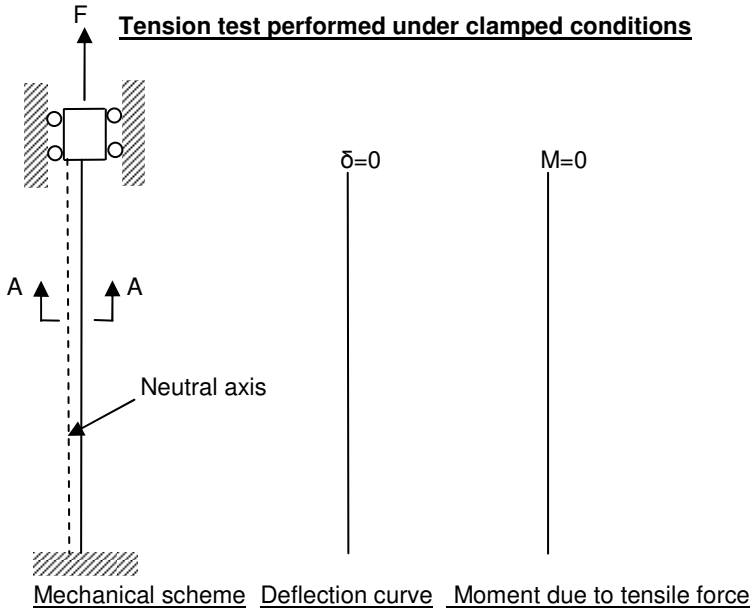

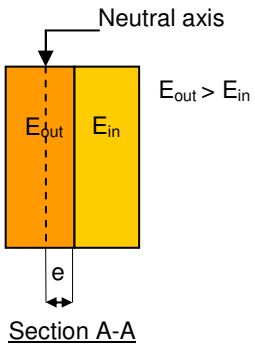

Figure 4.4: Differences between free tension test and tension test under clamped conditions

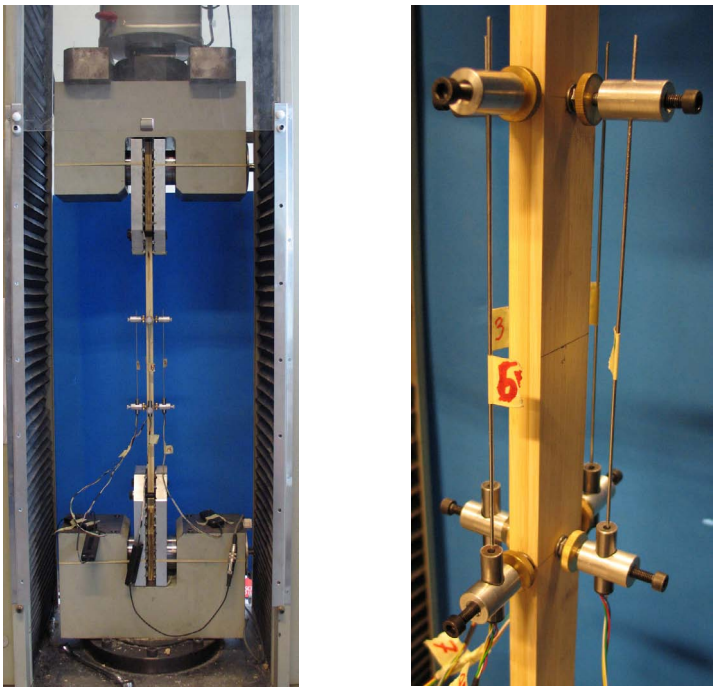

Figure 4.5: Left: test setup of tension test on triple-layer laminations; right: positioning of four LVDT-transducers

The tensile strength is computed by:

$$f_{t;0} = \frac{F_{max}}{A} \qquad \text{eq.4.1}$$

where:

F_{max}	= maximum load	[N]
$f_{t;0}$	= tensile strength parallel to the grain	[N/mm^2]
A	= reduced cross-sectional area	[mm^2]

Most of the laminations failed within the gauge section, the ones who failed within the supporting area were excluded from the determination of the tensile strength. Deformation was measured by two LVDT-transducers[1] applied on the wide faces of the test specimens over a length of 200 mm. Measuring the deformation over a relatively large part of the test specimen enabled to compute a mean modulus of elasticity taking into account the influence of nodes which were irregular distributed troughout the lamination. The modulus of elasticity in tension is computed by:

$$E_{t;0} = \frac{l_1 \cdot (F_2 - F_1)}{A \cdot (w_2 - w_1)} \qquad \text{eq.4.2}$$

where:

$E_{t;0}$	= modulus of elasticity in tension parallel to the grain	[N/mm^2]
l_1	= gauge length	[mm]
$F_2 - F_1$	= increment of loading on the straight portion of the load deformation curve	[N]
$w_2 - w_1$	= increment of deformation corresponding to $F_2 - F_1$	[mm]

[1] LVDT = Linear Variable Differential Transformer

The increment of loading was computed between 10% and 40% of the maximum load. The LVDT-transducers were taken away before failure to prevent damage. The displacement of the cross-head was measured until failure in order to describe the load deformation behavior. During the first series (A(Phyll.Pub)-TT-I) test specimens were equipped with four LVDT-transducers on each side of the test specimen in order to verify that no bending occurred. The positioning of the four LVDT-transducers is shown in Figure 4.5 (right). All test specimens were conditioned in a conditioning chamber (temperature = 20°C and relative humidity = 65%) before they were tested.

Moisture Content and Density

Since moisture and density affect the mechanical properties it was decided to determine these variables. This was done according to ISO 22157-1:2004 (International Standard Organization, 2004). Moisture content was determined by weighing of the loss in mass of the test piece on drying to constant mass using an oven at a temperature of approximately 103°C. After 24 hours the mass was recorded at regular intervals of 2 hours. Drying was considered complete when the difference in mass between the successive determinations of the weight did not exceed 0.1 g. The moisture content is computed by eq.2.2.

Density was determined on the basis of the same test pieces that were used for the determination of the moisture content. The density was determined at the moisture content of the test specimen: the mass was taken as the oven-dry mass and the volume was taken at the moisture content of the test specimen. The density is computed by:

$$\rho_0 = \frac{m}{V} \cdot 10^6 \qquad \text{eq.4.3}$$

where:

ρ_0 = density at the moisture content of the test specimen [kg/m^3]
m = oven-dry mass [g]
V = volume determined at the moisture content of the test specimen [mm^3]

Statistical Test

In order to investigate whether there were significant differences between the two samples, described in paragraph 4.2.1, with respect to tensile strength and modulus of elasticity in tension, statistical tests were carried out using SPSS 11.5. The two samples were considered independent from each other and both populations were assumed to be normal distributed. This was verified by normal probability plots and the tests of Kolmogorov-Smirnov and Shapiro-Wilk, respectively. An independent-samples t test was executed based on a level of significance of $\alpha = 0.05$. The null hypothesis was stated as:

$$H_0 : \mu_1 = \mu_2 \qquad \text{eq.4.4}$$

The alternative hypothesis was stated as:

$$H_1 : \mu_1 \neq \mu_2 \qquad \text{eq.4.5}$$

4.3 Results and Discussion

4.3.1 Properties of Bamboo Laminations Loaded in Tension

The experimental results are represented by Table 4.3. The individual results of each test specimen can be found in appendix H (H.1.1).

Table 4.3: Experimental results: properties of triple-layer laminations loaded in tension

Test series		A(Phyll.Pub)-TT-I	C(Phyll.Pub)-TT-I
Tensile strength parallel to the grain ($f_{t;0}$)			
Useful samples	**[-]**	8	8
Mean	**[N/mm^2]**	82	91
Standard deviation	**[N/mm^2]**	15 (18.2%)	6 (7.0%)
Modulus of elasticity in tension parallel to the grain ($E_{t;0}$)			
Useful samples	**[-]**	12	15
Mean	**[N/mm^2]**	9591	9503
Standard deviation	**[N/mm^2]**	730 (7.6%)	641 (6.7%)
Moisture content (*MC*)			
Sample size	**[-]**	24	30
Mean	**[%]**	7.7	8.5
Standard deviation	**[%]**	0.2 (2.3%)	0.4 (4.2%)
Density (ρ_0)			
Sample size	**[-]**	24	30
Mean	**[kg/m^3]**	606	660
Standard deviation	**[kg/m^3]**	31 (5.2%)	27 (4.1%)

Note: the value in parenthesis refers to the coefficient of variation

The results are in poor agreement to the results found by Nugroho (2000) who reported a mean tensile strength of 132 N/mm^2 (standard deviation = 21 N/mm^2) and a mean modulus of elasticity in bending of 10970 N/mm^2 (standard deviation = 1650 N/mm^2). These results were determined by node and internode test specimens. Compard to these results, the tensile strength of sample A is 38% lower and that of sample B 32%. The modulus of elasticity in tension of both samples is 13 % lower (it is assumed that the modulus of elasticity in bending is comparable to that in tension).

There can be many explanations for the found differences. Firstly, the used test specimens and method is different. Secondly, mechanical properties are affected by a number of variables e.g. age and density of the used culms which could have been significantly different. Strips originating from different positions along the culm height and along the culm wall thickness can also cause differences in mechanical properties.

Mechanical properties are predominantly affected by density. However, due to the small coefficient of variation, this variable was not responsible for the variation within samples (correlation between density and tensile strength was poor just as correlation between density and modulus of elasticity in tension).

The results of the statistical analyses can be found in appendix H (H.1.2, H.1.3 and H.1.4). From the results of the independent samples t test, it was found that density of sample A was significantly different from that of sample C, based on a significance of $\alpha = 0.05$. The null hypothesis was rejected. This means that, though not significantly, the considerably difference in tensile strength of sample A compared to that of sample C (82 N/mm^2 versus 91 N/mm^2), might be caused by density. This hypothesis is not confirmed by the difference in the modulus of elasticity in tension (9591 N/mm^2 versus 9503 N/mm^2) which was negligible and not significantly.

The use of the independent samples t test was justified since the involved populations were normal distributed according to the normal probability plot: the plotted points did not deviate significantly and systematically from the straight line. This followed also from the tests of Kolmogorov-Smirnov and Shapiro-Wilk in which the significance exceeded 0.05.

4.3.2 Stress-Strain Behavior

A bamboo lamination under tension behaved proportionally and failed in a brittle manner, which agrees to the results found by Arce-Villalobos (1993), for a strip loaded in tension. Figure 4.6 shows a typical stress strain curve for a bamboo lamination under tension.

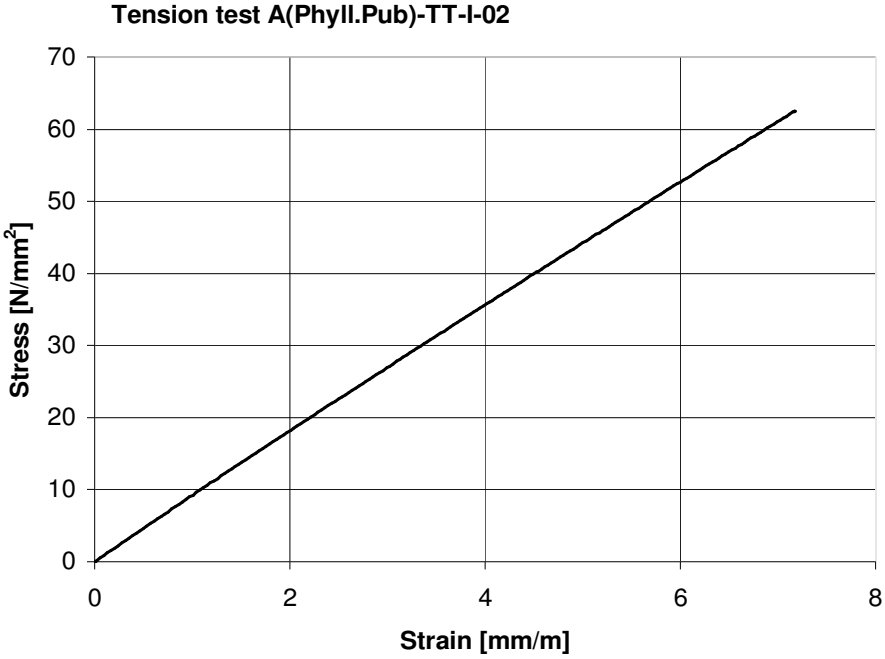

Note: deformation measured by two LVDT-transducers until failure

Figure 4.6: Stress-strain curve for bamboo lamination loaded in tension parallel to the grain

4.3.3 Failure Mode

It was observed that failure of most laminations was initiated by a node, shown in Figure 4.7. This is in agreement to the general statements on nodes found in the literature: nodes are the weakest link, see also paragraph 2.2.6. The influence of nodes on the tensile strength is extensively discussed in chapter 6.

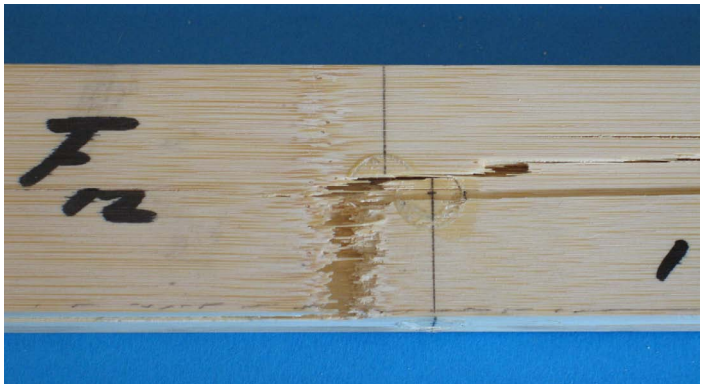

Figure 4.7: Failure within the gauge section of a bamboo lamination initiated by a node

Since the fact that some of the test specimens failed within the transition zone, the used radius of 500 mm may not be suitable. The change in section has to be slight: besides tensile stresses parallel to the grain, also tensile stresses perpendicular to the grain and shear stresses occur. The geometry of this transition zone is determined analytically in appendix D by taking the combined stresses into account. It was found that a radius of 1200 mm is required.

4.4 Conclusions

In this part of the research, the behavior of laminated bamboo loaded in tension was studied. To determine the tensile strength and modulus of elasticity in tension, tension tests were carried out. Two samples of different manufacturers were used. The geometry of the transition zone of the tension test specimen was determined analytically in appendix D. The following conclusions can be drawn:

- A bamboo lamination loaded in tension behaves proportionally and fails in a brittle manner.
- Failure of bamboo laminations is mostly initiated by a node.
- It can be recommended to adjust the radius for the test specimens used in this research to 1200 mm.

5 Influence of Joints on Tensile Strength and Stiffness

5.1 Introduction

When the length of beams exceeds the length of laminations, these have to be connected by end joints. A joint has to transmit a significant proportion of the strength parallel to the grain. The load a joint can withstand in shear has to approach the load that a lamination can withstand in tension.

In timber, scarf-joints are very efficient to accomplish this: joints with slopes of 1 in 10 or 1 in 12 were found to reach tensile strength equal to 85% to 90% of the strength of clear wood in tension. However, scarf joints exhibit besides this important advantage also some major disadvantages. Firstly, scarf joints are not economical. Secondly the accuracy at which the scarf is machined and the alignment and bonding of the two surfaces are critical in determining how well joints will perform. Nowadays, scarf-joints are replaced by finger-joints. These are in fact a modification of the plane scarf-joint: finger-joints can be seen as a series of short scarfs separated by a fingertip. It can be stated that, in timber, transferring forces by means of finger-joints is the most economical solution.

For lengthening bamboo laminations, both types of joints are interesting. Firstly, laminations can be connected by scarf-joints using different manufacturing systems with different levels of investment for equipment. This is favorable for the development of a glued-laminated bamboo industry in developing countries. Secondly, laminations can be connected by finger-joints using existing wood-technology. This is favorable for the application of glued-laminated bamboo in developed countries. No experience is available on both types of joints in relation to bamboo.

The purpose of this part of the research reported here is to study the effect of both scarf- and finger-joints on the tensile strength and stiffness of laminations. Paragraph 5.2.1 gives attention to the used materials. The used laminations, adhesives and test specimen are described. Paragraph 5.2.2 discusses the experimental test methods and the statistical tests used to investigate differences between samples. Paragraph 5.3 outlines the results after which they are discussed. Finally, paragraph 5.4 summarizes the conclusions.

5.2 Experimental

5.2.1 Materials

Laminations

To study the effect of joints on the tensile strength and stiffness, triple-layer laminations of batch A, B and C were used, described in paragraph 4.2.1.

Adhesive Used for Scarf-Jointing: Melamine-Urea-Formaldehyde

Melamine-urea formaldehyde was selected owing to the positive test results described in paragraph 8.3. More information on this adhesive can also be found in paragraph 8.2.1.

The mixing ratio adhesive – hardener was 100:30 by weight. A glue spread of about 500 g/m^2 was applied manually (by a brush) single-sided. This amount was recommended for hardwood by the manufacturer of the adhesive.

Adhesive Used for Finger-Jointing: Melamine Formaldehyde

Melamine formaldehyde (AKZO NOBEL, Cascomin 1250 with hardener 2550) is a thermosetting adhesive commonly used in the manufacturing of finger-joints for glued-laminated timber. This is an adhesive to be used where there is demand for light-colored bond lines with high water and weather resistance.

This adhesive was used at the glued-laminated timber factory where the laminations were finger-jointed.

The mixing ratio melamine formaldehyde – hardener was 100:100 by weight. It was not possible to quantify the glue spread.

Test Specimens: Tension Test on Scarf-Jointed Triple-Layer Laminations, Tension Test on Finger-Jointed Triple-Layer Laminations and Tension Test on Finger-Jointed Triple-Layer Laminations in Combination with ESPI Measurements

Dimensions of the test specimens were the same as those used for testing the tensile strength and modulus of elasticity in tension of triple-layer laminations, described in paragraph 4.2.1. However, for the finger-jointed laminations, the cross-section within the gauge length was not reduced since these test specimens were assumed to fail at the joint at a relatively low stress. Table 5.1 provides an overview of the number of test specimens and their denomination. Test specimens used for the tension test in combination with ESPI measurements were 60 mm in width instead of 80 mm.

Table 5.1: Number of test specimens and their denomination

Test	Sample	Specimen code	Number
Tension test on scarf-jointed triple-layer laminations	B	B(Phyll.Pub)-TT-II(sj)-01 to 15	15
Tension test on finger-jointed triple-layer laminations	A	A(Phyll.Pub)-TT-II(fj)-01 to 11	11
	C	C(Phyll.Pub)-TT-II(fj)-01 to 12	12
Tension test on finger-jointed triple-layer laminations in combination with ESPI-measurements	C	C(Phyll.Pub)-TT-II(fj)-13 to 17	5

The scarf-jointed laminations were manufactured by a table saw (CNC controlled). The slope applied was 1 in 10. They were machined across their thickness. To bond the two laminations together, pressure was applied by hand-screws, as shown in Figure 9.2. Hence, the pressure applied was not quantified. The geometry of the joint is shown in Figure 5.1.

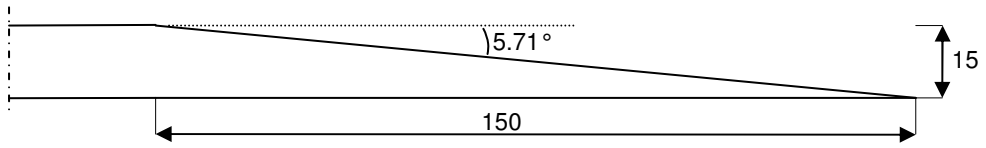

Note: dimensions in mm

Figure 5.1: Scarf-joint geometry

The finger-jointed laminations were manufactured under industrial conditions at the Nemaho in Doetinchem, the Netherlands, a glued-laminated timber factory. They were machined across their width in order to obtain horizontal finger-joints. To glue the pieces of laminations together end-pressure was applied. The optimal pressure was approximately 20 bar which corresponds to 2 N/mm^2, if a higher pressure was used, splitting of bamboo at the finger roots occurred. The finger profile concerns a standard profile used in glued-laminated timber. The geometry of this profile is shown in Figure 5.2.

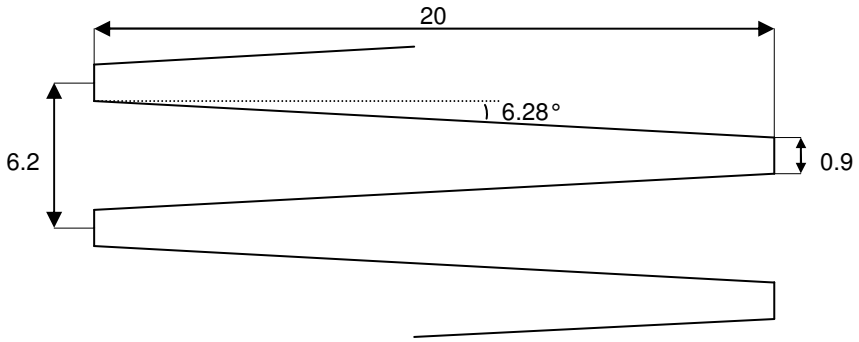

Note: dimensions in mm

Figure 5.2: Finger-joint geometry

Since the tensile strength perpendicular to the grain is poor, cracks occurred in the longitudinal direction when the end-pressure was too high. Test specimens pressed by using an optimal pressure of 20 bar had a gap of approximately 2.0 mm between the tip and the root.

Test Specimens: Moisture Content and Density

Moisture content and density were determined by using at least one test piece taken from each tension test specimen. These were based on ISO 22157-1:2004 (International Standard Organization, 2004). The dimensions of the pieces varied.

5.2.2 Method

Tension Test on Scarf-Jointed Triple-Layer Laminations and Tension Test on Finger-Jointed Triple-Layer Laminations

The tension test on both the scarf- and the finger-jointed triple-layer laminations was carried out according to that on triple-layer laminations described in paragraph 4.2.2. A constant cross-head movement of 1.5 and 1.0 mm/min was used for the scarf- and finger-jointed laminations, respectively. The test setups are shown in Figure 5.3.

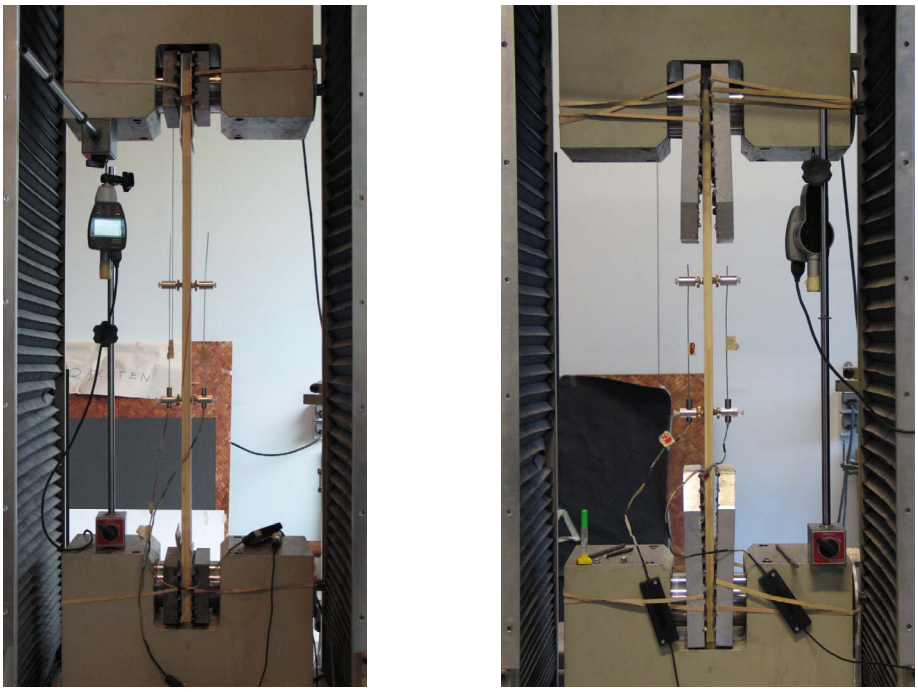

Figure 5.3: Left: test setup of tension test on scarf-jointed triple-layer laminations; right: test setup of tension test on finger-jointed triple-layer laminations

The tensile strength of the jointed lamination is computed by:

$$f_{t;j;0} = \frac{F_{max}}{A} \qquad \text{eq.5.1}$$

where

$f_{t;j;0}$ = tensile strength parallel to the grain of jointed lamination [N/mm^2]

A = reduced cross-sectional area / cross-sectional area [mm^2]

Deformation was measured by two LVDT-transducers applied on the wide faces of the test specimens over a length of 200 mm. Measuring the deformation over this length enabled to compare the results to those of the modulus of elasticity in tension (denoted E_a in the following) in order to quantify the influence of the joint on the stiffness. The stiffness of the jointed area (denoted E_b in the following) can be computed by subtracting the proportion of the deformation of the lamination (ΔL_a) from the total measured deformation ΔL_c (see Figure 5.4):

$$\Delta L_c = 2 \cdot \Delta L_a + \Delta L_b \qquad \text{eq.5.2}$$

hence:

$$\frac{L_c}{E_c} = 2 \cdot \frac{L_a}{E_a} + \frac{L_b}{E_b} \qquad \text{eq.5.3}$$

This results in:

$$E_b = \frac{L_b}{\frac{L_c}{E_c} - 2 \cdot \frac{L_a}{E_a}} \qquad \text{eq.5.4}$$

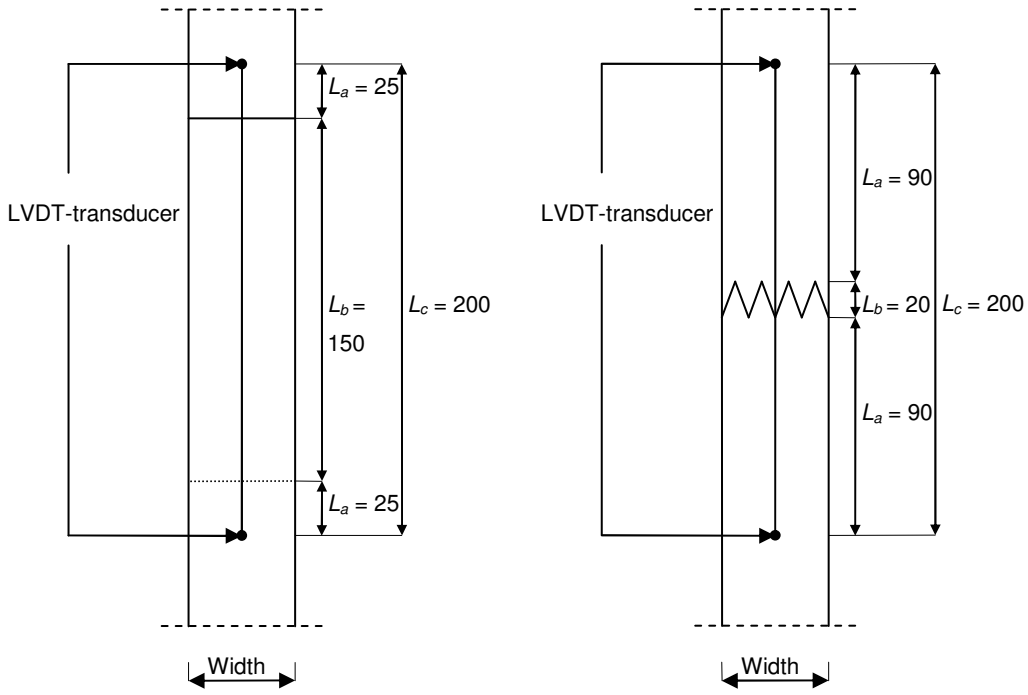

Note: dimensions in mm

Figure 5.4: Overview of variables used in eq.5.2 to eq.5.4 with respect to the scarf- (left) and the finger-jointed lamination (right)

E_c is computed by:

$$E_c = \frac{l_1 \cdot (F_2 - F_1)}{A \cdot (w_2 - w_1)} \qquad \text{eq.5.5}$$

The increment of loading was computed between 10% and 40% of the maximum load. The LVDT-transducers were taken away before failure to prevent damage. The displacement of the cross-head was measured until failure in order to describe the load deformation behavior. The positioning of LVDT-transducers is shown in Figure 5.5. All test specimens were conditioned in a conditioning chamber (temperature = 20℃ and relative humidity = 65%) before they were tested.

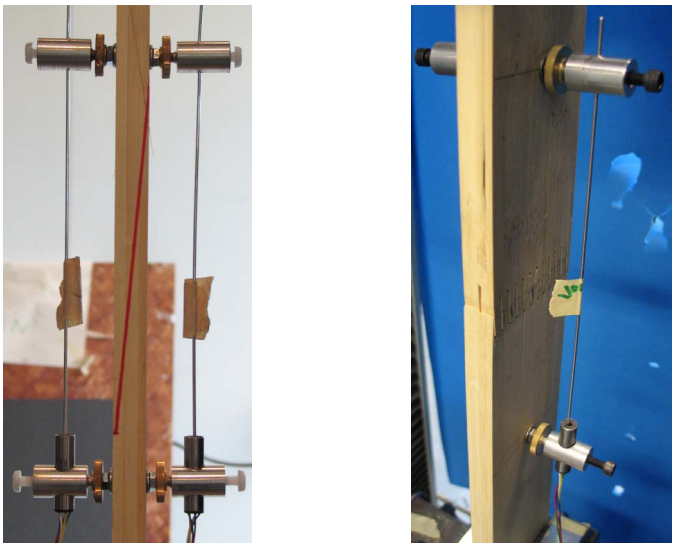

Figure 5.5: Left: positioning of LVDT-transducers mounted on scarf-jointed laminations; right: positioning of LVDT-transducers mounted on finger-jointed laminations

Tension Test on Finger-Jointed Triple-Layer Laminations in Combination with ESPI Measurements

Deformation over the surface of the finger-joint was measured by ESPI, a laser speckle technique. ESPI is the abbreviation for Electronic Speckle Pattern Interferometry. This technique is based on optical interference which allows for the observation of deformation of surfaces.

The working of ESPI will be explained based on the results of a finger-jointed test specimen. The test specimen was loaded in tension by a universal testing machine Schenck (100 kN). The front surface was illuminated over its full width and a height of approximately 50 mm, shown in Figure 5.6. The test setup is shown in Figure 5.7.

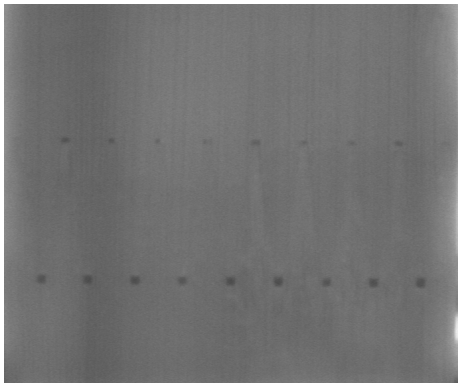

Figure 5.6: Photo of illuminated area by the digital camera of the apparatus

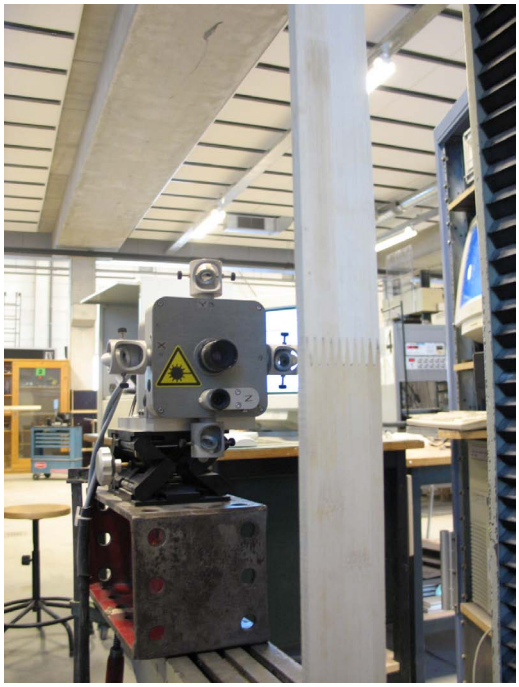

Figure 5.7: Test setup of tension test on finger-jointed triple-layer lamination in combination with ESPI measurements

The speckle interferometry uses the interference characteristics of electromagnetic waves. It is based on the fact that an optically rough surface appears granulated when it is lit by a coherent light (laser). This phenomenon is called a speckle and the individual grains are termed speckle. In Figure 5.8 can

be seen that an area is illuminated by two laser beams. These two beams are obtained by splitting the light beam produced by one laser diode.

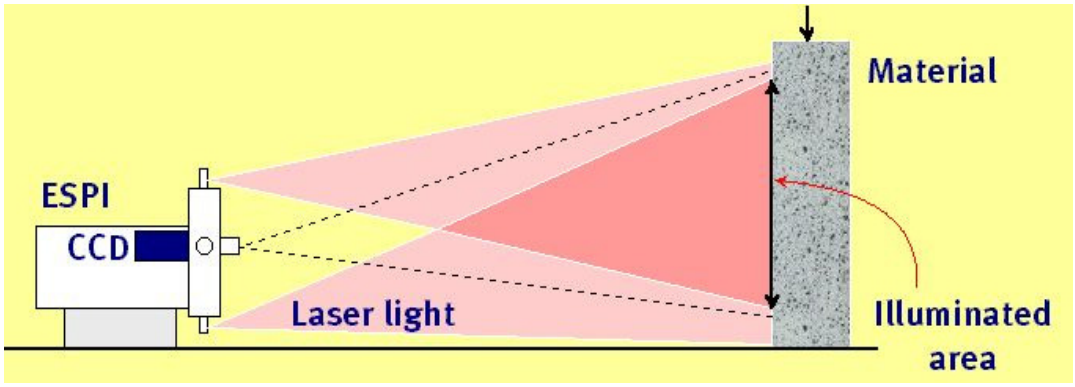

Figure 5.8: Principle of ESPI

After each load step, the reflected light was captured by a CCD camera. A speckle pattern, shown in Figure 5.9 (left) was found, which includes the deformation information of each point of the measured object. During the tests the constant cross-head movement was adjusted to 0.1 mm/m. Interference fringes, also shown in Figure 5.9 (right), were formed by subtracting speckle patterns from various phases of testing. The number of fringes and their widths are a measure of the displacements on the illuminated area. The displacements refer to an arbitrary zero, which was chosen to be the bottom of the illuminated area.

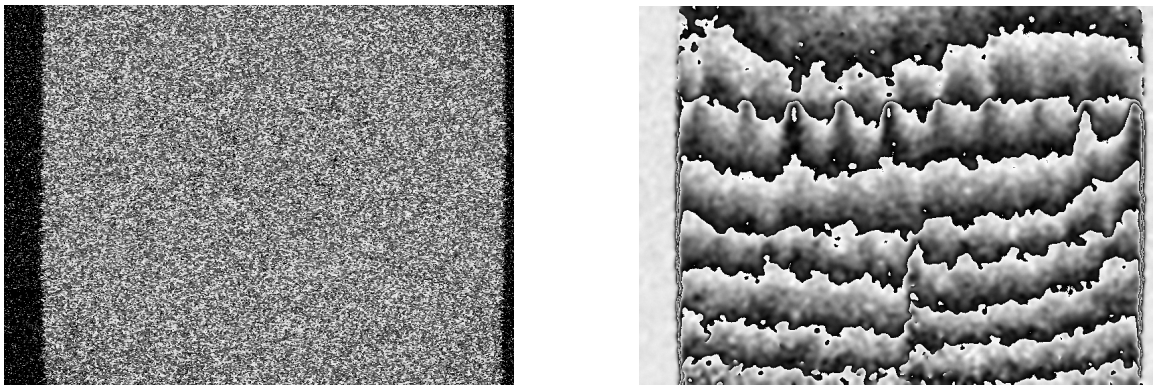

Figure 5.9: Left: speckle pattern; right: fringe pattern

Based on the fringe patterns, displacements shown in Figure 5.10 (left) were determined by calibrating the distance between 2 fringes. In this research displacements in *x* and in *y* direction were measured; the *y*-direction corresponded to the fiber direction. Finally the strains, shown in Figure 5.10 (right), were calculated from the measured displacements.

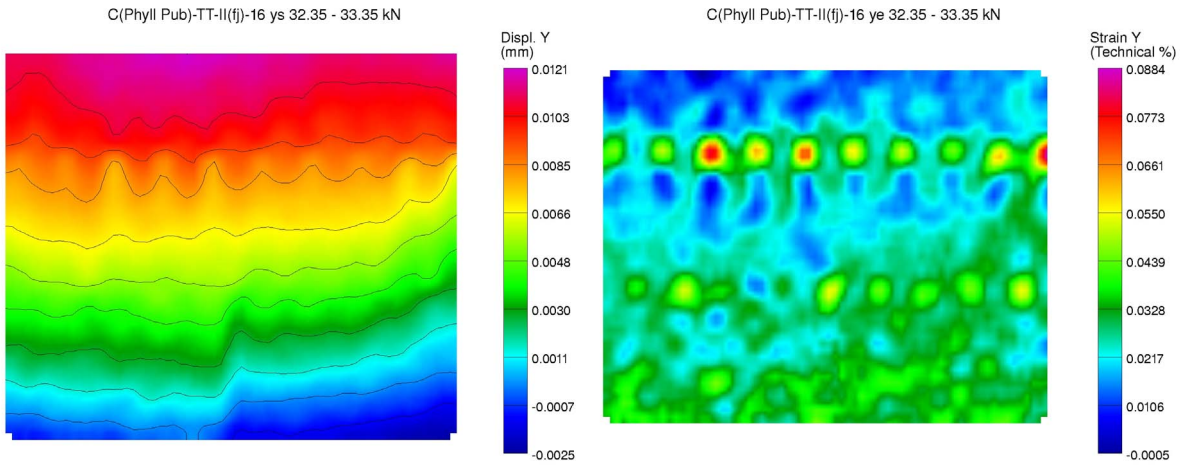

Figure 5.10: Left: displacement of test specimen C(Phyll.Pub)-TT-II(fj)-16 (load-phase: 32.35-33.35 kN); right: strain of test specimen C(Phyll.Pub)-TT-II(fj)-16 (load-phase: 32.35-33.35 kN)

It can be seen that the two plots are related to each other. The distance between lines of equal displacements, shown in the displacement plot is a measure for the strain that occurred, shown in the strain plot.

It has to be noticed that the ESPI system measures the deformation of the surface; the deformation in the test specimen can be totally different.

All test specimens were conditioned in a conditioning chamber (temperature = 20°C and relative humidity = 65%) before they were tested.

Moisture Content and Density

Moisture content and density were determined according to paragraph 4.2.2.

Statistical Tests

In order to investigate whether there were significant differences between finger-jointed test specimens of sample A and C, with respect to their tensile strength, statistical tests were carried out using SPSS 11.5, according to paragraph 4.2.2.

5.3 Results and Discussion

5.3.1 Properties of Jointed Bamboo Laminations Loaded in Tension

The experimental results are represented by Table 5.2 and Table 5.3. The individual results of each test specimen can be found in appendix H (H.2.1 and H.2.2).

Table 5.2: Experimental results: properties of scarf-jointed triple-layer laminations loaded in tension

Test series		B(Phyll.Pub)-TT-II(sj)
Tensile strength parallel to the grain of jointed lamination ($f_{t;j;0}$)		
Useful samples	**[-]**	12
Mean	**[N/mm^2]**	76
Standard deviation	**[N/mm^2]**	15 (19.7%)
Stiffness of jointed area ($E_{t;j;0}$)		
Mean	**[N/mm^2]**	8050
Moisture content (*MC*)		
Sample size	**[-]**	15
Mean	**[%]**	7.8
Standard deviation	**[%]**	0.3 (3.4%)
Density (ρ_0)		
Sample size	**[-]**	15
Mean	**[kg/m^3]**	609
Standard deviation	**[kg/m^3]**	54 (8.9%)

Note: the value in parenthesis refers to the coefficient of variation

Table 5.3: Experimental results: properties of finger-jointed triple-layer laminations loaded in tension

Test series		A(Phyll.Pub)-TT-II(fj)	C(Phyll.Pub)-TT-II(fj)
Tensile strength parallel to the grain of jointed lamination ($f_{t;j;0}$)			
Useful samples	**[-]**	11	15
Mean	**[N/mm^2]**	33	38
Standard deviation	**[N/mm^2]**	6 (19.0%)	11 (28.1%)
Stiffness of jointed area ($E_{t;j;0}$)			
Mean	**[N/mm^2]**	9243	6775
Moisture content (*MC*)			
Sample size	**[-]**	22	24
Mean	**[%]**	7.7	8.7
Standard deviation	**[%]**	0.1 (1.7%)	0.2 (2.1%)
Density (ρ_0)			
Sample size	**[-]**	22	24
Mean	**[kg/m^3]**	665	665
Standard deviation	**[kg/m^3]**	15 (2.3%)	15 (2.3%)

Note: the value in parenthesis refers to the coefficient of variation

Though all laminations failed at the joint, discussed in paragraph 5.3.3, the coefficient of variation for the tensile strength of the jointed laminations was larger than that of the unjointed laminations represented by Table 4.3. This means that the strength of the joints, like the strength of the material, is a stochastic variable.

Due to the small coefficient of variation, density was not responsible for the variation within the samples A and C (correlation between density and tensile strength of finger-jointed laminations was poor). The results of the statistical analyses can be found in appendix H (H.2.4 and H.2.5). From the results of the independent samples t test, it was found that density of sample A was not significantly different from that of sample C, based on a significance of $\alpha = 0.05$. The null hypothesis was not rejected. This means that, though not significantly, the considerably difference in tensile strength of finger-jointed laminations of sample A compared to that of those of sample C, is not caused by density.
It is believed that the difference is caused by the bond quality, which varied greatly.
The use of the independent samples t test was justified since the involved populations were normal distributed according to the normal probability plot: the plotted points did not deviate significantly and systematically from the straight line. This followed also from the tests of Kolmogorov-Smirnov and Shapiro-Wilk in which the significance exceeded 0.05.

5.3.2 Stress-Strain Behavior

The stress strain behavior of a jointed lamination loaded in tension corresponded to that of an unjointed lamination loaded in tension, discussed in paragraph 4.3.2. According to Serrano (1997), the linear-elastic behavior of a jointed lamination does not mean that the bondline behaves linear elastic: due to the fact that the bondline is very thin, its influence on the global response of a lamination is negligible.

5.3.3 Failure Mode

Scarf-Jointed Laminations

Failure of the scarf-jointed laminations was always initiated at the joint (except some test specimens that failed within the supporting area), cracks developed partly along the bondline, shown in Figure 5.11. The test specimens exhibited predominantly bamboo failure, though the percentage of bamboo failure was not as high as measured by the block shear test, discussed in paragraph 8.3.3.
Since the joint is applied under a slope, the surface is partly end-grain and partly tangential. According to Forest Products Laboratory (1999), end-grain surfaces are much more porous than radial or tangential surfaces. Overpenetration can occur because adhesives penetrate deeply into open fibers and vessles along the grain when pressure is applied to bond the assemblies together. This may explain the differences with the block shear test where the bonded surfaces are tangential.

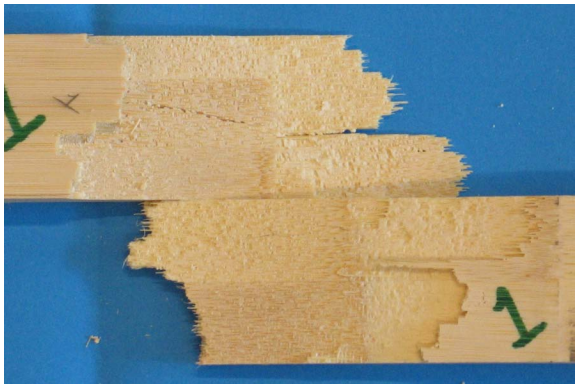

Figure 5.11: Failure of a scarf-jointed lamination partly along the bondline

Finger-Jointed laminations

Failure of the finger-jointed laminations was always initiated at the joint (except some test specimens that failed in the supporting area). Some test specimens failed predominantly along the fingers, shown in Figure 5.12 (left), whereas others failed partly along the fingers and partly in the net section, shown in Figure 5.12 (right). In both cases, failure was predominantly in the bondline and not in the bamboo. This may indicate a poor bond quality and suggests that melamine formaldehyde in the used mixing ratio and amount is not suitable for finger-jointing bamboo laminations.

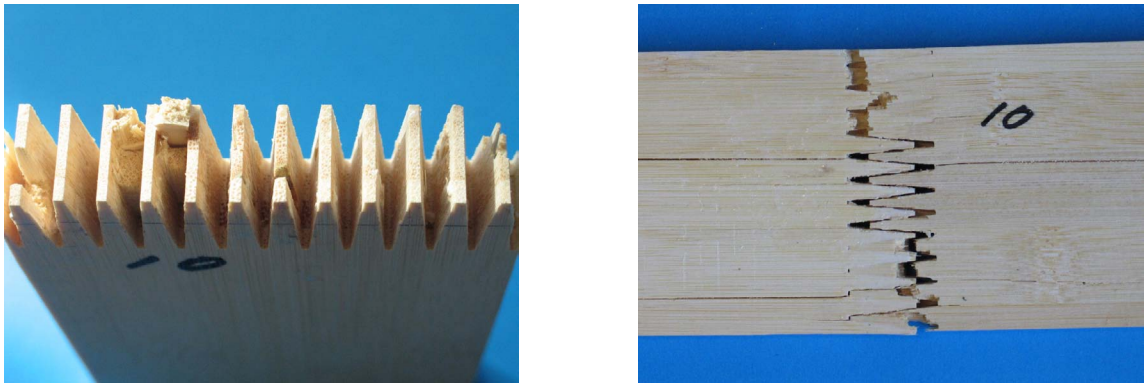

Figure 5.12: Left: failure of a finger-jointed lamination predominantly along the fingers; right: failure of a finger-jointed lamination partly along the fingers and partly in the net section

5.3.4 Strain Distribution over the Finger-Joint

The individual results of each test specimen can be found in appendix H (H.2.3). The results for the *x*-direction are left out of consideration.

The ESPI results of test specimen C(Phyll.Pub)-TT-II(fj)-13, 16 and 17 showed that high strain concentrations developed in the vicinity of the fingertip/root. Since it is assumed that this also applies for stresses, this is in agreement to the literature (Forest Products Laboratory, 1981): tips are a discontinuity and create stress concentrations. Furthermore, these results correspond also to the results of numerical simulations carried out by Serrano (1997) for wood.

It is believed that the scatter in the results is mainly caused by the presence and location of defects (e.g. voids in the bondline and longitudinal cracks in the lamination). For example, the results of test

specimen C(Phyll.Pub)-TT-II(fj)-13 showed high strains in the vicinity of one fingertip/root, caused by a defect which probably initiated failure. Also from the results of tests specimen C(Phyll.Pub)-TT-II(fj)-15, it can be seen that a small defect in the outermost bondline caused large strains which probably initiated failure.

The strain plots of test specimen C(Phyll.Pub)-TT-II(fj)-16 and 17 were predominantly symmetric and those test specimens exhibited the highest failure loads of all test specimens tested by ESPI.

5.3.5 Influence of Joints on Tensile Strength and Stiffness

The influence of the joint on the strength was quantified by computing the joint efficiency. This is expressed as a percentage of the strength of an unjointed lamination:

$$\frac{f_{t;j;0}}{f_{t;0}} \cdot 100 \qquad \text{eq.5.6}$$

The influence of the scarf-joint can not be compared directly to that of the finger-joints. The slopes of the joints are almost equal (5.71° versus 6.28°) however, the joint area of the scarf-joint is larger than that of the finger-joint. The joint area of the scarf-joint is computed by:

$$A_{sj} = L_2 \cdot W \qquad \text{eq.5.7}$$

and that of the finger-joint by:

$$A_{fj} = 2 \cdot L_2 \cdot h \cdot \frac{W}{P} \qquad \text{eq.5.8}$$

where:

A_{sj} = joint area of scarf-joint [mm^2]
A_{fj} = joint area of finger-joint [mm^2]
L_2 = slope length [mm]
W = width of lamination [mm]
h = height of lamination [mm]
P = pitch [mm]

(see also appendix E and F)

The ratio A_{sj} / A_{fj} is used to convert the influence of the finger-joint to the influence of a finger-joint containing a joint area equal to that of the scarf-joint by:

$$\frac{A_{sj}}{A_{fj}} \cdot \frac{f_{t;j;0}}{f_{t;0}} \cdot 100 \qquad \text{eq.5.9}$$

The influence of the joint on the modulus of elasticity in tension was also quantified. This influence is expressed as a percentage of the modulus of elasticity in tension of an unjointed lamination:

$$\frac{E_{t;j;0}}{E_{t;0}} \cdot 100 \qquad \text{eq.5.10}$$

where:

$E_{t;j;0}$ = stiffness of the jointed area (denoted E_b) [N/mm^2]

The results are represented by Table 5.4 and Table 5.5.

Table 5.4: Influence of scarf-joint on strength and stiffness

Test series		B(PhyII.Pub)-TT-II(sj)
Influence of the joint on the tensile strength	**[%]**	93.1
Influence of the joint on the modulus of elasticity in tension	**[%]**	83.9

Table 5.5: Influence of finger-joint on strength and stiffness

Test series		A(PhyII.Pub)-TT-II(fj)	C(PhyII.Pub)-TT-II(fj)
Influence of the joint on the tensile strength	**[%]**	40.6 (62.9)	42.2 (65.4)
Influence of the joint on the modulus of elasticity in tension	**[%]**	96.4	71.3

Note: the value in parenthesis refers to the influence of the finger-joint converted to the influence of a finger-joint containing a joint area equal to that of the scarf-joint

The influence of the finger-joint on the tensile strength was dramatic in contrast with the scarf-joint that turned out to be very efficient. Even when the influence of the finger-joints was converted to the influence of a finger-joint containing a joint area equal to that of the scarf-joint the difference was still significantly. There can be several reasons for the found differences. There are no tips present in scarf-joints and hence no stress-concentrations which may reduce the load-bearing capacity. Furthermore, the finger-jointed laminations exhibited low wood-failure while that of the scarf-jointed laminations was much higher. Using an adequate adhesive for the finger-jointed laminations may lead to better results.

The influence of the joints on the modulus of elasticity in tension was significantly, though not for the finger-jointed laminations of sample A. Based on this it is believed that stress redistributions may take place around joints in laminated beams. However, since this finding is very tentative, this is not taken into account in the prediction of the ultimate load-bearing capacity of the beam discussed in paragraph 9.3.4

5.3.6 Evaluation of Joint Profile

The best way to study the influence of the geometry on the behavior of joints is by numerical models. However, these methods are beyond the scope of this study and therefore it was attempted to evaluate the used profile analytically. In appendix E an analysis is carried out on the load-bearing capacity of the scarf-joint and in appendix F on that of the finger-joint.

The experimental results showed that the scarf-joint with a slope of 1 in 10 (5.71°) was very efficient. 93% of the tensile strength of an unjointed lamination could be transmitted. It is believed that by improving the bond quality, the efficiency might be further improved up to 100%. There is no need to adjust the geometry of the joint profile.

The finger-joint could transmit at least 41% of the tensile strength of an unjointed lamination. This may also be improved by improving the bond quality. However, based on the analysis, the geometry has to

be adjusted also. It was found that by reducing the slope angle to 3.7°, a joint efficiency of 81% could be achieved. Reducing the slope angle may also have a positive effect on the chance of splitting of the bamboo at the finger roots.

5.4 Conclusions

In this part of the research the effect of both scarf- and finger-joints on the tensile strength and stiffness of laminations was studied. To determine the tensile strength of the jointed laminations and the stiffness of the jointed area, tension tests were carried out. Three different samples were involved. The strain distribution over the surface of the finger-joint was determined. An analytical method elaborated in appendix E and F predicted the load-bearing capacity of the joints. The following conclusions can be drawn:

- The behavior of jointed laminations is up to a high extent similar to unjointed laminations. The behavior is also very stochastic and the stress-strain relationship is linear up to failure. The latter can be qualified as very brittle.
- Since all jointed laminations failed at the joint, the capacity of a lamination is directed by that of the joint.
- Joint efficiency (93%) of the scarf-joint is sufficient; small improvements might be possible by improvements of the bond quality. The used adhesive melamine-urea formaldehyde is suitable for scarf-jointing bamboo laminations. However, it can be recommended to study the effect of the variables involved in the bonding process on the performance of the joints. Important variables are the amount of adhesive and the pressure applied.
- Joint efficiency (at least 41%) of the finger-jointed laminations is poor. Improvements can be achieved by adjust the geometry of the joint in combination with the application of a suitable adhesive. Melamine formaldehyde in the used mixing ratio and amount is not suitable for finger-jointing bamboo laminations.
- The analytical method elaborated in appendix E and F is less suitable to predict the load-bearing capacity of joints. It can be recommended to develop a numerical model (FEM[1]) which accounts for the non-linear behavior of the bondline and the occurrence of a non-uniform stress distribution on the moment of failure. Such a model enables to study the effect of geometrical imperfections, presence and location of small defects (voids) in the bondline and differences in stiffness of the two scarf- or finger-joint halves.
- The results obtained by the laser speckle techniques can be used to verify numerical models, both qualitatively and quantitatively.

[1] FEM = Finite Element Method

6 Influence of Nodes on Tensile Strength

6.1 Introduction

Nodes have a negative influence on stiffness and strength. This can be explained by the anatomical structure of a node: a part of the vascular bundles bend away, explained in paragraph 2.2.6. In tension parallel to the grain, the direction of the load does not correspond to that of the grain of the node, and hence the tensile strength is reduced. The tensile strength of culms subjected to tension is directed by the tensile strength of the node since redistribution of stresses does not occur. However, in laminated members, redistribution of stresses may occur due to the fact that the negative influence of nodes might be counteracted by internodes depending on the probability of nodes coinciding in one cross section.

According to the literature, the reduction depends on the botanical species and property. In Table 6.1 the effect of nodes on mechanical properties is quantified for some botanical species. It can be seen that the reduction caused by nodes shows extreme variability. The reduction of nodes reported for *Bumbusa blumeana* by Arce-Villalobos (1993) is extreme. For *Phyllostachys pubescens*, the species used in this research, the reduction caused by nodes is significantly.
To compensate the negative effect caused by nodes in members assembled out of strips Wan Tarmeze (2005: p.195) proposed to glue the strips in such a way that the positions of nodes are uniformly scattered; nodes are compensated by internodes. However, in paragraph 2.2.1 can be found that the internode length increases from the base towards the middle part of the culm and then decreases further upwards. Consequently, the distribution of nodes along the culm height is not uniform. Furthermore, culms are not alike and in practice they are cross-cut to a length regardless of the position of the node. Since strips are randomly assembled into laminations it is not possible to uniformly scatter the nodes; hence it is possible that there is a cross-section where nodes are not counteracted by internodes.
But there is no study reported on the effects of nodes on the tensile strength of laminations randomly assembled out of strips.

Table 6.1: Effect of nodes on mechanical properties

Source	Botanical name	Property	Values	Ratio
[-]	[-]	[-]	[N/mm^2]	[-]
Arce-Villalobos (1993)	*Bumbusa blumeana*	Tension parallel to the grain	Node = 79.9 Internode = 271	0.30
		Modulus of elasticity in tension parallel to the grain	Node = 7453 Internode = 18858	0.40

Note: the ratio is computed by dividing the mechanical property of the node by that of the internode

Source: Arce-Villalobos (1993)

Table 6.1: Effect of nodes on mechanical properties (continuation)

Source [-]	Botanical name [-]	Property [-]	Values [N/mm^2]	Ratio [-]
Ahmad (2000)	*Dendrocalamus strictus*	Tension parallel to the grain	Node = 99.9 Internode = 160	0.62
		Modulus of elasticity in tension parallel to the grain	Node = 16777 Internode = 17422	0.96
		Modulus of rupture	Node = 149 Internode = 153	0.97
		Modulus of elasticity in bending	Node = 9685 Internode = 10434	0.93
Nugroho (2000)	*Phyllostachys pubescens*	Compression parallel to the grain	Node = 43.8 Internode = 49.2	0.89
		Tension parallel to the grain	Node = 123.6 Internode = 141.2	0.88
		Modulus of rupture	Node = 102.9 Internode = 116.7	0.88
		Modulus of elasticity in bending	Node = 10500 Internode = 11210	0.94

Note: the ratio is computed by dividing the mechanical property of the node by that of the internode

Source: Ahmad (2000); Nugroho (2000)

The purpose of this part of the research reported here is to study the effect of nodes on the tensile strength of laminations. Paragraph 6.2.1 gives attention to the used materials. The used laminations and test specimen are described. Paragraph 6.2.2 discusses the experimental test methods. Paragraph 6.3 outlines the results after which they are discussed in combination with analytical and numerical analyses. Finally, paragraph 6.4 summarizes the conclusions.

6.2 Experimental

6.2.1 Materials

Laminations

To study the influence of nodes on the tensile strength, single-layer laminations of batch C were used, described in paragraph 4.2.1. The laminations are assembled out of four strips side by side, shown in Figure 6.1.

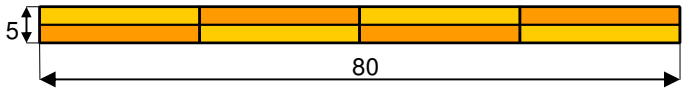

Note: dark color: outer part culm wall; light color: inner part culm wall

Figure 6.1: Composition single-layer laminations

Test Specimens: Tension Test on Single-Layer Laminations, Tension Test on Strips and Tension Test on Single-Layer Laminations in Combination with ESPI Measurements

Dimensions of the test specimens, used to determine the tensile strength and modulus of elasticity in tension of single-layer laminations, were the same as those used for testing the tensile strength and modulus of elasticity in tension of triple-layer laminations, described in paragraph 4.2.1, except for their thickness that was 5 mm.

To determine the tensile strength of nodes and modulus of elasticity in tension of nodes and internodes, strips were sawn out of single-layer laminations with a width varying from 9-19 mm. The cross-section was not reduced.

Test specimens used for the tension test in combination with ESPI measurements were sawn out of single-layer laminations with a width of 60 mm and the cross-section was not reduced. Table 6.2 provides an overview of the number of test specimens and their denomination.

Table 6.2: Number of specimens and their denomination

Test	Sample	Specimen code	Number
Tension test on single-layer laminations	C	C(Phyll.Pub)-TT-V-01 to 17	17
Tension test on strips	C	C(Phyll.Pub)-TT-IV-01 to 24	24
Tension test on single-layer laminations in combination with ESPI-measurements	C	C(Phyll.Pub)-TT-III-01 to 07	7

6.2.2 Method

Tension Test on Single-Layer Laminations and Tension Test on Strips

The tension test on single-layer laminations was carried out according to that on triple-layer laminations, described in paragraph 4.2.2. A constant cross-head movement of 1.5 mm/min was used.

The tension test on strips was carried out by a universal testing machine Schenck (100 kN). A constant cross-head movement of 1.5 mm/min was used. The charge of the test specimens was electrically acquired through the load cell installed between the test specimens and the cross-head. The test setup is shown in Figure 6.2.

Figure 6.2: Test setup of tension test on strips

The tensile strength of the node is computed by:

$$f_{t;n;0} = \frac{F_{max}}{A} \qquad \text{eq.6.1}$$

where

$f_{t;n;0}$ = tensile strength of node [N/mm^2]

Most of the strips failed at the node, the ones that failed within the supporting area were excluded from the determination of the tensile strength. To determine the modulus of elasticity in tension of the node, two strain gauges of 20 mm for each test specimen were used, applied on the front and back side of the wide faces. The deformation of the internode was measured by an extensiometer measuring over a length of 50 mm. The positioning of strain gauges and the extensiometer is shown in Figure 6.3.

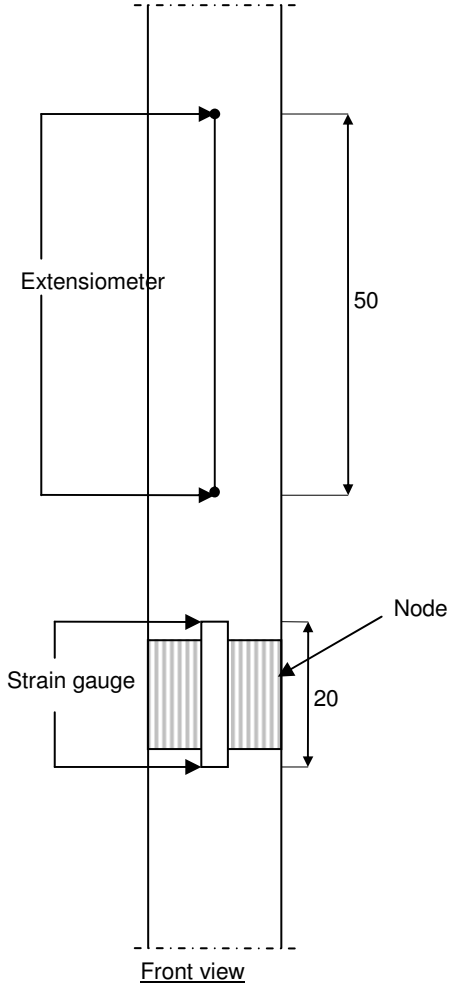

Note: dimensions in mm

Figure 6.3: Positioning of extensiometer and strain gauges

The modulus of elasticity in tension of the node is computed by:

$$E_{t;n;0} = \frac{F_2 - F_1}{A \cdot (\varepsilon_2 - \varepsilon_1)} \qquad \text{eq.6.2}$$

where:

$E_{t;n;0}$ = modulus of elasticity in tension parallel to the grain of the node [N/mm^2]

$\varepsilon_2 - \varepsilon_1$ = increment of strain corresponding to $F_2 - F_1$ [-]

The modulus of elasticity in tension of the internode is computed by:

$$E_{t;i;0} = \frac{l_1 \cdot (F_2 - F_1)}{A \cdot (w_2 - w_{1)}} \qquad \text{eq.6.3}$$

where:

$E_{t;i;0}$ = modulus of elasticity in tension parallel to the grain of the internode [N/mm^2]

The increment of loading was computed on the straight portion of the stress-strain or load deformation curve, mostly between 10% and 40% of the maximum load. The extensiometer was taken away before failure to prevent damage. One test specimen was used to verify whether there were significant differences between the results obtained by the extensiometer and the strain gauges. This was accomplished by measuring the deformation over the internode by both the extensiometer and strain gauges, shown in Figure 6.4, so the results were comparable.

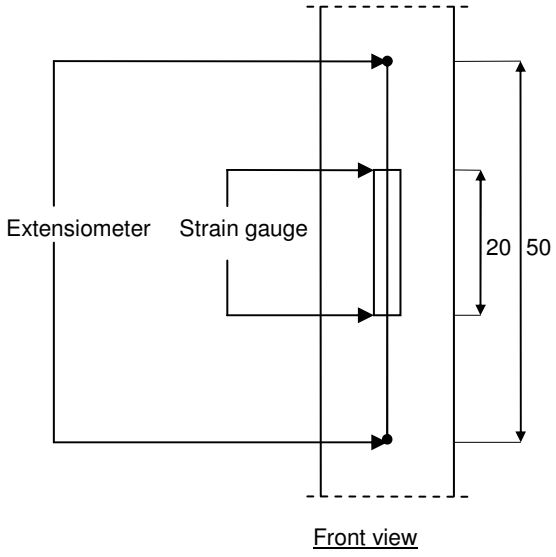

Note: dimensions in mm

Figure 6.4: Positioning of extensiometer and strain gauges during verification measurement

All test specimens were conditioned in a conditioning chamber (temperature = 20°C and relative humidity = 65%) before they were tested.

Tension Test on Single-Layer Laminations in Combination with ESPI Measurements

Deformation over the surface of the single-layer laminations was measured by ESPI. The working of this system is explained in paragraph 5.2.2. The test specimen was loaded in tension by a universal testing machine Schenck (100 kN). The front surface was illuminated over its full width and a height of approximately 50 mm and contained various configurations of nodes. The test setup is shown in Figure 6.5.

Figure 6.5: Test setup of tension test on single-layer laminations in combination with ESPI measurements

All test specimens were conditioned in a conditioning chamber (temperature = 20°C and relative humidity = 65%) before they were tested.

6.3 Results and Discussion

6.3.1 Properties of Nodes and Internodes Loaded in Tension

The experimental results of the strips (series C(Phyll.Pub)-TT-IV)) are represented by Table 6.3. The individual results of each test specimen can be found in appendix H (H.3.1).

Table 6.3: Experimental results: properties of nodes and internodes loaded in tension

Test series		**C(Phyll.Pub)-TT-IV**
Tensile strength parallel to the grain of the node ($f_{t;n;0}$)		
Useful samples	**[-]**	22
Mean	**[N/mm^2]**	79
Standard deviation	**[N/mm^2]**	16 (20.2%)
Modulus of elasticity in tension parallel to the grain of the node ($E_{t;n;0}$)		
Useful samples	**[-]**	6
Mean	**[N/mm^2]**	9199
Standard deviation	**[N/mm^2]**	1716 (18.7%)
Modulus of elasticity in tension parallel to the grain of the internode ($E_{t;i;0}$)		
Useful samples	**[-]**	7
Mean	**[N/mm^2]**	7365
Standard deviation	**[N/mm^2]**	1217 (16.5%)

Note: the value in parenthesis refers to the coefficient of variation

It was found that the modulus of elasticity in tension of the node is higher than that of the internode. This does not agree to the literature. Nugroho (2000) reported a value of 10500 N/mm^2 for the modulus of elasticity in bending of the node and 11210 N/mm^2 for the internode. When it is assumed that the modulus of elasticity in bending is comparable to that in tension, than the first value is in the same order of magnitude to the value of 9199 N/mm^2 found in this research. However, the modulus of elasticity in tension of the internodes does not correspond to the value of 7365 N/mm^2 found in this research. This discrepancy is not caused by the test method. There were no significant differences between the results obtained by the extensiometer and the strain gauges; deviation was less than 3%. Since the sample size was not sufficient to recognize the tendency, no hard statements can be made. Furthermore, the modulus of elasticity in tension of the internode (7365 N/mm^2) does not correspond to that of the single-layer laminations (10135 N/mm^2) measured over a length of 200 mm (a comparison is made with single-layer laminations since the node test specimens were sawn out of the same raw material). This value can be seen as a mean modulus of elasticity taken into account the influence of nodes. The modulus of elasticity in tension of the internode has to be at least equal to this value. Based on these figures the ratio $E_{t;n;0}$ / $E_{t;i;0}$ is taken as at most 0.91.

6.3.2 Stress-Strain Behavior

The stress strain behavior of a strip loaded in tension corresponded to that of a triple-layer lamination loaded in tension discussed in paragraph 4.3.2.

6.3.3 Strain Distribution over Single-Layer Lamination Measured by ESPI

The individual results of each test specimen (series C(Phyll.Pub)-TT-III)) can be found in appendix H (H.3.3). The results for the x-direction are left out of consideration. The ESPI results showed that local, high strain concentrations developed at the location of nodes. Up to a load level of approximately at most 70% (coefficient of variation = 19%) of the maximum load, the sections where nodes are located remain plane. It seems that, above this load level, nodes start to fail and initiate failure of the total lamination.

6.3.4 Analytical Prediction of Node Failure

The experimental results of the single-layer laminations (series C(Phyll.Pub)-TT-V)) are represented by Table 6.4, along with the results of the triple-layer laminations represented by table 4.3 and the results of the strips reported in paragraph 6.3.1. The individual results of each single-layer test specimen can be found in appendix H (H.3.2).

Table 6.4: Experimental results: tensile strength parallel to the grain of strips (nodes), single-layer laminations, and triple layer-laminations

Test series		Strips (node) C(Phyll.Pub)-TT-IV	Single-layer laminations C(Phyll.Pub)-TT-V	Triple-layer laminations C(Phyll.Pub)-TT-I
$f_{t;n;0}$ / $f_{t;0}$				
Useful samples	[-]	22	10	8
Mean	[N/mm^2]	79	93	91
Standard deviation	[N/mm^2]	16 (20.2%)	19 (20.1%)	6 (7.0%)

Note: the value in parenthesis refers to the coefficient of variation

Failure of single-layer laminations and triple-layer-laminations is mostly initiated by a node. However, the tensile strength of laminations is higher than that of the strips. This phenomenon was studied analytically. The following assumptions are made:

- The section remains plane.
- The node and internode behave linear elastic.

These assumptions are not in agreement to the local behavior of nodes measured by ESPI. However, for an analytical understanding these are suitable.

A lamination subjected to tension under clamped conditions, shown in Figure 6.6, is considered. Section A-A consists partly out of a node and an internode. Due to the fact that the test is performed under clamped conditions, no bending moment occurs and hence no additional stresses, see also paragraph 4.2.2.

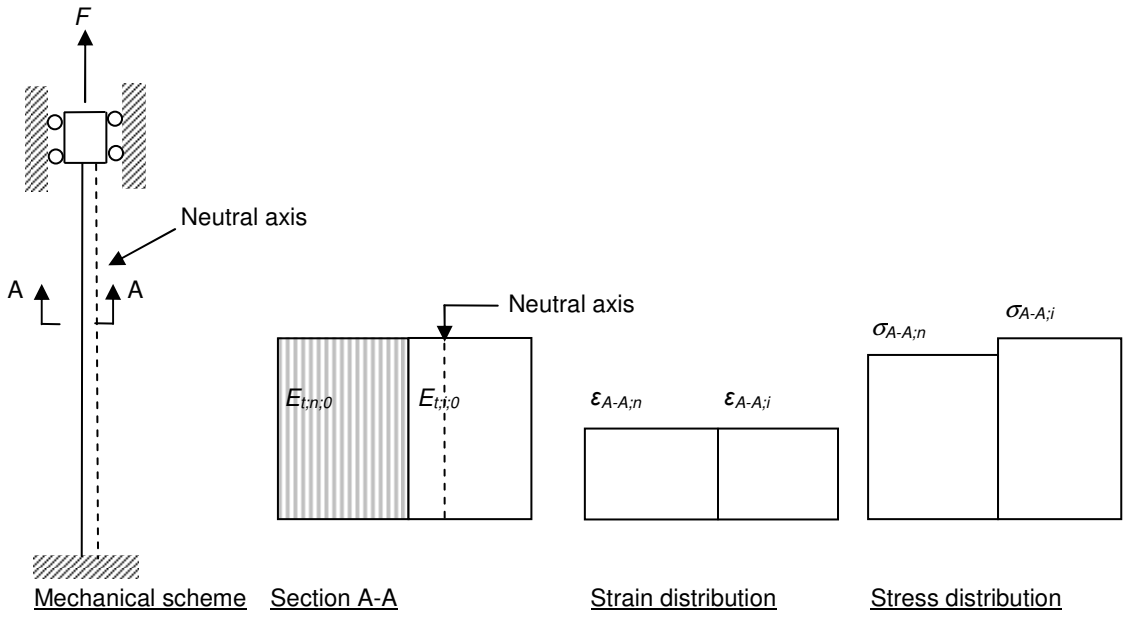

Figure 6.6: Lamination loaded in tension performed under clamped conditions

The strain in section A-A can be computed by:

$$\varepsilon_{A-A;n} = \varepsilon_{A-A;i} = \varepsilon_{A-A} = \frac{F}{A_n \cdot E_{t;n;0} + A_i \cdot E_{t;i;0}} \qquad \text{eq.6.4}$$

where:

$\varepsilon_{A\text{-}A;n}$ = strain in node in section A-A [-]
$\varepsilon_{A\text{-}A;i}$ = strain in internode in section A-A [-]
$\varepsilon_{A\text{-}A}$ = strain in section A-A [-]
F = load [N]
A_n = area of nodes in section A-A [mm^2]
A_i = area of internodes in section A-A [mm^2]

The stress in the nodes can be computed by:

$$\sigma_{A-A;n} = E_{t;n;0} \cdot \varepsilon_{A-A} \qquad \text{eq.6.5}$$

and in the internodes by:

$$\sigma_{A-A;i} = E_{t;i;0} \cdot \varepsilon_{A-A} \qquad \text{eq.6.6}$$

where:

$\sigma_{A\text{-}A;n}$ = stress in node [N/mm^2]
$\sigma_{A\text{-}A;i}$ = stress in internode [N/mm^2]

The ratio $E_{t;n;0}/\ E_{t;i;0} = 0.91$; the ratio $f_{t;n;0}/\ f_{t;i;0} = 0.88$, according to Nugroho (2000). Hence:

$$\frac{\sigma_{A-A;n}}{\sigma_{A-A;i}} = \frac{E_{t;n;0} \cdot \varepsilon_{A-A}}{E_{t;i;0} \cdot \varepsilon_{A-A}} = 0.91 \qquad \text{eq.6.7}$$

The ultimate stress in the nodes is reached before the ultimate stress in the internodes is reached:

$$\sigma_{A-A;n} = f_{t;n;0} = 0.88 \cdot f_{t;i;0} \qquad \text{eq.6.8}$$

$$\sigma_{A-A;i} = \frac{\sigma_{A-A;n}}{0.91} = \frac{0.88 \cdot f_{t;i;0}}{0.91} = 0.97 \cdot f_{t;i;0} \qquad \text{eq.6.9}$$

where:

$f_{t;i;0}$ = tensile strength of the internode [N/mm^2]

The stress distribution over nodes and internodes at the time just before failure of nodes is shown in Figure 6.7

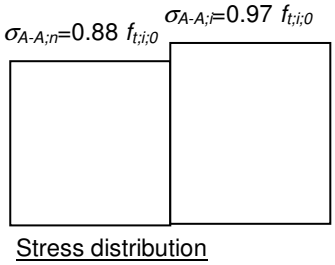

Figure 6.7: Stress distribution over nodes and internodes just before failure

After failure of the nodes, the force which is transferred can increase depending on the ratio A_i / A_n, by redistribution of stresses; stresses in internodes can increase. The force which is transferred at the time of failure of the nodes can be computed by:

$$F_n = \sigma_{A-A;n} \cdot A_n + \sigma_{A-A;i} \cdot A_i \qquad \text{eq.6.10}$$

After failure of the nodes at least the same force has to be transferred:

$$F_n = \sigma_{A-A;i} \cdot A_i \qquad \text{eq.6.11}$$

The area of the internodes can be substituted by the area of the nodes:

$$\frac{A_i}{A_n} = n \Rightarrow A_i = n \cdot A_n \qquad \text{eq.6.12}$$

where:

n = ratio A_i / A_n [-]

The force which can be transferred, when failure is initiated by the nodes and stresses are not able to redistribute, is:

$$F_n = 0.88 \cdot f_{t;i;0} \cdot A_n + 0.97 \cdot f_{t;i;0} \cdot n \cdot A_n \qquad \text{eq.6.13}$$

When it is possible, after the nodes have failed, for stresses to redistribute the force which can be transferred is:

$$F_i = f_{t;i;0} \cdot n \cdot A_n \qquad \text{eq.6.14}$$

Whether redistribution occurs depends on the ratio A_i / A_n:

$$F_n = F_i = 0.88 \cdot f_{t;i;0} \cdot A_n + 0.97 \cdot f_{t;i;0} \cdot n \cdot A_n = f_{t;i;0} \cdot n \cdot A_n \Rightarrow n = 29 \qquad \text{eq.6.15}$$

Thus when $n \leq 29$ the force which can be transferred is F_n (failure is initiated by a node); when $n > 29$ the force which can be transferred is F_i (failure does not have to be initiated by a node). The tensile strength of laminations assembled out of strips is mostly higher than that of the strips. Based on the results obtained by the tension test this is computed by:

$$f_{t;0} = \frac{F_{\max}}{A} \qquad \text{eq.6.16}$$

The cross-sectional area can be computed by:

$$A = A_n + A_i = A_n + n \cdot A_n = A_n \cdot (1 + n) \qquad \text{eq.6.17}$$

The single- and triple-layer laminations used in this research consist out of two and four strips in the gauge section, respectively. In case of the single-layer laminations, n is at most 1 and in case of the triple-layer laminations, n is at most 3. This means (theoretically) that failure, for both types of laminations, is always initiated by a node, which corresponds to the observations. For example, in case of single-layer laminations, the tensile strength is computed by:

$$f_{t;0} = \frac{F_n}{A} = \frac{0.88 \cdot f_{t;i;0} \cdot A_n + 0.97 \cdot f_{t;i;0} \cdot n \cdot A_n}{A_n \cdot (1+n)} = \frac{0.88 \cdot \frac{79}{0.88} \cdot 1 + 0.97 \cdot \frac{79}{0.88} \cdot 1 \cdot 1}{1 \cdot (1+1)} = 83 \qquad \text{eq.6.18}$$

and in the case of triple-layer laminations:

$$f_{t;0} = \frac{F_n}{A} = \frac{0.88 \cdot f_{t;i;0} \cdot A_n + 0.97 \cdot f_{t;i;0} \cdot n \cdot A_n}{A_n \cdot (1+n)} = \frac{0.88 \cdot \frac{79}{0.88} \cdot 1 + 0.97 \cdot \frac{79}{0.88} \cdot 3 \cdot 1}{1 \cdot (1+3)} = 85 \qquad \text{eq.6.19}$$

It can be seen that the measured tensile strength is higher than that of the nodes (79 N/mm^2). Differences with the experimental values are among other things caused by the ratio $f_{t;n;0}$ / $f_{t;i;0}$ (= 0.88) which is assumed.

When n (> 29) approaches to infinity, the measured tensile strength approaches to the tensile strength of the internodes:

$$\lim_{n\to\infty} f_{t;0}(n) = \lim_{n\to\infty} \frac{f_{t;i;0} \cdot n \cdot A_n}{A_n \cdot (1+n)} = f_{t;i;0} \qquad \text{eq.6.20}$$

Hence, the measured tensile strength varies between $f_{t;n;0}$ for n = 0 and $f_{t;i;0}$ for n = infinity. It is believed that the scatter in the results is, among other things, caused by n. This parameter can be seen as a stochastic variable and depends on the number of strips which is assembled into a lamination.

6.3.5 Probability of Nodes Coinciding

Based on the ratio A_i / A_n, the percentage of nodes coinciding expressed in relation to the total cross-section can be computed by:

$$k = \frac{A_n}{A} \cdot 100 = \frac{A_n}{A_n \cdot (1+n)} \cdot 100 \qquad \text{eq.6.21}$$

where:

k = percentage of nodes coinciding related to the total cross-section [-]

For the found value of n = 29, follows k = 3.3%. By the analysis carried out in appendix G, the probability of *at least* a certain percentage of nodes coinciding within a certain area, expressed in relation to the total cross-section, within *at least* one section, is computed depending on the total number of strips. It appears that this probability is 1.0 for $k \geq 3.3\%$ and a total number of strips of at least 12. This means that failure is always initiated by a node. Furthermore, it was found that the probability is affected by size, though not for $k \geq 3.3\%$ up to a maximum number of 400 strips.

6.4 Conclusions

In this part of the research, the influence of nodes on the tensile strength of laminations was studied. The properties of nodes and internodes were determined by tension tests on strips. The tensile strength of nodes was compared to that of single- and triple-layer laminations. The strain distribution over the surface of single-layer laminations was determined in order to study the behavior of nodes at the moment of failure. An analytical analysis was carried out on the conditions that lead to failure initiated by nodes. Numerical simulations in order to predict the probability of failure initiated by nodes were elaborated in appendix G. The following conclusions can be drawn:

- The modulus of elasticity in tension parallel to the grain of the node is lower than that of the internode. The ratio $E_{t;n;0}$ / $E_{t;i;0}$ is at most 0.91.
- Above a load level of at most 70% of the maximum load, high strain concentrations develop at the locations of nodes. It is believed that above this load level, nodes start to fail and initiate failure of the total lamination.

- It is shown based on an analytical analysis in combination with numerical simulations that a node always initiates failure of single- and triple-layer laminations loaded in tension, used in this research.

7 Laminated Bamboo Loaded in Compression

7.1 Introduction

Since bending is a combination of tension and compression, the behavior of laminated bamboo loaded in compression is also important. Since it is believed that the joints in the compression zone have little or no effect on the strength of the beam only the compressive strength is studied and the influence of joints on the compressive strength is left out of consideration.

Comprehensive information exists on the compression behavior of bamboo culms (Janssen, 1981; Arce-Villalobos, 1993). However, this experimental data is not representative for laminated bamboo and no information is available on the properties of laminated bamboo loaded in compression.

The purpose of this part of the research reported here is to study the behavior of laminated bamboo loaded in compression and to determine the compressive strength and modulus of elasticity in compression. Paragraph 7.2.1 gives attention to the used materials. The used laminations, adhesives and test specimens are described. Paragraph 7.2.2 discusses the experimental test methods. Paragraph 7.3 outlines the results after which they are discussed. Finally, paragraph 7.4 summarizes the conclusions.

7.2 Experimental

7.2.1 Materials

Laminations

To study the compressive strength and modulus of elasticity in compression, triple-layer laminations of batch B were used, described in paragraph 4.2.1.

Adhesives Used for Bonded Joints: Melamine-Urea-Formaldehyde

For the adhesion of laminations, melamine-urea formaldehyde was selected owing to the positive test results described in paragraph 8.3. More information on this adhesive can also be found in paragraph 8.2.1.

The mixing ratio adhesive – hardener was 100:30 by weight. To bond the laminations with their wide faces to each other, a glue spread of about 500 g/m^2 was applied manually (by a brush) single-sided. This amount was recommended for hardwood by the manufacturer of the adhesive.

Test Specimens: Compression Test on Laminated Test Specimens

Test specimens were based on those used for wood according to EN 408 (European Committee for Standardization, 1995a) and were sawn out of laminated pieces. These pieces were obtained by bonding 11 triple-layer laminations on top of each other, in a steel clamping system, described in

paragraph 9.2.1. A pressure of approximately 1.0 N/mm^2 was applied by three hydraulic jacks. The laminated pieces were finished by planing the wide faces to remove the adhesive that had squeezed out between adjacent laminations.

The test specimens had a length to width ratio (slenderness) of six. The end surfaces were accurately prepared to ensure that they were plane to one another and perpendicular to the axis of the test specimen. The geometry of the test specimens is shown in Figure 7.1.

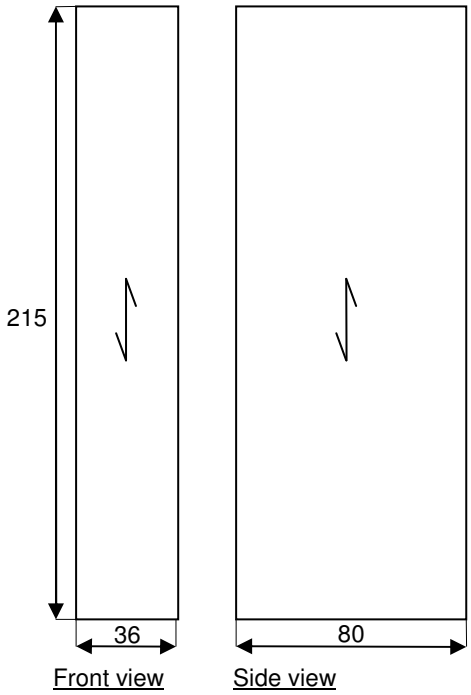

Note: dimensions in mm

Figure 7.1: Geometry compression test specimen

Table 7.1 provides an overview of the number of test specimens and their denomination.

Table 7.1: Number of test specimens and their denomination

Test	Sample	Specimen code	Number
Compression test on laminated test specimens	B	B(Phyll.Pub)-CT-Preliminary Test-01 and 02 B(Phyll.Pub)-CT-01 to 06	8

Furthermore, two test specimens were prepared to investigate the influence of the slenderness ratio on the compressive strength (B(Phyll.Pub)-CT-Additional Test-01 and 02). These test specimens had a length of 140 mm.

Test Specimens: Moisture Content and Density

Moisture content and density were determined by using one test piece taken from each compression test specimen. These were based on ISO 22157-1:2004 (International Standard Organization, 2004). The test pieces were approximately 25 mm in thickness, 36 mm in width and 80 mm in height.

7.2.2 Method

Compression Test on Laminated Test Specimens

The compression test was carried out in accordance with EN 408 (European Committee for Standardization, 1995a). The test specimen was concentrically loaded by a universal testing machine Schenck (250 kN). The upper plate of the testing machine was hinged, so a compressive load was applied without inducing bending. No special measures were taken to avoid friction between the test specimen and the loading plates. The charge of the test specimens was electrically acquired through the load cell installed between the test specimens and the cross-head. A constant cross-head movement of 1.5 mm/min was used. The test setup is shown in Figure 7.2 (left).

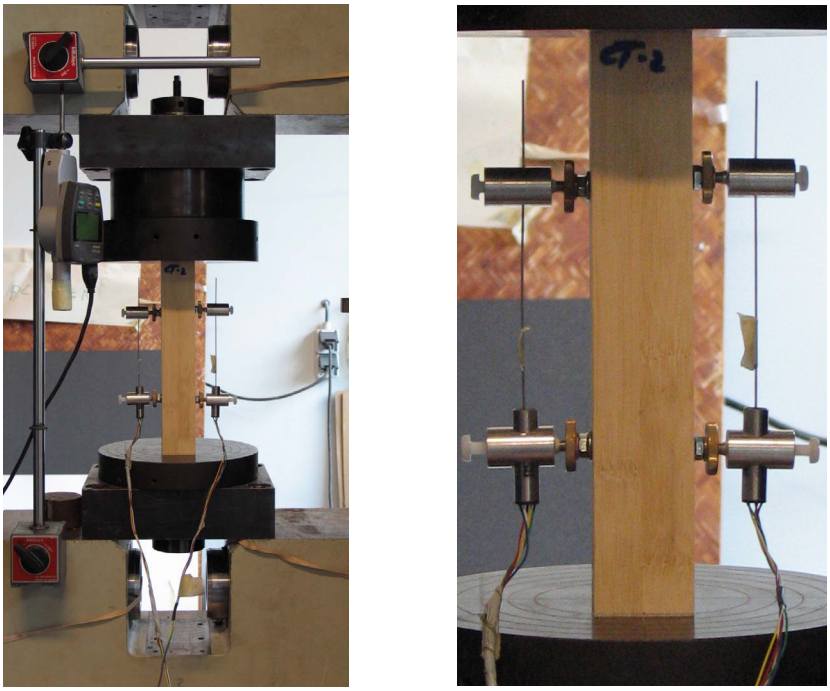

Figure 7.2: Left: test setup of compression test on laminated test specimens; right: positioning of LVDT-transducers

The compressive strength is computed by:

$$f_{c;0} = \frac{F_{max}}{A} \qquad \text{eq.7.1}$$

where:

$f_{c;0}$ = compressive strength parallel to the grain [N/mm^2]

Deformation was measured by two LVDT-transducers applied on the wide faces of the test specimens over a length of 100 mm. The modulus of elasticity in compression is computed by:

$$E_{c;0} = \frac{l_1 \cdot (F_2 - F_1)}{A \cdot (w_2 - w_1)} \qquad \text{eq.7.2}$$

where:

$E_{c,0}$ = modulus of elasticity in compression parallel to the grain [N/mm^2]

The increment of loading was computed between 10% and 40% of the maximum load. The positioning of the two LVDT-transducers is shown in Figure 7.2 (right). All test specimens were conditioned in a conditioning chamber (temperature = 20°C and relative humidity = 65%) before they were tested.

Moisture Content and Density

Moisture content and density were determined according to ISO 22157-1:2004 (International Standard Organization, 2004), described in paragraph 4.2.2.

7.3 Results and Discussion

7.3.1 Properties of Laminated Bamboo Loaded in Compression

The experimental results are represented by Table 7.2. The individual results of each test specimen can be found in appendix H (H.4.1).

Table 7.2: Experimental results: properties of laminated bamboo loaded in compression

Test series		**B(Phyll.Pub)-CT**
Compressive strength parallel to the grain ($f_{c;0}$)		
Sample size	**[-]**	8
Mean	**[N/mm^2]**	48
Standard deviation	**[N/mm^2]**	1 (1.6%)
Modulus of elasticity in compression parallel to the grain ($E_{c;0}$)		
Sample size	**[-]**	6
Mean	**[N/mm^2]**	8305
Standard deviation	**[N/mm^2]**	359 (4.3%)
Moisture content (*MC*)		
Sample size	**[-]**	6
Mean	**[%]**	8.2
Standard deviation	**[%]**	0.2 (2.2%)
Density (ρ_0)		
Sample size	**[-]**	6
Mean	**[kg/m^3]**	611
Standard deviation	**[kg/m^3]**	12 (1.9%)

Note: the value in parenthesis refers to the coefficient of variation

It can be observed that, especially the value of the coefficient of variation for the compressive strength is remarkably small. This might be caused by the “ductile” behavior of laminated bamboo loaded in compression. When failure is brittle, as in the case of laminated bamboo loaded in tension, the coefficient of variation for the tensile strength is higher since the material fails at the weakest link; no redistribution takes place.

The value for the modulus of elasticity in compression (8305 N/mm^2), is a bit lower than the value for the modulus of elasticity in tension (9591 N/mm^2), see Table 4.3. It can be stated that laminated bamboo loaded in compression behaves less stiff than when loaded in tension.

7.3.2 Stress-Strain Behavior

Figure 7.3 shows the stress-strain curve of one of the test specimens. Laminated bamboo loaded in compression behaved proportional up to a certain limit, which may be referred to as the proportional limit. This can be defined as the point where the curve deviates from the straight line; beyond this point, stress is no longer proportional to the strain. The stress corresponding to this point is termed stress at proportional limit, and the corresponding strain as strain at proportional limit. Beyond the proportional limit, strain increases at a faster rate than does the load. The upper limit of the curvilinear region is the ultimate stress (is equal to the compressive strength), which the material can sustain. The corresponding strain is termed the strain at ultimate stress. The post-failure region can also be important in some applications; however, during the experiments this was not determined.

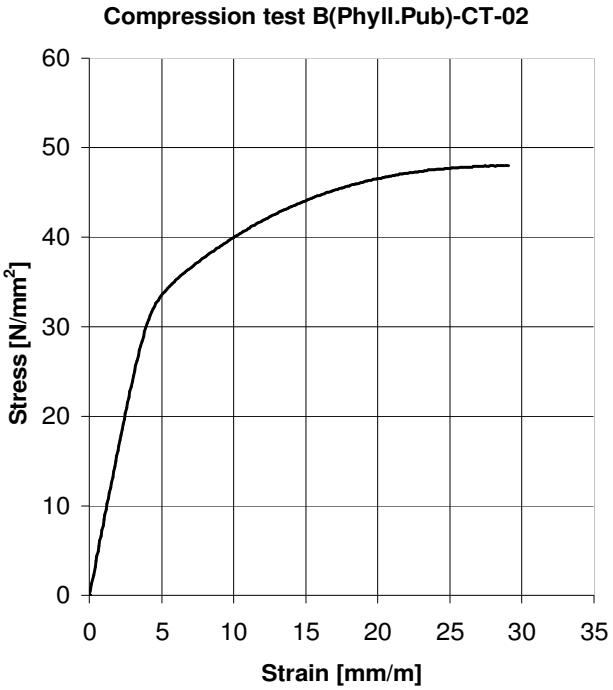

Figure 7.3: Stress-strain curve for a laminated test specimen loaded in compression

7.3.3 Failure Mode

During the experiments, it was observed that all test specimens failed in the same mode: just before reaching the maximum load, buckling was initiated. This is shown in Figure 7.4. No local damage, like wrinkles, was observed at the surfaces, even not at the location of nodes.

Figure 7.4: Failure initiated by buckling

Since the fact that during all tests buckling occurred when the proportional limit was exceeded, this type of buckling is termed inelastic buckling (Gere, 2006). The slenderness ratio is too small for elastic stability (Euler buckling) to govern and too large for strength consideration alone to govern. Because the proportional limit is exceeded, the slope of the stress-strain curve for the material is less than the modulus of elasticity; hence, the critical load for inelastic buckling is always less than the Euler load. This behavior differs from that of wood test specimens with the same slenderness loaded in compression. In these specimens, failure can be initiated in several ways but inelastic buckling is not likely to occur.

It is believed that the maximum load, measured during the experiments, does not resemble the ultimate load, and hence the compressive strength might be underestimated. To investigate this phenomenon, two additional tests were performed with a length of 140 mm. The experimental results are represented by Table 7.3.

Table 7.3: Experimental results: influence length of test specimen on the compressive strength

Length test specimen [mm]	**Slenderness [-]**	**Compressive strength parallel to the grain ($f_{c;0}$) [N/mm^2]**
215	6	48
140	4	50

Though failure of the additional test specimens was also initiated by buckling, the results of the compressive strength were only slightly higher. Since the number of test specimens was small, no hard statement can be made. The conjecture that the compressive strength might be underestimated by the mean value of 48 N/mm^2 cannot be confirmed. Specific research is needed on an adequate test

specimen to determine the compressive strength of laminated bamboo. However, this is beyond the scope of this research.

7.4 Conclusions

In this part of the research, the behavior of laminated bamboo loaded in compression was studied. The compressive strength and modulus of elasticity in compression were determined by compression tests. The following conclusions can be drawn:

- Laminated bamboo loaded in compression behaves less stiff than when loaded in tension.
- Laminated bamboo loaded in compression behaves proportional up to a certain limit, beyond this limit, strain increases at a faster rate than does the load. The behavior can be typified as “ductile”.
- It can be recommended to study the slenderness of the test specimens on the failure behavior in order to find a reliable value for the compressive strength.

8 Bond Quality

8.1 Introduction

In laminated beams, bondlines between laminations are subjected to shear forces. For optimal material use, the shear strength of bonded joints has to be higher than, or at least equal to, the material: the strength of bonded joints is not governing so this can be ignored in structural design. To guarantee this, a suitable adhesive has to be used.

To the author's knowledge the most extensive research carried out on the bonding feasibility of *Phyllostachys pubescens* was by Amino (2002). Two representative indices of the bonding feasibility were studied: the shear strength and the bamboo failure ratio. Additionally, moisture resistance tests were carried out. The test specimens consisted out of single-layer laminations glued together. The shear strength was determined by loading the test specimens until failure by compression loading. Several variables were investigated on the shear strength of the bonded joints namely: the orientation of laminations in relation to each other, the direction of the grain, the density and the type of glue used (phenol-resorcinol formaldehyde and epoxy resin).
It was found that the type of glue used had no remarkable influence on the results, for phenol-resorcinol formaldehyde parallel to the grain a shear strength of 10.5 N/mm^2 was found and for epoxy resin 10.3 N/mm^2 (mean values). Bamboo failure ratio of the test specimens was low; especially for phenol-resorcinol formaldehyde (the bamboo failure ratio rarely exceeded 10%). The influence of moisture variation did not affect the results of specimens bonded by epoxy resin. The other variables mentioned are already discussed in paragraph 3.4.2.
Other researches related to the subject worth mentioning are the study of Li (2004) who determined the contact angle of urea formaldehyde resin on the surface of test specimens of *Phyllostachys pubescens*, the study of Ahmad (2000) who studied the glueability of *Dendrocalamus strictus*, the study of Zaidon et al. (2004) who studied the glueability of *Gigantochloa scortechinii* and the study of Chen et al. (2000) who studied the bonding of *Phyllostachys pubescens* with copolymer resins made of biomass residue extracts with phenol and formaldehyde.
But there is no experience available on the adhesives available for this research in relation to *Phyllostachys pubescens*.

The purpose of this part of the research reported here is to study the bond quality of face joints by using two commercial adhesives commonly used in the manufacturing of glued-laminated timber: melamine-urea-formaldehyde and resorcinol-phenol. Paragraph 8.2.1 gives attention to the used materials. The used laminations, adhesives and test specimen are described. Paragraph 8.2.2 discusses the experimental test methods and the statistical tests used to investigate differences between samples. Paragraph 8.3 outlines the results after which they are discussed. Finally, paragraph 8.4 summarizes the conclusions.

8.2 Experimental

8.2.1 Materials

Laminations

To study the bond quality, single-layer laminations of batch A and triple-layer laminations of batch C were used, described in paragraph 4.2.1.

Adhesives Used for Bonded Joints: Melamine-Urea-Formaldehyde

Melamine-urea-formaldehyde (AKZO NOBEL, Cascomin 1240 with hardener 2540) is a thermosetting adhesive commonly used in the manufacturing of glued-laminated timber. This is an adhesive to be used where there is demand for light-colored bond lines with high water and weather resistance of the bond line. It is used in hardwood plywood, end-jointing and edge-gluing of lumber, and scarf joining softwood plywood.

The mixing ratio adhesive – hardener was 100:30 by weight. For the plywood shear test, a glue spread of about 250 g/m^2 was applied manually two-sided; for the block shear and delamination test, a glue spread of about 500 g/m^2 was applied manually single-sided. This amount was recommended for hardwood by the manufacturer of the adhesive.

Adhesives Used for Bonded Joints: Resorcinol-Phenol

Resorcinol-phenol (AKZO NOBEL, combination 1712 with hardener 2520) is a thermosetting adhesive commonly used in the manufacturing of glued-laminated timber. This is an adhesive to be used where there is demand for weather resistance of the bond line. The color of the bondline is dark red. It is used in laminated timbers and in the assembly of joints that must withstand severe service conditions.

The mixing ratio adhesive – hardener was 100:15 by weight. For the block shear and delamination test a glue spread of about 500 g/m^2 was applied manually single-sided. This amount was recommended for hardwood by the manufacturer of the adhesive.

Test Specimens: Plywood Shear Test

Test specimens were based on a typical plywood shear test according to EN 314-1 (European Committee for Standardization, 2004). Also modified test specimens were used. Plywood shear test specimens were modified by combining two test specimens which resulted in symmetric test specimens. Test specimens were assembled out of single-layer laminations glued on top of each other with their grain parallel to each other. Notches were applied by a precision saw. Pressure was applied by hand-screws: hence, the pressure applied was not quantified. The geometry of the test specimens is shown in Figure 8.1.

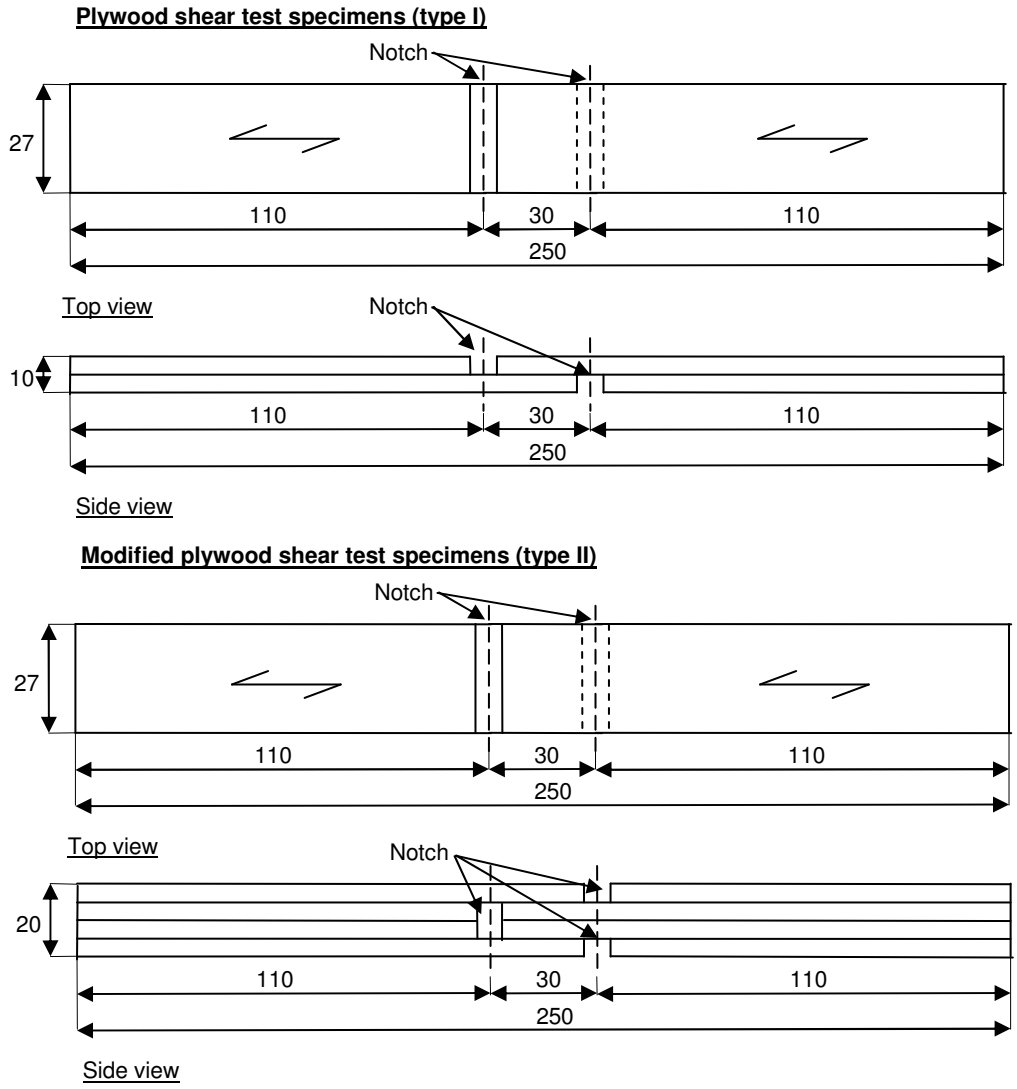

Note: dimensions in mm

Figure 8.1: Geometry test specimens

Table 8.1 provides an overview of the number of test specimens and their denomination.

Table 8.1: Number of test specimens and their denomination

Test	Sample	Adhesive used	Specimen code	Number
Plywood shear test	A	Melamine-urea-formaldehyde	A(PhyII.Pub)-ST-MUF-I-01 to 04	4
Modified plywood shear test	A	Melamine-urea-formaldehyde	A(PhyII.Pub)-ST-MUF-II-01 to 07	7

Test Specimens: Block Shear Test

Test specimens were based on a typical glued-laminated timber block shear test according to EN 392 (European Committee for Standardization, 1995b). Two different types of test specimens were distinguished: test specimens glued with melamine-urea-formaldehyde and test specimens glued with

resorcinol-phenol. For each type, three test bars were assembled out of 14 triple-layer laminations glued on top of each other with their grain parallel to each other. These laminations were bonded together in a steel clamping system. A pressure of 1 N/mm^2 was applied by compression loading. The glued surface was the square of 50 mm. The geometry of the test specimens is shown in Figure 8.2.

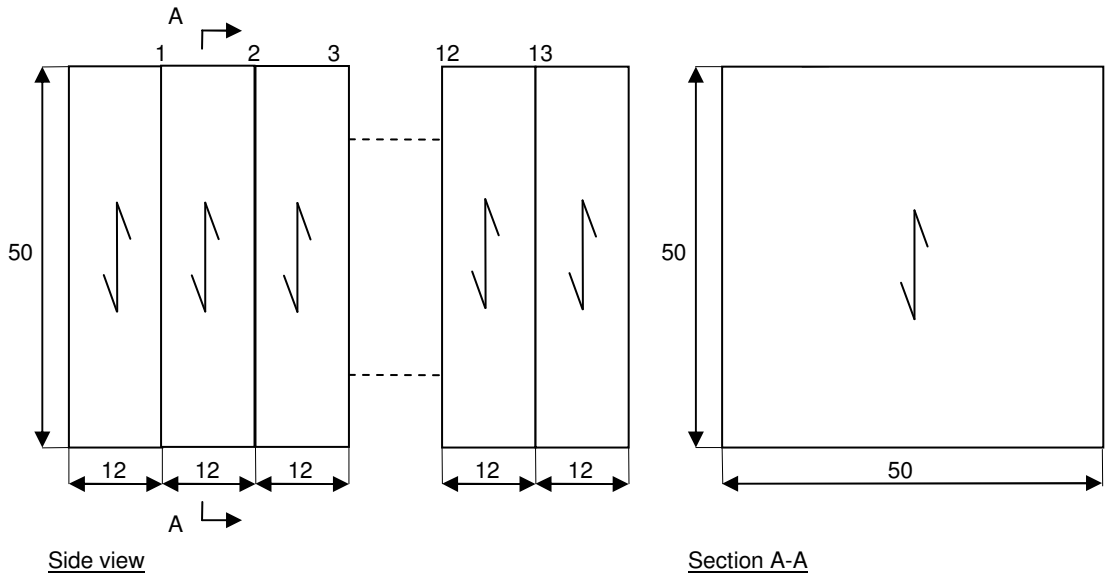

Note: dimensions in mm

Figure 8.2: Geometry block shear test specimens

Table 8.2 provides an overview of the number of test specimens and their denomination.

Table 8.2: Number of test specimens and their denomination

Test	Sample	Adhesive used	Specimen code	Number
Block shear test	C	Melamine-urea-formaldehyde	C(Phyll.Pub)-ST-MUF-01 to 39	39
	C	Resorcinol-phenol	C(Phyll.Pub)-ST-RP-01 to 39	39

Test Specimens: Delamination Test

Test specimens were based on a typical glued-laminated timber delamination test according to prEN 391 (European Committee for Standardization, 2001b). Two different test specimens were distinguished: test specimens glued with melamine-urea-formaldehyde and test specimens glued with resorcinol-phenol. The test specimens were assembled out of 21 single-layer laminations glued on top of each other with their grain parallel to each other. These laminations were bonded together in a steel clamping system. A pressure of 1 N/mm^2 was applied by compression loading. The geometry of the test specimens is shown in Figure 8.3.

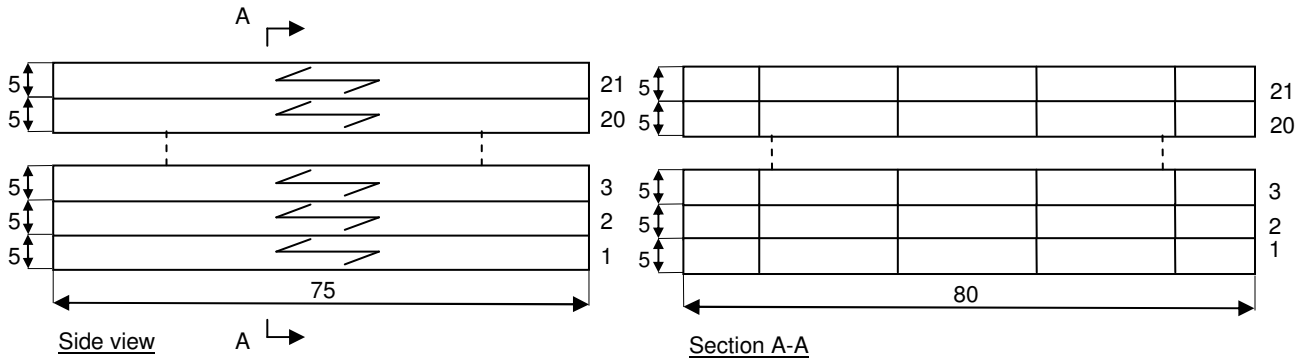

Note: dimensions in mm

Figure 8.3: Geometry delamination test specimens

Table 8.3 provides an overview of the number of test specimens and their denomination.

Table 8.3: Number of test specimens and their denomination

Test	Sample	Adhesive used	Specimen code	Number
Delamination test	C	Melamine-urea-formaldehyde	C(Phyll.Pub)-DT-MUF	1
	C	Resorcinol-phenol	C(Phyll.Pub)-DT-RP	1

8.2.2 Method

All test specimens were conditioned in a conditioning chamber (temperature = 20℃ and relative humidity = 65%) for at least one week before they were tested, resulting in a moisture content of 8.5 – 8.7%.

Pywood Shear Test and Block Shear Test

For the shear tests it was decided to choose a constant cross-head movement of 0.6 mm/min as is prescribed by ISO 22157-1:2004(E) (International Organization for Standardization, 2004) for the shear test. This enabled to compare the experimental values with values given in the literature for pure shear strength since it is believed that the speed of loading affects the results.

Plywood shear test specimens were loaded in tension parallel to the grain until failure by a universal testing machine Schenck (100 kN), shown in Figure 8.5. Block shear test specimens were loaded in compression parallel to the grain until failure, shown in Figure 8.4. In both tests, the charge of the test specimens was electrically obtained trough the load cell installed between the test specimens and the cross-head.

Figure 8.4: Test setup of block shear test

It was assumed that the short length of the bondline assures a uniform stress distribution, which enables to compute the shear strength by:

$$f_v = \frac{F_{max}}{A} \qquad \text{eq.8.1}$$

where

f_v = shear strength [N/mm^2]

A = sheared area [mm^2]

The percentage of bamboo failure was visually determined by use of the written guidelines in Annex A of EN 314-1 (European Committee for Standardization, 2004). This consisted of an area assessment and a determination of the failure surface. The percentage is expressed as a proportion of the damaged surface by the shear test to the entire bond area.

Delamination Test

Before the test, the total length of the glue lines on the end-grain surfaces of the test specimens was measured. The test specimens were submerged in a pressure vessel at a vacuum of 200 kPa for about 15 minutes. Then the vaccum was released and a pressure was applied of 600-700 kPa for about 2 hours. While the test specimens were still completely submerged, this cycle was repeated. Then the test specimens were dried in a climate room at 30 °C for about 4 days.

The cycle described above was repeated one more time which resulted in 2 cycles. After the final drying treatment the total glue line delamination on both end-grain surfaces of the test specimens was measured.

The total delamination percentage of a test specimen is calculated by:

$$100 \cdot \frac{l_{tot;delam}}{l_{tot;glueline}} \qquad \text{eq.8.2}$$

where

$l_{tot;delam}$ = delamination length of all glue lines in the test specimen [mm]

$l_{tot;glueline}$ = entire length of glue lines on the two end-grain surfaces of each test specimen [mm]

The maximum delamination percentage for a single glue line in a test specimen is calculated by:

$$100 \cdot \frac{l_{\max;delam}}{2 \cdot l_{glueline}} \qquad \text{eq.8.3}$$

where

$l_{max;delam}$ = maximum delamination length of one glue line in the test specimen [mm]

$l_{glueline}$ = length of one glue line [mm]

Statistical Test

In order to investigate whether there were significant differences between the shear strength of adhesive joints of test specimens bonded with melamine-urea-formaldehyde and test specimens bonded with resorcinol-phenol, statistical tests were carried out using SPSS 11.5 according to paragraph 4.2.2.

8.3 Results and Discussion

8.3.1 Plywood Shear Test

The experimental results are represented by Table 8.4. The individual results of each test specimen can be found in appendix H (H.5.1).

Table 8.4: Experimental results: shear strength determined by plywood shear tests

Test series		A(PhyII.Pub)-ST-MUF-I	A(PhyII.Pub)-ST-MUF-II
Shear strength (f_v)			
Useful samples	[-]	4	7
Mean	[N/mm^2]	5.6	8.1
Standard deviation	[N/mm^2]	0.2 (3.2%)	0.7 (8.2%)

Note: the value in parenthesis refers to the coefficient of variation

The results obtained by test specimens of type I are in poor agreement to the results of the block shear test presented in paragraph 8.3.2. The tested bond line is subjected to a combination of shear stress and normal (peel) stress perpendicular to the plane of the bond line due to eccentricity of loading. Further, due to the low bending stiffness at the section of the notches the specimen will deform as shown in Figure 8.5. Due to the geometrical non-linear behavior of the specimen normal stresses will magnify. Hence, a very low value for the shear strength was found in this test.

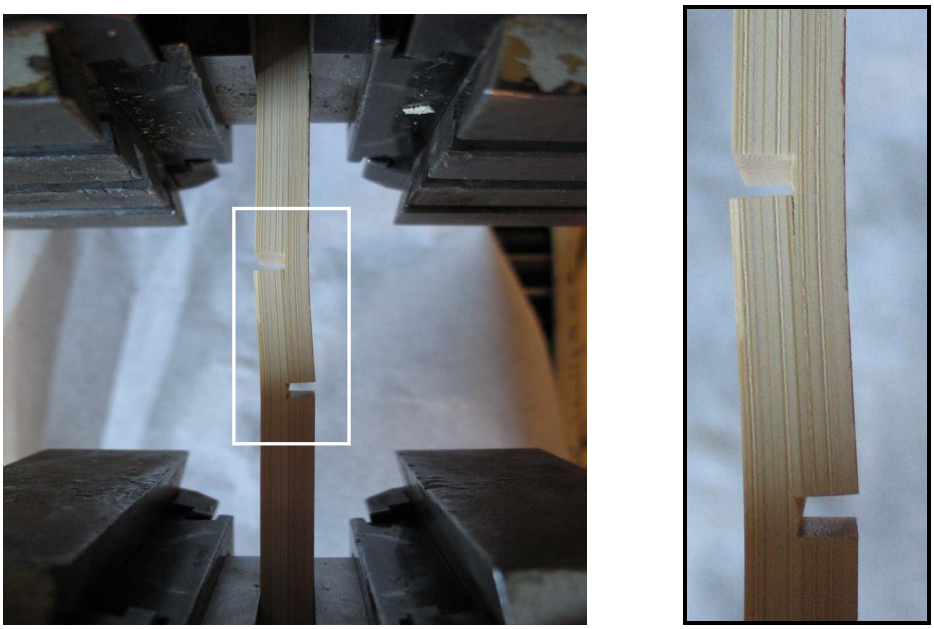

Figure 8.5: Deformed state of test specimen just before failure

The results obtained by the modified test specimens, test specimens of type II, were higher than those obtained by type I. The test specimens were symmetric and the occurrence of normal stresses perpendicular to the plane of the bondline were reduced. However, the shear strength is still lower than that found by the block shear test in paragraph 8.3.2.

It is believed that the occurrence of normal stresses had still a significant influence on the results. Further, the way of gluing the adherends to each other could be of influence. Pressure was applied by handscrews; the recommended pressure of 1.0 N/mm^2 was probably not achieved. Summarized it can be said that it is not recommended to use a plywood shear test specimen or a modified one since the results are not representative for the strength of face joints in laminated beams subjected to shear forces.

8.3.2 Block Shear Test

The experimental results are represented by Table 8.5. The individual results of each test specimen can be found in appendix H (H.5.2). The results of the statistical analysis can be found in appendix H (H.5.3).

Table 8.5: Experimental results: shear strength determined by shear block tests

Test series		**C(Phyll. pub)-ST-MUF**	**C(Phyll. pub)-ST-RP**
Shear strength (f_v)			
Useful samples	[-]	38	36
Mean	[N/mm^2]	13.3	12.4
Standard deviation	[N/mm^2]	1.7 (12.8%)	1.7 (13.3%)

Note: the value in parenthesis refers to the coefficient of variation

The mean shear strength of the test specimens bonded with melamine-urea-formaldehyde was found to be higher than those bonded with resorcinol-phenol. From the results of the independent samples t

test, the difference was found to be significant based on a significance of $\alpha = 0.05$. The null hypothesis was rejected. Furthermore, with 95% confidence, the mean shear strength of adhesive joints bonded with melamine-urea-formaldehyde exceeded the mean shear strength of adhesive joints bonded with resorcinol-phenol by between 0.12 and 1.67 N/mm^2.
The use of the independent samples t test was justified since the two populations were normal distributed according to the normal probability plot. For both populations, the plotted points did not deviated significantly and systematically from the straight line. This followed also from the tests of Kolmogorov-Smirnov and Shapiro-Wilk in which the significance exceeded 0.05.

To determine whether the strength of the adhesive joints exceeds the shear strength of bamboo parallel to the grain a comparison is made with values published in previous research. According to the experimental data found in Janssen (1991: pp. 98-99) the shear strength of *Phyllostachys pubescens* varied from 10.3 N/mm^2 (standard deviation = 0.4 N/mm^2) to 13.5 N/mm^2 (standard deviation = 3.1 N/mm^2) depending on the dimensions of the test specimens (width and height). These values were mean values based on a moisture content of 15.2%, a density of 722 kg/m^3 and 5 tests for each combination of width and height. The specimen used was a so-called stairtype specimen shown in Figure 8.6. The thickness of the specimen was equal to the wallthickness of a bamboo culm.

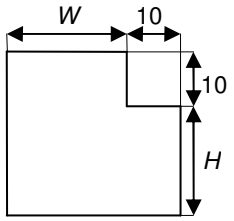

Note: *W* varied from 10-30 mm; *H* varied from 10-40 mm

Figure 8.6: “Stairtype” test specimen for determining the shear strength

For adhesive joints based on both types of adhesives the shear strength is in the same order of magnitude to that of the material. Based on these results it can be stated that the strength of the bonded joints can be ignored in structural design. However, it has to be said that a comparison like this is doubtful. Better is to determine the shear strength of the material also experimentally.

With respect to the performance requirements of glued-laminated timber according prEN 386 (European Committee for Standardization, 2001a) the shear strength of each bondline has to be at least 6.0 N/mm^2. The adhesive joints studied in this research easily meet these requirements.

8.3.3 Bamboo Failure

Besides the shear strength, another important indicator of bond quality is the percentage of bamboo failure. This percentage should be above 90% (for mean values) according to prEN 386 (European Committee for Standardization, 2001a). The combination of high shear strength along with high bamboo failure is a good indicator of the load-carrying capability of the joint. When bamboo failure is low, probably durability might be lacking in the bond.

The experimental results are represented by Figure 8.7. The individual results for each test specimen can be found in appendix H (H.5.2).

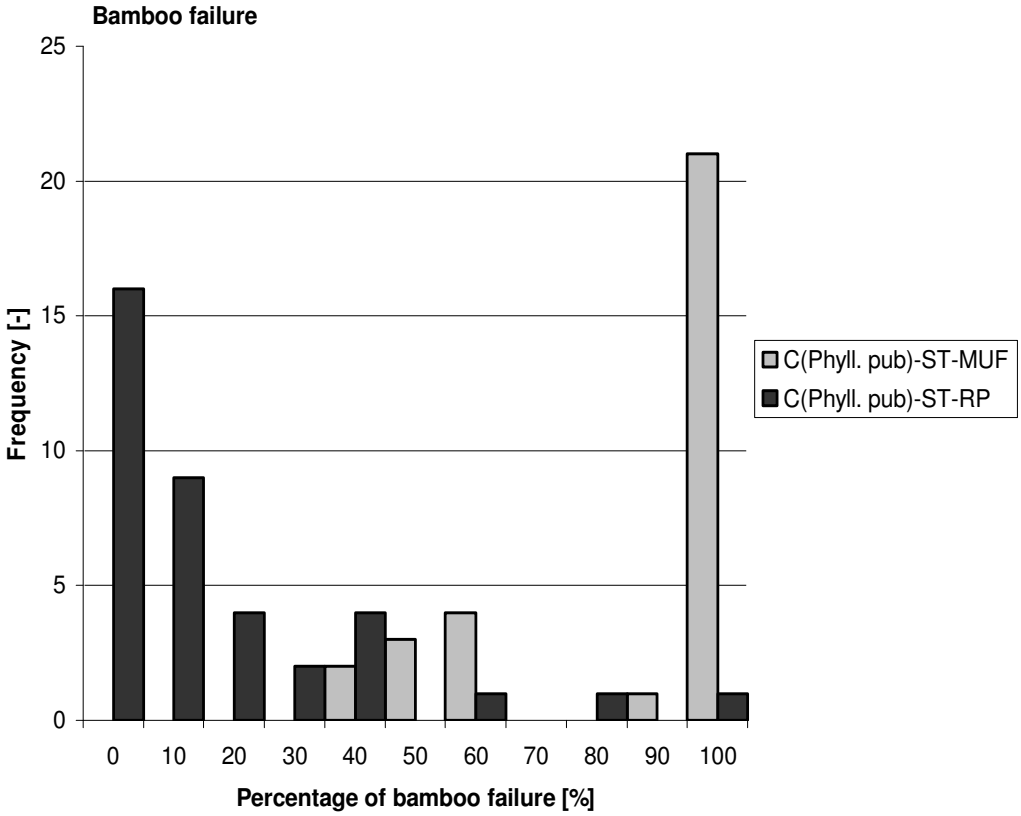

Figure 8.7: Experimental results: bamboo failure

The test specimens bonded with melamine-urea-formaldehyde exhibited high bamboo failure in contrast to those bonded with resorcinol-phenol, shown in Figure 8.8

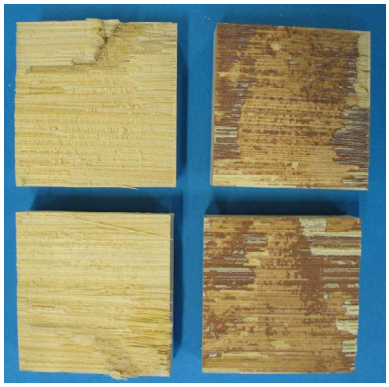

Figure 8.8: Bamboo failure: specimens of type MUF (left); specimens of type RP (right)

This is in accordance with Amino (2002) who found a low bamboo failure for test specimens bonded with phenol-resorcinol formaldehyde. Based on these results resorcinol-phenol is not suitable for bonding laminations of *Phyllostachys pubescens.* Adhesive joints bonded with melamine-urea-formaldehyde satisfy the requirements according to prEN 386 (European Committee for Standardization, 2001a).

8.3.4 Delamination

In addition to shear strength and wood failure, delamination is an indicator of the durability of a structural bond. Delamination can be defined as the separation between laminations (Forest Products Laboratory, 1999). Internal stresses are build up by introducing a gradient in the moisture content. This will result in tensile stresses perpendicular to the bond line. Poor bonding quality will result in delamination. Delamination can occur either in the adhesive or at the interface between adhesive and adherend. This depends on the strength of the adhesive. If the strength of the adhesive is stronger than that of the adherend, then the laminations will fail adjacent to the bondline. The laminations will fail within the bondline when the adhesive is weaker than the adherend. The experimental results are represented by Table 8.6.

Table 8.6: Experimental results: delamination

Test series		**C(Phyll.Pub)-DT-MUF**	**C(Phyll.Pub)-DT-RP**
Total delamination	[%]	0	5.8
Maximum delamination	[%]	0	39.4

Delamination occurred at the test specimen bonded with resorcinol-phenol in contrast to that bonded with melamine-urea-formaldehyde where no delamination occurred (delamination of vertical glue lines is not included). However, since for each type of adhesive only one test specimen was involved, the results are only indicative and cannot be generalized.

According to prEN 386 (European Committee for Standardization, 2001a), the total delamination percentage depends on the method and the number of cycles. The lowest maximum total delamination percentage for 2 cycles is 5%. Furthermore, the maximum delamination percentage shall be less or equal to 40%. Based on this, resorcinol-phenol is not suitable for bonding laminations of *Phyllostachys pubescens*.

8.4 Conclusions

In this part of the research, the bond quality of face joints was studied by plywood shear tests, block shear tests parallel to the grain and delamination tests. The shear strength was determined, the percentage of bamboo failure and the percentage of total and maximum delamination. Two types of adhesives were involved: melamine-urea-formaldehyde and resorcinol-phenol. Regarding the bond quality the following conclusions can be drawn:

- The results of the shear strength determined by a plywood shear test are not representative for the strength of face joints in laminated beams subjected to shear forces.
- The mean shear strength of adhesive joints bonded with melamine-urea-formaldehyde exceeds the mean shear strength of adhesive joints bonded with resorcinol-phenol. The difference is significant on the basis of a significance of $\alpha = 0.05$.
- The strength of bonded joints based on both types of adhesives can be ignored in structural design.

- Bonded joints based on melamine-urea-formaldehyde meet the requirements of glued-laminated timber according to prEN 386 (European Committee for Standardization, 2001a) with respect to the shear strength, bamboo failure and delamination.
- Resorcinol-phenol is not suitable for bonding laminations of *Phyllostachys pubescens* due to the low bamboo failure in combination with the relative high percentage of total delamination and maximum delamination.
- It can be recommended to study the long-term behavior of bonded joints based on melamine-urea-formaldehyde.

9 Bending Behavior of Laminated Bamboo Beams

9.1 Introduction

To develop a reliable model to predict the bending strength of glued-laminated bamboo beams, the behavior of these beams has to be studied in an experimental way with the aim of full-scale tests. It was decided to lengthen the laminations by means of scarf-joints due to the positive test results discussed in paragraph 5.3.5.

Considering the model aimed at, a close relationship with glued-laminated timber is considered with respect to manufacturing aspects and the bending behavior of the beams. The latter is discussed in paragraph 2.5. To the author's knowledge, the only study available on glued-laminated bamboo beams is the one by Wan Tarmeze (2005). This study consists of a numerical analysis and is already discussed in paragraph 2.4.4. However, there is no experimental study reported on the behavior of laminated bamboo beams: full-size structural beams have never been produced and tested.

The purpose of this part of the research reported here, together with the findings in the previous chapters, is to present a model which predicts the bending strength of glued-laminated bamboo beams. Paragraph 9.2.1 gives attention to the used materials. Paragraph 9.2.2 discusses the experimental test methods. Paragraph 9.3 outlines the results after which they are discussed. Finally, paragraph 9.4 summarizes the conclusions.

9.2 Experimental

9.2.1 Materials

Laminations

The laminated beams were assembled out of triple-layer laminations of batch B, described in paragraph 4.2.1.

Adhesives Used for Scarf-Joints and Bonded Joints: Melamine-Urea-Formaldehyde

For the adhesion of laminations, both for scarf and bonded joints, melamine-urea formaldehyde was selected owing to the positive test results described in paragraph 5.3 and 8.3, respectively. More information on this adhesive can also be found in paragraph 8.2.1.

The mixing ratio adhesive – hardener was 100:30 by weight. To lengthen the laminations by means of scarf joints and to bond the laminations with their wide faces to each other, a glue spread of about 500 g/m^2 was applied manually (by a brush) single-sided. This amount was recommended for hardwood by the manufacturer of the adhesive.

Test Specimens: Four-Point Bending Test on Laminated Bamboo Beams

It was decided to produce full-scale beams with a length of approximately 2900 mm long. The depth of the section was about 165 mm: 11 laminations on top of each other, and the width about 70 mm. The geometry of the test specimens is shown in Figure 9.1.

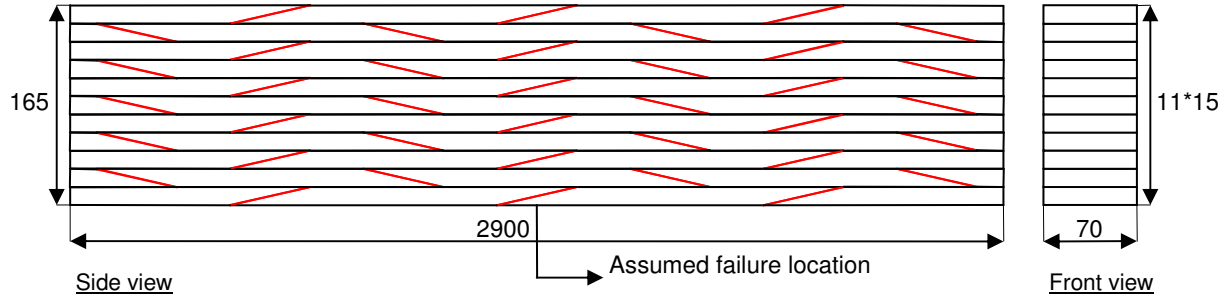

Figure 9.1: Geometry and configuration of joints

The laminated bamboo beams were assumed to fail at the joint in the outermost lamination at the tension side. To realize the most unfavorable and decisive situation, a joint in this lamination was located in the middle were the highest bending stress occured. Furthermore, the joints were configured alternately in relation to each other with respect to their position and their slope, also shown in Figure 9.1.

The beams were made in three steps, shown in Figure 9.2. Firstly, the individual laminations were lengthened by the use of scarf joints. Pressure was applied by hand-screws: hence, the pressure applied was not quantified. Secondly, the lengthened laminations were bonded together in a steel clamping system. A pressure of 1 N/mm^2 was applied by 3 hydraulic jacks. Finally, the beams were finished by planing the wide faces to remove the adhesive that had squeezed out between adjacent laminations.

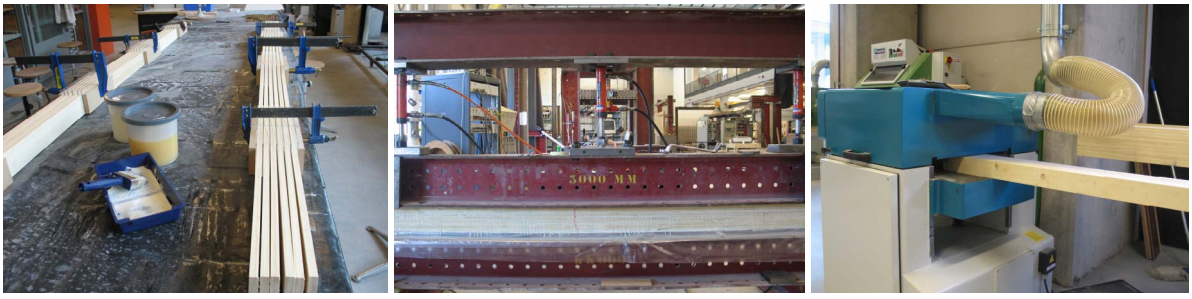

Figure 9.2: Left: lengthening of the individual laminations by scarf joints; middle: bonding the individual laminations together in a steel clamping system; right: finishing of the beams by planing the wide faces

Table 9.1 provides an overview of the number of test specimens and their denomination.

Table 9.1: Number of test specimens and their denomination

Test	Sample	Specimen code	Number
Four-point bending test on laminated beams	B	B(Phyll.Pub)-BT-Preliminary Test B(Phyll.Pub)-BT-01 to 06	7

Test Specimens: Moisture Content and Density

Moisture content and density were determined by using one test piece taken from each bending test specimen at the end of the beam. The test pieces were approximately 25 mm in thickness, 70 mm in width and 165 mm in height.

9.2.2 Method

Four-Point Bending Test on Laminated Bamboo Beams

A four-point bending test configuration was used to ensure pure bending at mid span and maximum shear at the supports. The proportion of the span to the beam height followed the standard four-point bending method defined by EN 408 (European Committee for Standardization, 1995a). According to this standard this proportion may vary between fifteen and twenty-one, shown in Figure 9.3. The span was decided to be 2720 mm which resulted in a proportion of approximately sixteen. By this configuration, it was assumed that bending failure was facilitated.

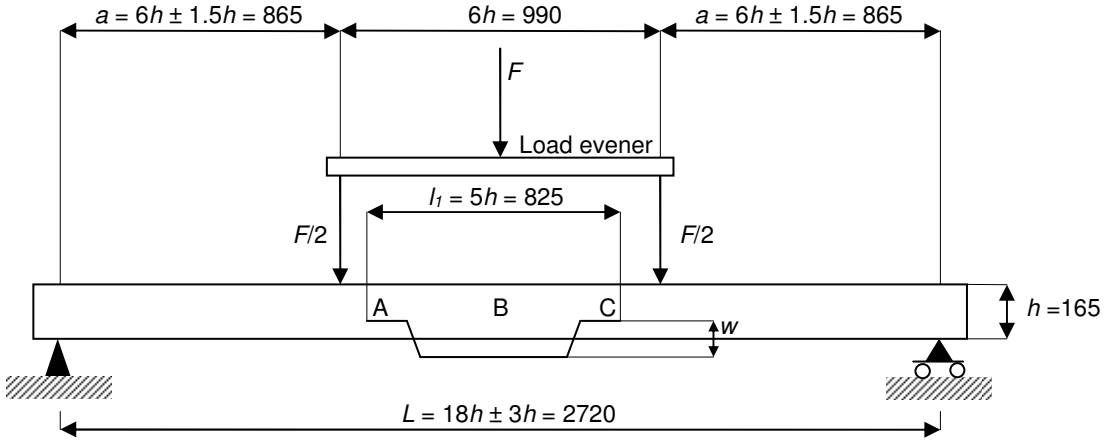

Note: dimensions in mm

Figure 9.3: Test arrangement for measuring the modulus of elasticity in bending and the bending strength according to EN 408

The test specimen was simply supported. The load was applied by an electrically operated hydraulic jack (capacity 150 kN; stroke length 100 mm) through a load evener. When failure of the test specimen did not occur by using the full stroke length of the latter hydraulic jack, a second manually operated hydraulic jack, placed in serial order, was used (capacity 200 kN; stroke length 51 mm). Small steel plates were inserted between the test specimen and the loading heads and supports to minimize local indentation. Lateral restraint near the supports was provided to prevent the risk of buckling. Between the hydraulic jack and the load evener a hinge was installed. The load applied was electrically acquired trough the load cell inserted between the two hydraulic jacks. The test setup is shown in Figure 9.4

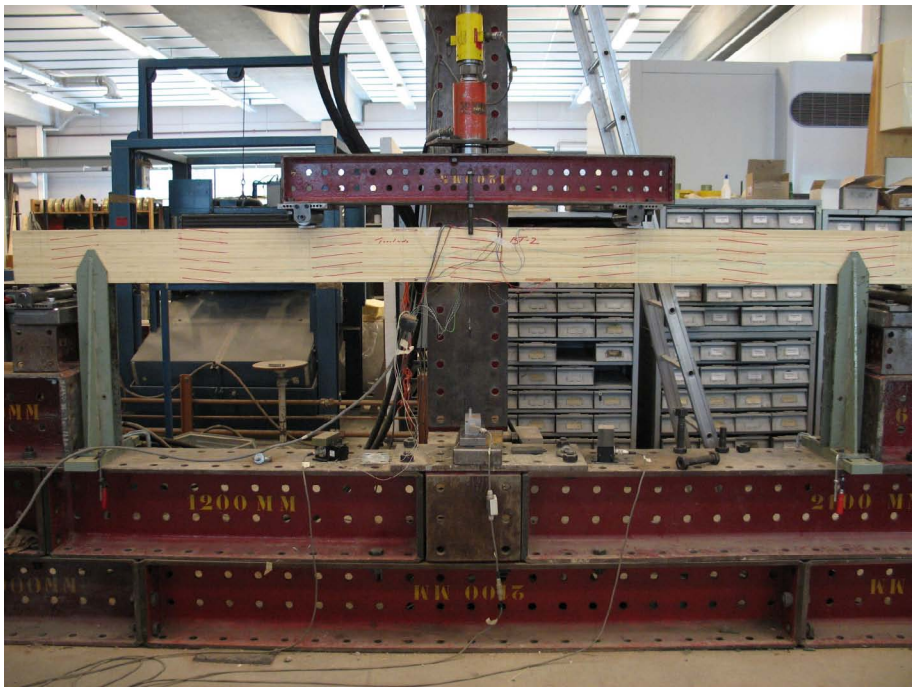

Figure 9.4: Test setup of four-point bending test on laminated bamboo beams

The modulus of elasticity and the bending strength were determined in one run. The loading speed was set at 20 mm/min. The bending strength is computed by:

$$f_m = \frac{a \cdot F_{\max}}{2 \cdot W} \qquad \text{eq.9.1}$$

where:

f_m	= bending strength	[N/mm^2]
a	= distance between a loading position and the nearest support	[mm]
F_{max}	= maximum load, applied by the hydraulic jack	[N]
W	= section modulus	[mm^3]

Note that the bending strength obtained by eq.9.1, which is equal to the modulus of rupture, is an accepted criterion of strength. It has considerable value as a parameter for comparing the various types of composites used in bending. However, it is not a true stress because the formula is only valid to the elastic limit.

To determine the modulus of elasticity in bending, deformations were measured over a length l_1 equal to five times the depth of the section centered within the test span, i.e. the deformation of point B was measured relative to points A and C by three LVDT-transducers, see Figure 9.3. Since the length l_1 was located in the shear free zone between the loading points, shear deformation was not incorporated.

The strain was measured at the compression and tension zone in the middle of a lamination 7.5 mm from the top and bottom side of the beam, respectively. This was done at two sections by applying strain gauges of 60 mm on the front and back side of the wide faces. In total 8 strain gauges were

used. The strain over the height of the section was assumed to vary linear; this was verified by one test specimen by measuring the strains over the height at one section by applying strain gauges of 30 mm located 30 mm center to center on the front and back side of the wide faces. The positioning of the LVDT-transducers and strain gauges is shown in Figure 9.5.

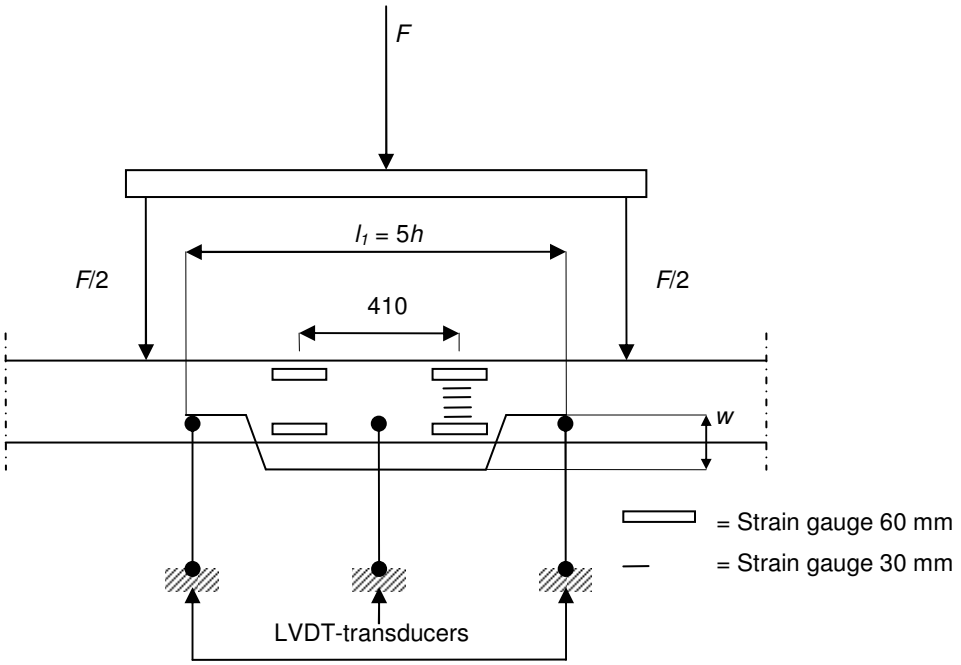

Note: Configuration strain gauges at the backside is identically to that of strain gauges on the front side; strain gauges of 30 mm were applied at only one test specimen

Figure 9.5: Positioning of LVDT-transducers and strain gauges

The modulus of elasticity in bending is computed by:

$$E_m = \frac{a \cdot l_1^2 \cdot (F_2 - F_1)}{16 \cdot I \cdot (w_2 - w_1)}$$

where:

E_m = modulus of elasticity in bending [N/mm^2]

I = moment of inertia [mm^4]

The increment of loading was computed between 10 % and 40 % of the maximum load. All test specimens were conditioned in a conditioning chamber (temperature = 20℃ and relative humidity = 65%) before they were tested.

Moisture Content and Density

Moisture content and density were determined according to paragraph 4.2.2.

9.3 Results and Discussion

9.3.1 Properties of Laminated Bamboo Loaded in Bending

The experimental results are represented by Table 9.2. The individual results of each test specimen can be found in appendix H (H.6.1).

Table 9.2: Experimental results: properties of laminated bamboo loaded in bending

	Test series		B(Phyll.Pub)-BT
Bending strength (f_m)			
	Sample size	**[-]**	7
	Mean	**[N/mm^2]**	72
	Standard deviation	**[N/mm^2]**	5 (6.9%)
Modulus of elasticity in bending (E_m)			
	Sample size	**[-]**	7
	Mean	**[N/mm^2]**	8357
	Standard deviation	**[N/mm^2]**	1230 (14.7%)
Moisture content (*MC*)			
	Sample size	**[-]**	6
	Mean	**[%]**	8.3
	Standard deviation	**[%]**	0.1 (1.6%)
Density (ρ_0)			
	Sample size	**[-]**	6
	Mean	**[kg/m^3]**	614
	Standard deviation	**[kg/m^3]**	8 (1.3%)

Note: the value in parenthesis refers to the coefficient of variation; the loading speed used during the preliminary test (5 mm/min) differed from the other tests (20 mm/min)

It can be observed that, the value for the standard deviation for the bending strength is remarkably small. This is discussed in paragraph 9.3.4.

It can be expected that the modulus of elasticity in bending lies in between the modulus of elasticity in compression and in tension: bending is a combination of tension and compression, and laminated bamboo loaded in compression behaves less stiff than when loaded in tension. However, the modulus of elasticity in bending (8357 N/mm^2) was in the same order of magnitude to the modulus of elasticity in compression (8305 N/mm^2), see Table 4.3. This may be explained by the influence of the scarf-joints on the stiffness, discussed in paragraph 5.3.5. The stiffness is reduced at the location of joints which may lead to a global reduction of the stiffness.

9.3.2 Load-Displacement Behavior

Figure 9.6 shows a typical load displacement curve for a laminated bamboo beam loaded in bending. It can be seen that the beam behaved linear elastic up to a certain limit termed the proportional limit. When the beam was loaded beyond the proportional limit, the behavior can be qualified as elastic-plastic. The results obtained by the strain gauges showed that the tension side of the beam behaved predominantly linear-elastic, whereas the compression zone behaved elastic-plastic.

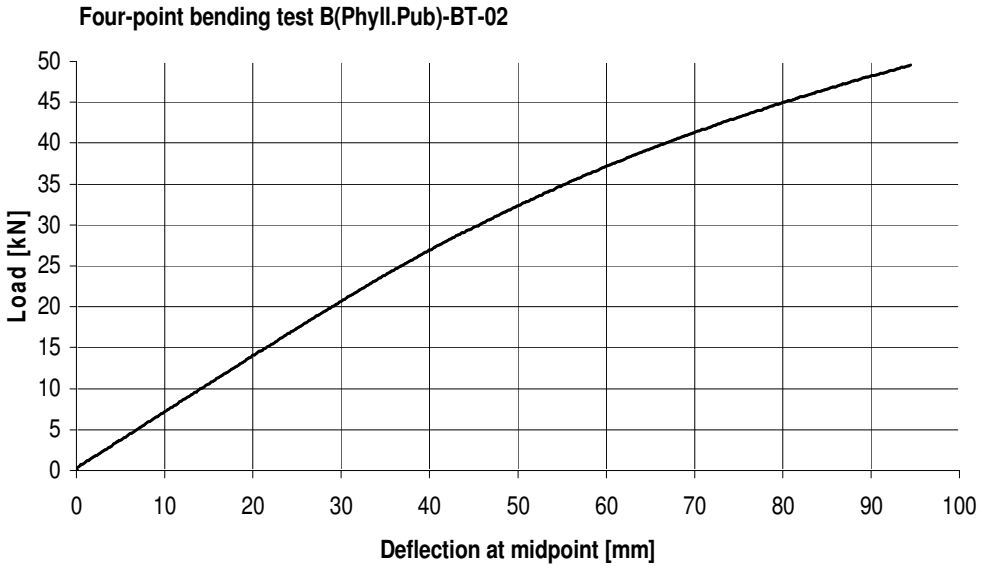

Figure 9.6: Load deflection curve of a laminated bamboo beam loaded in bending

9.3.3 Failure Mode

It was observed that failure of the laminated bamboo beams, which was accompanied by large deflections, occurred suddenly and was very brittle. Most of the beams (4 test specimens) failed at the scarf-joint located in the middle of the outermost lamination at the tension side, shown in Figure 9.7.

Figure 9.7: Failure of a laminated bamboo beam initiated at the scarf-joint

Failure of the other three test specimens was initiated by a node, at the outermost lamination at the tension side between the two loading positions.

Failure of all test specimens correlated with cracks running parallel to the grain formed at the failed section. It is believed that these cracks were not stable and that redistribution of stresses did not occur. A crack is stable when it only will propagate when the load is increased. In that case, stresses can redistribute and the initial failure does not lead to a total collapse of the beam. Notice that this behavior can only be observed by using a constant rate of displacement.

In the nonlinear range of stress-strain behavior, a constant rate of displacement causes a reduced rate of loading, whereas a constant rate of loading produces an accelerated deformation, shown in Figure 9.8. A constant rate of displacement has to be used to quantify the nonlinear behavior of a material.

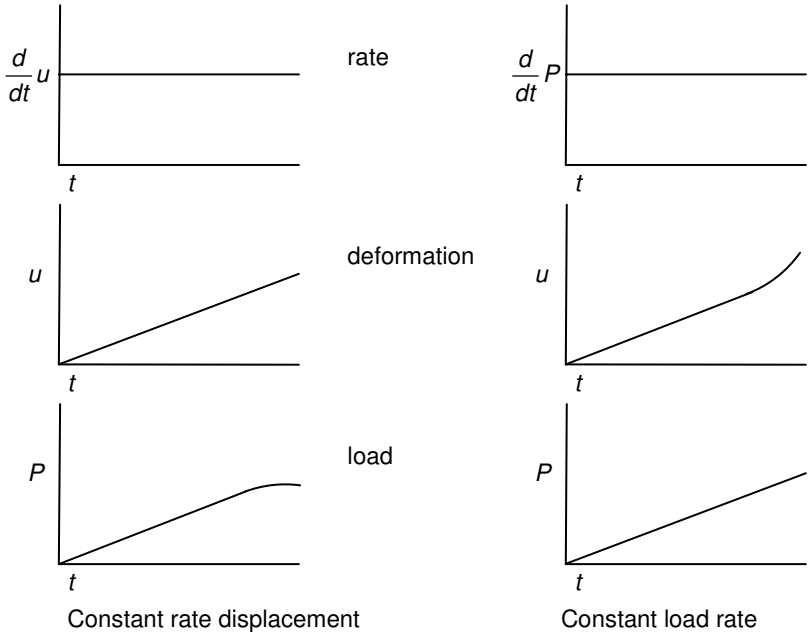

Figure 9.8: Deformation versus time and load versus time responses for a constant rate of displacement and a constant rate of loading

Source: Bodig and Jayne (1982)

The assumption that cracks were not stable and that redistribution of stresses did not occur was verified by one representative test specimen. This test specimen was loaded to failure only by the electrically operated hydraulic jack and hence, the full test was carried out using a constant rate of displacement.

The other test specimens were loaded to failure (5 tests specimens) by using the manually operated hydraulic jack during the last part of the test. Hence, the last part of the test was not carried out using a constant rate of displacement.

In general, it can be stated that the bending strength of glued-laminated bamboo beams is directed by the tensile strength of its outermost lamination, where failure can be initiated either at the joint or at a node. The fact that failure is accompanied by large deflections can be an advantage: in the ultimate limit state there is visible warning of danger.

9.3.4 Prediction of the Ultimate Load-Bearing Capacity of the Beam

The loading capacity of the beams was predicted analytically, by taking into account the elastic-plastic behavior, and compared to the experimental data. The ultimate bending moment is computed by:

$$M_u = \frac{a \cdot F_{\max}}{2} \qquad \text{eq.9.2}$$

where:

M_u = ultimate bending moment [Nmm]

To simplify the analytical computation the following assumptions are made:

- For the modulus of elasticity in tension, a value of 9591 N/mm^2 is used; for that in compression, a value of 8305 N/mm^2 is used.
- The section remains plane before and after bending.
- The stress-strain diagram is modeled according to Figure 9.10.

The second assumption was verified by the results of test specimen B(Phyll.Pub)-BT-06. The strains varied linear with the distance from the neutral axis at various load levels, shown in Figure 9.9. It was found that, as the stress increased the neutral plane shifted towards the tension side.

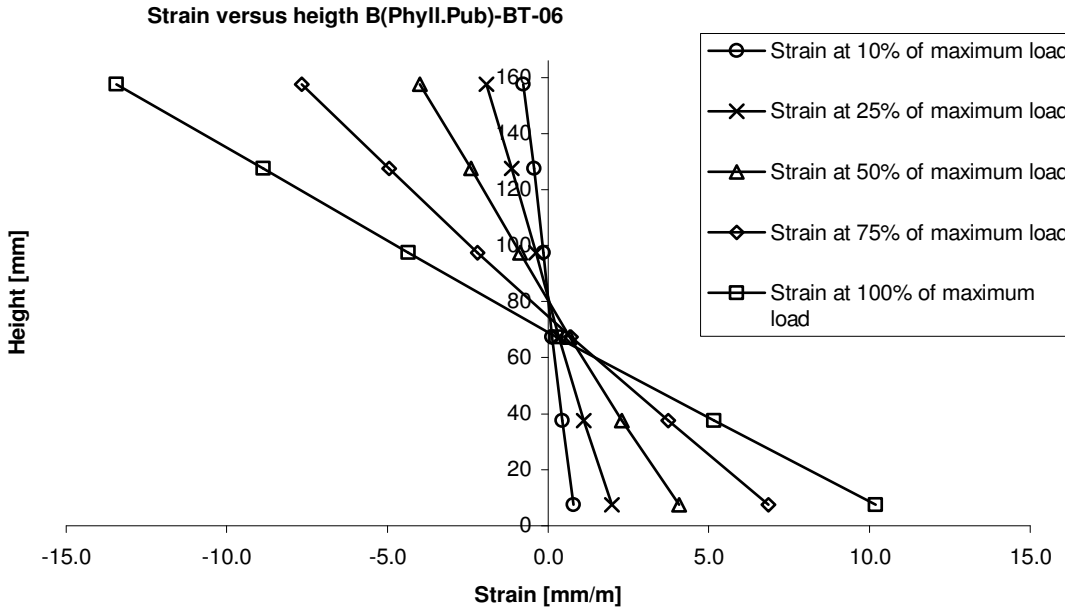

Figure 9.9: Strain versus height at various load levels for test specimen B(Phyll.Pub)-BT-06

Since the beams that exhibited joint failure failed at a lower stress than those that exhibited node failure, the ultimate bending moments were also different. Hence, two computations were made.

To compute the ultimate bending moment analytically, the stress-strain relationship of laminated bamboo loaded in tension and in compression was modeled: the first by a linear diagram; the latter by a bi-linear diagram. The first branch of the stress-strain relationship for laminated bamboo loaded in compression resembled the behavior up to the proportional limit; the second branch resembled the ductile behavior where the stress still increased slightly when the strain increased considerably.

For laminated bamboo loaded in tension exhibiting joint and node failure the mean value for the ultimate stress was computed by taking the average of the experimental values, represented by Table 5.2 and 4.3, respectively. The strain at ultimate stress was computed by dividing the ultimate stress by the modulus of elasticity in tension. The results are represented by Table 9.3.

For laminated bamboo loaded in compression the mean values for the stress and strain at proportional limit were determined graphically. The mean value for the ultimate stress and strain at ultimate stress

were computed by taking the average of the experimental values, represented by Table 7.2. The results are represented by Table 9.4.

Table 9.3: Stress and strain values for laminated bamboo loaded in tension

Node failure		**Joint failure**	
Ultimate stress ($\sigma_{t;u} = f_{t;0}$) **[N/mm^2]**	**Strain at ultimate stress** ($\varepsilon_{t;u}$) **[mm/m]**	**Ultimate stress** ($\sigma_{t;u} = f_{t;j;0}$) **[N/mm^2]**	**Strain at ultimate stress** ($\varepsilon_{t;u}$) **[mm/m]**
82	8.5	76	7.9

Table 9.4: Stress and strain values for laminated bamboo loaded in compression

Stress at proportional limit ($\sigma_{c;pl}$) **[N/mm^2]**	**Strain at proportional limit** ($\varepsilon_{c;pl}$) **[mm/m]**	**Ultimate stress** ($\sigma_{c;u} = f_{c;0}$) **[N/mm^2]**	**Strain at ultimate stress** ($\varepsilon_{c;u}$) **[mm/m]**
34	4.1	48[1]	27.0

Note: [1]) the ultimate compressive stress might be underestimated, see also paragraph 7.3.3

The model of the stress-strain relationship defined by the variables discussed above is shown in Figure 9.10.

Model of stress-strain relationship

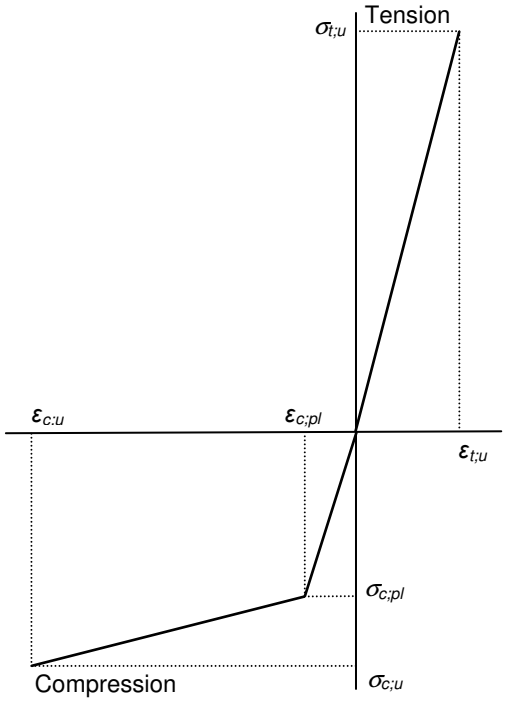

Figure 9.10: Model of stress-strain relationship

The strain- and stress-distribution over the cross-section at the moment of failure was modeled by the diagrams shown in Figure 9.11.

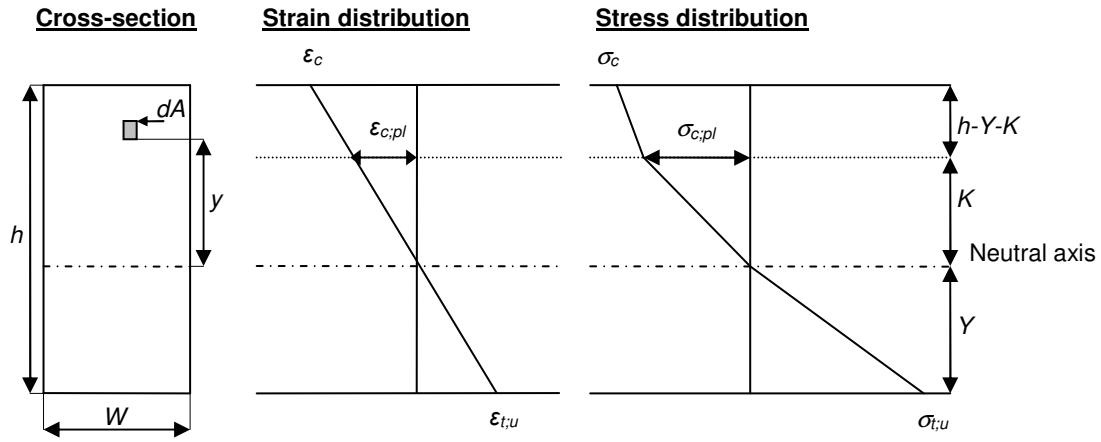

Figure 9.11: Left: cross-section; middle: strain distribution at the moment of failure; right: stress distribution at the moment of failure

Since the ultimate bending moment is the moment resultant of the stresses acting on the cross-section, it can be computed by integrating over the cross-sectional area *A*:

$$M_u = -\int_A \sigma \cdot y \cdot dA \qquad \text{eq.9.3}$$

where:

σ = stress [N/mm^2]

y = coordinate of the element of area *dA* related to the neutral axis [mm]

This formula can be written in the following concrete form:

$$M_u = W \sum S_i y_i = W\left(S_1 \cdot y_1 + S_2 \cdot y_2 + S_3 \cdot y_3 + S_4 \cdot y_4\right) \qquad \text{eq.9.4}$$

where:

W = width of the beam [mm]

y_i = vertical distance from the neutral axis to the centroid of the i^{th} surface S_i, (see Figure 9.12) [mm]

$$S_1 \cdot y_1 = \frac{\left(\sigma_c - \sigma_{c;pl}\right) \cdot W \cdot \left(h - Y - K\right)}{2} \cdot \left(\frac{2}{3} \cdot \left(h - Y - K\right) + K\right)$$

$$S_2 \cdot y_2 = \sigma_{c;pl} \cdot W \cdot \left(h - Y - K\right) \cdot \left(\frac{h - Y - K}{2} + K\right)$$

$$S_3 \cdot y_3 = \frac{\sigma_{c;pl} \cdot W \cdot K}{2} \cdot \frac{2}{3} \cdot K$$

$$S_4 \cdot y_4 = \frac{\sigma_{t;u} \cdot W \cdot Y}{2} \cdot \frac{2}{3} \cdot Y$$

Stress Distribution

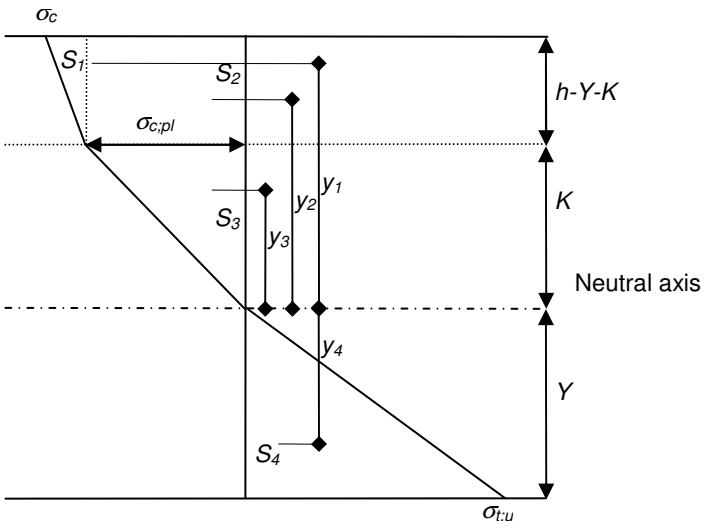

Figure 9.12: Variables used to compute M_u

To obtain the ultimate bending moment, the position of the neutral axis has to be computed. The neutral axis is positioned to realize the equilibrium between the resultant compressive force and the resultant tensile force:

$$F_c = F_t \qquad \text{eq.9.5}$$

where:

F_c = resultant compressive force [N]

F_t = resultant tensile force [N]

Hence:

$$\frac{(\sigma_c - \sigma_{c;pl}) \cdot W \cdot (h - Y - K)}{2} + \sigma_{c;pl} \cdot W \cdot (h - Y - K) + \frac{\sigma_{c;pl} \cdot W \cdot K}{2} = \frac{\sigma_{t;u} \cdot W \cdot Y}{2} \qquad \text{eq.9.6}$$

The unknown variables besides Y, are σ_c and K. K can be substituted by:

$$K = \frac{\varepsilon_{c;pl} \cdot Y}{\varepsilon_{t;u}} \qquad \text{eq.9.7}$$

and σ_c, for which applies $\sigma_{c;pl} < \sigma_c \leq \sigma_{c;u}$, by:

$$\sigma_c = \frac{\sigma_{c;u} - \sigma_{c;pl}}{\varepsilon_{c;u} - \varepsilon_{c;pl}} \cdot (\varepsilon_c - \varepsilon_{c;pl}) + \sigma_{c;pl} = \frac{\sigma_{c;u} - \sigma_{c;pl}}{\varepsilon_{c;u} - \varepsilon_{c;pl}} \cdot \left(\frac{h - Y}{Y} \cdot \varepsilon_{t;u} - \varepsilon_{c;pl} \right) + \sigma_{c;pl} \qquad \text{eq.9.8}$$

Doing so, the position of the neutral axis Y is written in term of one variable Y:

$$\frac{\left(\left(\frac{\sigma_{c;u} - \sigma_{c;pl}}{\varepsilon_{c;u} - \varepsilon_{c;pl}} \cdot \left(\frac{h - Y}{Y} \cdot \varepsilon_{t;u} - \varepsilon_{c;pl} \right) + \sigma_{c;pl} \right) - \sigma_{c;pl} \right) \cdot W \cdot \left(h - Y - \left(\frac{\sigma_{c;pl} \cdot Y}{\sigma_{t;u}} \right) \right)}{2} + \sigma_{c;pl} \cdot W \cdot \left(h - Y - \left(\frac{\sigma_{c;pl} \cdot Y}{\sigma_{t;u}} \right) \right)$$

$$+ \frac{\sigma_{c;pl} \cdot W \cdot \left(\frac{\sigma_{c;pl} \cdot Y}{\sigma_{t;u}} \right)}{2} = \frac{\sigma_{t;u} \cdot W \cdot Y}{2} \qquad \text{eq.9.9}$$

This equation can be solved for Y by the method of trial and error. The analytical results along with the experimental results are represented by Table 9.5 and Table 9.6.

Table 9.5: Analytical and experimental results for test specimens that failed at the joint

	$\varepsilon_{t;u}$ [mm/m]	ε_c [mm/m]	Y [mm]	M_u [kNm]
Analytical	7.9[1]	10.6	71.0	19.8
Experimental	9.6[2]	12.2	73.2	22.7

Note: [1]) mean based on 12 tests; [2]) mean based on 4 tests

Table 9.6: Analytical and experimental results for test specimens that failed at the node

	$\varepsilon_{t;u}$ [mm/m]	ε_c [mm/m]	Y [mm]	M_u [kNm]
Analytical	8.5[1]	11.8	69.5	20.7
Experimental	10.7[2]	14.0	72.1	24.2

Note: [1]) mean based on 8 tests; [2]) mean based on 3 tests

The ultimate bending moment computed by the analytical method underestimated the experimental values by 15% and 17% for the test specimens that failed at the joint and at the node, respectively. This can be explained by the "real" laminating effect discussed in the next paragraph.

9.3.5 Empirical Model

In general, two methods can be distinguished to predict the strength of glued-laminated bamboo members. The first method can be qualified statistically. By using a sample size sufficiently large, taking into account each variable affecting the strength, the properties of glued-laminated members of bamboo can be determined.

The second method links the properties of the individual laminations to those of the members assembled out of these laminations by a numerical model verified by experiments. The variables are taken into account by the numerical model. The latter method is desirable since the first is expensive and time-consuming.

In the following, the properties of the individual laminations are linked to those of the beams by an empirical model. This empirical model can be used to calibrate a numerical model, which in turn can be used to carry out a parameter study taking into account all variables affecting the bending strength. However, the latter is beyond the scope of this study.

In glued-laminated timber the properties of the individual laminations are linked to those of the beams by means of the laminating factor, discussed in paragraph 2.5.1. This factor quantifies the increase in strength of lumber laminations when bonded in a glued-laminated timber beam compared with their strength when tested by standard test procedures, based on ordinary beam theory. The laminating effect can be explained by three physical factors: an effect of testing procedure, a reinforcement of defects and an effect of dispersion, also discussed in paragraph 2.5.1.

To explain these effects with respect to glued-laminated bamboo the laminating effect should be quantified by the "real" laminating factor based on "real" strains rather than the laminating factor based on ordinary beam theory. The "real" laminating factor can be computed by:

$$\lambda_{lam;2} = \frac{\varepsilon_{m;ten;u}}{\varepsilon_{t;u}} \qquad \text{eq.9.10}$$

where:

$\lambda_{lam;2}$ = "real" laminating factor based on "real" strains [-]

$\varepsilon_{m;ten;u}$ = strain at ultimate bending stress at the tension side of the beam [-]

$\varepsilon_{t;u}$ = strain at ultimate tensile stress [-]

The results are represented by Table 9.7.

Table 9.7: "Real" laminating factor computed by mean strain values

	$\varepsilon_{m;ten;u}$ [1]	$\varepsilon_{t;u}$ [2]	$\lambda_{lam;2}$
	[-]	[-]	[-]
Joint	9.6 [3]	7.9 [4]	1.22
Node	10.7 [5]	8.5 [6]	1.26

Note: [1]) corresponds to the experimental value for $\varepsilon_{t;u}$, represented by Table 9.5 and Table 9.6; [2]) corresponds to the analytical value for $\varepsilon_{t;u}$, represented by Table 9.5 and Table 9.6; [3]) mean based on 4 tests; [4]) mean based on 12 tests; [5]) mean based on 3 tests; [6]) mean based on 8 tests

Gain in strength was 22% and 26% for jointed and unjointed laminations, respectively. This increase in strength quantified by the "real" laminating effect can be explained by a reinforcement effect in combination with an effect of dispersion. The low value of the coefficient of variation for the bending strength can also be explained by these effects.

The weak parts and joints within laminations at the tension side of the beam were reinforced by adjacent stiffer laminations that provided alternative paths for stresses to flow around them. Hence they sustained a higher tensile stress compared to that when tested by the tension test discussed in paragraph 4.2.2 and 5.2.2. For this reason, it is important to configure the joints alternately in relation to each other.

The effect of dispersion depends on the coefficient of variation for the tensile strength of laminations, which was significantly. In beams, the low-strength laminations are distributed throughout the volume. Hence, there is a decreased probability that the lowest strength laminations will initiate beam failure. This effect includes a "size-effect" and is discussed in the next paragraph.

The effect of the testing procedure was not present since the tensile strength was determined by tension tests performed under clamped conditions, see also paragraph 4.2.2.

The empirical model should be based on the most unfavorable situation. Beams that failed at the joints exhibited the lowest bending strength and are decisive. For practical use, the properties of the jointed laminations are linked to those of the beams that exhibited joint failure by the laminating factor based on ordinary beam theory:

$$\lambda_{lam;1} = \frac{f_m}{f_{t;j;0}} \qquad \text{eq.9.11}$$

In engineering, characteristic values (typically, lower 5th percentiles) are used to establish design values. For this reason, the laminating effect at the characteristic strength level has to be determined by:

$$\lambda_{lam;1;k} = \frac{f_{m;k}}{f_{t;j;0;k}} \qquad \text{eq.9.12}$$

where *k* refers to characteristic. For a normal distribution when the variance is unknown, a characteristic strength value can be computed by:

$$f_k = f \cdot \left(1 - \frac{t_{5/n-1} \cdot \frac{v}{100}}{\sqrt{n}}\right) \qquad \text{eq.9.13}$$

where:

f_k	= characteristic strength value	[N/mm^2]
f	= mean strength value	[N/mm^2]
v	= coefficient of variation	[%]
$t_{5/n-1}$	= Student's t value to calculate the 5th percentile	[-]
n	= sample size	[-]

The results are represented by Table 9.8.

Table 9.8: Laminating factor computed by characteristic strength values

	f_m	$f_{m;k}$	$f_{t;j;0}$	$f_{t;j;0;k}$	$\lambda_{lam;1;k}$
	[N/mm^2]	[N/mm^2]	**[N/mm^2]**	[N/mm^2]	**[-]**
Joint	70[1] (8.0%)	63	76[2] (19.7%)	68	0.93

Note: [1]) mean based on 4 tests; [2]) mean based on 12 tests; the value in parenthesis refers to the coefficient of variation

The laminating effect quantified by the laminating factor based on ordinary beam theory did not exceeded 1.0. When the proportional limit was exceeded at the compression side of the beam, the stiffness dropped. Hence, the compressive stress σ_c developed at the outermost lamination at the compression side was much lower than the tensile stress developed at the outermost lamination at the tension side. By dividing the result of eq.9.8 by $f_{t;j;0}$ the difference is estimated. It turned out that the compressive stress is only half of the tensile stress. Hence, the tensile stress at the outermost lamination at the tension side of the beam is underestimated when computed by ordinary beam theory. Consequently, the compressive stress at the outermost lamination at the compression side of the beam is overestimated. Notice that these values are equal to each other when computed by ordinary beam theory. This explains why the laminating factor did not exceeded 1.0.

By the empirical relationship expressed by the laminating factor, the characteristic bending strength of the beam can be computed by:

$$f_{m;k} = 0.93 \cdot f_{t;0;j;k} \qquad \text{eq.9.14}$$

Subsequently, the loading capacity can be computed linear-elastic. Note that the value of 0.93 can only be used when one strength class is distinguished. It is believed that the laminating effect decreases with increasing strength of laminations. Furthermore, due to the small sample size the findings are very tentative.

9.3.6 Size-effect

The empirical model elaborated in the preceding paragraph using the laminating factor is in principle only valid for members of the same botanical species with the same dimensions as those of the test specimens used in the experiments. It is believed that the most important variable which affects the bending strength of the beams is the size.

As discussed in the preceding paragraph, the effect of dispersion includes a “size-effect”. The strength decreases with an increasing size. This can be explained on the basis of Weibull’s weakest link theory for brittle materials discussed in literature related to timber engineering (e.g. Bodig and Jayne, 1982; Centrum Hout, 1995; Smith, 2003). In summary, this theory explains volume effects for brittle materials loaded in tension. The theory says that ”when loaded in tension, a chain is as strong as its weakest link”. The theory can also be used for stress fields other than tension like bending. The formulation of the theory yields:

$$\frac{\sigma_2}{\sigma_1} = \left(\frac{V_1}{V_2}\right)^{1/m} \qquad \text{eq.9.15}$$

where:

V_1 = volume of member 1 [mm^3]
V_2 = volume of member 2 [mm^3]
σ_1 = strength of member 1 [N/mm^2]
σ_2 = strength of member 2 [N/mm^2]
m = size parameter [-]

For the derivation of this formula, the reader is referred to the cited literature. For deep beams loaded in bending, it can be assumed that failure can also be initiated in the second or third lamination; hence, it is believed that the size-effect is a combination of a depth effect and a length effect. This can be represented by a depth effect only, when the ratio between the length and depth is fixed. Additionally, the width may influence the size-effect.

The size-effect is also affected by the loading configuration. For example, the probability of failure of a simply supported beam loaded in four-point bending compared to that of one loaded in three-point bending is higher. In the latter, only the cross-section at mid-point is subjected to the maximum bending stress, while in the first case the volume between the loading positions is subjected to the maximum bending stress.

By quantifying the size-effect, the formula for the bending strength can be adjusted by a factor taking into account the size of the member.

9.3.7 Competitiveness of Glued-laminated Bamboo

In order to say something about the competitiveness of glued-laminated bamboo compared to engineered wood products as glued-laminated timber and LVL with respect to their mechanical properties, these can be compared to each other. The properties of glued-laminated timber are represented by Table 9.9, those of LVL by Table 9.10 and those of glued-laminated bamboo by Table 9.11.

Table 9.9: Characteristic bending strength and mean modulus of elasticity in bending for homogenous glued-laminated timber

Glulam strength classes	**Bending strength ($f_{m;k}$) [N/mm^2]**	**Modulus of elasticity in bending (E_m) [N/mm^2]**
GL 24h	24	11600
GL 28h	28	12600
GL 32h	32	13700
GL 36h	36	14700

Source: European Committee for Standardization (1999)

Table 9.10: Characteristic bending strength and mean modulus of elasticity in bending for Kerto-S-LVL

Bending strength ($f_{m;k}$) [N/mm^2]	**Modulus of elasticity in bending (E_m) [N/mm^2]**
51[1]	14000

Note: [1]) Edgewise bending strength

Source: Centrum Hout (1995)

Table 9.11: Characteristic bending strength and mean modulus of elasticity in bending for glued-laminated bamboo

Bending strength ($f_{m;k}$) [N/mm^2]	**Modulus of elasticity in bending (E_m) [N/mm^2]**
63	8357

It can be seen that the bending strength of glued-laminated bamboo is superior tot that of glued-laminated timber and LVL. This is caused by the high tensile strength of the laminations that can be transferred to a large extent by the joint in combination with the small coefficient of variation for the bending strength.

The modulus of elasticity in bending of glued-laminated bamboo is rather poor. This implies that glued-laminated bamboo is suitable for structural applications where strength is governing above stiffness. When the serviceability limit state is decisive, the cross-section has to be made higher. This can be illustrated by the following example.

Consider a simply supported rectangular beam loaded by a uniform load. The deformation in the middle of the span can be computed by:

$$\delta = \frac{5 \cdot q \cdot L^4}{384 \cdot E_m \cdot I} \qquad \text{eq.9.16}$$

where:

δ = deflection in the middle of the span [mm]

The moment of inertia follows from:

$$I = \frac{1}{12} \cdot W \cdot h^3 \qquad \text{eq.9.17}$$

When the allowed deformation δ_a is known, the relative height of the beam made of glued-laminated bamboo can be compared to that made of glued-laminated timber GL 36h:

$$\frac{h_{bamboo}}{h_{timber}} = \frac{\sqrt[3]{\frac{60 \cdot q \cdot L^4}{384 \cdot E_{m;g;bamboo} \cdot W \cdot \delta_a}}}{\sqrt[3]{\frac{60 \cdot q \cdot L^4}{384 \cdot E_{m;g;timber} \cdot W \cdot \delta_a}}} = \sqrt[3]{\frac{E_{m;g;timber}}{E_{m;g;bamboo}}} = \sqrt[3]{\frac{14700}{8357}} = 1.21 \qquad \text{eq.9.18}$$

Thus in the case of a rectangular cross-section, the height of a beam made of glued-laminated bamboo has to be made 21% higher to satisfy the requirements when the serviceability limit state is decisive compared to a beam made of glued-laminated timber GL 36h.

9.4 Conclusions

In this part of the research, the behavior of glued-laminated bamboo beams was studied with the aim of full-scale tests. Together with the findings in the previous chapters an empirical model, which links the properties of the individual laminations to those of the beams, was established. The following conclusions can be drawn:

- The modulus of elasticity in bending, which is rather low, might be affected by the stiffness of the joints.
- The bending strength of a glued-laminated bamboo beam is directed by the tensile strength of its outermost lamination where failure can be initiated either by a joint or a node, this because bamboo under compression has a large yield capacity. The stress-strain response can be qualified elastic-plastic. Failure occurs suddenly and is very brittle; redistribution of stresses does not occur.
- The loading capacity of the beams can be predicted analytically, taking into account the elastic-plastic behavior. The stress-strain relationship for laminated bamboo loaded in tension and compression can be modeled by a linear and a bi-linear diagram, respectively.
- The tensile strength of the individual laminations can be linked to the bending strength of the beams by the laminating factor. The increase in strength of laminations bonded in a glued-laminated bamboo beam can be attributed to an effect of reinforcement and dispersion. The latter effect is believed to include a size-effect.
- It can be recommended to study the effect of the size on the bending strength by a numerical model (FEM) calibrated by experiments. On the basis of this, the formula for the bending strength can be adjusted by a factor taking into account the size of the member.

- The bending strength of glued-laminated bamboo is superior compared to that of glued-laminated timber and LVL. However, the stiffness is rather poor. This implies that glued-laminated bamboo is suitable for structural applications where strength is governing above stiffness.

10 Overall Conclusions and Recommendations

10.1 Overall Conclusions

Based on the experimental and analytical results discussed in the preceding chapters some major conclusions can be drawn on bamboo applied in laminated beams:

- The proposed structural members can be applied both by developing countries and developed countries using different manufacturing systems with different levels of investment for equipment.
- Bamboo laminations can be successfully lengthened by means of scarf-joints with a slope of 1 in 10. A joint efficiency of 93% can be achieved.
- The bending strength of glued-laminated bamboo beams is directed by the tensile strength of its outermost lamination, where failure can be initiated either at a joint or a node.
- Commercial adhesives used in timber can successfully be applied to bamboo. This means that the knowledge on these adhesives available in relation to timber can be consulted.
- The bending strength of laminated beams can be predicted on the basis of the tensile strength of jointed laminations. The increase in strength is caused by a reinforcement effect in combination wit an effect of dispersion.
- Regarding applications where strength is determining above stiffness, glued-laminated bamboo is a very promising material compared to engineered timber products.

10.2 Recommendations for Further Research on Glued-Laminated Bamboo

The present work on glued-laminated bamboo can be seen as an introduction and the results are limited to the botanical species *Phyllostachys pubescens*. To successfully apply glued-laminated bamboo as engineering material supplemental studies are necessary. In the following, recommendations are made for further research on glued-laminated bamboo. These are discussed on the basis of two themes: fundamental relations and glued-laminated bamboo beams.
In both themes it can be recommended to involve, besides *Phyllostachys pubescens*, a second botanical species like *Guadua angustifolia*. The latter is one of the most potential species, with respect to availability, dimensions and structural properties of Latin-America. Furthermore, it can be recommended to involve wide strips.

10.2.1 Fundamental Relations

Modification Factors for Moisture Content and Duration of Load

Fibrous materials experience a significant loss of strength over a period of time. For example, the strength values to be used in design for timber structures for long-term permanent loads are approximately only 60% of the strength values found in a short-term laboratory test.
Experimental research on bamboo results in a load modification factor to convert short-term laboratory results to long-term results.

Mechanical properties of bamboo are dependant on the moisture content. The moisture content correlates negatively with the mechanical properties. Some properties are more sensitive to moisture than others. Thus, the influence of moisture content on important mechanical properties, like compressive strength, tensile strength, bending strength and shear strength has to be studied experimentally. This may also lead to a moisture modification factor. Additionally, the equilibrium moisture content as function of the relative humidity and temperature has to be studied.

For design purposes it might be possible, corresponding to timber structures, to assign bamboo structures to service classes and actions to load duration classes. In timber a modification factor depending on the combination of the two classes is chosen.

Durability aspects

As wood, bamboo can suffer from fungi. In fact, bamboo is less durable than most softwood species and some treatment is necessary to obtain durable structures. Mostly the treatment is carried out in a non-sustainable way. Modern sustainable modification techniques are currently developed for wood treatments and should certainly be considered for the treatment of bamboo as well.

10.2.2 Glued-Laminated Bamboo Beams

Modeling of Failure in End-Joints of Bamboo Laminations by Numerical Methods (FEM)

This study showed that both scarf-joints and finger-joints can be applied to lengthen bamboo laminations. However, the latter joints exhibited a poor joint efficiency. Regarding finger-joints, the further aim could be to develop an optimal finger-joint using a suitable model.

Since the analytical model used in this study based on stress equilibrium overestimates the load-bearing capacity of the joints, a numerical model (FEM) which accounts for the non-linear behavior of the bondline and the occurrence of a non-uniform stress distribution on the moment of failure can be recommended according to the approach described in Serrano (1997; 2000). In this approach, the properties of the bond line have to be determined experimentally by using small test specimens after which they can be implemented in the model. Electronic Speckle Pattern Interferometric techniques can be used to calibrate the model.

Based on this model, also a parameter study on variables affecting the load-bearing capacity of the finger-joint can be carried out. The effect of geometrical imperfections, presence and location of small defects (voids) in the bondline and differences in stiffness of the two finger-joint halves are the most important variables.

This parameter study can also be carried out to investigate the influence of these variables on the load-bearing capacity of the scarf-joint.

Modeling of Failure in Glued-Laminated Bamboo Beams by Numerical Methods (FEM)

In addition to the empirical model employed in this report, which is only valid for a small range of parameters, a numerical model (FEM) has to be established which can be used to carry out a parameter study to determine the effect of size on the bending strength. This model should be calibrated by experiments.

The model for the joint discussed above can be simplified for its use in the global model for predicting the bending strength. By implementing the variables defined by their mean value and coefficient of variation it should be possible to study the effect of size on the bending strength.

Influence of Beam Configuration

The scarf-joints used for lengthening bamboo laminations exhibit a major disadvantage: they are not economical since they are wasteful of bamboo. Since these joint are only believed to be efficient in the outer highly tensile stressed zones, in the inner zones and compression zones laminations lengthened by butt-joints can be used. Based on this it can be recommended to study the bending strength of a beam partly constructed out of laminations lengthened by butt-joints and the outermost laminations at the tension zone lengthened by scarf-joints.

Furthermore, according to the findings by Serrano (1997; 2000) discussed in paragraph 2.5.2 it is interesting to study the bending strength of a beam constructed out of laminations lengthened by butt-joints, where the thickness of the outer laminations at the tension zone is relatively thin (less than 10 mm).

Local Bearing Capacity at Supporting Points

The actions working on beams have to be transferred by supporting points to the foundation of the structure. Regarding the local bearing capacity at the supporting points both the compressive strength perpendicular to the grain and modulus of elasticity perpendicular to the grain are of importance. These properties have to be determined experimentally just as the state of stress diffusion.

Long-Term Performance: Creep

Another important field of study is the creep behavior of glued-laminated bamboo beams loaded in bending. Creep can be defined as the increase of deformation under a constant applied action. Based on experiments, carried out by Janssen (1981) on bamboo culms, bamboo can be considered as a viscoelastic material. The creep behavior is schematically shown in Figure 10.1. The creep part of the deformation starts after the instantaneous deformation u_{inst}.

The parameters influencing creep are believed to be the following:

- load duration;
- moisture content;
- temperature;
- stress level.

Thus the creep behavior of glued-laminated bamboo beams loaded in bending has to be studied taken into account the variables discussed above.

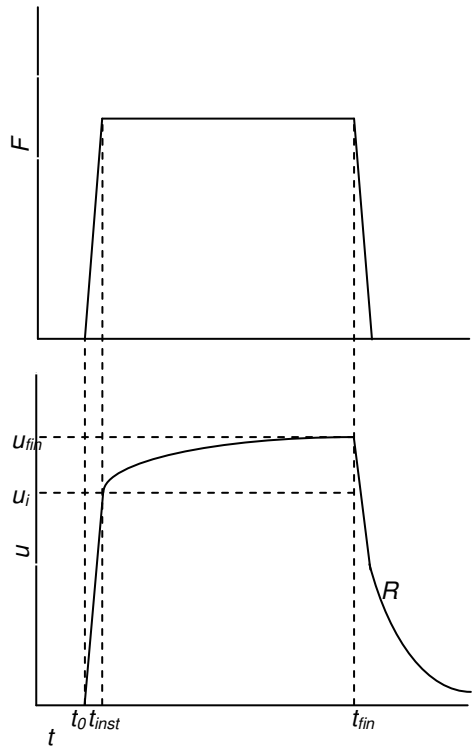

Figure 10.1: Schematic representation of viscoelastic behavior of a material. *U* is the deformation, *F* the load and *t* the time. Creep at time t_{fin} is $u_{fin} - u_{inst}$. *R* is the recovery.

Source: Centrum Hout (1995)

Bond Quality

Regarding the bond-quality the long-term behavior of bonded joints based on melamine-urea-formaldehyde has to be studied. Additionally, it can be recommended to study the effect of different preservation techniques / preservatives on the bond quality.

Furthermore, in relation to scarf-joints, the variables involved in the bonding process on the performance of the joints have to be studied. Important variables are the amount of adhesive and the pressure applied.

References

Ahmad, M. 2000. Analysis of Calcutta bamboo for structural composite materials. PhD Thesis. Virginia Polytechnic Institute and State University, Blacksburg, Virginia, U.S.A. 210 pp.

Amino, Y. 2002. Mechanical performance evaluation of bamboo-timber composite beams. PhD Thesis No. 2585. Swiss Federal Institute of Technology, Lausanne, Switzerland. 125 pp.

Amino, Y. 2003. Conception and feasibility of bamboo–precocious wood composite beams. Journal of Bamboo and Rattan, Vol. 2, No. 3, pp. 261–279.

Amino, Y. 2004. Bamboo-precocious wood composite beams: theoretical prediction of the bending behaviour. Journal of Bamboo and Rattan, Vol. 3, No. 2, pp. 107-121.

Amino, Y. 2005. Bamboo-precocious wood composite beams: bending capacity for long-term loading. Journal of Bamboo and Rattan, Vol. 4, No. 1, pp. 55-70.

Arce-Villalobos, O.A. 1993. Fundamentals of the design of bamboo structures. PhD. Thesis. Eindhoven University of Technology, Eindhoven, The Netherlands. 261 pp.

Bodig, J. and B.A. Jayne. 1982. Mechanics of wood and wood composite. Van Nostrand Reinhold Co, New York, U.S.A. 311 pp.

Centrum Hout. 1995. Timber Engineering STEP 1. Centrum Hout, Almere, The Netherlands.

Chen, C.H. et al. 2000. Bonding Moso bamboo with copolymer resins made of biomass residue extracts with phenol and formaldehyde. Forest Products Journal, Vol. 50, No. 9, pp. 70-74.

Chunwarin, W. 1975. Culm structure, composition and properties of three Thai bamboos. PhD Thesis. State University of New York College of Environmental Science and Forestry, Syracuse, New York, U.S.A.

Dransfield, S. and E.A. Widjaja (Editors). 1995. Plant Resources of South-East Asia No.7. Bamboos. Backhuys Publishers, Leiden, The Netherlands.

Dunkelberg, K. 1985. Bambus als Baustoff [Bamboo as a building material]. In: IL31, Institute for Lightweight Structures, Stuttgart, Germany. pp. 38-260.

European Committee for Standardization. 1995a. Timber structures – Structural timber and glued-laminated timber – Determination of some physical and mechanical properties. EN 408. European Committee for Standardization, Brussels, Belgium.

European Committee for Standardization. 1995b. Glued-laminated timber - Shear test of glue lines. EN 392. European Committee for Standardization, Brussels, Belgium.

European Committee for Standardization. 1999. Timber structures – Glued-laminated timber – Strength classes and determination of characteristic values. EN 1194. European Committee for Standardization, Brussels, Belgium.

European Committee for Standardization. 2001a. Glued-laminated timber - Performance requirements and minimum production requirements. prEN 386. European Committee for Standardization, Brussels, Belgium.

European Committee for Standardization. 2001b. Glued-laminated timber – Delamination test of glue lines. prEN 391. European Committee for Standardization, Brussels, Belgium.

European Committee for Standardization. 2004. Plywood – Bonding quality - Part 1: Test methods. EN 314-1. European Committee for Standardization, Brussels, Belgium.

Forest Products Laboratory. 1981. Finger-Jointed Wood Products. Research Paper FPL 382. U.S. Department of Agriculture, Madison, Wisconsin, U.S.A. 23 pp.

Forest Products Laboratory. 1999. Wood handbook - Wood as an engineering material. U.S. Department of Agriculture, Forest Service, Forest Products Laboratory, Madison, Wisconsin, U.S. 463 pp.

Ganapathy, P.M. et al. 1999. Bamboo panel boards – a state of the art review - INBAR Technical Report No. 12. International Network for Bamboo and Rattan, Beijing, China. 115 pp.

Gere, J.M. 2006. Mechanics of Materials. Thomson, Londen, United Kingdom.

Gnanaharan, R. 1993. Shrinkage behaviour of bamboos grown in Kerala, India. BIC-India Bulletin, Vol. 3 (2), pp. 1-6.

International Organization for Standardization. 2004. Bamboo - Determination of physical and mechanical properties. Standard No. ISO 22157-1:2004(E). International Organization for Standardization, Geneva, Switzerland.

Janssen, J.J.A. 1981. Bamboo in building structures. PhD Thesis. Eindhoven University of Technology, Eindhoven, The Netherlands, 238 pages.

Janssen, J.J.A. 1991. Mechanical properties of bamboo. Kluwer Academic Publishers, Dordrecht, The Netherlands. 134 pp.

Janssen, J.J.A. 1995. Building with bamboo - A handbook. Intermediate Technology Publications, London, U.K. 65 pp.

Janssen, J.J.A. 2000. Designing and Building with Bamboo - INBAR Technical Report No. 20. International Network for Bamboo and Rattan, Beijing, China. 208 pp.

Jayanetti, D.L. and P.R. Follet. 1998. Bamboo in construction: An Introduction – INBAR Technical Report No. 16. International Network for Bamboo and Rattan, Beijing, China.

Kumar, S. et al. 1994. Bamboo preservation techniques: a review. Published jointly by International Network of Bamboo and Rattan and Indian Council of Forestry Research Education, Beijing, China. 59 pp.

Lee, A.W.C. et al. 1997. Flexural properties of bamboo-reinforced southern pine OSB beams. Forests Products Journal, Vol. 47, No. 6, pp. 74-78.

Li, S.H. et al. 1994. Reformed bamboo and reformed bamboo/aluminum composite – Part I Manufacturing technique, structure and static properties. Journal of materials science, 29, pp. 5990-5996.

Li, X. 2004. Physical, chemical, and mechanical properties of bamboo and its utilization potential for fiberboard manufacturing. MSc Thesis. Louisiana State University and Agriculture and Mechanical College, Louisiana, United States of America. 68 pp.

Liese, W. 1987. Research on bamboo. Wood Science and Technology, 21, pp. 189-209.

Liese, W. 1992. The structure of bamboo in relation to its properties and utilization. In: Zhu, S.; Li, W.; Zhang, X.; Wang, Z. ed., Bamboo and its use. Proceedings of the International Symposium on Industrial Use of Bamboo, Beijing, China: 7-11 December 1992. International Tropic Timber Organization; Chinese Academy of Foresrty, Beijing, China.

Liese, W. 1998. The anatomy of bamboo culms. Technical Report No. 18. International Network of Bamboo and Rattan, Beijing, China. 207 pp.

Liese, W. and S. Kumar. 2003. Bamboo preservation compendium. Technical Report No. 22. International Network of Bamboo and Rattan, Beijing, China. 231 pp.

Nugroho, N. 2000. Development of processing methods for bamboo composite materials and its structural performance. PhD Thesis. The University of Tokyo, Tokyo, Japan.

Nugroho, N., and N. Ando. 2000. Development of structural composite products made from bamboo I: fundamental properties of bamboo zephyr board. Journal of Wood Sciences, 46, pp. 68-74.

Nugroho, N., and N. Ando. 2001. Development of structural composite products made from bamboo II: fundamental properties of laminated bamboo lumber. Journal of Wood Sciences, 47, pp. 237-242.

Qisheng, Z. et al. 2001. Industrial utilization on bamboo - INBAR Technical Report No. 26. International Network for Bamboo and Rattan, Beijing, China. 207 pp.

Serrano, E. 1997. Finger-joints for laminated beams. Experimental and numerical studies of mechanical behavior. Lund University, Lund, Sweden.

Serrano, E. 2000. Adhesive joints in timber engineering – modeling and testing of fracture properties. Doctoral thesis. Lund University, Lund, Sweden.

Smith, I. et al. 2003. Fracture and fatigue in wood. Wiley, West Sussex, England. 234 pp.

Wan Tarmeze, 2005. Numerical analysis of laminated bamboo strip lumber (LBSL). PhD Thesis. The University of Birmingham, Birmingham, United Kingdom. 239 pp.

Wang, Z., and W. Guo. 2003. Current status and prospects of new architectural materials from bamboo - INBAR Working Paper No. 47. International Network for Bamboo and Rattan, Beijing, China.

Zaidon, A. et al. 2004. Bonding characteristics of Gigantochloa scortechinii. Journal of Bamboo and Rattan, Vol. 3, No. 1, pp. 57-65.

Further Reading

De Flander, K. 2005. The role of bamboo in global modernity: from traditional to innovative construction material. Barriers and opportunities to the greater development and use of Guadua Bamboo for Construction Products. MSc Thesis. Wageningen University, Wageningen, The Netherlands.

Seethalakshmi, K.K and M.S.M. Kumar. 1998. Bamboos of India - a compendium. Published jointly by Kerala Forest Research Institute, India and International Network of Bamboo and Rattan, Beijing, China. 342 pp.

Appendices

Appendix A: Properties of Several Bamboo Species

A.1 Physical Properties

Table A.1: Physical properties of several bamboo species

Common and botanical names	Condition and relative density[1]	[-]	Base of shrinkage value measurement (moisture content)	Radial shrinkage[2] [%]	Tangential shrinkage[2] [%]	Longitudinal shrinkage[2] [%]
Giant Timber Bamboo	Green	0.48	Green to air-dry	18.21	9.25	0.02
Phyllostachys bambusoides	Dry	-	(170.9% to 12.1%)			
Thorny Bamboo	Green	0.690	Green to oven-dry	17.76	-	-
Bambusa arundinacea	Dry	0.790	(70.0% to 0.0%)			
Mitenga	Green	0.650	Green to oven-dry	18.77	-	-
Bambusa longispiculata	Dry	0.910	(82.0% to 0.0%)			
Buloh Gading	Green	0.580	Green to oven-dry	22.45	-	-
Bambusa vulgaris	Dry	0.790	(94.0% to 0.0%)			
Giant Bamboo	Green	0.620	Green to oven-dry	7.87	-	-
Dendrocalamus giganteus	Dry	0.730	(79.0% to 0.0%)			
Buloh Duri	Green	0.537	Green to oven-dry	13.30	6.2	-
Bambusa blumeana	Dry	-	(114.0% to 0.0%)			
Bolo	Green	0.539	Green to oven-dry	11.30	6.5	-
Gigantochloa levis	Dry	-	(115.1% to 0.0%)			
Thorny bamboo	-	-	Green to 12 %	13.39	-	-
Bambusa arundinacea	-	-	Green to oven-dry	16.41	-	-
Calcutta bamboo	Green	0.661	Green to oven-dry	8.80	-	0.1
Dendrocalamaus strictus	Dry	0.757	(58.0% to 0.0%)			

Note: [1]) based on oven-dry weight and the volume at the specified moisture content; [2]) expressed as a percentage of the green dimension

Source: Ahmad (2000)

A.2 Mechanical Properties

Table A.2: Mechanical properties of several bamboo species

Common and botanical names	Condition [-]	Relative density [-]	Modulus of rupture [N/mm^2]	Modulus of elasticity [N/mm^2]	Stress at proportional limit^2 [N/mm^2]
Giant Timber Bamboo	Green	0.48	70	7171	-
Phyllostachys bambusoides	Dry	-	103	10687	-
Thorny Bamboo	Green	0.583	73	9239	45
Bambusa arundinacea	Dry	0.649	95	12135	62
Terai Bamboo	Green	0.751	52	11170	32
Melocanna beccifera	Dry	0.817	56	12686	42
Thanawa	Green	0.733	61	9515	33
Thyrsostachys oliverii	Dry	0.758	88	11859	50
Buloh Semantan	Green	-	59	4964	41
Gigantochloa scortechinii	Dry	-	-	-	-
Moso Bamboo	Green	0.666	97	7929	48
Phyllostachys pubescens	Dry	-	-	-	-
Balku Bans[1]	Green	0.785	64	7308	-
Bambusa balcooa	Dry	-	-	-	-
Pichle[1]	Green	0.631	61	9584	33
Bambusa nutans	Dry	0.693	85	12135	48
Tulda	Green	-	-	-	-
Bambusa tulda	Dry	0.64	120	12617	73
Punting Pole Bamboo[1]	Green	-	-	-	-
Bambusa tuldoides	Dry	0.83	151	15858	83
Guadua[1]	Green	-	-	-	-
Guadua angustifolia	Dry	0.82	142	17237	82

Note: it is not sure if the represented values are mean values; dry condition not specified; [1]) full size test (round bamboo); [2]) definition of stress at proportional limit is not known

Source: Ahmad (2000)

Table A.2: Mechanical properties of several bamboo species (continuation)

Common and botanical names	Condition [-]	Compression parallel to grain[2] [N/mm^2]	Tension parallel to grain [N/mm^2]	Shear parallel to grain [N/mm^2]
Giant Timber Bamboo	Green	31	101	-
Phyllostachys bambusoides	Dry	42	120	-
Thorny Bamboo	Green	34	-	-
Bambusa arundinacea	Dry	64	-	-
Terai Bamboo	Green	35	-	-
Melocanna beccifera	Dry	68	-	-
Thanawa	Green	46	-	-
Thyrsostachys oliverii	Dry	57	-	-
Buloh Semantan	Green	29	-	5
Gigantochloa scortechinii	Dry	-	-	-
Moso Bamboo	Green	41	12	11
Phyllostachys pubescens	Dry	-	-	-
Balku Bans[1]	Green	46	-	-
Bambusa balcooa	Dry	-	-	-
Pichle[1]	Green	44	-	-
Bambusa nutans	Dry	70	-	-
Tulda	Green	-	-	-
Bambusa tulda	Dry	64	-	-
Punting Pole Bamboo[1]	Green	-	-	-
Bambusa tuldoides	Dry	-	-	-
Guadua[1]	Green	-	-	-
Guadua angustifolia	Dry	-	-	-

Note: it is not sure if the represented values are mean values; dry condition not specified; [1]) full size test (round bamboo); [2]) it is not known if compression parallel to grain represents the plastic flow

Source: Ahmad (2000)

Table A.2: Mechanical properties of several bamboo species (continuation)

Common and botanical names	Condition	Relative density	Modulus of rupture	Modulus of elasticity	Stress at proportional limit[2]
	[-]	[-]	[N/mm^2]	[N/mm^2]	[N/mm^2]
Buloh Aur Bukit[1]	Green	0.57	58	10756	40
Bambusa burmanica	Dry	0.672	103	17444	53
Phai Songkham[1]	Green	0.731	54	12617	33
Bambusa pallida	Dry	-	-	-	-
Buddha's Belly Bamboo[1]	Green	0.626	33	3309	17
Bambusa ventricosa	Dry	-	-	-	-
Tinwa[1]	Green	0.601	51	10894	31
Cephalostachyum pergracile	Dry	0.64	70	18823	44
Wabo-myetsangye[1]	Green	0.515	39	2413	17
Dendrocalamus hamiltomii	Dry	-	-	-	-
Savannah Bamboo[1]	Green	0.688	82	14617	45
Oxytenanthera abyssinica	Dry	-	-	-	-
Mitenga[1]	Green	0.65	40	7929	27
Bambusa longispiculata	Dry	0.91	50	10066	34
Buloh Gading[1]	Green	0.58	62	11170	47
Bambusa vulgaris	Dry	0.79	76	11721	54
Giant Bamboo[1]	Green	0.62	15	1448	11
Dendrocalamus giganteus	Dry	0.73	51	9584	12
Buloh Duri[1]	Green	0.537	28	8825	20
Bambusa blumeana	Dry	-	-	-	-
Bolo[1]	Green	0.539	20	10411	15
Gigantochloa levis	Dry	-	-	-	-

Note: it is not sure if the represented values are mean values; dry condition not specified; [1]) full size test (round bamboo); [2]) definition of stress at proportional limit is not known

Source: Ahmad (2000)

Table A.2: Mechanical properties of several bamboo species (continuation)

Common and botanical names	Condition [-]	Compression parallel to grain[2] [N/mm^2]	Tension parallel to grain [N/mm^2]	Shear parallel to grain [N/mm^2]
Buloh Aur Bukit[1]	Green	36	-	-
Bambusa burmanica	Dry	65	-	-
Phai Songkham[1]	Green	48	-	-
Bambusa pallida	Dry	-	-	-
Buddha's Belly Bamboo[1]	Green	35	-	-
Bambusa ventricosa	Dry	-	-	-
Tinwa[1]	Green	35	-	-
Cephalostachyum pergracile	Dry	49	-	-
Wabo-myetsangye[1]	Green	41	-	-
Dendrocalamus hamiltomii	Dry	-	-	-
Savannah Bamboo[1]	Green	49	-	-
Oxytenanthera abyssinica	Dry	-	-	-
Mitenga[1]	Green	44	-	-
Bambusa longispiculata	Dry	54	-	-
Buloh Gading[1]	Green	36	-	-
Bambusa vulgaris	Dry	47	-	-
Giant Bamboo[1]	Green	31	-	-
Dendrocalamus giganteus	Dry	49	-	-
Buloh Duri[1]	Green	40	-	-
Bambusa blumeana	Dry	-	-	-
Bolo[1]	Green	42	-	-
Gigantochloa levis	Dry	-	-	-

Note: it is not sure if the represented values are mean values; dry condition not specified; [1]) full size test (round bamboo); [2]) it is not known if compression parallel to grain represents the plastic flow

Source: Ahmad (2000)

A.3 Features of Several Bamboo Species

Table A.3: Features of several bamboo species

Common and botanical names	Type [-]	Height [m]	Diameter [cm]	Wall thickness [mm]	Internode length [cm]	Maturity (harvesting) [yr]
Giant Timber Bamboo ***Phyllostachys bambusoides***	monopodial	2-12	2-9	4-8	10-20	-
Thorny Bamboo[1;2] ***Bambusa arundinacea***	sympodial	up to 30	15-18	very thick	20-40	3-4
Terai Bamboo[1] ***Melocanna beccifera***	sympodial	10-20	1.5-7.7	thick	25-30	2
Thanawa[1] ***Thyrsostachys oliverii***	sympodial	up to 25	5	thin	30-60	-
Buloh Semantan[1;2] ***Gigantochloa scortechinii***	sympodial	Up to 20	12-20	5-10	up to 60	3
Balku Bans[1] ***Bambusa balcooa***	sympodial	5-30	2.5-10	20	20-45	-
Tulda[1;2] ***Bambusa tulda***	sympodial	7-28	5-19	10-25	40-70	3-4
Punting Pole Bamboo[1] ***Bambusa tuldoides***	sympodial	6-10	3-5	4-5	30-36	-
Guadua[1;2] ***Guadua angustifolia***	sympodial	-	12	15	-	-

Note: [1]) used in construction; [2]) suitable for glued-laminated bamboo with respect to diameter and wall thickness

Source: Dransfield and Widjaja (1995)

Table A.3: Features of several bamboo species (continuation)

Common and botanical names	Type [-]	Height [m]	Diameter [cm]	Wall thickness [mm]	Internode length [cm]	Maturity (harvesting) [yr]
Buloh Aur Bukit[1;2] ***Bambusa burmanica***	-	15-20	8-10	thick	30	-
Buddha's Belly Bamboo[1] ***Bambusa ventricosa***	sympodial	6-10	3-5	4-5	30-36	-
Tinwa ***Cephalostachyum pergracile***	sympodial	7-30	2.5-7.5	thin	20-45	-
Wabo-myetsangye[1;2] ***Dendrocalamus hamiltomii***	-	up to 25	10-20	thick	-	-
Buloh Gading[1;2] ***Bambusa vulgaris***	sympodial	10-20	4-10	7-15	20-45	3
Giant Bamboo[1;2] ***Dendrocalamus giganteus***	sympodial	up to 30	18-25	up to 25	25-55	3
Buloh Duri[1;2] ***Bambusa blumeana***	sympodial	15-25	up to 20	5-30	25-60	3
Bolo ***Gigantochloa levis***	sympodial	up to 20	up to 16	-	up to 45	3

Note: [1]) used in construction; [2]) suitable for glued-laminated bamboo with respect to diameter and wall thickness

Source: Dransfield and Widjaja (1995)

Appendix B: Relations between Properties

In this appendix relations between several properties are investigated. This is appendix is related to paragraph 2.2.6.

B.1 Age

The relation between the age during harvesting and the density, the ultimate stresses in bending, compression, tension and shear according to the experimental data found in Janssen (1991: p. 120) is shown in Table B.1.

Table B.1: Several properties related to age

Ageclass [-]	Density [kg/m^3]	Tangential bending [N/mm^2]	Radial bending [N/mm^2]	Compression [N/mm^2]	Tension [N/mm^2]	Shear [N/mm^2]
1	542	118	96	45	106	8.3
2	583	129	104	49	161	10.1
3	620	141	113	53	186	11.7
4	641	147	119	54	188	12.1
5	630	144	114	52	187	11.6

Note: it is not sure if the represented values are mean values

Source: Janssen (1991: p.120)

These relations can be described by the following regression formulas:

Density: $\rho(A) = -8.57 \cdot A^2 + 74.83 \cdot A + 473.00$ eq.B.1

Ultimate tang. bend. strength: $\sigma_{b;\tan g;u}(A) = -2.43 \cdot A^2 + 21.57 \cdot A + 97.80$ eq.B.2

Ultimate rad. bend. strength: $\sigma_{b;rad;u}(A) = -2.07 \cdot A^2 + 17.53 \cdot A + 79.40$ eq.B.3

Ultimate compression strength: $\sigma_{c;u}(A) = -1.07 \cdot A^2 + 8.33 \cdot A + 37.40$ eq.B.4

Ultimate tensile strength: $\sigma_{t;u}(A) = -9.64 \cdot A^2 + 76.76 \cdot A + 41.40$ eq.B.5

Ultimate shear strength: $\tau_u(A) = -0.41 \cdot A^2 + 3.35 \cdot A + 5.28$ eq.B.6

where:

ρ	= density	[kg/m^3]
$\sigma_{b;tang;u}$	= ultimate tangential bending stress	[N/mm^2]
$\sigma_{b;rad;u}$	= ultimate radial bending stress	[N/mm^2]
$\sigma_{t;u}$	= ultimate tensile stress	[N/mm^2]
$\sigma_{c;u}$	=ultimate compression stress	[N/mm^2]
τ_u	= ultimate shear stress	[N/mm^2]
A	= age class	[-]

These formulas are based on the mean values of a research done with a Chinese bamboo species from the region Guizhou in 1980. The research used 90 culms with a diameter of 100 mm or more and

a length of 15 m. Tests were done on the lowest 6 m. The thickness of all species was their wall thickness. Other sizes were:

- for the mass per volume and compression tests: 20 mm to 20 mm;
- for bending: 300 mm long and 10 mm wide, 3-point bending test;
- for tension: 260 mm long, and in the centre a length of 60 mm with a wide of 4mm;
- for shear 50 mm high and 18 mm wide with a notch on one side of 12 mm wide and 30 mm high.

There were 5 age classes distinguished: I (1-2), II (3-4), III (5-6), IV (7-8) and V (9-10). The graphs of these functions together with the experimental results are shown in Figure B.1 and Figure B.2.

In the next example is shown how the optimum age for the ultimate tensile strength can be found. The determination of the optimum age for the other properties goes analogous. To find the optimum age first the derivative of the regression formula has to be computed.

$$\sigma'_{t;u}(A) = \frac{d}{dA} - 9.64 \cdot A^2 + 76.76 \cdot A + 41.40 = -19.28 \cdot A + 76.76 \qquad \text{eq.B.1-a}$$

The solution of the following equation represents the optimum age class:

$$-19.28 \cdot A + 76.76 = 0 \Rightarrow A = 3.98$$

This corresponds to an age of approximately 7-8 years. In Table B.2 the optimum age for the other properties is summarized. It appears that the optimum age is the same for all properties.

Table B.2: Optimum age at time of harvesting for several properties

Property [N/mm^2] / [kg/m^3]	**Optimum age** [years]
Density	7-8
Ultimate tangential bending stress	7-8
Ultimate radial bending stress	7-8
Ultimate compression stress	7-8
Ultimate tensile stress	7-8
Ultimate shear stress	7-8

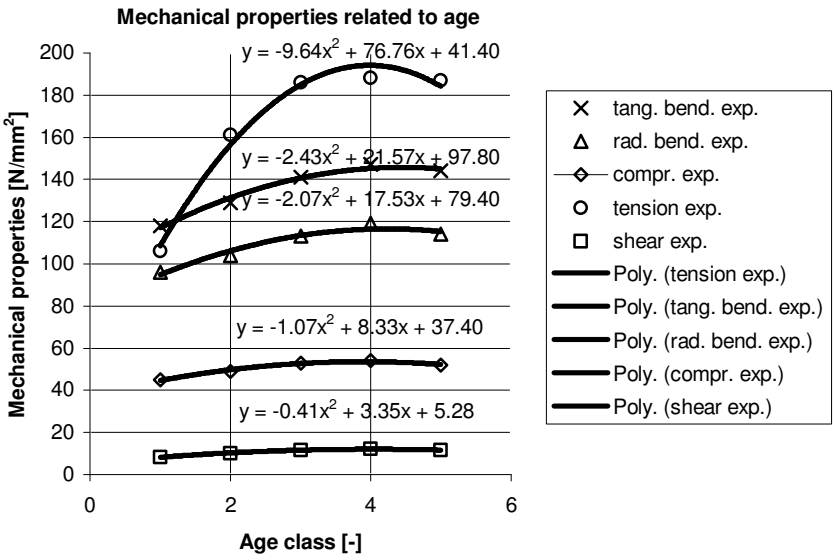

Figure B.1: Mechanical properties related to age

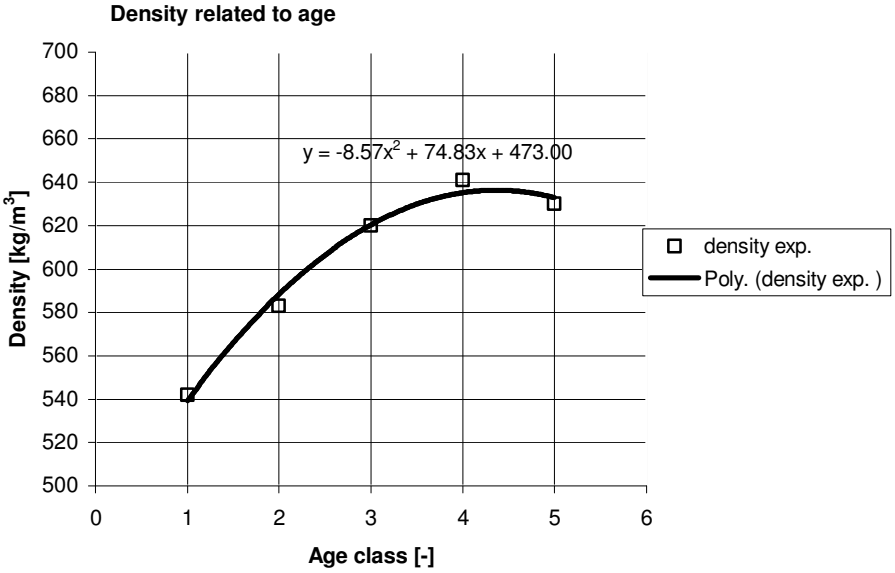

Figure B.2: Density related to age

B.2 Moisture Content

The relation between moisture content and the modulus of elasticity in bending, the tensile strength, the compression strength, and the shear strength according to the experimental data found in Janssen (1991: p. 126) is shown in Table B.3.

Table B.3: Mechanical properties related to moisture content

Moisture content [%]	Modulus of elasticity in bending x 10^2 [N/mm^2]	Tension [N/mm^2]	Compression [N/mm^2]	Shear [N/mm^2]
0	225.00	238	63	10.0
7.5	215.00	201	55	9.3
38.2	155.00	175	36	6.4
81.2	117.60	150	43	7.0

Note: it is not sure if the represented values are mean values

Source: Janssen (1999: p.126)

These relations can be described by the following regression formulas:

Modulus of elasticity in bending: $E(MC) = 1.19 \cdot MC^2 - 232.74 \cdot MC + 22786.23$ eq.B.7

Ultimate tensile strength: $\sigma_{t;u}(MC) = 0.01 \cdot MC^2 - 2.01 \cdot MC + 228.45$ eq.B.8

Ultimate compression strength: $\sigma_{c;u}(MC) = 0.01 \cdot MC^2 - 1.13 \cdot MC + 62.98$ eq.B.9

Ultimate shear strength: $\tau_u(MC) = -0.15 \cdot MC + 10.14$ eq.B.10

where:

E = modulus of elasticity in bending [N/mm^2]

MC = moisture content [%]

These formulas are based on a research on the effect of water absorption on mechanical properties. The specified moisture contents of 7.5, 38.2 and 81.2% were respectively obtained by coating in epoxy and soaking the bamboo in distilled water for 144 hours, boiling the bamboo in distilled water for 2 hours and soaking in distilled water for 144 hours. The graphs of these functions together with the experimental results are shown in Figure B.3.

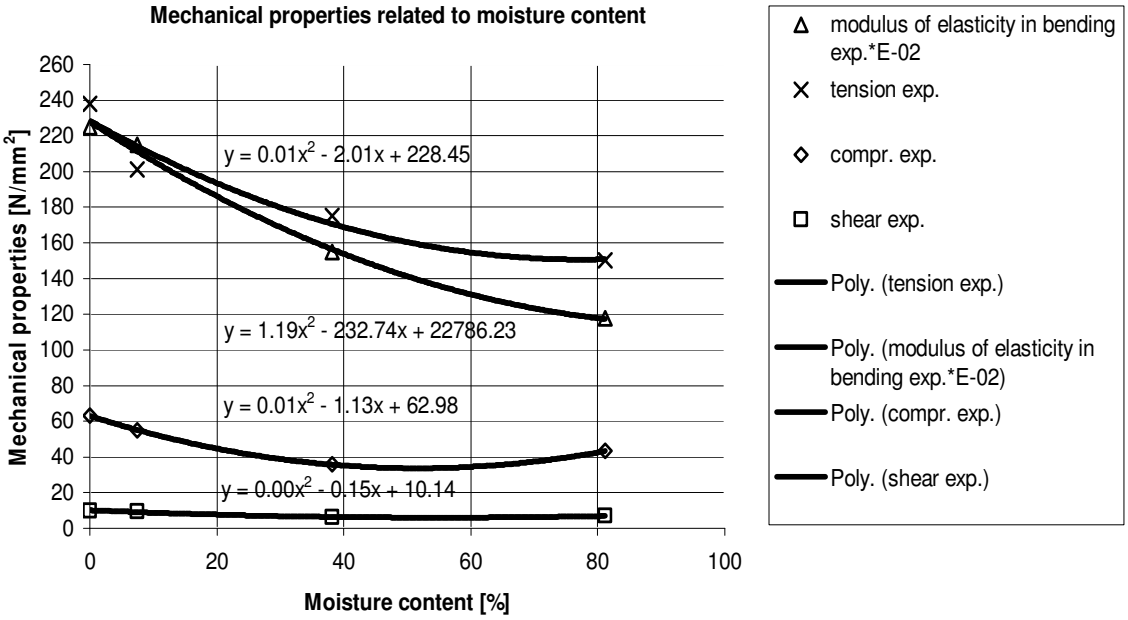

Figure B.3: Mechanical properties related to moisture content

B.3 Density

The experimental relation between the density and the bending strength, the modulus of elasticity and the compression strength according to the experimental data found in Janssen (1991: p. 128) is shown in Table B.4.

Table B.4: Mechanical properties related to density

Density [kg/m^3]	Bending [N/mm^2]	Modulus of elasticity in bending x 10^2 [N/mm^2]	Compression [N/mm^2]
499	52	45.70	55
626	94	87.60	63
726	124	165.60	51
732	124	186.00	72
797	128	170.20	75
854	157	205.00	71
862	160	205.30	79

Note: it is not sure if the represented values are mean values

Source: Janssen (1991: p.128)

These relations can be described by the following regression formulas:

Ultimate bending strength: $\sigma_{b;u}(\rho) = 0.28 \cdot \rho - 86.44$ eq.B.11

Modulus of elasticity in bending: $E(\rho) = 45.43 \cdot \rho - 17855.86$ eq.B.12

Ultimate compression strength: $\sigma_{c;u}(\rho) = 0.06\rho + 23.82$ eq.B.13

These formulas are based on a research done with bamboo from 7 different localities, consisting of 10 culms of about 3.3 m long from each locality. The graphs of these functions together with the experimental results are shown in Figure B.4.

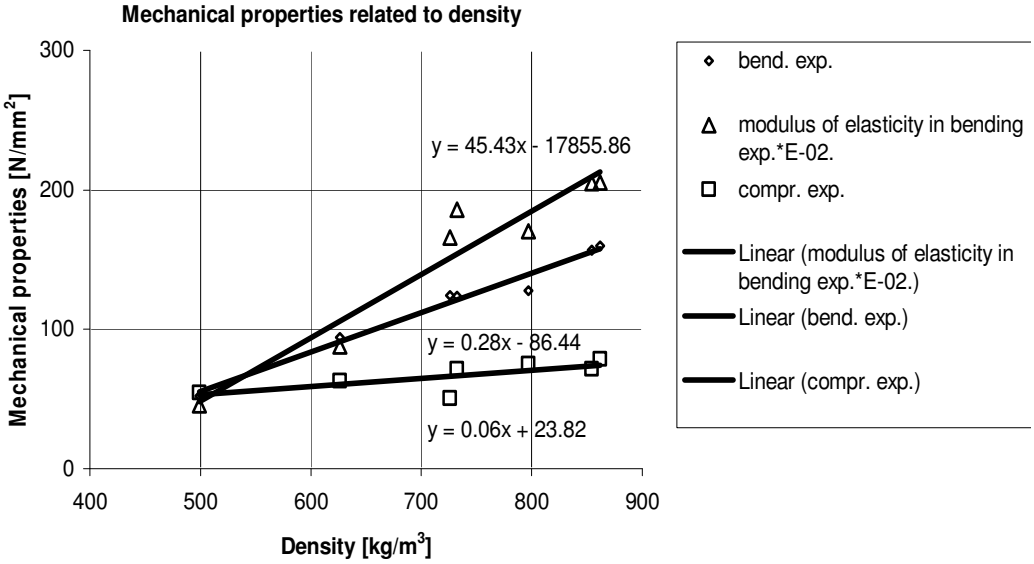

Figure B.4: Mechanical properties related to density

B.4 Position along the Culm

The experimental relation between the position along the culm and the number of vascular bundles, the density, the bending strength (tangential and radial), the compression strength, the tensile strength and the shear strength according to the experimental data found in Janssen (1991, p. 122) is shown in Table B.5.

Table B.5: Several properties related to position along the culm

Position [-]	No.vasc.b [n/mm^2]	Density [kg/m^3]	Tangential bending [N/mm^2]	Radial bending [N/mm^2]	Compression [N/mm^2]	Tension [N/mm^2]	Shear [N/mm^2]
1	1.58	554	127	116	42	139	11.2
2	2.39	635	147	120	53	185	12.0
3	2.67	660	149	125	56	202	13.2

Note: it is not sure if the represented values are mean values

Source: Janssen (1991: p.122)

These relations can be described by the following regression formulas:

No. vasc. b.: $V(x) = -0.27 \cdot x^2 + 1.61 \cdot x + 0.24$ eq.B.14

Density: $\rho(x) = -28.00 \cdot x^2 + 165.00 \cdot x + 417.00$ eq.B.15

Ultimate tang. bend. strength: $\sigma_{b;\tan g;u}(x) = -9.00 \cdot x^2 + 47.00 \cdot x + 89.00$ eq.B.16

Ultimate rad. bend. strength: $\sigma_{b;rad;u}(x) = 0.50 \cdot x^2 + 2.50 \cdot A + 113.00$ eq.B.17

Ultimate compression strength: $\sigma_{c;u}(x) = -4.45 \cdot x^2 + 24.95 \cdot x + 21.10$ eq.B.18

Ultimate tensile strength: $\sigma_{t;u}(x) = -14.50 \cdot x^2 + 89.50 \cdot x + 64.00$ eq.B.19

Ultimate shear strength: $\tau_u(x) = 0.20 \cdot x^2 + 0.20 \cdot x + 10.80$ eq.B.20

where:

x = position along the culm [-]

V = number of vascular bundles [n/mm^2]

These formulas are based on the same research as the research which investigated the relations between the mechanical properties and age.

There were 3 positions distinguished: I (1-2 m), II (3-4 m) and III (5-6 m). The graphs of these functions together with the experimental results are shown in Figure B.5, Figure B.6 and Figure B.7. In Figure B.8 the graph of the density related to number of vascular bundles is shown.

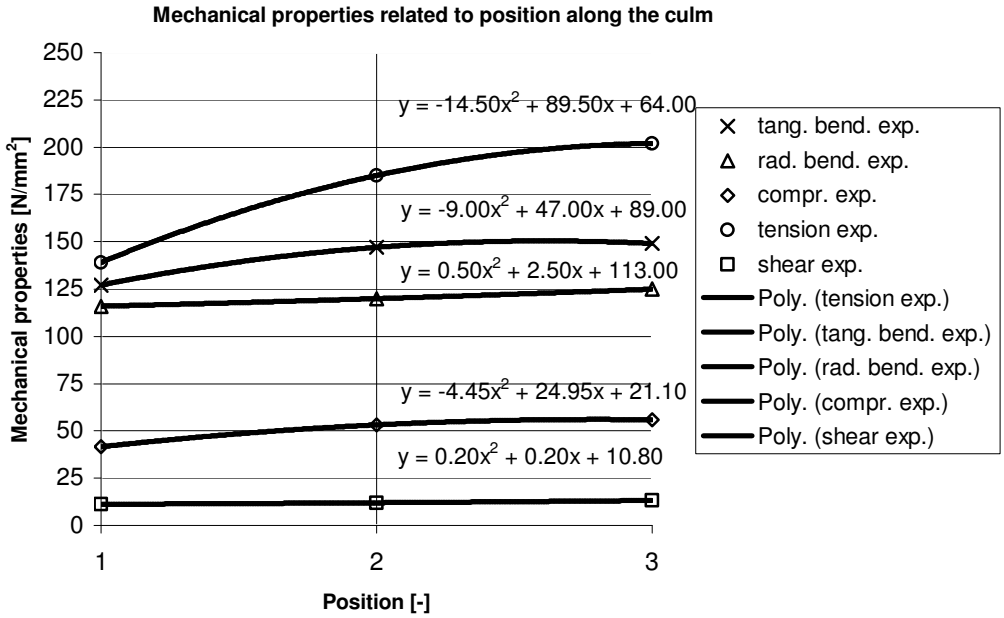

Figure B.5: Mechanical properties related to position along the culm

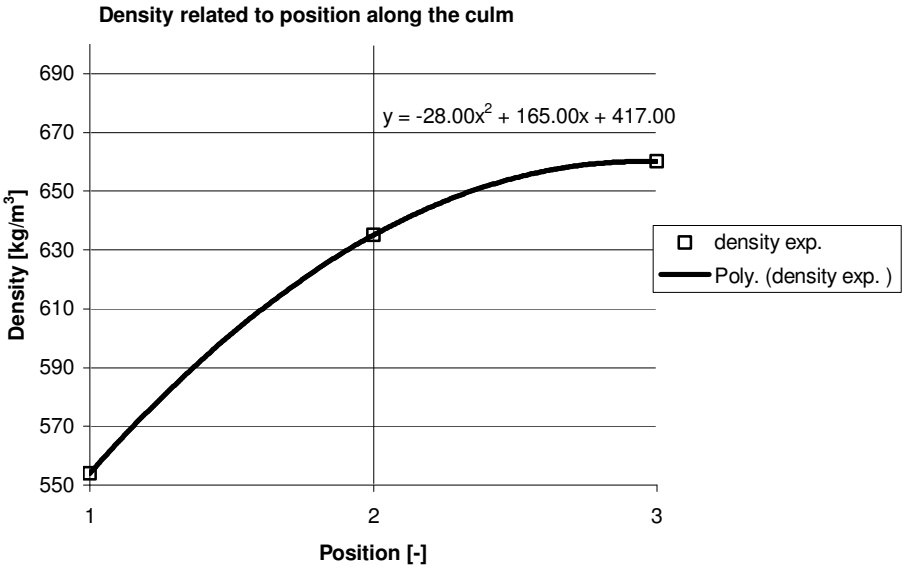

Figure B.6: Density related to position along the culm

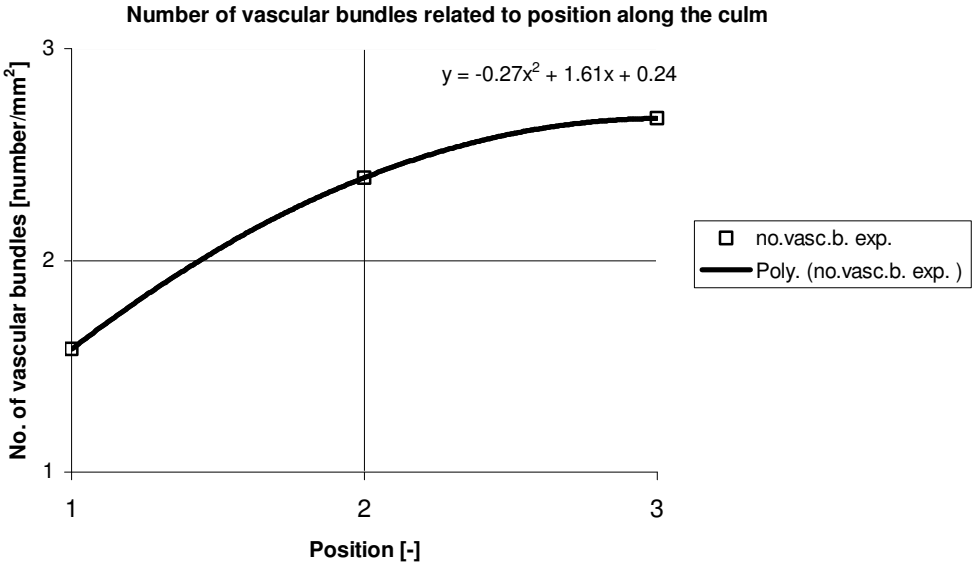

Figure B.7: Number of vascular bundles related to position along the culm

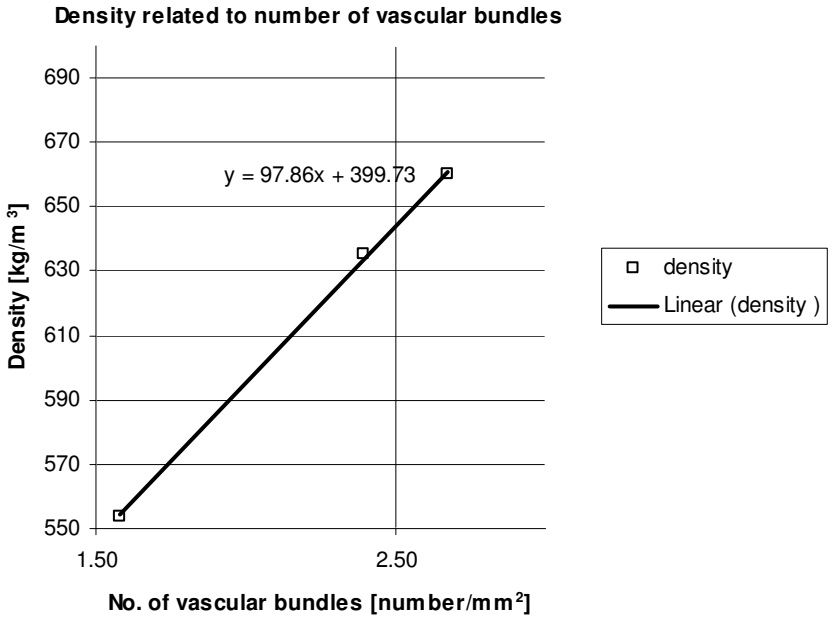

Figure B.8: Density related to number of vascular bundles

B.5 Consistency Analysis

The formula (eq.B.1) for the density as function of the age can be expressed as the age as function of the density:

Density: $$\rho(A) = -8.57 \cdot A^2 + 74.83 \cdot A + 473.00$$ eq.B.1

Age: $$A(\rho) = 4.37 - 5.83 \cdot 10^{-4} \cdot \sqrt{2.18 \cdot 10^8 - 3.43 \cdot 10^5 \cdot \rho}$$ eq.B.21

Now this formula can be substituted in the average of eq.B.2 and eq.B.3, to obtain the bending strength as function of the density and in eq.B.4 to obtain the compression strength as function of the density, respectively. Hence:

Ultimate bend. strength:

$$\sigma_{b;u}(\rho) = -2.25\cdot\left(4.37-5.83\cdot10^{-4}\cdot\sqrt{2.18\cdot10^{8}-3.43\cdot10^{5}\cdot\rho}\right)^{2} + 173.95 - 1.14\cdot10^{-2}\cdot\sqrt{2.18\cdot10^{8}-3.43\cdot10^{5}\cdot\rho} \qquad \text{eq.B.22}$$

Ultimate compression strength:

$$\sigma_{c;u}(\rho) = -1.07\cdot\left(4.37-5.83\cdot10^{-4}\cdot\sqrt{2.18\cdot10^{8}-3.43\cdot10^{5}\cdot\rho}\right)^{2} + 73.77 - 4.86\cdot10^{-3}\cdot\sqrt{2.18\cdot10^{8}-3.43\cdot10^{5}\cdot\rho} \qquad \text{eq.B.23}$$

These formulas (only valid on a certain interval) can be compared to eq.B.11 and eq.B.13 respectively. The formulas are graphically represented by Figure B.9.

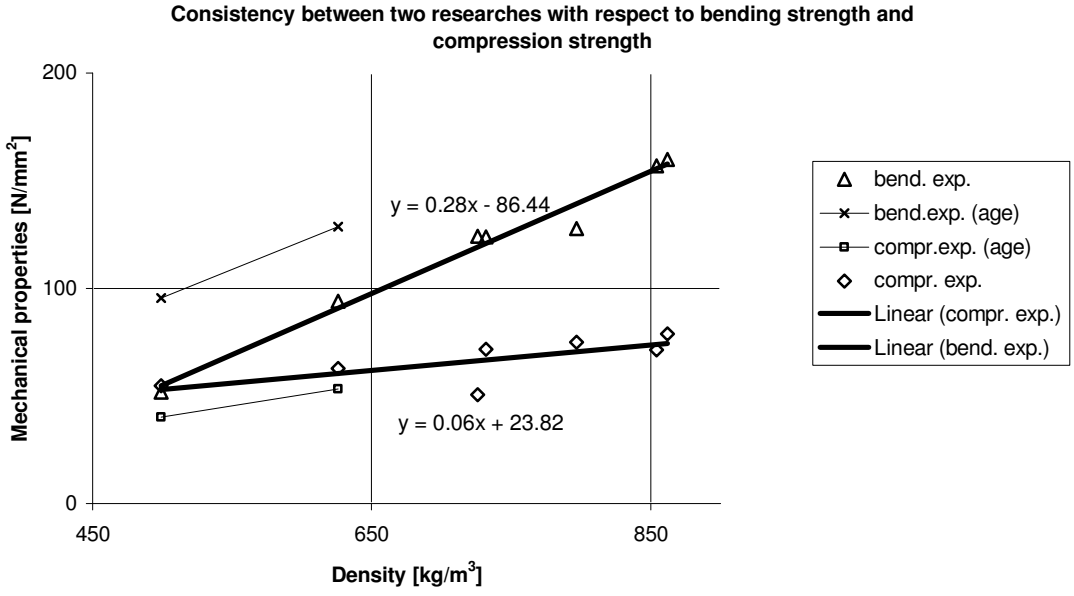

Figure B.9: Consistency between two researches with respect to bending strength and compression strength

It can be said that the slopes of the graphs are roughly the same which means that both researches are consistent with each other. The magnitudes of the values are not the same. This can be explained by the fact that the species used in both researches was not the same.

Appendix C: Analysis of Vertical and Horizontal Laminated Bamboo

In this appendix vertical and horizontal laminated bamboo is compared to each other with respect to the effective modulus of elasticity related to the total cross-section. This appendix is related to paragraph 3.4.1.

C.1 Modeling of Strips

Since the distribution of fibers varies along the culm wall thickness and hence the modulus of elasticity, there is a difference between vertical and horizontal laminated bamboo with respect to the effective modulus of elasticity related to the total cross-section. The strips can be modeled by the two layer model described in paragraph 3.4.1. The standard formulas for the location of the neutral plane in relation to the bottom of the beam and the effective modulus of elasticity are:

$$Y = \frac{\sum_{i=1}^{n} A_i \cdot E_i \cdot y_i}{\sum_{i=1}^{n} A_i \cdot E_i} \qquad \text{eq.C.1}$$

$$E_{eff} = \frac{12}{B \cdot H^3} \sum_{i=1}^{n} E_i \cdot \left(I_i + A_i \cdot d_i^2 \right) \qquad \text{eq.C.2}$$

where:

Y	= location of the neutral plane in relation to the bottom of the beam	[mm]
y_i	= centroidal plane of the i^{th} strip in relation to the bottom of the beam	[mm]
A_i	= cross-sectional area of the i^{th} strip	[mm^2]
E_i	= modulus of elasticity of the i^{th} strip	[N/mm^2]
I_i	= moment of inertia of the the i^{th} strip about its neutral plane	[mm^4]
B	= total width of the cross-section	[mm]
H	= total height of the cross-section	[mm]
d_i	= distance between the neutral plane and the centroidal plane of the i^{th} strip	[mm]

C.2 Vertical Laminated Bamboo

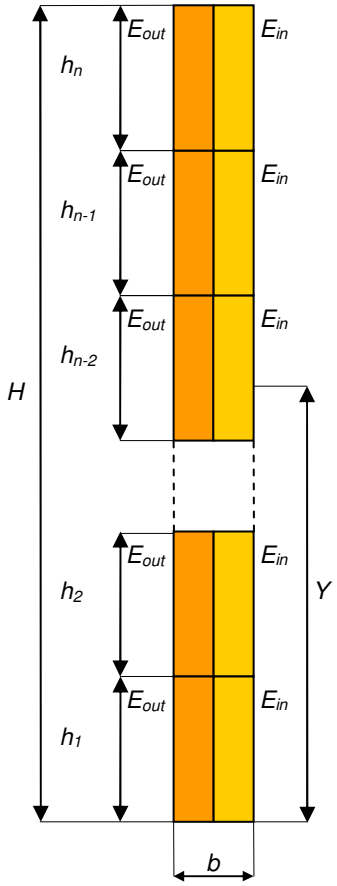

Figure C.1: Vertical laminated bamboo

Consider a rectangular cross-section consisted out of n strips on top of each other (Figure C.1). Each strip has an outer and inner layer with E_{out} and E_{in}, respectively. Each strip has the same height h so the formula for Y, in this case can be written as:

$$Y = \frac{\sum_{i=1}^{n}\left(\frac{1}{2}\cdot b\cdot h\cdot E_{out}\cdot\left((i-1)\cdot h+\frac{1}{2}\cdot h\right)+\frac{1}{2}\cdot b\cdot h\cdot E_{in}\cdot\left((i-1)\cdot h+\frac{1}{2}\cdot h\right)\right)}{n\cdot\left(\frac{1}{2}\cdot b\cdot h\cdot E_{out}+\frac{1}{2}\cdot b\cdot h\cdot E_{in}\right)} \qquad \text{eq.C.3}$$

where:

h	= height of the strip	[mm]
b	= width of the strip	[mm]
E_{out}	= modulus of elasticity of the outer layer of the strip	[N/mm^2]
E_{in}	= modulus of elasticity of the inner layer of the strip	[N/mm^2]
n	= number of strips	[-]

Y, which can be written as a function of n, is the half of the height H when h is substituted by H / n:

$$Y(n)=\frac{\sum_{i=1}^{n}\left(\frac{1}{2}\cdot b\cdot\frac{H}{n}\cdot E_{out}\cdot\left((i-1)\cdot\frac{H}{n}+\frac{1}{2}\cdot\frac{H}{n}\right)+\frac{1}{2}\cdot b\cdot\frac{H}{n}\cdot E_{in}\cdot\left((i-1)\cdot\frac{H}{n}+\frac{1}{2}\cdot\frac{H}{n}\right)\right)}{n\cdot\left(\frac{1}{2}\cdot b\cdot\frac{H}{n}\cdot E_{out}+\frac{1}{2}\cdot b\cdot\frac{H}{n}\cdot E_{in}\right)}=\frac{1}{2}\cdot H \qquad \text{eq.C.4}$$

The effective modulus of elasticity of the total cross-section, which can be written as a function of *n*, is the average of E_{out} and E_{in}:

$$E_{eff}(n)=\frac{12}{b\cdot(n\cdot h)^3}\sum_{i=1}^{n}\left(\begin{array}{l}\left(\frac{1}{24}\cdot b\cdot h^3+\frac{1}{2}\cdot b\cdot h\cdot\left((i-1)\cdot h+\frac{1}{2}\cdot h-\bar{y}\right)^2\right)\cdot E_{out}\\+\left(\frac{1}{24}\cdot b\cdot h^3+\frac{1}{2}\cdot b\cdot h\cdot\left((i-1)\cdot h+\frac{1}{2}\cdot h-\bar{y}\right)^2\right)\cdot E_{in}\end{array}\right)=\frac{E_{out}+E_{in}}{2} \qquad \text{eq.C.5}$$

C.3 Horizontal Laminated Bamboo

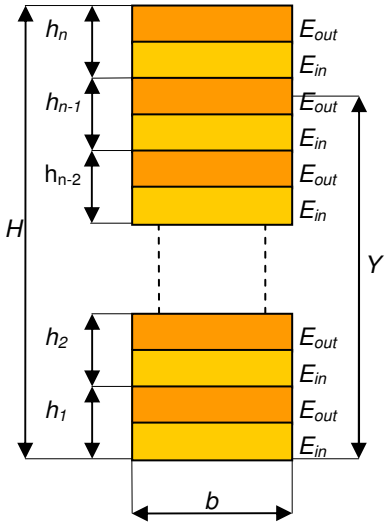

Figure C.2: Horizontal laminated bamboo

Consider a rectangular cross-section consisted out of *n* strips on top of each other (Figure C.2). Each strip has an outer and inner layer with E_{out} and E_{in}, respectively. Each strip has the same height *h* so the formula for *Y*, in this case can be written as:

$$Y=\frac{\sum_{i=1}^{n}\left(b\cdot\frac{1}{2}\cdot h\cdot E_{out}\cdot\left((i-1)\cdot h+\frac{3}{4}\cdot h\right)+b\cdot\frac{1}{2}\cdot h\cdot E_{in}\cdot\left((i-1)\cdot h+\frac{1}{4}\cdot h\right)\right)}{n\cdot\left(b\cdot\frac{1}{2}\cdot h\cdot E_{out}+b\cdot\frac{1}{2}\cdot h\cdot E_{in}\right)} \qquad \text{eq.C.6}$$

When *n* approaches to infinity, *Y*, which can be written as a function of *n*, approaches to the half of the height *H* when *h* is substituted by *H* / *n*:

$$\lim_{n\to\infty}Y(n)=\lim_{n\to\infty}\frac{\sum_{i=1}^{n}\left(b\cdot\frac{1}{2}\cdot\frac{H}{n}\cdot E_{out}\cdot\left((i-1)\cdot\frac{H}{n}+\frac{3}{4}\cdot\frac{H}{n}\right)+b\cdot\frac{1}{2}\cdot\frac{H}{n}\cdot E_{in}\cdot\left((i-1)\cdot\frac{H}{n}+\frac{1}{4}\cdot\frac{H}{n}\right)\right)}{n\cdot\left(b\cdot\frac{1}{2}\cdot\frac{H}{n}\cdot E_{out}+b\cdot\frac{1}{2}\cdot\frac{H}{n}\cdot E_{in}\right)}=\frac{1}{2}\cdot H \qquad \text{eq.C.7}$$

When n approaches to infinity the effective modulus of elasticity of the total cross-section, which can be written as a function of *n*, approaches to the average of E_{out} and E_{in}:

$$\lim_{n\to\infty} E_{eff}(n) = \lim_{n\to\infty} \frac{12}{b\cdot(n\cdot h)^3} \sum_{i=1}^{n} \left(\begin{array}{l} \left(\frac{1}{96}\cdot b\cdot h^3 + b\cdot\frac{1}{2}\cdot h\cdot\left((i-1)\cdot h+\frac{3}{4}\cdot h-\bar{y}\right)^2\right)\cdot E_{out} \\ +\left(\frac{1}{96}\cdot b\cdot h^3 + b\cdot\frac{1}{2}\cdot h\cdot\left((i-1)\cdot h+\frac{1}{4}\cdot h-\bar{y}\right)^2\right)\cdot E_{in} \end{array} \right) = \frac{E_{out}+E_{in}}{2} \quad \text{eq.C.8}$$

To investigate the behavior of the function $E_{eff}(n)$, the function is plotted in Figure C.3. For the variables values are taken which are summarized in Table C.1.

Table C.1: Strip features

Width [mm]	Height [mm]	E_{out} [N/mm^2]	E_{in} [N/mm^2]
20	5	20000	10000

The variables *b* and *h* do not affect the results. Obviously the results are affected by E_{out} and E_{in}. It appears that the function very rapidly converges which means that the following formula is valid for $n \geq 12$:

$$E_{eff}(n) \approx \frac{E_{out}+E_{in}}{2} \quad \text{eq.C.9}$$

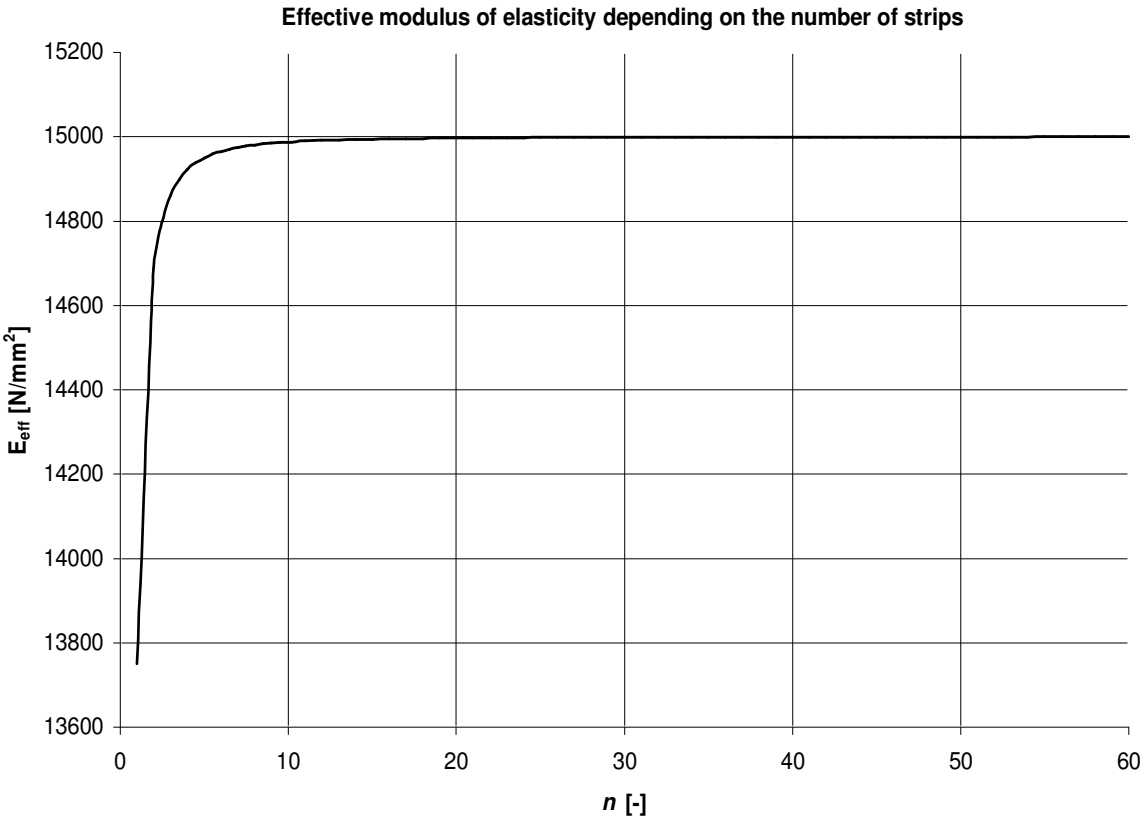

Figure C.3: Effective modulus of elasticity depending on the number of strips

On the basis of this analysis it can be stated that strip orientation, vertical or horizontal, has no significant effect on the effective modulus of elasticity when a beam is assembled out of more than 12 strips on top of each other.

Appendix D: Configuration Radius Tension Test Specimen

In this appendix the configuration of the radius of the transition zone of the tension test specimen used in this research is determined. This appendix is related to chapter 4.

D.1 Derivation of Combined Stresses in the Transition Zone

It is common to reduce the cross section within the gauge length of tension test specimens. The section of failure can be kept under control which enables to calculate the stresses accurately. However, the change in section has to be slight to prevent failure within the transition zone. This is the zone between the gauge length and the supporting area. Combined stresses occur in this zone: besides tensile stresses parallel to the grain, also tensile stresses perpendicular to the grain and shear stresses occur. The geometry of the transition zone is shown in Figure D.1.

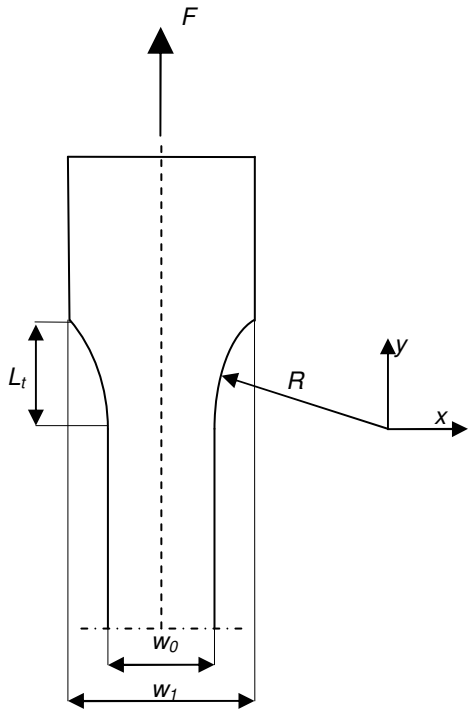

Figure D.1: Geometry of the transition zone

The geometry of the transition zone can be described on the basis of the following variables:

L_t	= length of the transition zone	[mm]
w_0	= width of the gauge zone	[mm]
w_1	= maximum width of the transition zone	[mm]
R	= radius of the transition zone	[mm]
F	= tension force	[N]

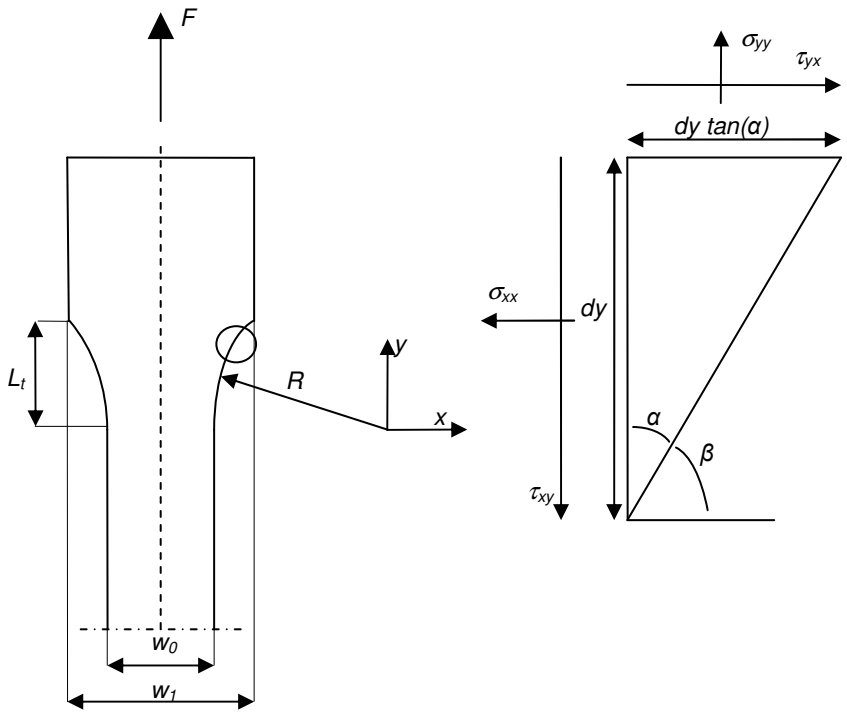

Figure D.2: Infinitesimal element in the transition zone

To derive the stresses, an infinitesimal element along the side of the transition zone of the tension test specimen is considered, see Figure D.2. The dimension in vertical direction is denoted *dy* and the other dimensions are depending on the angle *α*. From the equilibrium of forces it follows:

$$\sum H = 0 \rightarrow \sigma_{yy} \cdot dy \cdot \tan(\alpha) = \tau_{xy} \cdot dy$$
$$\sum V = 0 \rightarrow \tau_{yx} \cdot dy \cdot \tan(\alpha) = \sigma_{xx} \cdot dy \qquad \text{eq.D.1}$$
$$\sum M = 0 \rightarrow \sigma_{yy} \cdot dy \cdot \tan(\alpha) \cdot \frac{1}{2} \cdot dy \cdot \tan(\alpha) = \sigma_{xx} \cdot dy \cdot \frac{1}{2} \cdot dy$$

hence:

$$\tau_{xy} = \sigma_{yy} \cdot \tan(\alpha)$$
$$\sigma_{xx} = \tau_{yx} \cdot \tan(\alpha) \rightarrow \tau_{xy} = \tau_{yx} \qquad \text{eq.D.2}$$
$$\sigma_{xx} = \sigma_{yy} \cdot \tan^2(\alpha)$$

where:

$\tau_{xy} = \tau_{yx}$	= shear stress	[N/mm^2]
σ_{xx}	= normal stress in x-direction	[N/mm^2]
σ_{yy}	= normal stress in y-direction	[N/mm^2]

The interaction between tensile stresses parallel to the grain, tensile stresses perpendicular to the grain and shear stresses can be determined by the following interaction formula according to Norris:

$$\left(\frac{\sigma_{yy}}{\sigma_{yy;\max}}\right)^2 + \left(\frac{\tau_{xy}}{\tau_{xy;\max}}\right)^2 + \left(\frac{\sigma_{xx}}{\sigma_{xx;\max}}\right)^2 \leq 1 \qquad \text{eq.D.3}$$

where:

$\tau_{xy;max} = \tau_{yx}$ = ultimate shear stress [N/mm^2]

$\sigma_{xx;max}$ = ultimate normal stress in x-direction [N/mm^2]

$\sigma_{yy;max}$ = ultimate normal stress in y-direction [N/mm^2]

τ_{xy} and σ_{xx} in eq.D.3 can be substituted by σ_{yy} according to eq.D.2:

$$\left(\frac{\sigma_{yy}}{\sigma_{yy;\max}}\right)^2 + \left(\frac{\sigma_{yy}}{\tau_{xy;\max}}\right)^2 \cdot \tan^2(\alpha) + \left(\frac{\sigma_{yy}}{\sigma_{xx;\max}}\right)^2 \cdot \tan^4(\alpha) \le 1 \qquad \text{eq.D.4}$$

Solving the equation for σ_{yy} gives:

$$\sigma_{yy} = \frac{\sigma_{xx;\max} \cdot \tau_{xy;\max} \cdot \sigma_{yy;\max}}{\sqrt{\tau_{xy;\max}^2 \cdot \sigma_{xx;\max}^2 + \tan^2(\alpha) \cdot \sigma_{yy;\max}^2 \cdot \sigma_{xx;\max}^2 + \tan^4(\alpha) \cdot \sigma_{yy;\max}^2 \cdot \tau_{xy;\max}^2}} \qquad \text{eq.D.5}$$

The transition zone can be described by a circle with equation:

$$y^2 + x^2 = R^2 \rightarrow y = \pm\sqrt{R^2 - x^2} \qquad \text{eq.D.6}$$

The angle β can be determined from eq.D.6 by computing the arctangent of the derivative of y:

$$\beta = \arctan(y') = \arctan\left(\frac{d}{dx}\sqrt{R^2 - x^2}\right) = \arctan\left(\frac{-x}{\sqrt{R^2 - x^2}}\right) \qquad \text{eq.D.7}$$

Hence:

$$\alpha = 90 - \beta = 90 - \arctan\left(\frac{-x}{\sqrt{R^2 - x^2}}\right) \qquad \text{eq.D.8}$$

In the transition zone w is a function of y:

$$w(y) = w_0 + 2 \cdot \left(R - \sqrt{R^2 - y^2}\right) \qquad \text{eq.D.9}$$

The force which has to be transferred by the transition zone to the gauge portion follows from:

$$F = \sigma_{yy;\max} \cdot t \cdot w_0 \qquad \text{eq.D.10}$$

where:

t = thickness test specimen [mm]

In the transition zone the following criterion should be satisfied:

$$\frac{F}{t \cdot w(y)} \le \sigma_{yy}(y) \qquad \text{eq.D.11}$$

After substitution follows:

$$\frac{\left(\sigma_{yy;\max} \cdot t \cdot w_0\right)}{t \cdot \left(w_0 + 2 \cdot \left(R - \sqrt{R^2 - y^2}\right)\right)} \le \frac{\sigma_{xx;\max} \cdot \tau_{xy;\max} \cdot \sigma_{yy;\max}}{\sqrt{\tau_{xy;\max}^2 \cdot \sigma_{xx;\max}^2 + \tan^2\left(90 - \arctan\left(\frac{-x}{\sqrt{R^2 - x^2}}\right)\right) \cdot \sigma_{yy;\max}^2 \cdot \sigma_{xx;\max}^2 + \tan^4\left(90 - \arctan\left(\frac{-x}{\sqrt{R^2 - x^2}}\right)\right) \cdot \sigma_{yy;\max}^2 \cdot \tau_{xy;\max}^2}} \qquad \text{eq.D.12}$$

D.2 Optimal Radius for Tension Test Specimen

Based on the ultimate stresses, represented by Table D.1, the optimal radius *R* can be determined of the tension test specimen used in this research.

Table D.1: Properties of tension test specimen

$\sigma_{yy;max}$ [N/mm^2]	$\tau_{xy;max}$ [N/mm^2]	$\sigma_{xx;max}$ [N/mm^2]
90[1]	13.5[2]	2.7[3]

Note: [1]) based on tensile strength of bamboo laminations, see Table 4.3; [2]) according to Janssen (1991: pp. 98-99); [3]) tensile strength perpendicular to the grain is assumed to be 3% of the tensile strength parallel to the grain

Analytically solving for *R* is not possible; the equation can be solved by using the method of trial and error with the help of an EXCEL spreadsheet. The results are represented by Table D.2.

Table D.2: Configuration transition zone

w_0 [mm]	w_1 [mm]	R [mm]	L_t [mm]
40	80	1200	220

It can be seen that the length of the transition zone has to be relatively large. Considering wood, a radius for a tension test specimen of 800 mm is common. The difference is caused by the high tensile strength parallel to the grain of bamboo in relation to the shear strength and the tensile strength perpendicular to the grain which are relatively low. Since the fact that not only tensile stresses parallel to the grain occur but also combined stresses in the transition zone this large radius has to be taken into account.

Appendix E: Analysis of Load-Bearing Capacity of Scarf-Joint

In this appendix the load-bearing capacity of the scarf-joint used in this research, see also chapter 5, is analyzed based on stress equilibrium. It is assumed that failure takes place at completely uniform stress distributions along the bondlines, and the ratio of normal to shear stress is equal to the slope of the scarf. This corresponds to the bondline being elastic – perfectly plastic. The analytical results are compared to the experimental results.

E.1 Geometric Variables

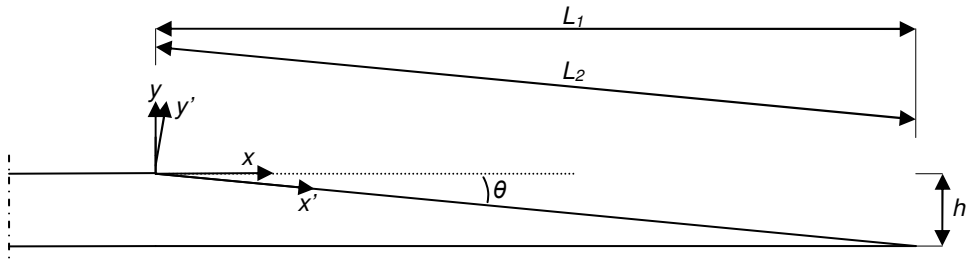

Figure E.1: Scarf-joint geometry

The geometry of a scarf-joint can be described on the basis of the following variables, see :

h = height [mm]
L_1 = scarf length [mm]
L_2 = slope length [mm]
θ = slope angle [°]

The *x-y* coordinate system is defined parallel to the axis of the grain and parallel to the length-axis of the lamination. The *x'-y'* coordinate system is defined parallel to the slope of the scarf. The angle between both coordinate systems is denoted theta.

E.2 Derivation of Formulas

The load a scarf-joint can withstand in shear has to approach the load that a lamination can withstand in tension. However, besides shear stresses, also stresses normal to the bondline occur since the scarf is applied under a slope. The interaction between shear stresses and normal stresses can be described by the following failure criterion according to Norris:

$$\left(\frac{\sigma_{y'y'}}{\sigma_{y'y';\max}}\right)^m + \left(\frac{\tau_{x'y'}}{\tau_{x'y';\max}}\right)^m = 1 \qquad \text{eq.E.1}$$

where:

$\sigma_{y'y'}$ = normal stress [N/mm^2]
$\sigma_{y'y';max}$ = ultimate normal stress [N/mm^2]
$\tau_{x'y'}$ = shear stress [N/mm^2]
$\tau_{x'y';max}$ = ultimate shear stress [N/mm^2]

m = calibration constant (for wood, typically $m = 2$) [-]

The exponent depends on the type of adhesive just as the maximum shear and normal stress. These parameters are influenced by the adherent and the interface. In this analysis it is assumed that the maximum shear stress of the adhesive is equal to the maximum shear stress of the adherent. The ultimate normal stress is assumed to be one third of the ultimate shear stress. This ratio is based on experimental research for wood reported in Serrano (1997; 2000). The assumed parameters are represented by Table E.1.

Table E.1: Assumed properties of adhesive

$\tau_{x'y';max}$ [N/mm^2]	$\sigma_{y'y';max}$ [N/mm^2]	m [-]
13.5[1]	4.5	2.0

Note: [1]) ultimate shear stress according to Janssen (1991: pp. 98-99)

Figure E.2 shows the failure criterion in a graphical way. Theoretically, combinations inside the graph will not result in failure, combinations outside the graph will.

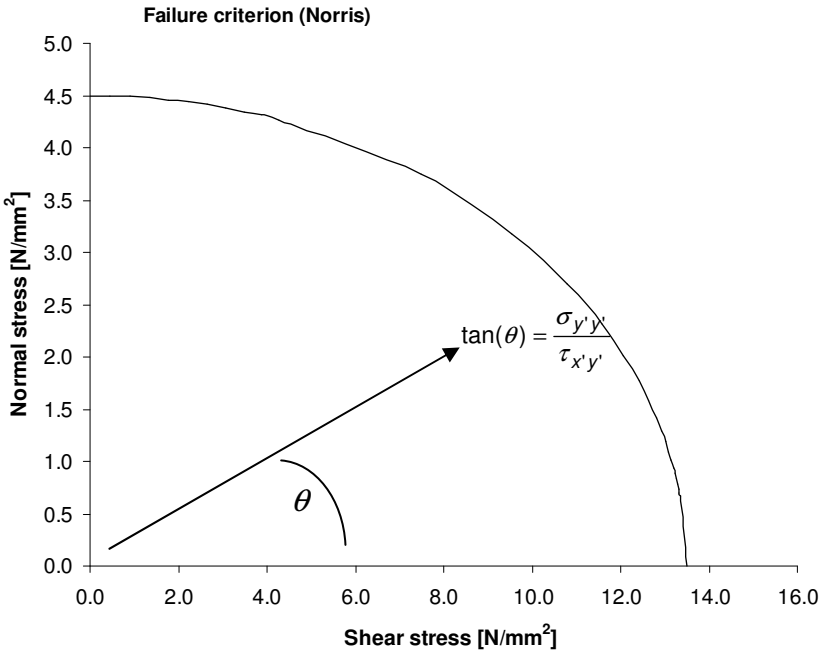

Figure E.2: Failure criterion

The stresses working along the sloping area of the scarf are represented by Figure E.3.

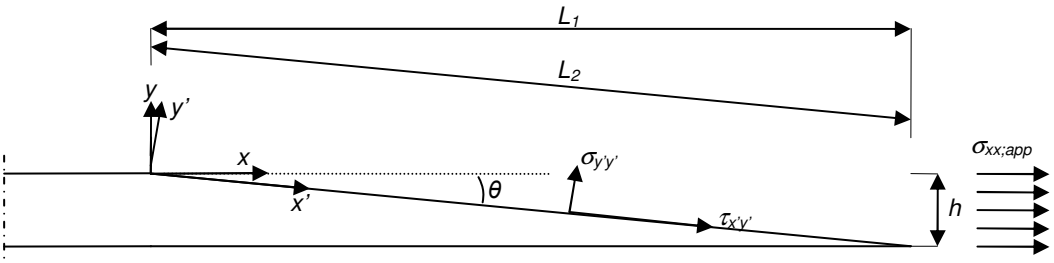

Figure E.3: Representation of stresses working along the sloping area of the scarf

The ratio of normal to shear stress is equal to the slope of the scarf:

$$\sigma_{y'y'} = \tau_{x'y'} \cdot \tan(\theta) \qquad \text{eq.E.2}$$

This relation can be used to substitute $\sigma_{y'y'}$ by $\tau_{x'y'}$ in eq.E.1:

$$\left(\frac{\tau_{x'y'} \cdot \tan(\theta)}{\sigma_{y'y';max}}\right)^2 + \left(\frac{\tau_{x'y'}}{\tau_{x'y';max}}\right)^2 = 1 \qquad \text{eq.E.3}$$

This equation can be solved for $\tau_{x'y'}$:

$$\tau_{x'y'} = \frac{\sigma_{y'y';max} \cdot \tau_{x'y';max}}{\sqrt{\sigma_{y'y';max}^2 + \tau_{x'y';max}^2 \cdot \tan^2(\theta)}} \qquad \text{eq.E.4}$$

The shear stress working along the sloping side of the fingers can be converted to the stress that can be applied, by:

$$\sigma_{xx;app} = \frac{\tau_{x'y'} \cdot L_2}{h \cdot \cos(\theta)} \qquad \text{eq.E.5}$$

where:

$\sigma_{xx;app}$ = stress which can be applied [N/mm^2]

E.3 Evaluation of Joint Profile

The joint profile used in this research can be described based on the following variables: scarf length (L_1 = 150 mm), height (h = 15 mm), and slope (θ = 5.71°). The stress which can be transmitted computed by eq.E.5 is along with the experimental results represented by Table E.2.

Table E.2: Analytical and experimental results

	Analytical [N/mm^2]	**Experimental [N/mm^2]**
Tensile strength parallel to the grain of jointed lamination ($f_{t;j;0}$)	131	76

It can be concluded that the load-bearing capacity of the scarf-joint is overestimated by the analytical method. Differences between the analytical method and the experimental behavior of the bondline are caused by:

- non-linear behavior of the bondline;
- occurrence of a non-uniform stress distribution on the moment of failure;
- geometrical imperfections which causes peak stresses;

- presence and location of small defects (voids) in the bondline;
- differences in stiffness of the two scarf-joint halves.

Appendix F: Analysis of Load-Bearing Capacity of Finger-Joint

In this appendix the load-bearing capacity of the finger-joint used in this research, see also chapter 5, is analyzed. This appendix can be seen as a continuation of the preceding appendix.

F.1 Geometric Variables

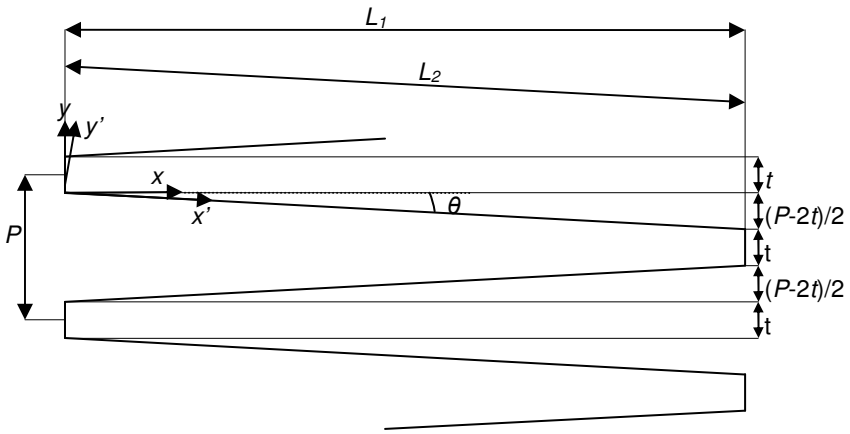

Figure F.1: Finger-joint geometry

The geometry of a finger-joint can be described on the basis of the following variables, see Figure F.1:

- P = pitch [mm]
- L_1 = finger length [mm]
- L_2 = slope length [mm]
- t = tip width [mm]
- θ = slope angle [°]

The bond area contains the area of the sloping side of the fingers: it is assumed that the tip does not transfer any forces. The *x-y* coordinate system is defined parallel to the axis of the grain and parallel to the length-axis of the lamination. The *x'-y'* coordinate system is defined parallel to the slope of the finger. The angle between both coordinate systems is denoted theta.

F.2 Derivation of Formulas

The interaction formula and adhesive properties used in this appendix are described in the preceding appendix. The stresses working along the sloping areas of the fingers are represented by Figure F.2.

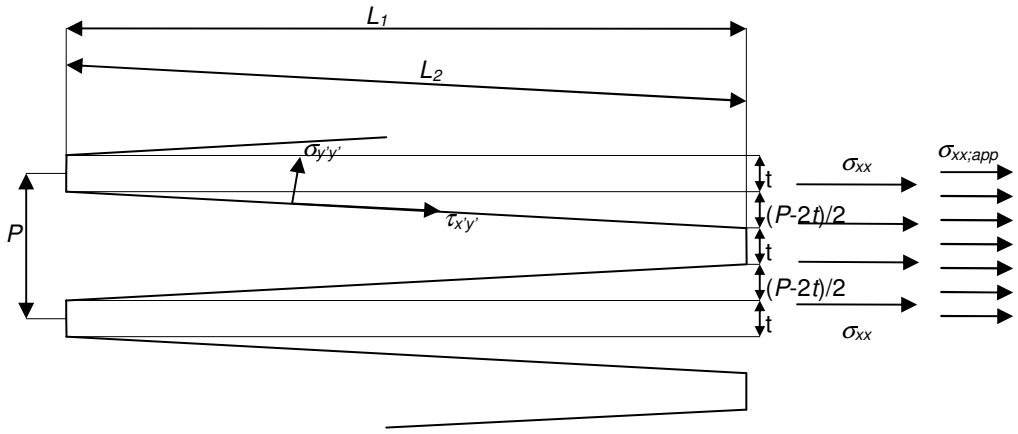

Figure F.2: Representation of stresses working along the sloping areas of the fingers

The derivation of formulas is the same as in the preceding appendix up to eq.E.4. It is assumed that the tip does not transfer any forces. The shear stress working along the sloping side of the fingers can be converted to the stress that can be applied, by:

$$\sigma_{xx;app} = \sigma_{xx} \cdot \left(1 - \frac{2 \cdot t}{P}\right) = \frac{\tau_{x'y'} \cdot 2 \cdot L_2}{(P - 2 \cdot t) \cdot \cos(\theta)} \cdot \left(1 - \frac{2 \cdot t}{P}\right) = \frac{\tau_{x'y'} \cdot 2 \cdot L_2}{P \cdot \cos(\theta)} = \frac{\dfrac{\sigma_{y'y';\max} \cdot \tau_{x'y';\max}}{\sqrt{\sigma_{y'y';\max}^{\,2} + \tau_{x'y';\max}^{\,2} \cdot \tan^2(\theta)}} \cdot 2 \cdot L_2}{P \cdot \cos(\theta)} \qquad \text{eq.F.1}$$

where:

$\sigma_{xx;app}$ = stress which can be applied [N/mm^2]

F.3 Evaluation of Joint Profile

The load-bearing capacity of the scarf-joint was overestimated by the analytical method. This is also the case for the load-bearing capacity of the finger-joint. Serrano (1997; 2000) derived a formula for the finger-joint strength depending on the shear strength of the bondline for wood:

$$\sigma_{xx;app;\exp;Ser} = 9.93 \cdot \tau_{x'y';\max}^{\,0.59} \qquad \text{eq.F.2}$$

where:

$\sigma_{xx;app;exp;Ser}$ = stress which can be applied according to Serrano (1997; 2000) [N/mm^2]

This relation is based on several adhesives and a joint profile which can be described on the basis of the following variables: finger length (L_1 = 20 mm), pitch (P = 6.2 mm), slope (θ = 5.99°) and tip thickness (t = 1.0 mm). This formula can be used to adjust eq.F.1:

$$\frac{9.93 \cdot \tau_{x'y';\max}^{\,0.59}}{\dfrac{\sigma_{y'y';\max} \cdot \tau_{x'y';\max}}{\sqrt{\sigma_{y'y';\max}^{\,2} + \tau_{x'y';\max}^{\,2} \cdot \tan^2(\theta)}} \cdot 2 \cdot L_2} = \frac{9.93 \cdot 13.5^{0.59}}{\dfrac{4.5 \cdot 13.5}{\sqrt{4.5^2 + 13.5^2 \cdot \tan^2(5.99)}} \cdot 2 \cdot 20} = 0.55 \Rightarrow \qquad \text{eq.F.3}$$

$$\sigma_{xx;app;\exp} = 0.55 \cdot \frac{\dfrac{\sigma_{y'y';\max} \cdot \tau_{x'y';\max}}{\sqrt{\sigma_{y'y';\max}^{\,2} + \tau_{x'y';\max}^{\,2} \cdot \tan^2(\theta)}} \cdot 2 \cdot L_2}{P \cdot \cos(\theta)}$$

where:

$\sigma_{xx;app;exp}$ = stress which can be applied adjusted by experimental research [N/mm^2]

The joint profile used in this research can be described on the basis of the following variables: finger length (L_1 = 20 mm), pitch (P = 6.2 mm), slope (θ = 6.3°) and tip thickness (t = 0.9 mm). The stress which can be transmitted computed by eq.F.3 along with the experimental results is represented by Table F.1.

Table F.1: Analytical and experimental results

	Analytical [N/mm^2]	**Experimental (A(PhyII.Pub)-TT-II(fj))** [N/mm^2]	**Experimental (C(PhyII.Pub)-TT-II(fj))** [N/mm^2]
Tensile strength parallel to the grain of jointed lamination ($f_{t;j;0}$)	46	33	38

The difference with the experimental results is mainly caused by the fact that bond quality was poor. Since joint efficiency was far from satisfying, the influence of the geometry on the load-bearing capacity of the finger-joint is studied in the next paragraph.

F.4 Influence Geometry

The stress in the net section (total section minus thickness of fingertips) has to be bounded by the tensile strength parallel to the grain:

$$\frac{\sigma_{xx;app;\exp}}{\left(1-\frac{t}{P}\right)} \le f_{t;0} \qquad \text{eq.F.4}$$

The tensile strength parallel to the grain, represented by Table 4.3, is 82 N/mm^2 for sample A. This value can be used as an upper boundary for the stress in the net section.

F.4.1 Influence of Slope Angle on Stress in Net Section and Applied Stress Adjusted by Experimental Research

The influence of the slope angle on the stress in the net section and the applied stress adjusted by experimental research can be investigated. The finger length is held constant and hence the pitch will vary. In Figure F.3 the geometry is represented for three different finger-joints ($\theta_A > \theta_B > \theta_C$). It can be seen that the pitch varies. It is assumed that the minimum tip width is 0.9 mm constantly. Practical limitations are imposed by knives of cutting heads: if they are too thin, they rapidly overheat which results in permanent damage or dulling.

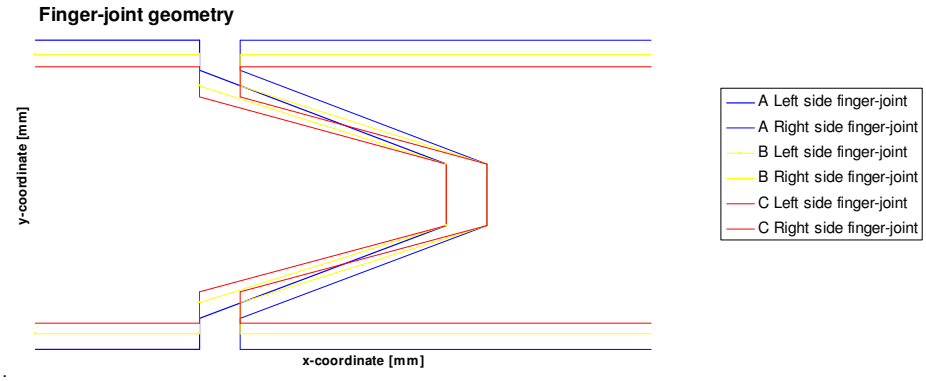

Figure F.3: Finger joint geometry – variable = slope angle

The slope angle versus the normal stress in the net section and applied stress is shown in Figure F.4.

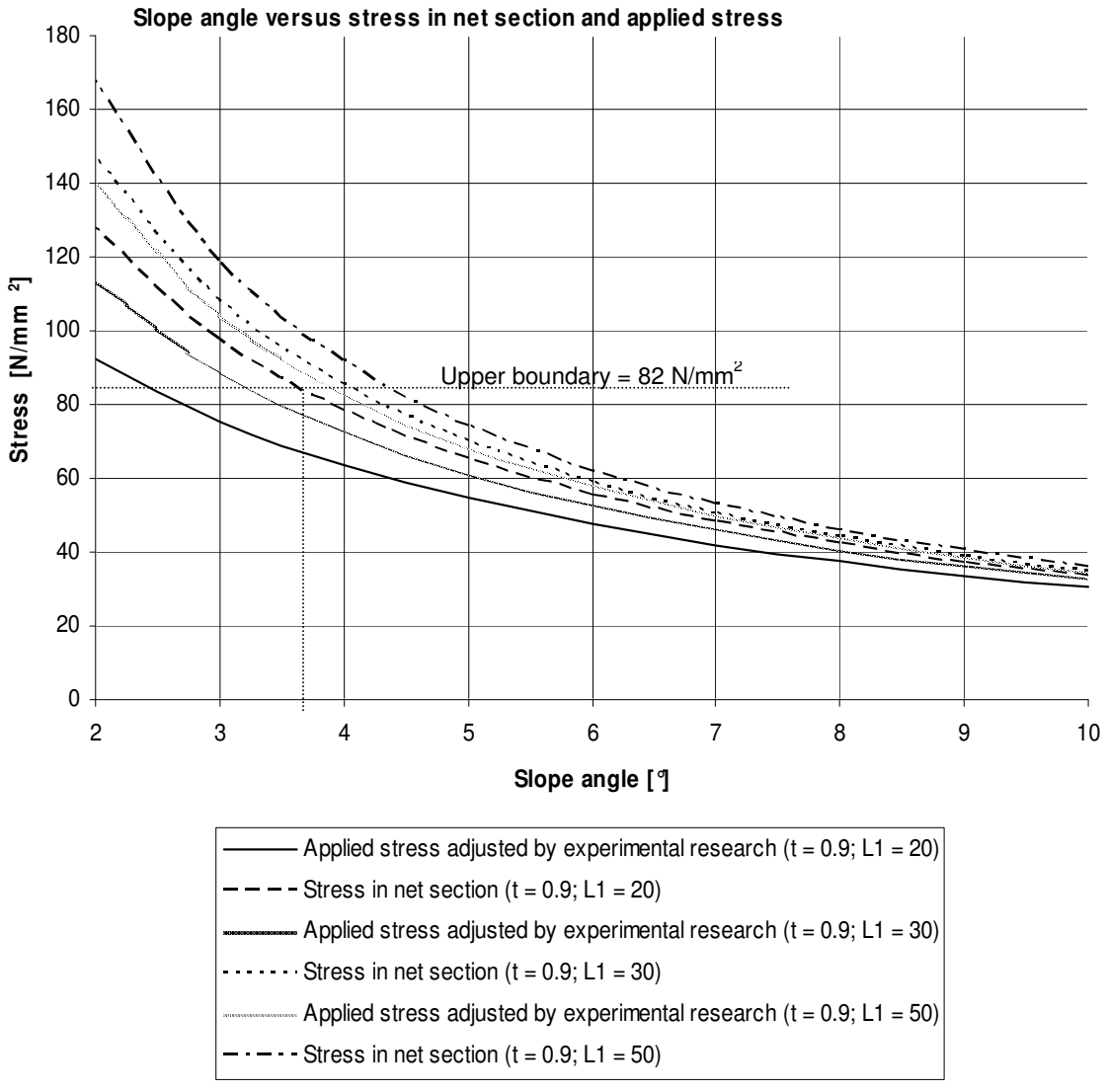

Note: applied stress adjusted to experimental research computed according to eq.F.3; stress in net section computed according to eq.F.4

Figure F.4: Slope angle versus stress

It can be seen that up to an angle of approximately 3.7°, it is useful to reduce the angle (finger length = 20 mm). Further, it can be seen that increasing the finger length at a slope angle of 3.7° is useless since the stress in the net section becomes too high.

F.4.2 Influence of Finger Length (or Pitch) on Stress in Net Section and Applied Stress

The influence of the finger length (or pitch) on the stress in the net section and the applied stress can be investigated. The slope angle is held constant and hence the pitch will also vary. In Figure F.5 the geometry is represented for three different finger-joints ($L_{1A}<L_{1b}<L_{1c}$). It can be seen that the pitch varies. It is assumed that the minimum tip width is 0.9 mm constantly.

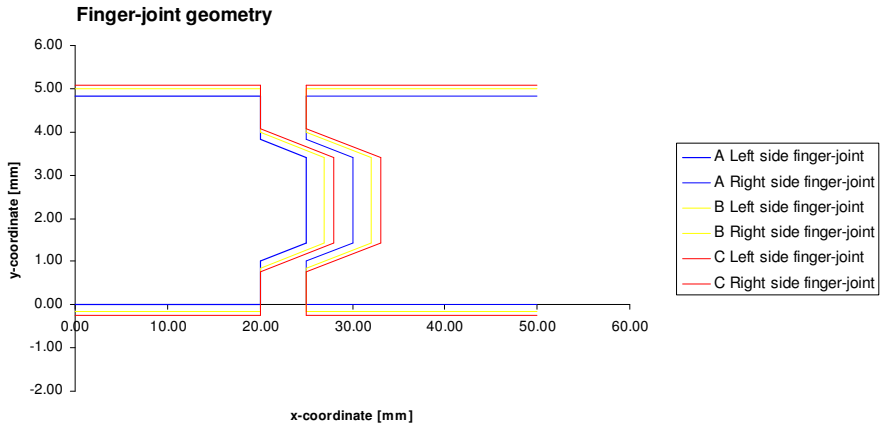

Figure F.5: Finger joint geometry – variable = finger length

The finger length versus the normal stress in the net section and the applied stress is shown in Figure F.6.

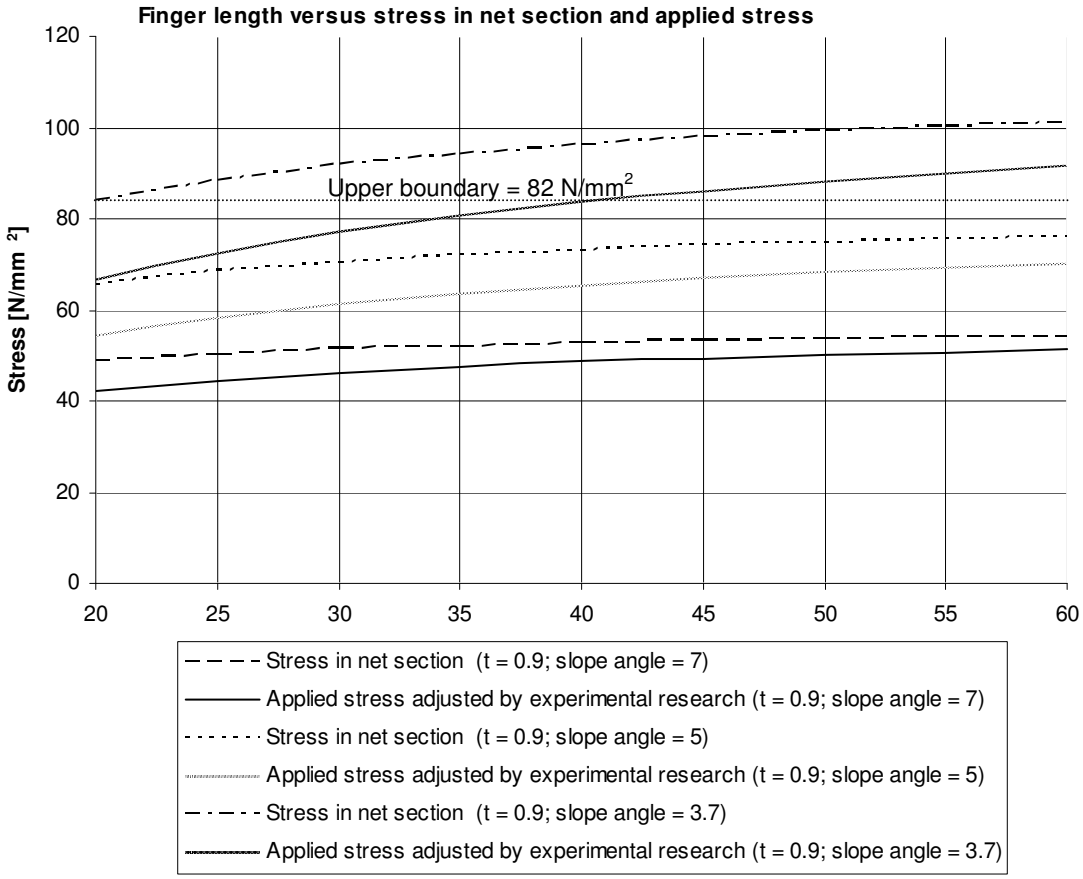

Note: applied stress adjusted to experimental research computed according to eq.F.3; stress in net section computed according to eq.F.4

Figure F.6: Finger length versus stress

In general it can be seen that, with slope and tip thickness held constant, joint strength increases with increase in pitch (and length) but at a decreasing rate. Again, it can be seen that by applying a slope angle of 3.7°, it is useless to apply a finger length longer than 20 mm.

Based on this analysis it can be said that the slope angle of the used profile has to be reduced to 3.7°. It is believed that reducing the angle has also a positive effect on the chance of splitting of the bamboo at the finger roots when end pressure is applied during manufacturing. The stress which can be applied is 66.6 N/mm^2 (base on the following variables: finger length (L_1 = 20 mm), pitch (P = 4.39 mm), slope (θ = 3.7°) and tip thickness (t = 0.9 mm) which makes the joint efficiency 81%.

Appendix G: Prediction of Probability of Nodes Coinciding

In this appendix the probability of nodes coinciding is predicted by Monte Carlo simulations and is related to chapter 6.

G.1 Configuration of Nodes along the Culm Height

The distribution of nodes along the culm height is not uniform. The internode length increases from the base towards the middle part of the culm and then decreases further upwards. Parametric functional data analysis on several samples of 15 botanical species has lead to the following expressions for the internode length as a function of the internode number. The following expression holds for the lower part of a culm:

$$L_{i;lower} = 25.13 + 4.8080 \cdot x - 0.0774 \cdot x^2 \qquad \text{eq.G.1}$$

and for the upper part:

$$L_{i;upper} = 178.84 - 2.3927 \cdot x + 0.0068 \cdot x^2 \qquad \text{eq.G.2}$$

where:

$L_{i;lower}$ = internode length lower part of the culm [%]
$L_{i;upper}$ = internode length upper part of the culm [%]
x = total number of internodes [%]

Phyllostachys pubescens contains out of 73 nodes. It is assumed that the height of a culm is 20 m and hence, the maximum length of an internode is 457 mm. The plot of the culm height versus the internode length by using the formula for the lower part is shown in Figure G.1.

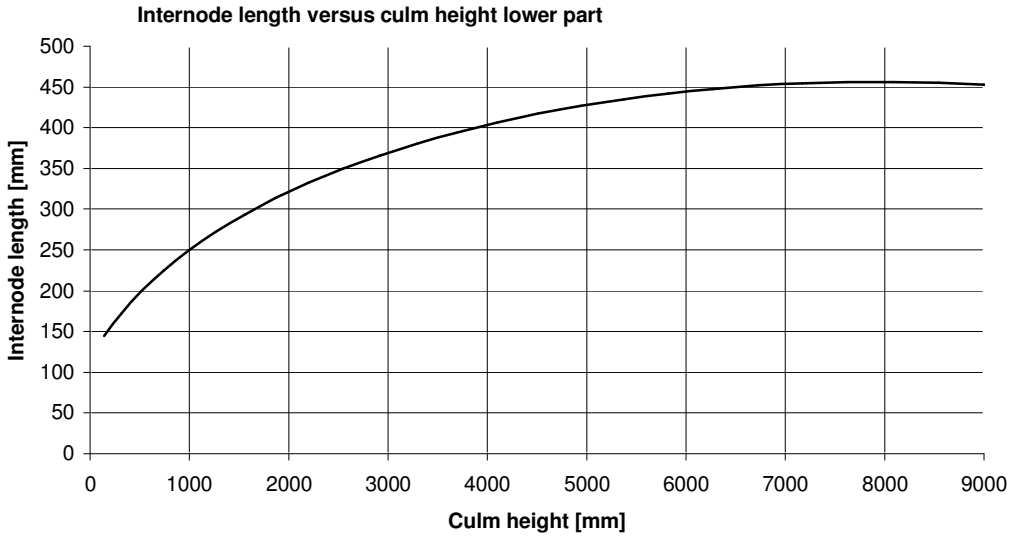

Figure G.1: Plot of internode length versus culm height lower part

G.2 Configuration of Nodes along the Strip Length

It is assumed that the first 9 m of the culm is cut into required lengths of 1 m after which it is split into strips, see Figure G.2. Additionally, since culms are not alike it is assumed that the length of the internodes is normally distributed around the values given by the expressions in eq.G.1 and eq.G.2. Furthermore, the position of the first saw cut is assumed to be uniformly distributed on the interval [0, 1000]. Hence, the coordinates of nodes in relation to the saw cuts vary and the number of different strips is infinitely.

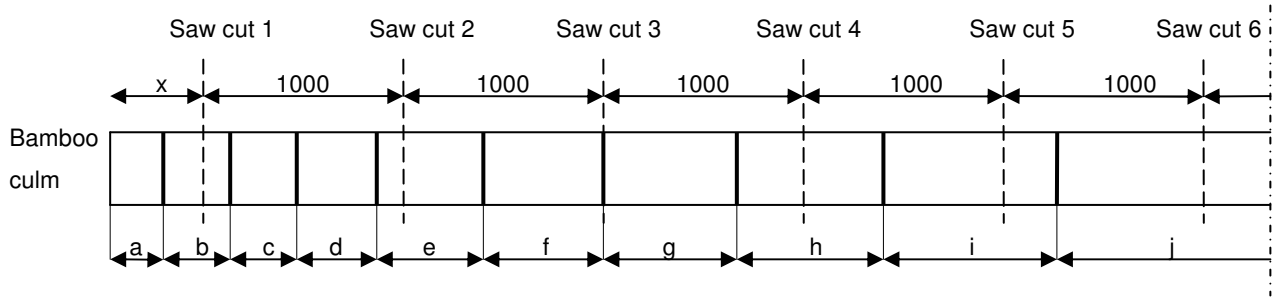

Figure G.2: Configuration of nodes along the strip length

G.3 Numerical Simulations

Strips are randomly assembled into laminations. The probability of *at least* a certain percentage of nodes coinciding within a certain area (denoted interaction area), expressed in relation to the total cross-section, within *at least* one section, can be computed. This problem is to complex to solve analytically since multidimensional integrals with complex boundary conditions are involved. The problem was simulated by the Monte Carlo method. A program was written in MATLAB 6.1 to simulate the assembly of strips into laminations. The following assumptions are made:

- The probability of strips originating from the same culm assembled into the same lamination is negligible, in other words, strips are independent from each other.
- Strips are randomly assembled into laminations.

Based on these assumptions, it is justified to assemble the lamination out of one strip of each culm. Hence, the first saw cut is located uniformly on the interval [0, 8000] and the second saw cut is 1000 mm shifted in relation to the first. The probability is estimated by:

$$\hat{p} = \frac{X}{n} \qquad \text{eq.G.3}$$

where:

$\hat{p}$ = estimated probability [-]

X = the number of laminations that belong to the class of interest [-]

n = number of simulations/sample size [-]

It can be assumed that X is binomially distributed. According to the central limit theorem, the estimator $\hat{p}$ is approximately normally distributed with expected value:

$$\mu = E(\hat{p}) = \frac{n \cdot p}{n} = p \qquad \text{eq.G.4}$$

where:

μ = mean [-]

p = probability [-]

The variance of the estimator can be computed by:

$$\sigma^2 = V(\hat{p}) = \frac{n \cdot p \cdot (1-p)}{n^2} = \frac{p \cdot (1-p)}{n} \qquad \text{eq.G.5}$$

where:

σ^2 = variance [-]

The number of simulations, based on an accuracy of two digits, follows from:

$$3 \cdot \sigma = 0.005$$
$$3 \cdot \sqrt{\frac{p \cdot (1-p)}{n}} = 0.005 \qquad \text{eq.G.6}$$
$$\Rightarrow n = \left(\frac{3}{0.005}\right)^2 \cdot p \cdot (1-p)$$

The maximum number of simulations should be used, hence:

$$n = \left(\frac{3}{0.005}\right)^2 \cdot 0.5 \cdot (1-0.5) = 90000 \qquad \text{eq.G.7}$$

G.4 Parameter Study

Since there are several variables involved it is important to known in what way each variable affects the estimated probability. The influence of the following variables was investigated:

- Standard deviation of nodes
- Interaction area (nodes are assumed to interact within a certain distance from each other)
- Number of strips (size effect)

To investigate the influence of the standard deviation of nodes and the interaction area, a lamination consisted out of 12 strips was considered. It was found that the standard deviation of nodes within a range of 0 to 60 mm did not have any influence on the results. This might be explained by the fact that the standard deviation of nodes compared to the standard deviation of the first saw cut on the interval [0, 8000] is very small. It is believed that, when the standard deviation increases, the influence on the result becomes significant.

On the other hand, the interaction area had a considerable effect on the results within a range of 10 to 60 mm. This is shown in Figure G.3. It seems that the graphs are horizontally shifted in relation to each other.

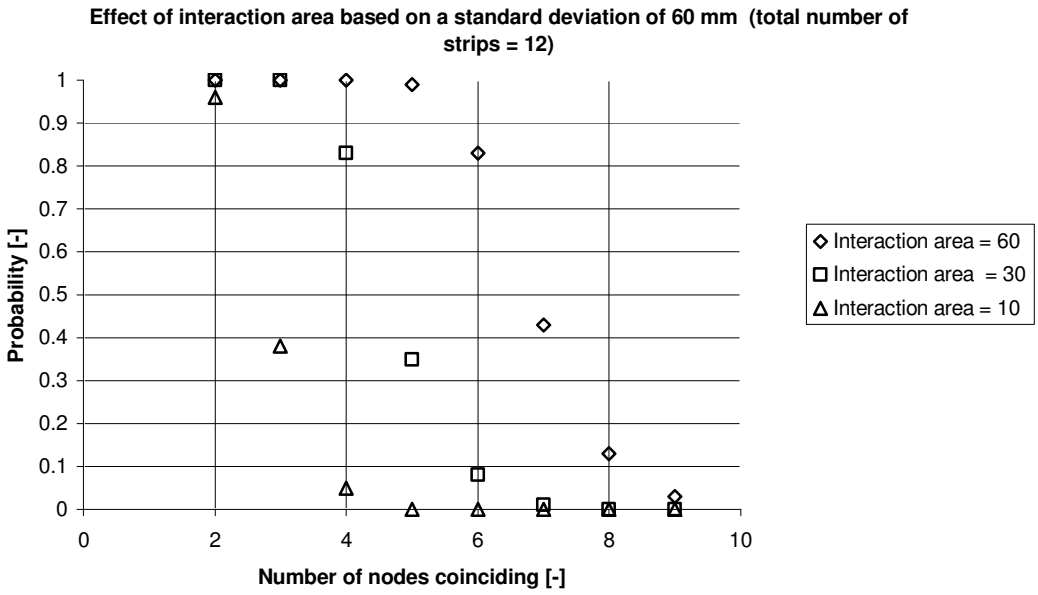

Figure G.3: Effect of interaction area based on a standard deviation of 60 mm

The effect of size was investigated by varying the total number of strips and the percentage of nodes coinciding was held constant. Due to memory capacity, percentages of 50% and 33% were chosen. These percentages do not resemble a practical situation and are only of academic interest. The results are shown in Figure G.4 and Figure G.5. It can be seen that the probability is affected by size. In contrast to wood, size has a positive influence on strength. It seems that if the number of strips converges to infinity, the probability converges to 0. This is convincing since it is believed that the possibilities of nodes coinciding will decrease when the total number of strips increases.

However, for the found value of k = 3.3% (see paragraph 6.3.5), the probability is not affected by size up to 400 strips, based on an accuracy of 1 digit and an area of influence of 50 mm.

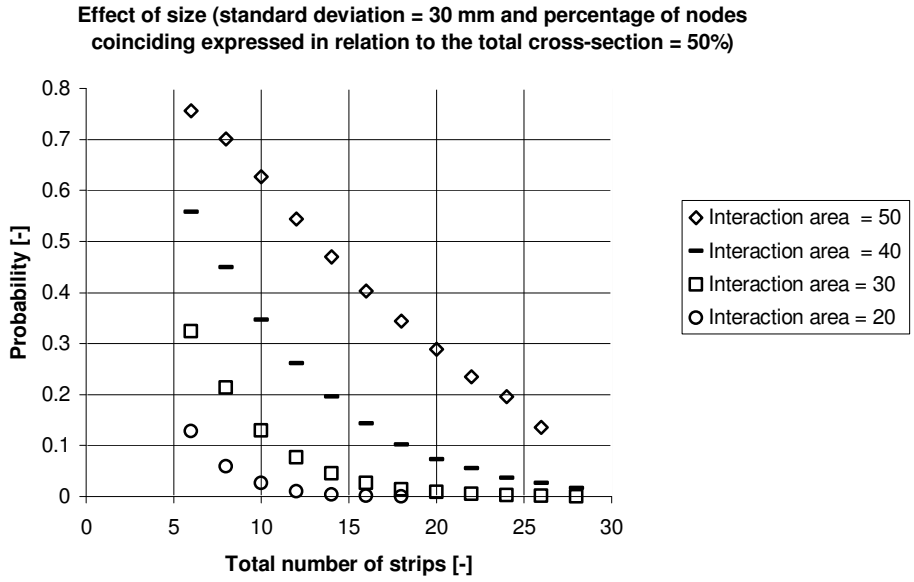

Figure G.4: Effect of size (standard deviation = 30 mm and percentage of nodes coinciding expressed in relation to the total cross-section = 50%).

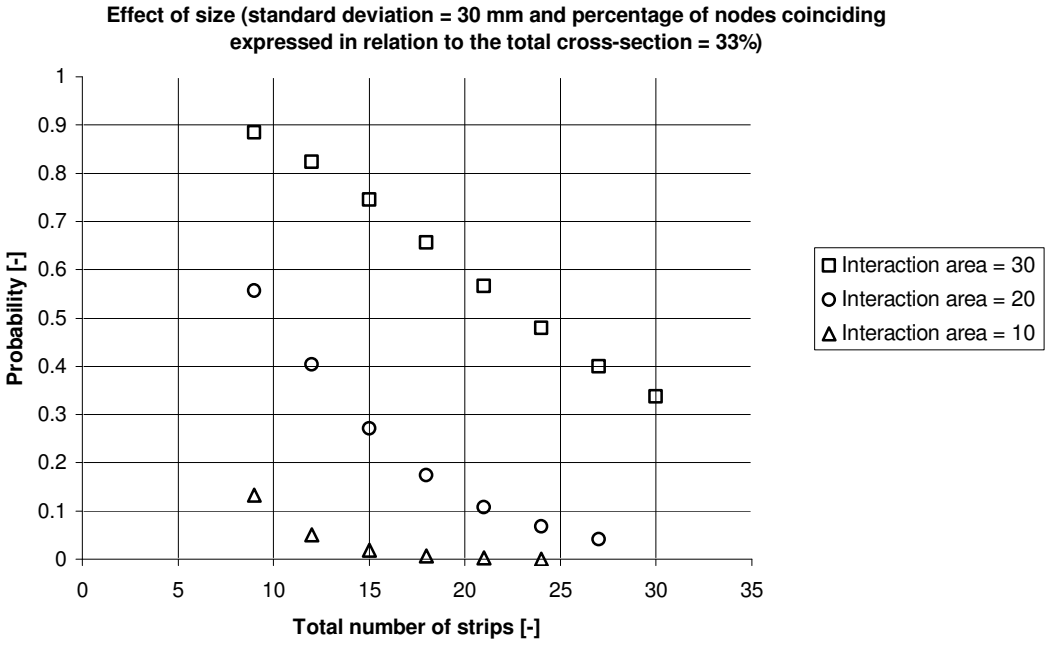

Figure G.5: Effect of size (standard deviation = 30 mm and percentage of nodes coinciding expressed in relation to the total cross-section = 33%).

Appendix H: Experimental and Statistical Results

H.1 Laminated Bamboo Loaded in Tension

H.1.1 Experimental Results: Tension Test on Triple-Layer Laminations

Table H.1: Properties of triple-layer laminations loaded in tension (sample A)

Test specimen [-]	$f_{t;0}$ [N/mm^2]	$E_{t;0}$ [N/mm^2]	MC [%]	ρ_0 [kg/m^3]
A(PhyII.Pub)-TT-I-01	102	10667	7.9	656
A(PhyII.Pub)-TT-I-02	64	8898	7.8	620
A(PhyII.Pub)-TT-I-03	65	8874	7.3	603
A(PhyII.Pub)-TT-I-04	82	10016	7.8	618
A(PhyII.Pub)-TT-I-05	-[1]	8870	7.7	580
A(PhyII.Pub)-TT-I-06	90	9370	7.8	591
A(PhyII.Pub)-TT-I-07	-[1]	8975	7.7	562
A(PhyII.Pub)-TT-I-08	-[1]	8932	7.8	658
A(PhyII.Pub)-TT-I-09	-[1]	10041	7.7	571
A(PhyII.Pub)-TT-I-10	69	10102	7.8	603
A(PhyII.Pub)-TT-I-11	83	9470	7.4	631
A(PhyII.Pub)-TT-I-12	99	10880	7.7	585

Note: [1]) failed within supporting area

Table H.2: Properties of triple-layer laminations loaded in tension (sample C)

Test specimen [-]	$f_{t;0}$ [N/mm^2]	$E_{t;0}$ [N/mm^2]	MC [%]	ρ_0 [kg/m^3]
C(PhyII.Pub)-TT-I-01	-[1]	9832	8.7	692
C(PhyII.Pub)-TT-I-02	91	8967	9.2	619
C(PhyII.Pub)-TT-I-03	85	9243	8.3	670
C(PhyII.Pub)-TT-I-04	-[1]	10439	8.6	669
C(PhyII.Pub)-TT-I-05	82	10337	8.2	679
C(PhyII.Pub)-TT-I-06	86	9457	8.4	644
C(PhyII.Pub)-TT-I-07	93	9778	8.0	650
C(PhyII.Pub)-TT-I-08	-[1]	9174	9.0	645
C(PhyII.Pub)-TT-I-09	102	10472	8.4	695
C(PhyII.Pub)-TT-I-10	93	9147	8.3	682
C(PhyII.Pub)-TT-I-11	-[1]	10090	8.5	647
C(PhyII.Pub)-TT-I-12	-[1]	8904	8.2	633
C(PhyII.Pub)-TT-I-13	94	9528	9.0	701
C(PhyII.Pub)-TT-I-14	-[1]	8805	8.4	615
C(PhyII.Pub)-TT-I-15	-[1]	8378	8.2	661

Note: [1]) failed within supporting area

H.1.2 Statistical Results: Paired Samples T Test (Density)

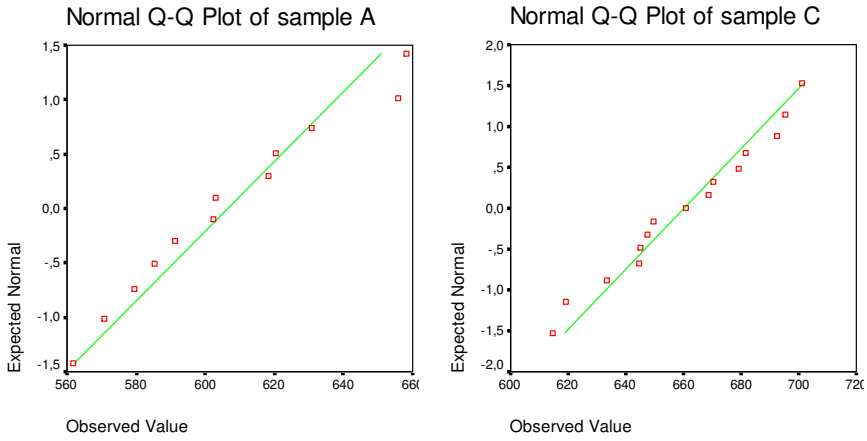

Figure H.1: Normal probability plots of sample A and C

Table H.3: Results of tests of normality

SAMPLE	Kolmogorov-Smirnov[2]			Shapiro-Wilk		
	Statistic	df	Sig.	Statistic	df	Sig.
A	.126	12	.200[1]	.953	12	.685
C	.119	15	.200[1]	.962	15	.725

Note: [1]) this is a lower bound of the true significance; [2]) lilliefors Significance Correction

Table H.4: Results of independent samples t test

	Levene's Test for Equality of Variances		t-test for Equality of Means						
	F	Sig.	t	df	Sig. (2-tailed)	Mean Difference	Std. Error Difference	95% Confidence Interval of the Difference	
								Lower	Upper
Equal variances assumed	.231	.635	-4.799	25	.000	-53.7313	11.19638	-76.79071	-30.67195
Equal variances not assumed			-4.718	21.898	.000	-53.7313	11.38788	-77.35471	-30.10796

H.1.3 Statistical Results: Paired Samples T Test (Tensile Strength)

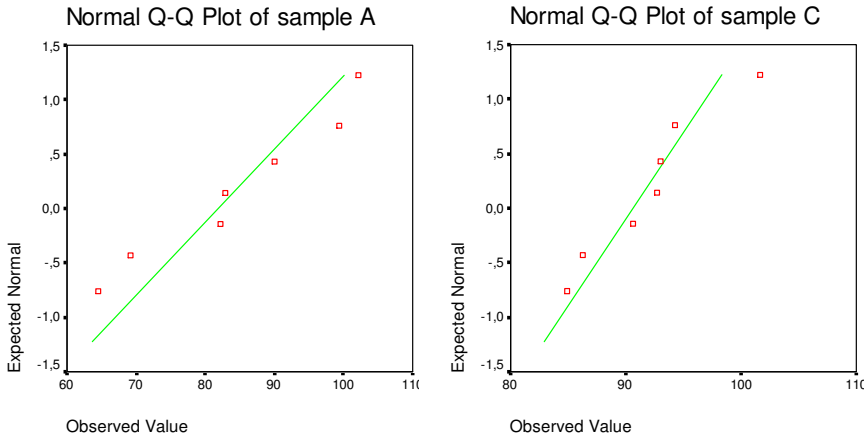

Figure H.2: Normal probability plots of sample A and C

Table H.5: Results of tests of normality

SAMPLE	Kolmogorov-Smirnov[2]			Shapiro-Wilk		
	Statistic	df	Sig.	Statistic	df	Sig.
A	.177	8	.200[1]	.909	8	.345
C	.156	8	.200[1]	.967	8	.871

Note: [1]) this is a lower bound of the true significance; [2]) lilliefors Significance Correction

Table H.6: Results of independent samples t test

	Levene's Test for Equality of Variances		t-test for Equality of Means						
	F	Sig.	t	df	Sig. (2-tailed)	Mean Difference	Std. Error Difference	95% Confidence Interval of the Difference	
								Lower	Upper
Equal variances assumed	5.320	.037	-1.531	14	.148	-8.7612	5.72132	-21.03226	3.50976
Equal variances not assumed			-1.531	9.438	.158	-8.7612	5.72132	-21.61277	4.09027

H.1.4 Statistical Results: Paired Samples T Test (Modulus of Elasticity in Tension)

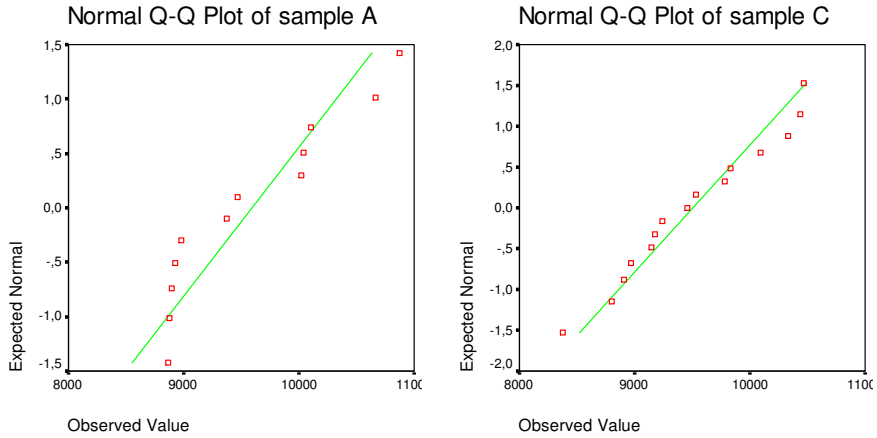

Figure H.3: Normal probability plots of sample A and C

Table H.7: Results of tests of normality

SAMPLE	Kolmogorov-Smirnov[2]			Shapiro-Wilk		
	Statistic	df	Sig.	Statistic	df	Sig.
A	.218	12	.122	.868	12	.062
C	.124	15	.200[1]	.958	15	.652

Note: [1]) this is a lower bound of the true significance; [2]) lilliefors Significance Correction

Table H.8: Results of independent samples t test

	Levene's Test for Equality of Variances		t-test for Equality of Means						
	F	Sig.	t	df	Sig. (2-tailed)	Mean Difference	Std. Error Difference	95% Confidence Interval of the Difference	
								Lower	Upper
Equal variances assumed	.582	.453	.333	25	.742	87.7522	263.80736	-455.56927	631.07360
Equal variances not assumed			.328	22.138	.746	87.7522	267.77937	-467.38747	642.89180

H.2 Influence of Joints on Tensile Strength and Stiffness

H.2.1 Experimental Results: Tension Test on Scarf-Jointed Triple-Layer Laminations

Table H.9: Properties of scarf-jointed triple-layer laminations loaded in tension (sample B)

Test specimen [-]	$f_{t;j;0}$ [N/mm^2]	E_c[3] [N/mm^2]	MC [%]	ρ_0 [kg/m^3]
B(PhyllPub)-TT-II(sj)-01	96	9714	8.1	601
B(PhyllPub)-TT-II(sj)-02	79	8047	7.6	603
B(PhyllPub)-TT-II(sj)-03	90	8059	8.0	503
B(PhyllPub)-TT-II(sj)-04	81	8365	7.5	731
B(PhyllPub)-TT-II(sj)-05	71	7335	8.2	593
B(PhyllPub)-TT-II(sj)-06	57	8695	7.8	664
B(PhyllPub)-TT-II(sj)-07	92	-[2]	7.8	573
B(PhyllPub)-TT-II(sj)-08	74	8063	7.6	610
B(PhyllPub)-TT-II(sj)-09	50	7384	8.5	585
B(PhyllPub)-TT-II(sj)-10	78	8270	7.7	636
B(PhyllPub)-TT-II(sj)-11	57	8184	7.7	649
B(PhyllPub)-TT-II(sj)-12	89	9764	7.9	663
B(PhyllPub)-TT-II(sj)-13	-[1]	-[2]	7.6	545
B(PhyllPub)-TT-II(sj)-14	-[1]	8513	7.9	598
B(PhyllPub)-TT-II(sj)-15	-[1]	8636	7.5	581

Note: [1]) failed within supporting area; [2]) not measured; [3]) see eq.5.5

H.2.2 Experimental Results: Tension Test on Finger-Jointed Triple-Layer Laminations

Table H.10: Properties of finger-jointed triple-layer laminations loaded in tension (sample A)

Test specimen [-]	$f_{t;j;0}$ [N/mm^2]	E_c[2] [N/mm^2]	MC [%]	ρ_0 [kg/m^3]
A(Phyll.Pub)-TT-II(fj)-01	25	8300	7.6	695
A(Phyll.Pub)-TT-II(fj)-02	26	-[1]	7.7	681
A(Phyll.Pub)-TT-II(fj)-03	35	8875	7.7	651
A(Phyll.Pub)-TT-II(fj)-04	35	9784	7.6	674
A(Phyll.Pub)-TT-II(fj)-05	28	10383	7.6	665
A(Phyll.Pub)-TT-II(fj)-06	29	9531	7.6	680
A(Phyll.Pub)-TT-II(fj)-07	35	8962	7.8	649
A(Phyll.Pub)-TT-II(fj)-08	38	10519	7.8	662
A(Phyll.Pub)-TT-II(fj)-09	45	10274	8.0	657
A(Phyll.Pub)-TT-II(fj)-10	40	9191	7.6	652
A(Phyll.Pub)-TT-II(fj)-11	31	9734	7.7	653

Note:[1]) discarded; [2]) see eq.5.5

Table H.11: Properties of finger-jointed triple-layer laminations loaded in tension (sample C)

Test specimen [-]	$f_{t;j;0}$ [N/mm^2]	E_c[2] [N/mm^2]	MC [%]	ρ_0 [kg/m^3]
C(Phyll.Pub)-TT-II(fj)-01	48	9732	8.6	648
C(Phyll.Pub)-TT-II(fj)-02	32	9905	8.7	677
C(Phyll.Pub)-TT-II(fj)-03	41	8747	8.9	679
C(Phyll.Pub)-TT-II(fj)-04	46	8457	8.9	694
C(Phyll.Pub)-TT-II(fj)-05	31	9415	8.8	674
C(Phyll.Pub)-TT-II(fj)-06	21	8953	8.8	648
C(Phyll.Pub)-TT-II(fj)-07	37	8753	8.8	652
C(Phyll.Pub)-TT-II(fj)-08	42	10121	8.8	678
C(Phyll.Pub)-TT-II(fj)-09	48	8902	8.7	651
C(Phyll.Pub)-TT-II(fj)-10	-[1]	8522	8.7	650
C(Phyll.Pub)-TT-II(fj)-11	18	9523	8.3	659
C(Phyll.Pub)-TT-II(fj)-12	53	8598	8.5	669

Note: [1]) failed within supporting area; [2]) see eq.5.5

H.2.3 Experimental Results: Tension test on Finger-Jointed Triple-Layer Laminations in Combination with ESPI Measurements

Table H.12: Failure load and tensile strength of finger-jointed triple-layer laminations loaded in tension (sample C)

Test specimen [-]	F_{max} [kN]	$f_{t;j;0}$ [N/mm^2]
C(Phyll.Pub)-TT-II(fj)-13	27	32
C(Phyll.Pub)-TT-II(fj)-14	-[1]	-[1]
C(Phyll.Pub)-TT-II(fj)-15	27	33
C(Phyll.Pub)-TT-II(fj)-16	43	55
C(Phyll.Pub)-TT-II(fj)-17	30	38

Note: [1]) discarded

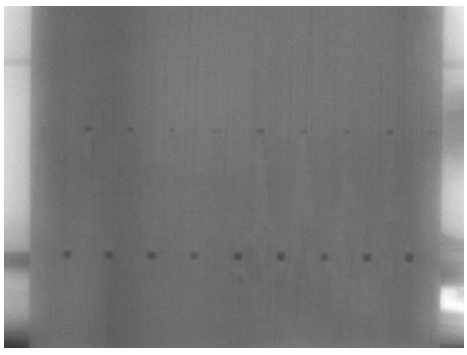

Figure H.4: Photo of illuminated area test specimen C(Phyll.Pub)-TT-II(fj)-13

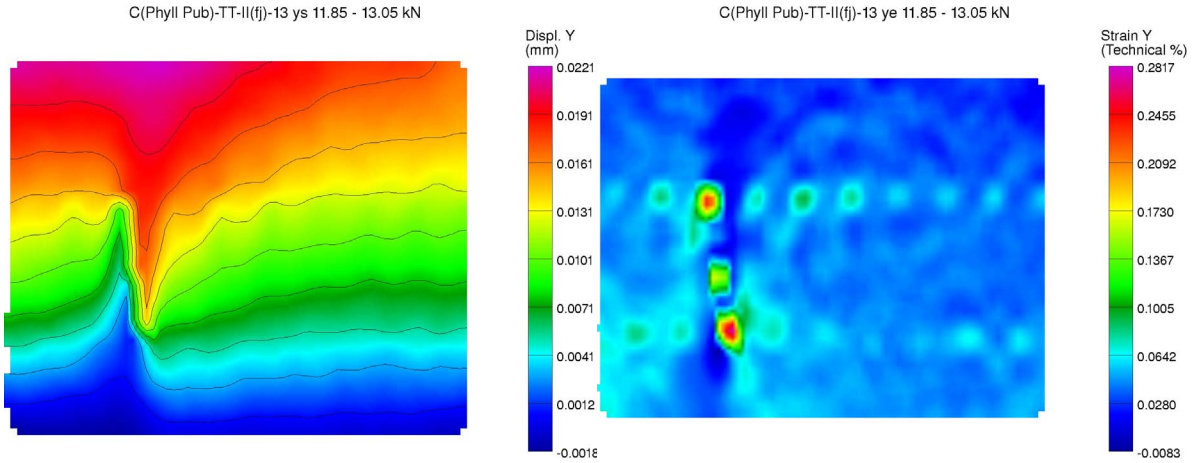

Figure H.5: Displacement and strain of test specimen C(Phyll.Pub)-TT-II(fj)-13; load-phase: 11.85-13.05 kN

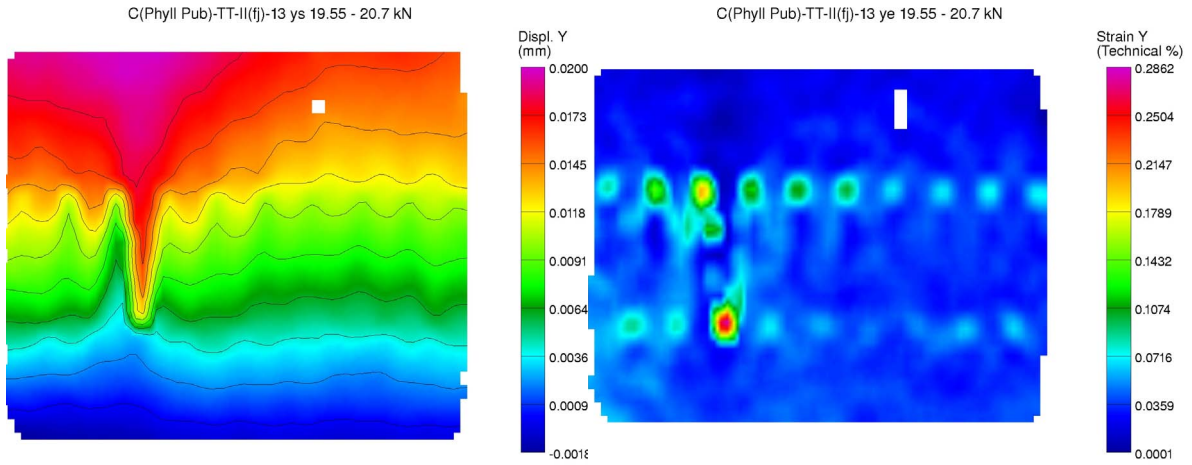

Figure H.6: Displacement and strain of test specimen C(Phyll.Pub)-TT-II(fj)-13; load-phase: 19.55-20.7 kN

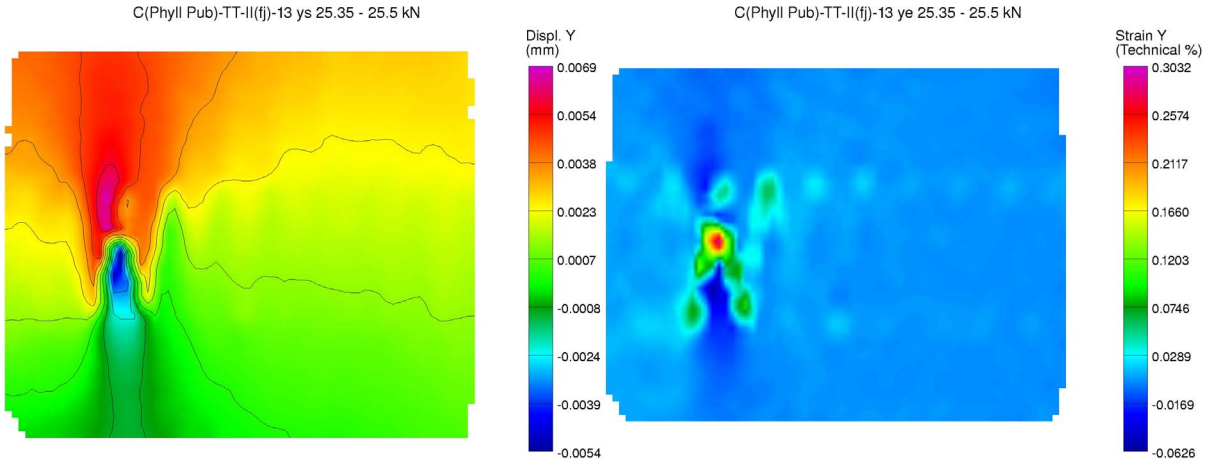

Figure H.7: Displacement and strain of test specimen C(Phyll.Pub)-TT-II(fj)-13; load-phase: 25.35-25.5 kN

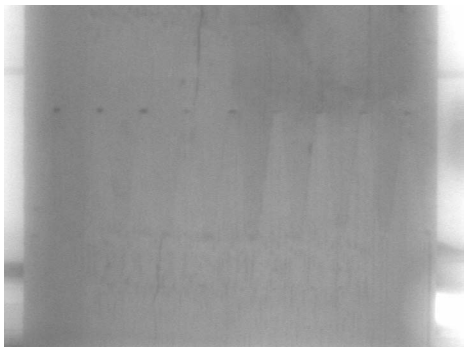

Figure H.8: Photo of illuminated area test specimen C(Phyll.Pub)-TT-II(fj)-15

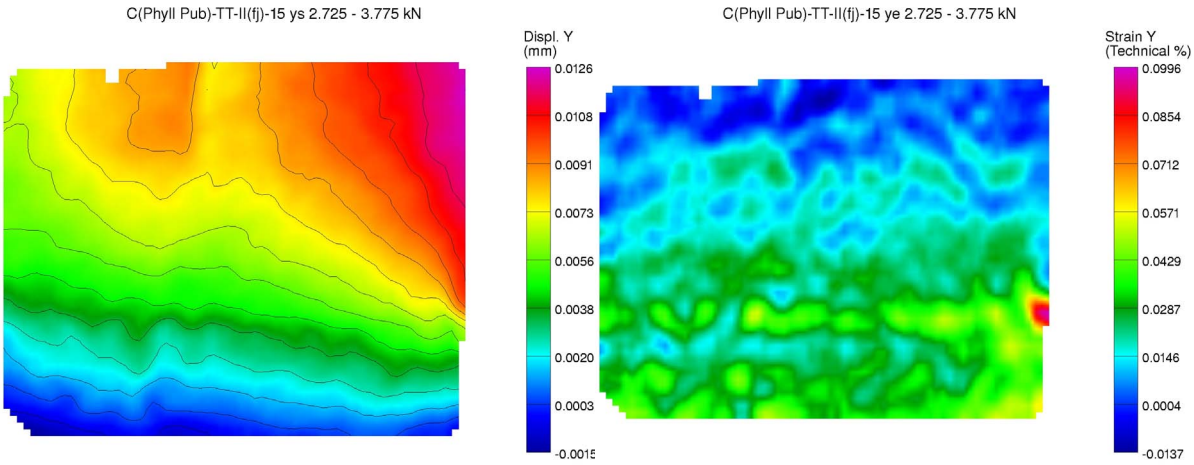

Figure H.9: Displacement and strain of test specimen C(Phyll.Pub)-TT-II(fj)-15; load-phase: 2.725-3.3775 kN

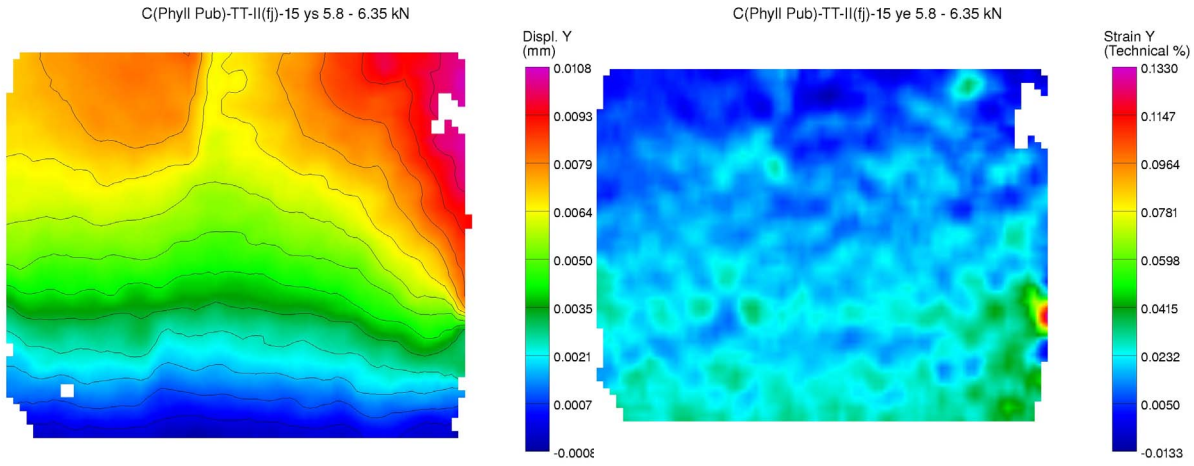

Figure H.10: Displacement and strain of test specimen C(Phyll.Pub)-TT-II(fj)-15; load-phase: 5.8-6.35 kN

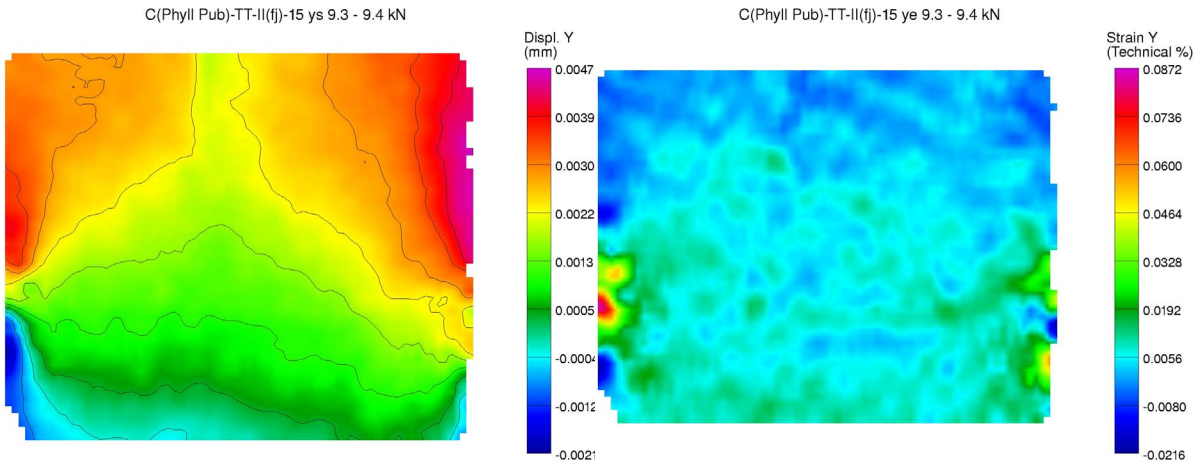

Figure H.11: Displacement and strain of test specimen C(Phyll.Pub)-TT-II(fj)-15; load-phase: 9.3-9.4kN

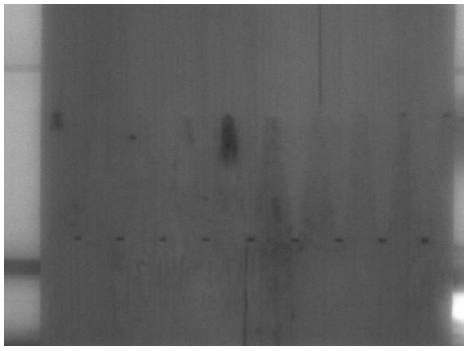

Figure H.12: Photo of illuminated area test specimen C(Phyll.Pub)-TT-II(fj)-16

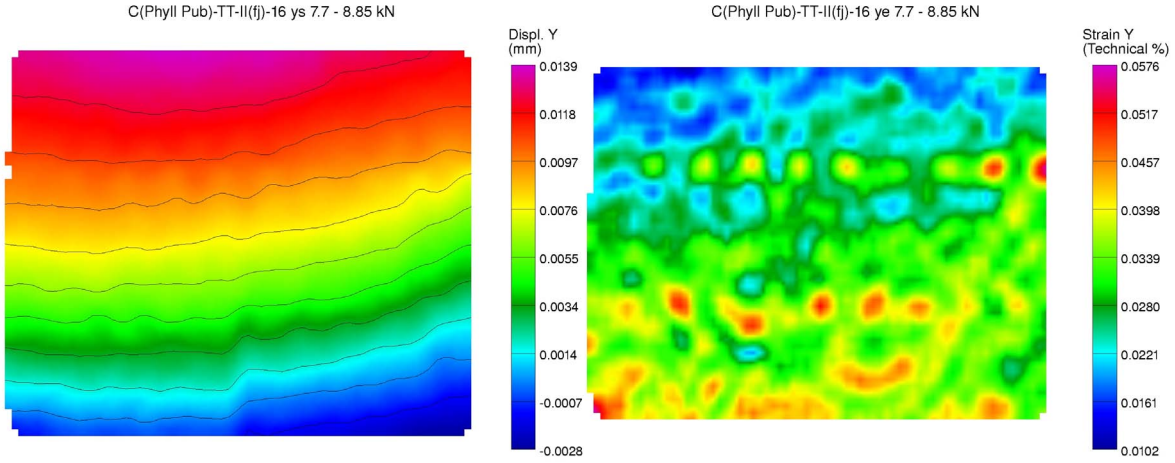

Figure H.13: Displacement and strain of test specimen C(Phyll.Pub)-TT-II(fj)-16; load-phase: 7.7-8.85 kN

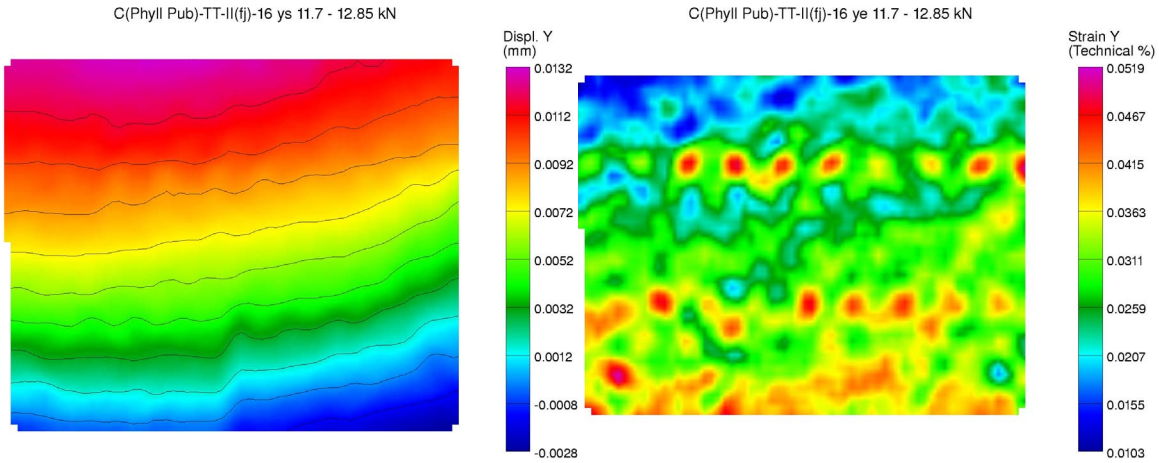

Figure H.14: Displacement and strain of test specimen C(Phyll.Pub)-TT-II(fj)-16; load-phase: 11.7-12.85 kN

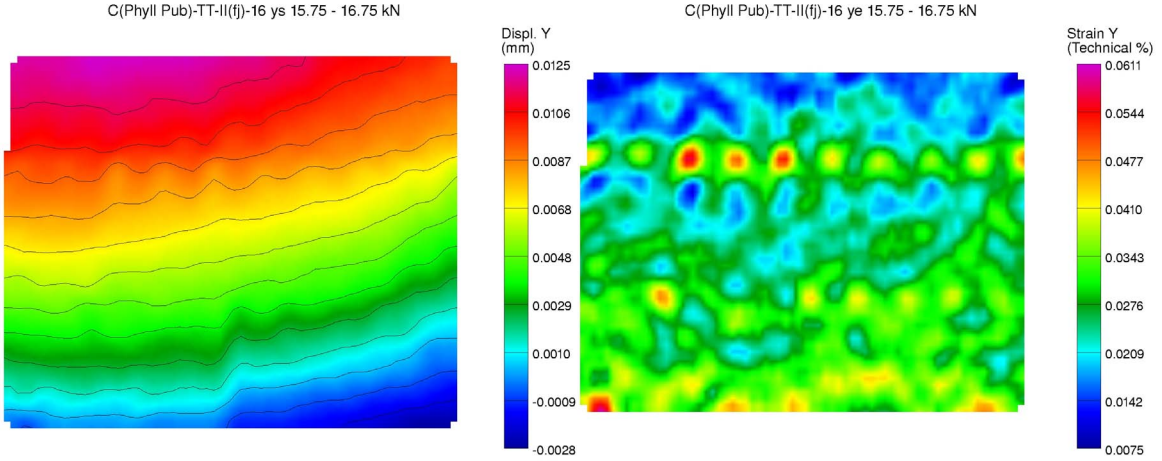

Figure H.15: Displacement and strain of test specimen C(Phyll.Pub)-TT-II(fj)-16; load-phase: 15.75-16.75 kN

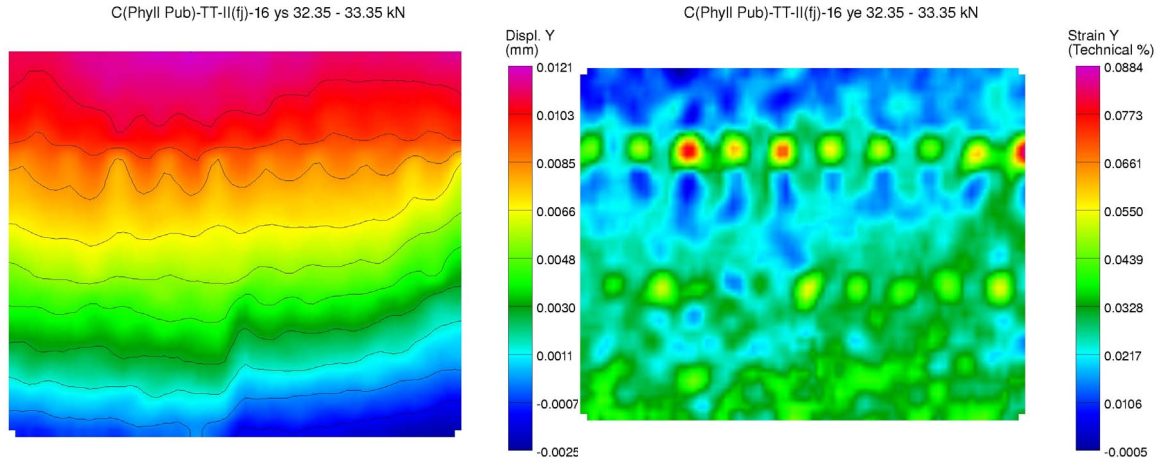

Figure H.16: Displacement and strain of test specimen C(Phyll.Pub)-TT-II(fj)-16; load-phase: 32.35-33.35 kN

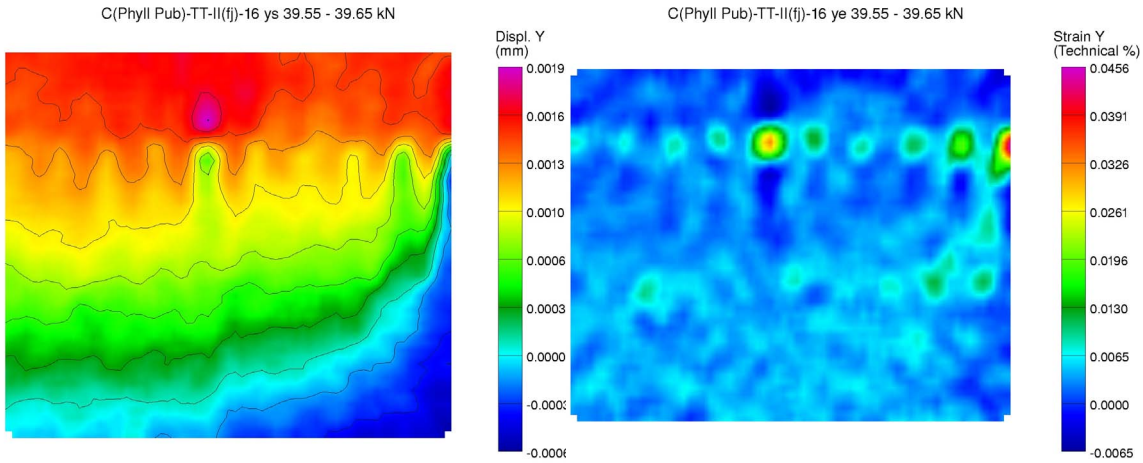

Figure H.17: Displacement and strain of test specimen C(Phyll.Pub)-TT-II(fj)-16; load-phase: 39.55-39.65 kN

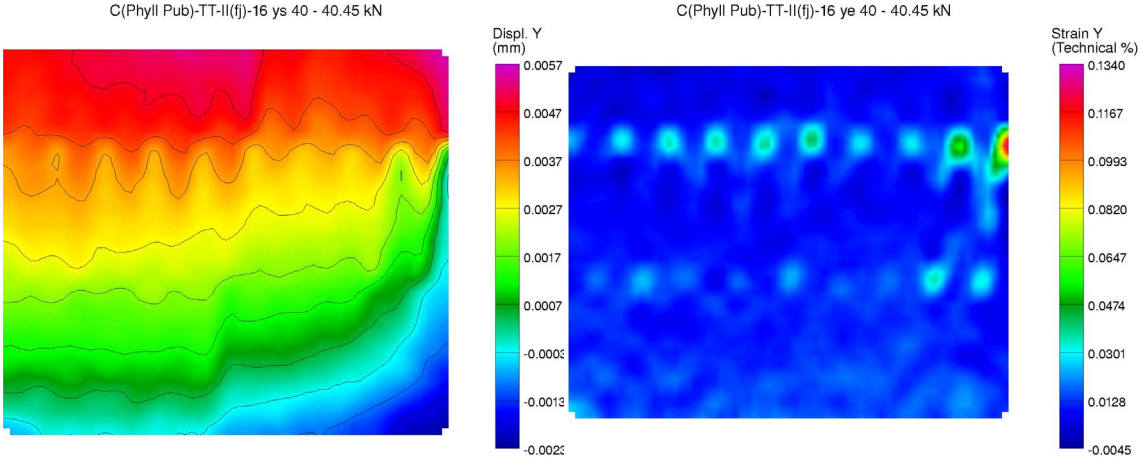

Figure H.18: Displacement and strain of test specimen C(Phyll.Pub)-TT-II(fj)-16; load-phase: 40-40.45 kN

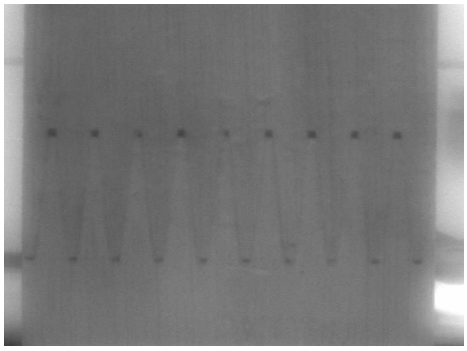

Figure H.19: Photo of illuminated area test specimen C(Phyll.Pub)-TT-II(fj)-17

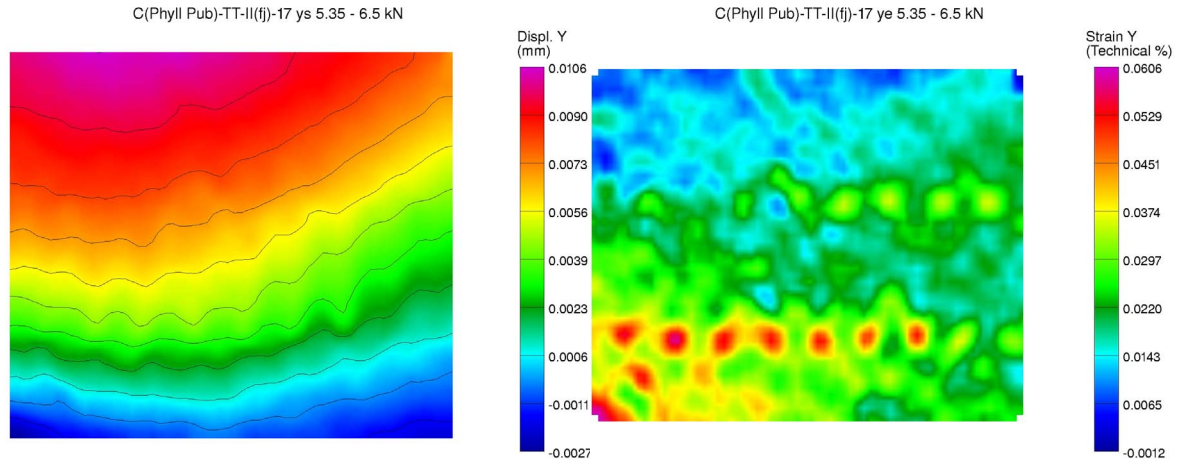

Figure H.20: Displacement and strain of test specimen C(Phyll.Pub)-TT-II(fj)-17; load-phase: 5.35-6.5 kN

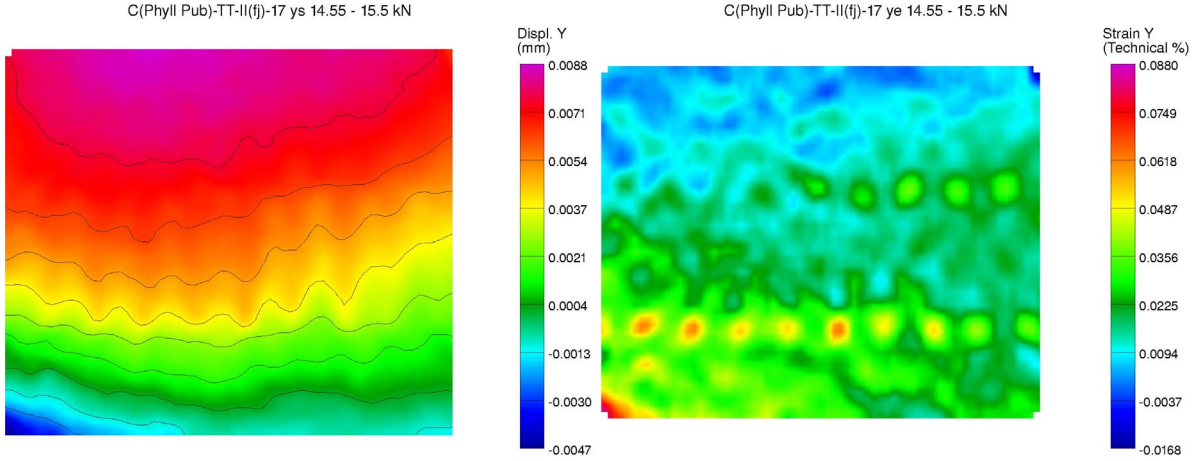

Figure H.21: Displacement and strain of test specimen C(Phyll.Pub)-TT-II(fj)-17; load-phase: 14.55-15.55 kN

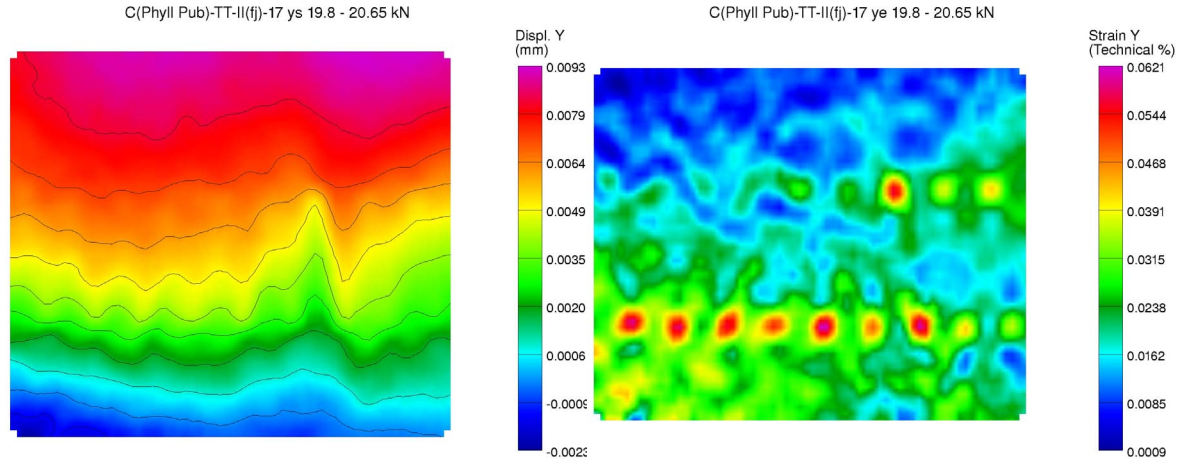

Figure H.22: Displacement and strain of test specimen C(Phyll.Pub)-TT-II(fj)-17; load-phase: 19.8-20.65 kN

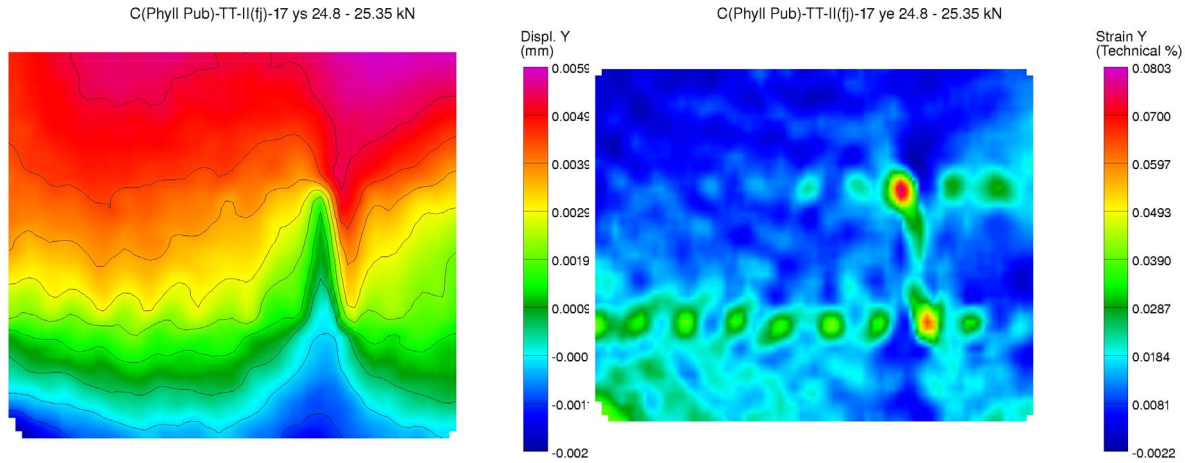

Figure H.23: Displacement and strain of test specimen C(Phyll.Pub)-TT-II(fj)-17; load-phase: 24.8-25.35 kN

H.2.4 Statistical results: Paired Samples T Test (Density)

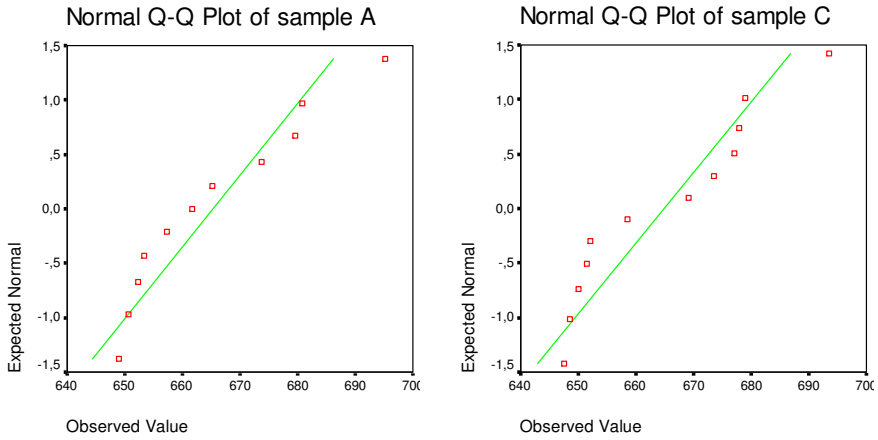

Figure H.24: Normal probability plots of sample A and C

Table H.13: Results of tests of normality

SAMPLE	Kolmogorov-Smirnov[2]			Shapiro-Wilk		
	Statistic	df	Sig.	Statistic	df	Sig.
A	.156	11	.200[1]	.910	11	.242
C	.213	12	.137	.892	12	.127

Note: [1]) this is a lower bound of the true significance; [2]) lilliefors Significance Correction

Table H.14: Results of independent samples t test

	Levene's Test for Equality of Variances		t-test for Equality of Means						
	F	Sig.	t	df	Sig. (2-tailed)	Mean Difference	Std. Error Difference	95% Confidence Interval of the Difference	
								Lower	Upper
Equal variances assumed	.155	.698	.075	21	.941	.4755	6.37320	-12.77834	13.72925
Equal variances not assumed			.075	20.891	.941	.4755	6.36768	-12.77107	13.72198

H.2.5 Statistical results: Paired Samples T Test (Tensile Strength of Finger-Jointed Laminations)

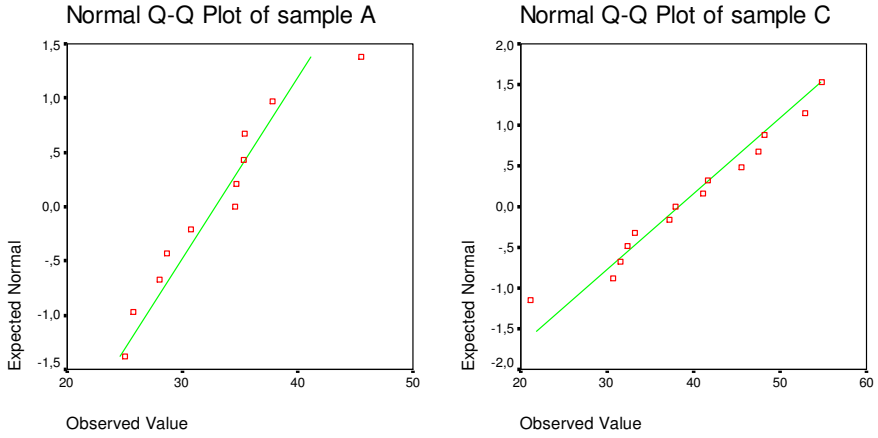

Figure H.25: Normal probability plots of sample A and C

Table H.15: Results of tests of normality

SAMPLE	Kolmogorov-Smirnov[2]			Shapiro-Wilk		
	Statistic	df	Sig.	Statistic	df	Sig.
A	.161	11	.200[1]	.936	11	.471
C	.108	15	.200[1]	.968	15	.834

Note: [1]) this is a lower bound of the true significance; [2]) lilliefors Significance Correction

Table H.16: Results of independent samples t test

	Levene's Test for Equality of Variances		t-test for Equality of Means						
	F	Sig.	t	df	Sig. (2-tailed)	Mean Difference	Std. Error Difference	95% Confidence Interval of the Difference	
								Lower	Upper
Equal variances assumed	3.415	.077	-1.502	24	.146	-5.4096	3.60251	-12.84485	2.02558
Equal variances not assumed			-1.633	22.706	.116	-5.4096	3.31289	-12.26779	1.44851

H.3 Influence of Nodes on Tensile Strength

H.3.1 Experimental Results: Tension Test on Strips

Table H.17: Experimental results: properties of nodes and internodes loaded in tension (sample C)

Specimen [-]	$f_{t;n;0}$ [N/mm^2]	$E_{t;n;0}$ [N/mm^2]	$E_{t;i;0}$ [N/mm^2]
C(Phyll.Pub)-TT-IV-01	52	-[3]	-[3]
C(Phyll.Pub)-TT-IV-02	91	-[3]	-[3]
C(Phyll.Pub)-TT-IV-03	65	-[3]	-[3]
C(Phyll.Pub)-TT-IV-04	58	-[3]	-[3]
C(Phyll.Pub)-TT-IV-05	79	-[3]	-[3]
C(Phyll.Pub)-TT-IV-06	91	-[3]	-[3]
C(Phyll.Pub)-TT-IV-07	60	-[3]	-[3]
C(Phyll.Pub)-TT-IV-08	89	-[3]	-[3]
C(Phyll.Pub)-TT-IV-09	94	-[3]	-[3]
C(Phyll.Pub)-TT-IV-10	101	-[3]	-[3]
C(Phyll.Pub)-TT-IV-11	92	8809	6617
C(Phyll.Pub)-TT-IV-12	102	9092	7445
C(Phyll.Pub)-TT-IV-13	53	6994	6341
C(Phyll.Pub)-TT-IV-14	65	8151	6221
C(Phyll.Pub)-TT-IV-15	-[1]	10190	7179
C(Phyll.Pub)-TT-IV-16	-[1]	11957	9701
C(Phyll.Pub)-TT-IV-17	90	-[3]	-[3]
C(Phyll.Pub)-TT-IV-18	95	-[3]	-[3]
C(Phyll.Pub)-TT-IV-19	76	-[3]	-[3]
C(Phyll.Pub)-TT-IV-20	75	-[3]	-[3]
C(Phyll.Pub)-TT-IV-21	61	-[3]	-[3]
C(Phyll.Pub)-TT-IV-22	81	-[3]	-[3]
C(Phyll.Pub)-TT-IV-23	80	-[3]	-[3]
C(Phyll.Pub)-TT-IV-24	-[2]	-[3]	8055

Note: [1]) failed within supporting area; [2]) not loaded until failure; [3]) not measured

H.3.2 Experimental Results: Tension Test on Single-Layer Laminations

Table H.18: Properties of single-layer laminations loaded in tension (sample C)

Specimen [-]	$f_{t;0}$ [N/mm^2]	$E_{t;0}$ [N/mm^2]
C(PhyII.Pub)-TT-V-01	-[1]	-[2]
C(PhyII.Pub)-TT-V-02	80	-[2]
C(PhyII.Pub)-TT-V-03	-[1]	8758
C(PhyII.Pub)-TT-V-04	68	-[2]
C(PhyII.Pub)-TT-V-05	-[1]	9213
C(PhyII.Pub)-TT-V-06	-[1]	10532
C(PhyII.Pub)-TT-V-07	83	9651
C(PhyII.Pub)-TT-V-08	81	10186
C(PhyII.Pub)-TT-V-09	128	10262
C(PhyII.Pub)-TT-V-10	-[1]	10780
C(PhyII.Pub)-TT-V-11	103	9803
C(PhyII.Pub)-TT-V-12	-[1]	11629
C(PhyII.Pub)-TT-V-13	102	10944
C(PhyII.Pub)-TT-V-14	100	9724
C(PhyII.Pub)-TT-V-15	-[1]	-[2]
C(PhyII.Pub)-TT-V-16	77	-[2]
C(PhyII.Pub)-TT-V-17	77	-[2]

Note: [1]) failed within supporting area; [2]) not measured

H.3.3 Experimental results: Tension Test on Single-Layer Laminations in Combination with ESPI Measurements

Table H.19: Failure load and tensile strength (sample C)

Specimen [-]	F_{max} [kN]	$f_{t;0}$ [N/mm^2]
C(PhyII.Pub)-TT-III-1	20	66
C(PhyII.Pub)-TT-III-2[2]	29	96
C(PhyII.Pub)-TT-III-3	26	-[1]
C(PhyII.Pub)-TT-III-4	22	71
C(PhyII.Pub)-TT-III-5[2]	24	79
C(PhyII.Pub)-TT-III-6	22	-[1]
C(PhyII.Pub)-TT-III-7	22	74

Note: [1]) failed within supporting area; [2]) failed within illuminated area

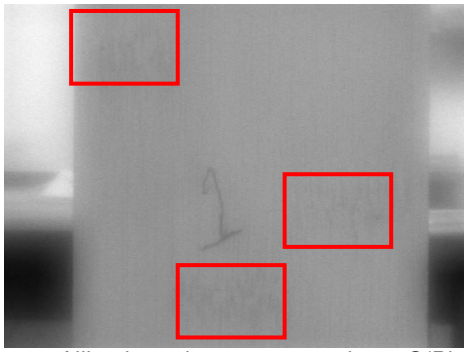

Figure H.26: Photo of illuminated area test specimen C(Phyll.Pub)-TT-III-1

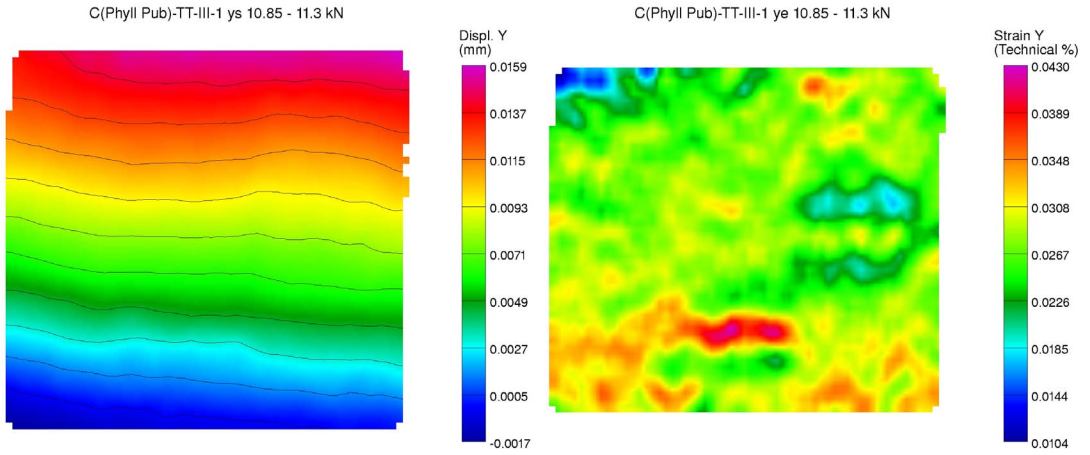

Figure H.27: Displacement and strain of test specimen C(Phyll.Pub)-TT-III-1; load-phase: 10.85-11.30 kN

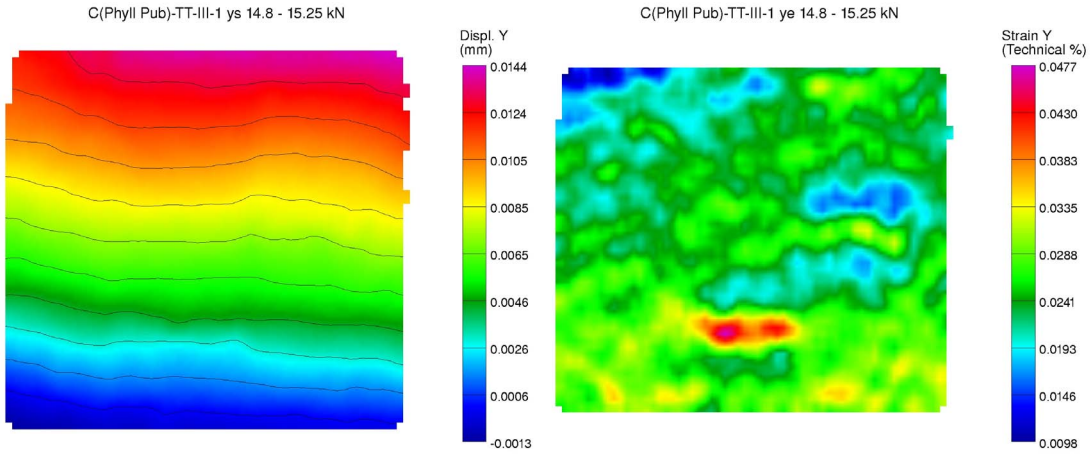

Figure H.28: Displacement and strain of test specimen C(Phyll.Pub)-TT-III-1; load-phase: 14.8-15.25 kN

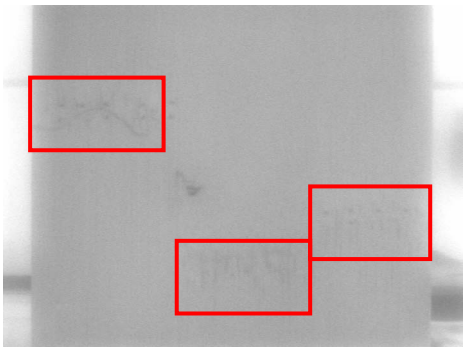

Figure H.29: Photo of illuminated area test specimen C(Phyll.Pub)-TT-III-2

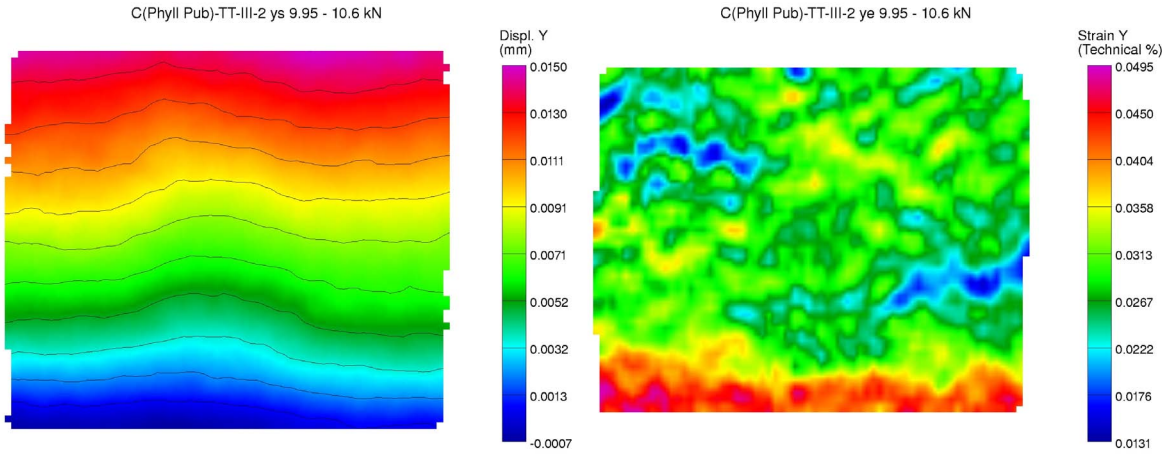

Figure H.30: Displacement and strain of test specimen C(Phyll.Pub)-TT-III-2; load-phase: 9. 95-10.6 kN

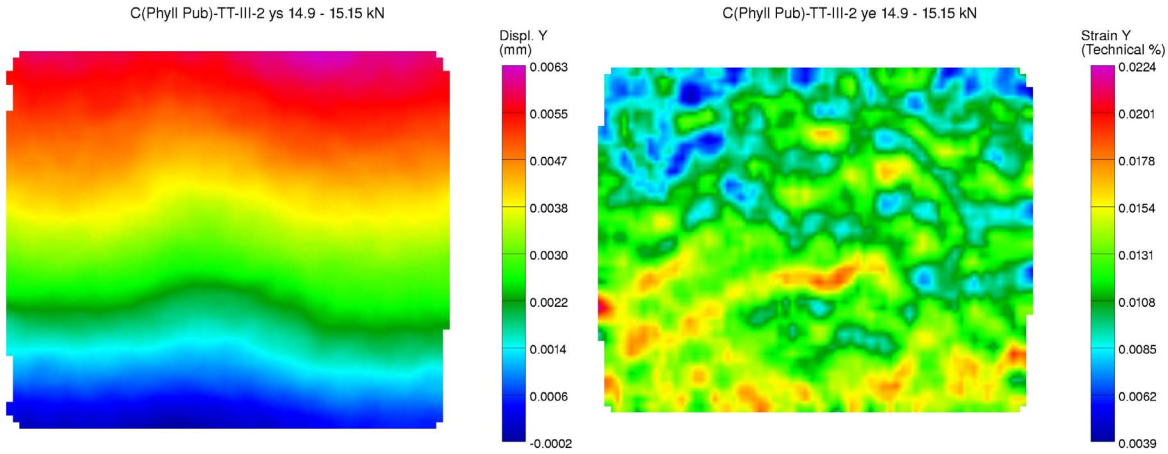

Figure H.31: Displacement and strain of test specimen C(Phyll.Pub)-TT-III-2; load-phase: 14.9-15.15kN

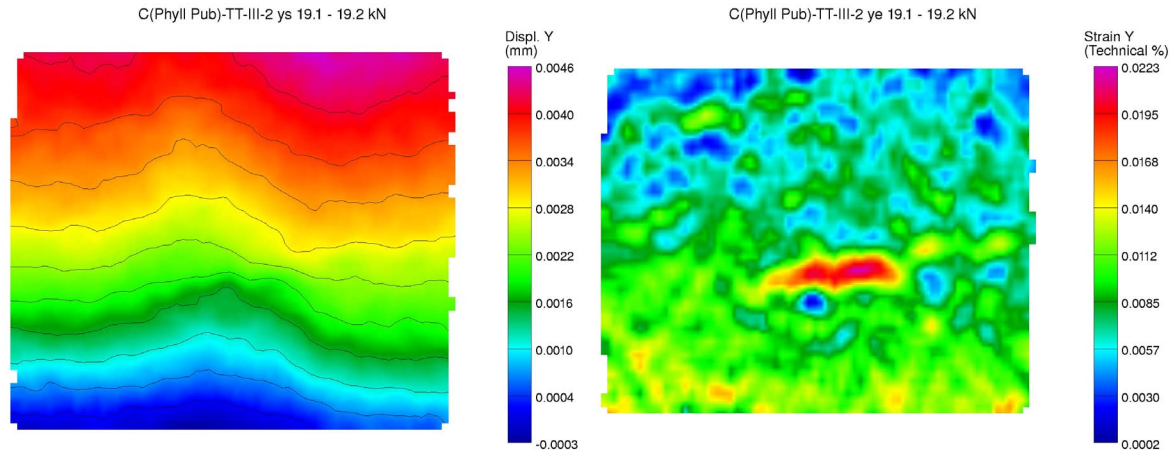

Figure H.32: Displacement and strain of test specimen C(Phyll.Pub)-TT-III-2; load-phase: 19.1-19.2 kN

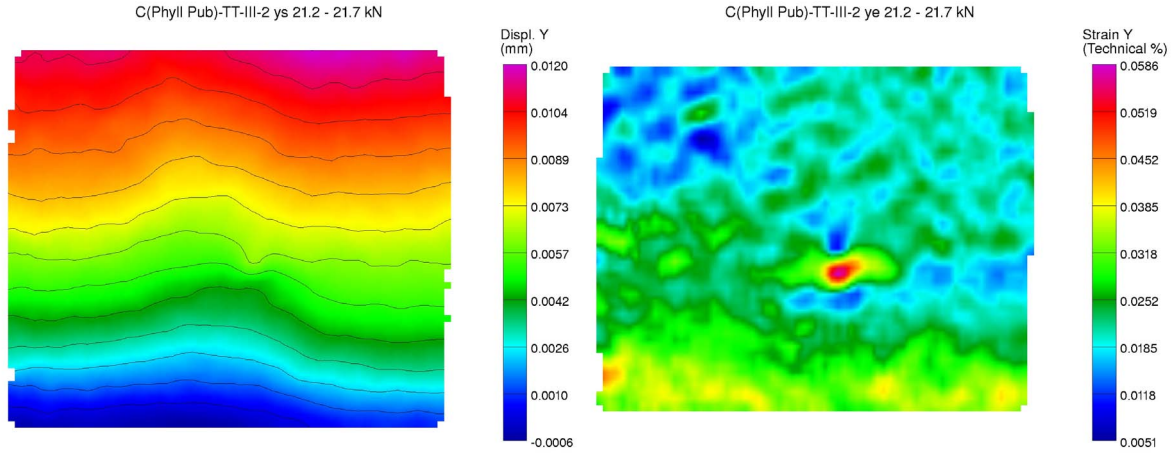

Figure H.33: Displacement and strain of test specimen C(Phyll.Pub)-TT-III-2; load-phase: 21.2-21.7 kN

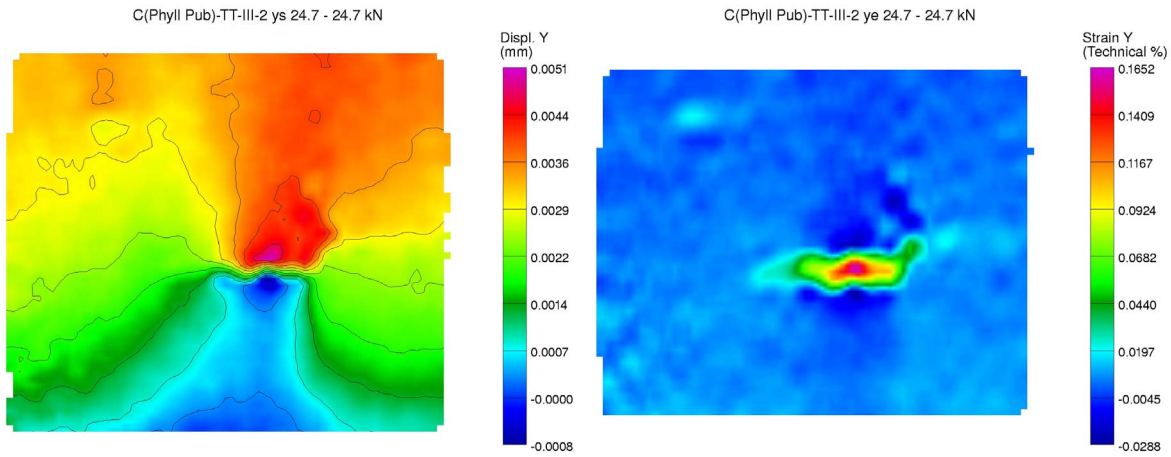

Figure H.34: Displacement and strain of test specimen C(Phyll.Pub)-TT-III-2; load-phase: 24.7-24.7 kN

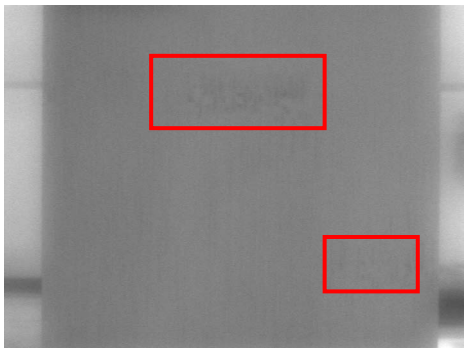

Figure H.35: Photo of illuminated area test specimen C(Phyll.Pub)-TT-III-3

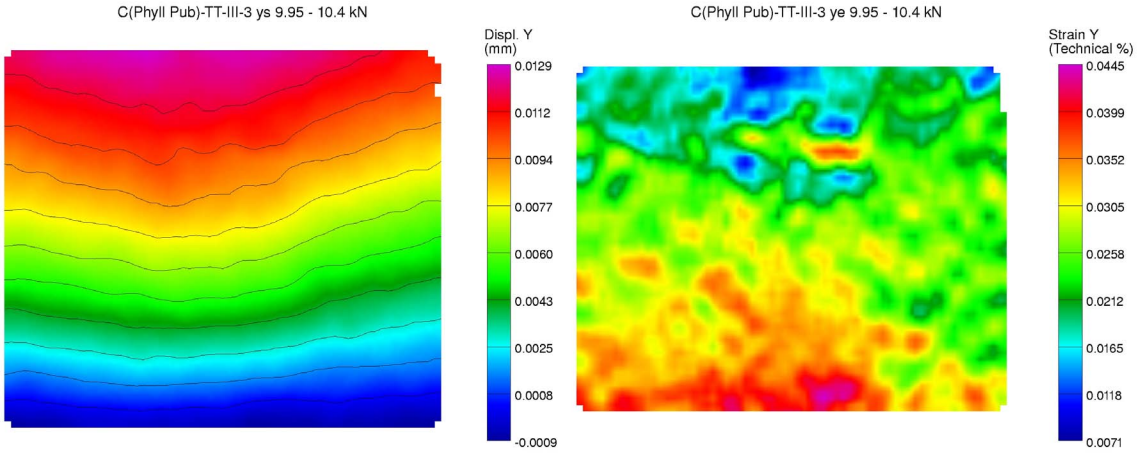

Figure H.36: Displacement and strain of test specimen C(Phyll.Pub)-TT-III-3; load-phase: 9.95-10.4 kN

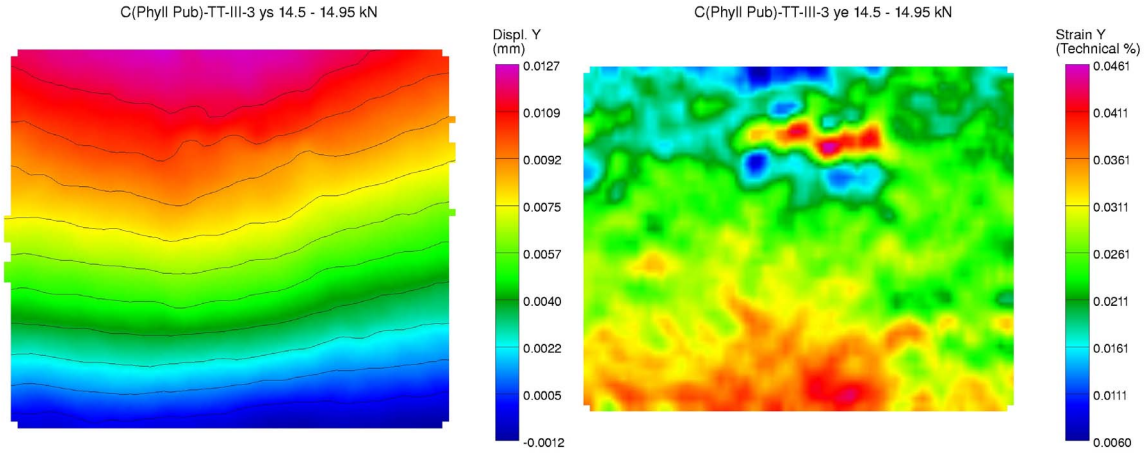

Figure H.37: Displacement and strain of test specimen C(Phyll.Pub)-TT-III-3; load-phase: 14.5-14.95 kN

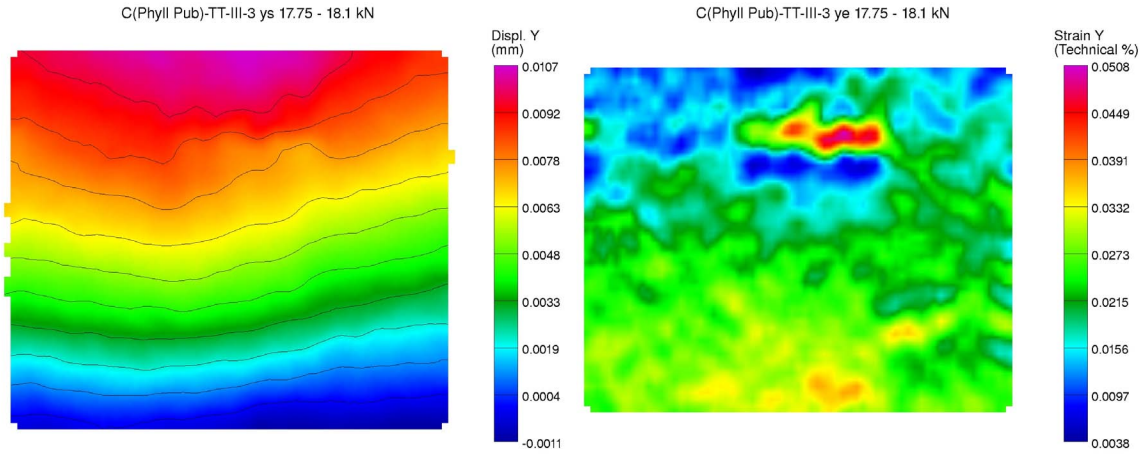

Figure H.38: Displacement and strain of test specimen C(Phyll.Pub)-TT-III-3; load-phase: 17.75-18.1 kN

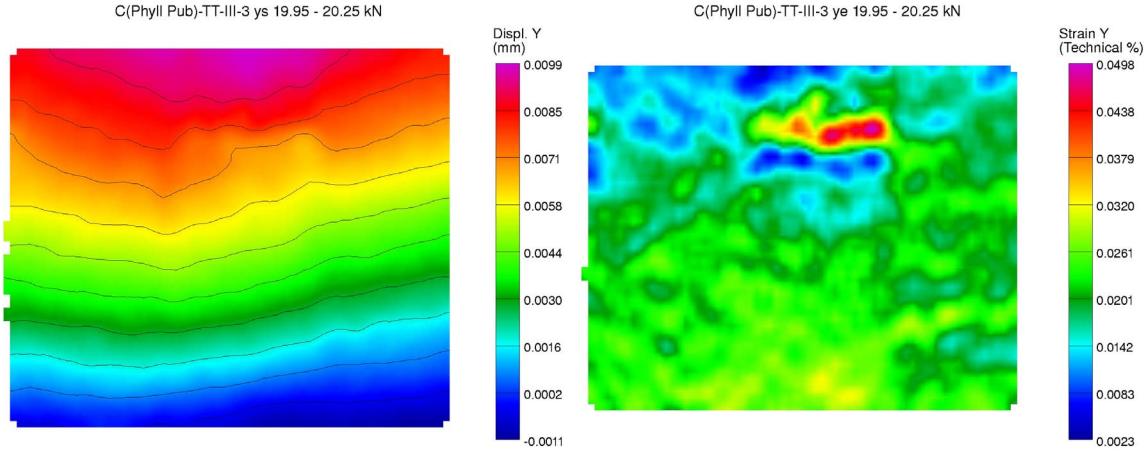

Figure H.39: Displacement and strain of test specimen C(Phyll.Pub)-TT-III-3; load-phase: 19.95-20.25 kN

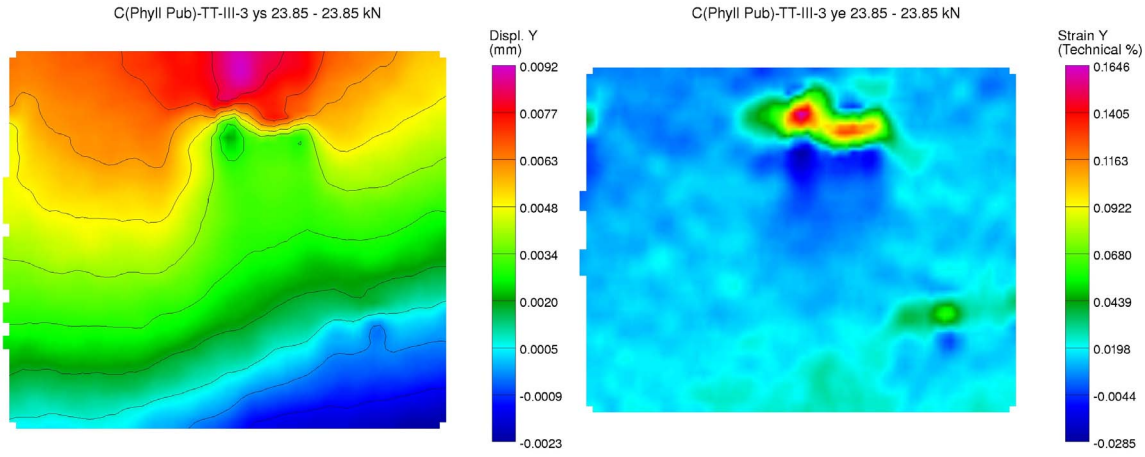

Figure H.40: Displacement and strain of test specimen C(Phyll.Pub)-TT-III-3; load-phase: 23.85-23.85 kN

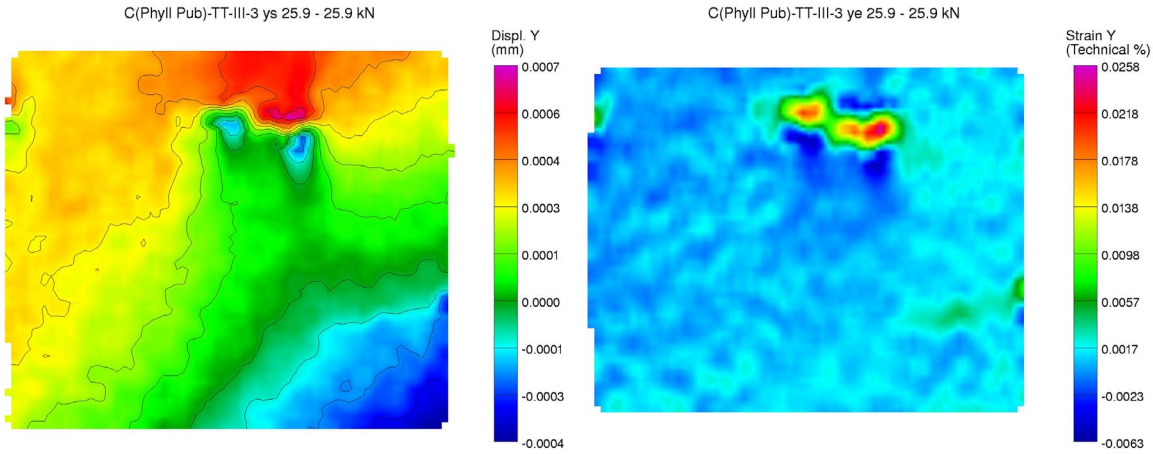

Figure H.41: Displacement and strain of test specimen C(Phyll.Pub)-TT-III-3; load-phase: 25.9-25.9 kN

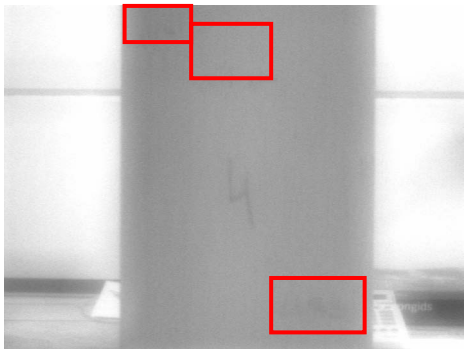

Figure H.42: Photo of illuminated area test specimen C(Phyll.Pub)-TT-III-4

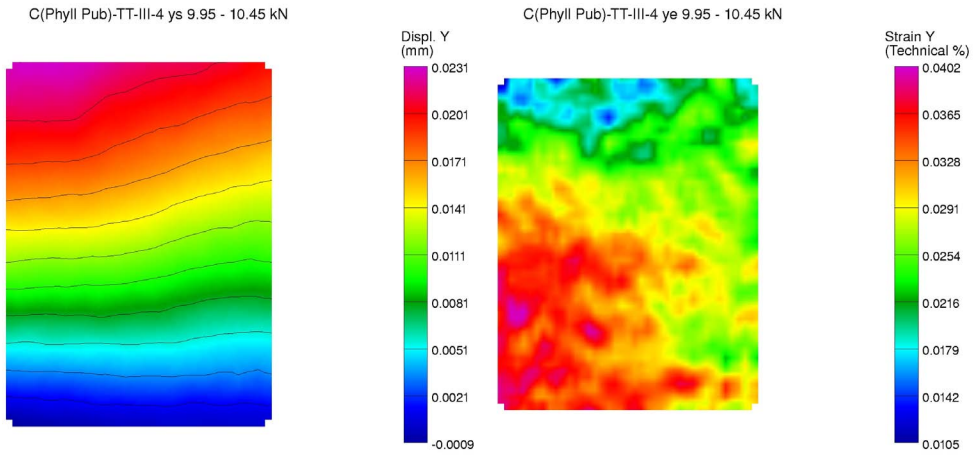

Figure H.43: Displacement and strain of test specimen C(Phyll.Pub)-TT-III-4; load-phase: 9.95-10.45 kN

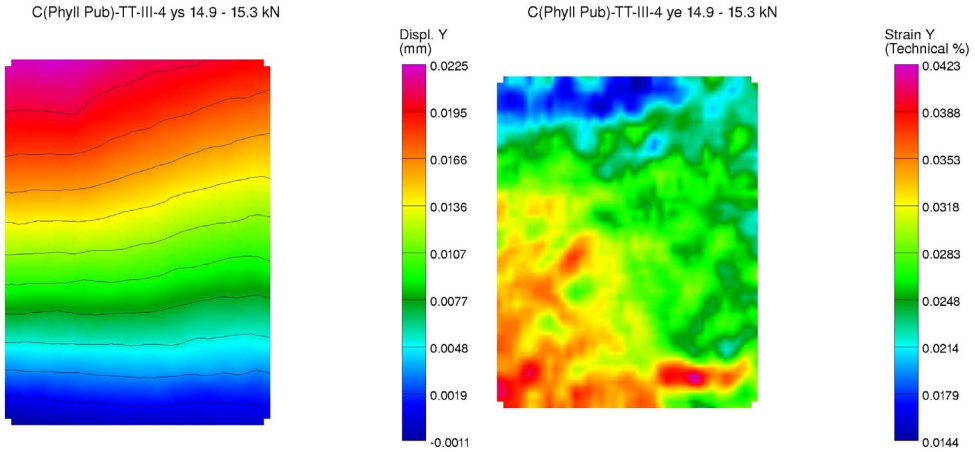

Figure H.44: Displacement and strain of test specimen C(Phyll.Pub)-TT-III-4; load-phase: 14.9-15.3 kN

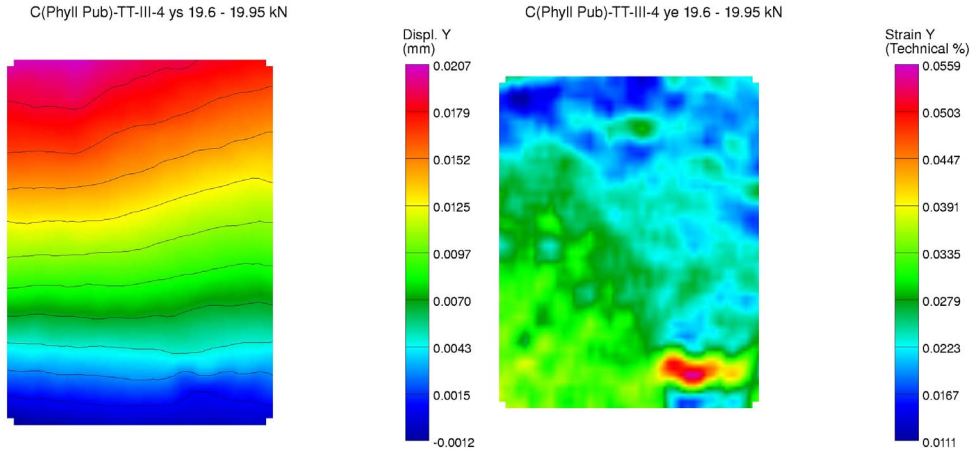

Figure H.45: Displacement and strain of test specimen C(Phyll.Pub)-TT-III-4; load-phase: 19.6-19.95 kN

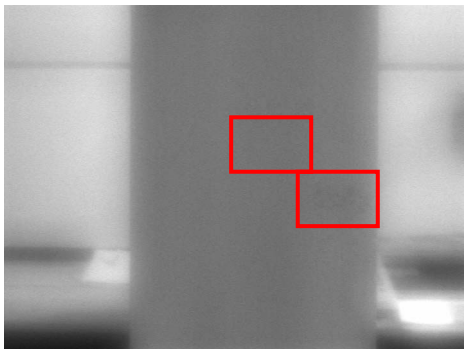

Figure H.46: Photo of illuminated area test specimen C(Phyll.Pub)-TT-III-5

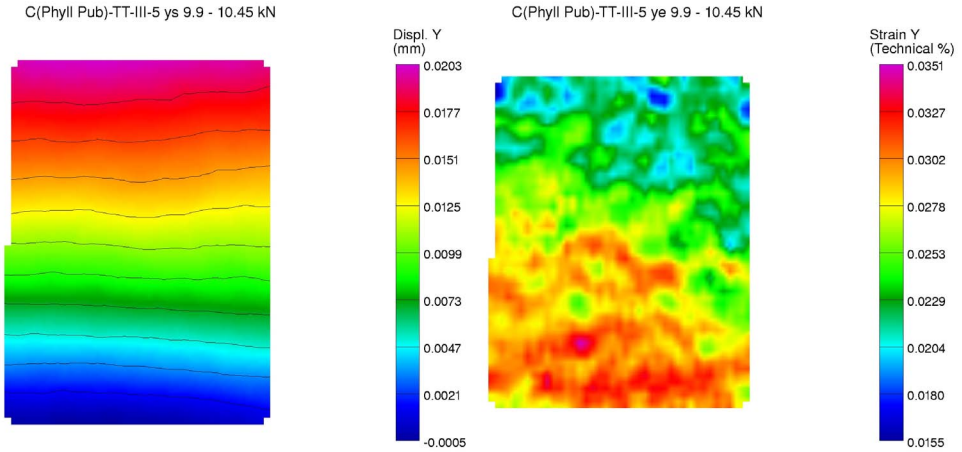

Figure H.47: Displacement and strain of test specimen C(Phyll.Pub)-TT-III-5; load-phase: 9.9-10.45 kN

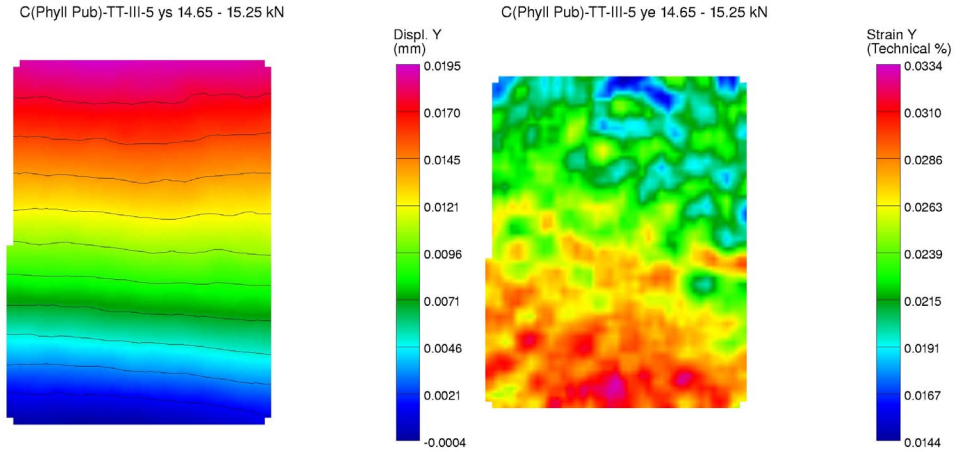

Figure H.48: Displacement and strain of test specimen C(Phyll.Pub)-TT-III-5; load-phase: 14.65-15.25 kN

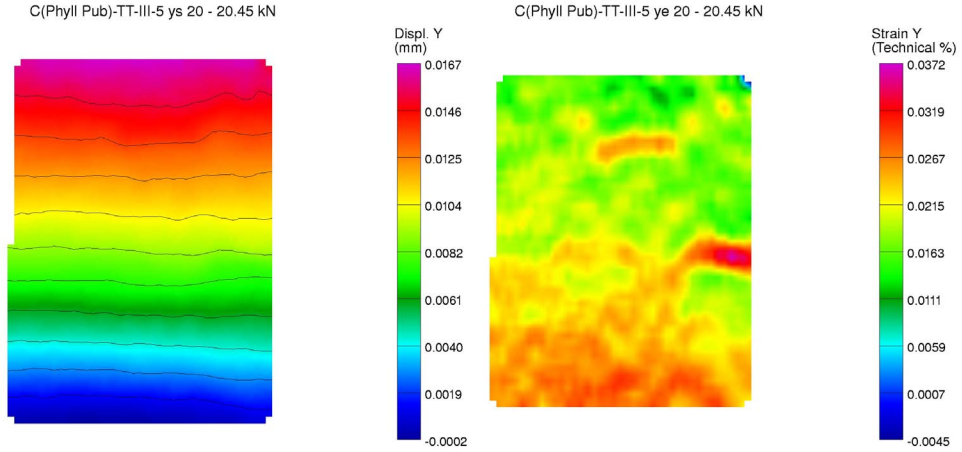

Figure H.49: Displacement and strain of test specimen C(Phyll.Pub)-TT-III-5; load-phase: 20-20.45 kN

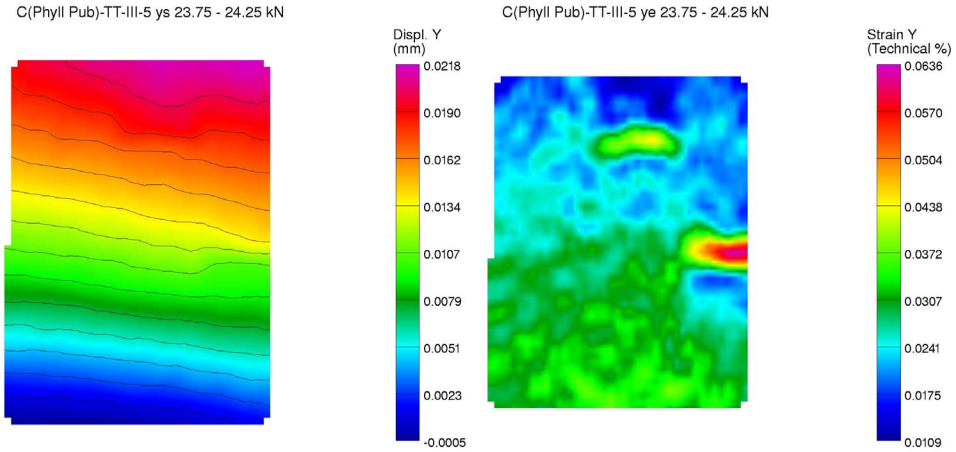

Figure H.50: Displacement and strain of test specimen C(Phyll.Pub)-TT-III-5; load-phase: 23.75-24.25 kN

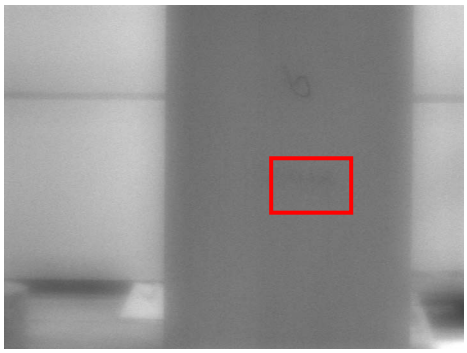

Figure H.51: Photo of illuminated area test specimen C(Phyll.Pub)-TT-III-6

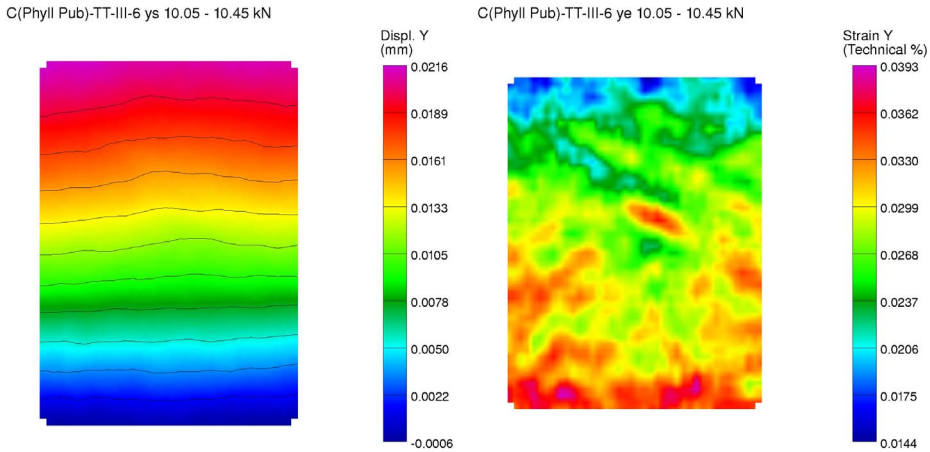

Figure H.52: Displacement and strain of test specimen C(Phyll.Pub)-TT-III-5; load-phase: 10.05-10.45 kN

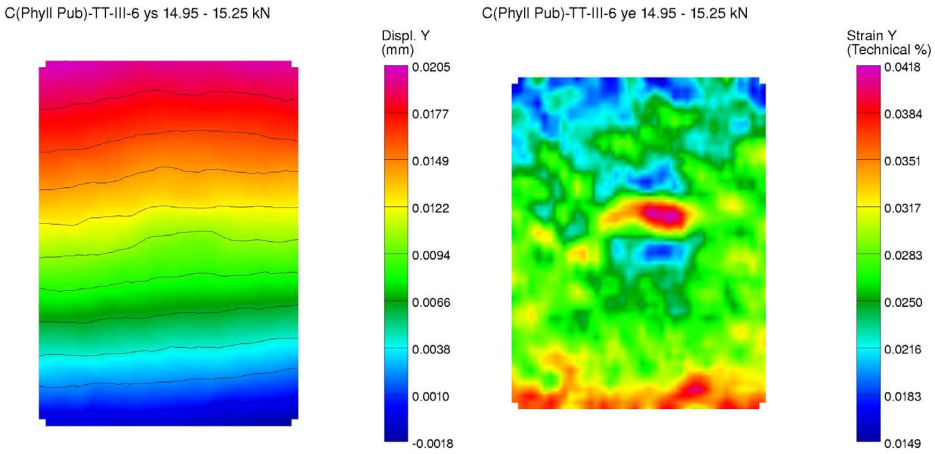

Figure H.53: Displacement and strain of test specimen C(Phyll.Pub)-TT-III-5; load-phase: 14.95-15.25 kN

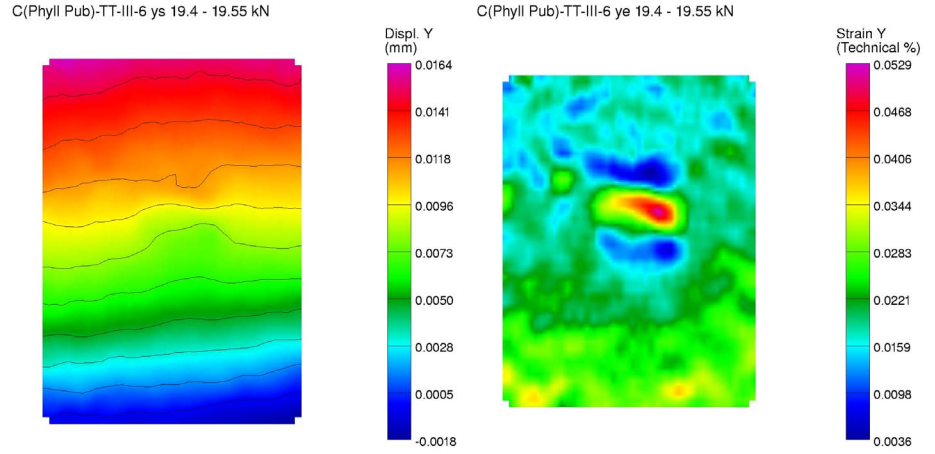

Figure H.54: Displacement and strain of test specimen C(Phyll.Pub)-TT-III-6; load-phase: 19.4-19.55 kN

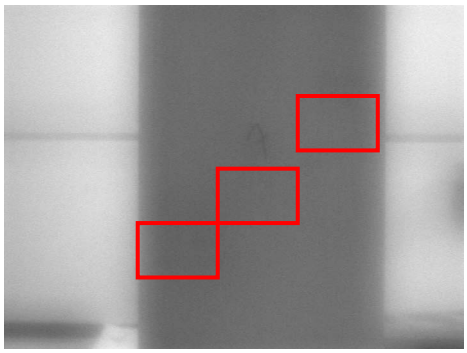

Figure H.55: Photo of illuminated area test specimen C(Phyll.Pub)-TT-III-7

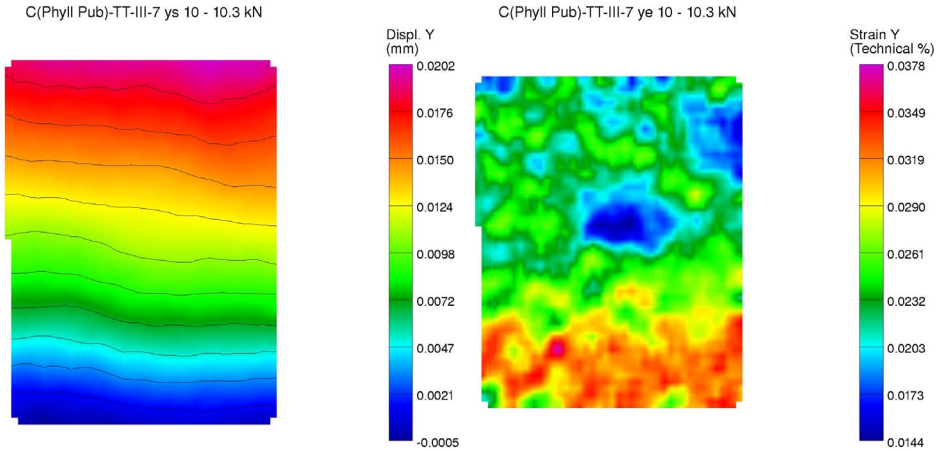

Figure H.56: Displacement and strain of test specimen C(Phyll.Pub)-TT-III-7; load-phase: 10-10.3 kN

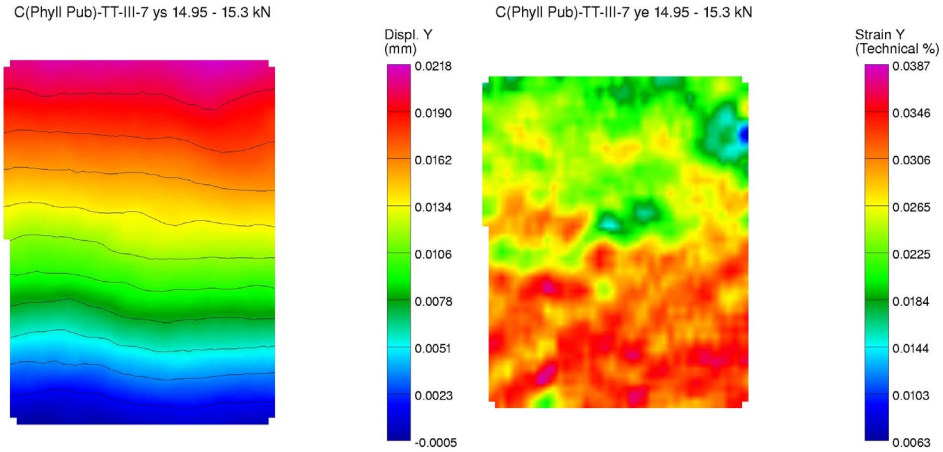

Figure H.57: Displacement and strain of test specimen C(Phyll.Pub)-TT-III-7; load-phase: 14.95-15.3 kN

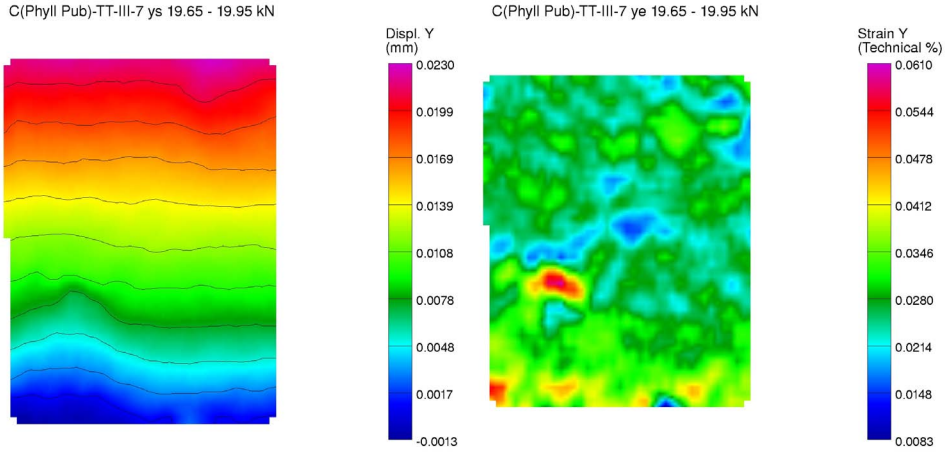

Figure H.58: Displacement and strain of test specimen C(Phyll.Pub)-TT-III-7; load-phase: 19.65-19.95 kN

H.4 Laminated Bamboo Loaded in Compression

H.4.1 Experimental Results: Compression Test on Laminated Test Specimens

Table H.20: Properties of laminated bamboo loaded in compression (sample B)

Test specimen [-]	$f_{c;0}$ [N/mm^2]	$E_{c;0}$ [N/mm^2]	MC [%]	ρ_0 [kg/m^3]
B(Phyll.Pub)-CT-Preliminary Test-01	47	-[1]	-[1]	-[1]
B(Phyll.Pub)-CT-Preliminary Test-02	48	-[1]	-[1]	-[1]
B(Phyll.Pub)-CT-01	48	8169	8.1	623
B(Phyll.Pub)-CT-02	48	8107	8.5	623
B(Phyll.Pub)-CT-03	47	8820	8.3	599
B(Phyll.Pub)-CT-04	47	8699	8.3	611
B(Phyll.Pub)-CT-05	48	8050	8.1	616
B(Phyll.Pub)-CT-06	50	7985	8.0	596
B(Phyll.Pub)-CT-Additional Test-01	49	-[1]	-[1]	-[1]
B(Phyll.Pub)-CT- Additional Test-02	51	-[1]	-[1]	-[1]

Note: [1]) not determined

H.5 Bond Quality

H.5.1 Experimental Results: Plywood Shear Test

Table H.21: Series A(Phyll.Pub)-ST-MUF-I

Test specimen [-]	f_v [N/mm^2]
A(Phyll.Pub)-ST-MUF-I-01	5.7
A(Phyll.Pub)-ST-MUF-I-02	5.8
A(Phyll.Pub)-ST-MUF-I-03	5.6
A(Phyll.Pub)-ST-MUF-I-04	5.4

Table H.22: Series A(Phyll.Pub)-ST-MUF-II

Test specimen [-]	f_v [N/mm^2]
A(Phyll.Pub)-ST-MUF-II-01	7.2
A(Phyll.Pub)-ST-MUF-II-02	8.5
A(Phyll.Pub)-ST-MUF-II-03	8.5
A(Phyll.Pub)-ST-MUF-II-04	8.6
A(Phyll.Pub)-ST-MUF-II-05	8.8
A(Phyll.Pub)-ST-MUF-II-06	7.8
A(Phyll.Pub)-ST-MUF-II-07	7.3

H.5.2 Experimental results: Block Shear Test

Table H.23: Series C(Phyll.Pub)-ST-MUF; bar I

Test specimen [-]	f_v [N/mm^2]	Bamboo failure [%]
C(Phyll.Pub)-ST-MUF-01	14.2	100
C(Phyll.Pub)-ST-MUF-02	11.9	100
C(Phyll.Pub)-ST-MUF-03	12.8	60
C(Phyll.Pub)-ST-MUF-04	14.3	-[1]
C(Phyll.Pub)-ST-MUF-05	12.0	100
C(Phyll.Pub)-ST-MUF-06	16.6	100
C(Phyll.Pub)-ST-MUF-07	11.6	100
C(Phyll.Pub)-ST-MUF-08	14.8	100
C(Phyll.Pub)-ST-MUF-09	14.1	100
C(Phyll.Pub)-ST-MUF-10	15.8	100
C(Phyll.Pub)-ST-MUF-11	11.8	100
C(Phyll.Pub)-ST-MUF-12	13.6	100
C(Phyll.Pub)-ST-MUF-13	12.0	90

Note: [1]) not possible to determine

Table H.24: Series C(Phyll.Pub)-ST-MUF; bar II

Test specimen [-]	f_v [N/mm^2]	Bamboo failure [%]
C(Phyll.Pub)-ST-MUF-14	12.9	50
C(Phyll.Pub)-ST-MUF-15	13.7	100
C(Phyll.Pub)-ST-MUF-16	14.3	60
C(Phyll.Pub)-ST-MUF-17	14.9	100
C(Phyll.Pub)-ST-MUF-18	14.3	100
C(Phyll.Pub)-ST-MUF-19	14.7	100
C(Phyll.Pub)-ST-MUF-20	13.4	50
C(Phyll.Pub)-ST-MUF-21	15.8	-[1]
C(Phyll.Pub)-ST-MUF-22	11.4	60
C(Phyll.Pub)-ST-MUF-23	10.9	-[1]
C(Phyll.Pub)-ST-MUF-24	11.2	-[1]
C(Phyll.Pub)-ST-MUF-25	12.8	100
C(Phyll.Pub)-ST-MUF-26	12.1	-[1]

Note: [1]) not possible to determine

Table H.25: Series C(Phyll.Pub)-ST-MUF; bar III

Test specimen [-]	f_v [N/mm^2]	Bamboo failure [%]
C(Phyll.Pub)-ST-MUF-27	13.9	60
C(Phyll.Pub)-ST-MUF-28	14.0	100
C(Phyll.Pub)-ST-MUF-29	14.8	100
C(Phyll.Pub)-ST-MUF-30	15.1	100
C(Phyll.Pub)-ST-MUF-31	14.7	100
C(Phyll.Pub)-ST-MUF-32	15.0	100
C(Phyll.Pub)-ST-MUF-33	9.8	40
C(Phyll.Pub)-ST-MUF-34	15.1	-[1]
C(Phyll.Pub)-ST-MUF-35	-[1]	40
C(Phyll.Pub)-ST-MUF-36	11.1	50
C(Phyll.Pub)-ST-MUF-37	11.3	-[1]
C(Phyll.Pub)-ST-MUF-38	12.0	100
C(Phyll.Pub)-ST-MUF-39	10.5	-[1]

Note: [1]) not possible to determine

Table H.26: Series C(Phyll.Pub)-ST-RP; bar I

Test specimen [-]	f_v [N/mm^2]	Bamboo failure [%]
C(Phyll.Pub)-ST-RP-01	11.0	30
C(Phyll.Pub)-ST-RP-02	12.3	10
C(Phyll.Pub)-ST-RP-03	12.9	10
C(Phyll.Pub)-ST-RP-04	14.5	0
C(Phyll.Pub)-ST-RP-05	-[1]	10
C(Phyll.Pub)-ST-RP-06	-[1]	0
C(Phyll.Pub)-ST-RP-07	14.5	0
C(Phyll.Pub)-ST-RP-08	13.7	0
C(Phyll.Pub)-ST-RP-09	13.5	0
C(Phyll.Pub)-ST-RP-10	14.0	0
C(Phyll.Pub)-ST-RP-11	15.3	30
C(Phyll.Pub)-ST-RP-12	12.8	100
C(Phyll.Pub)-ST-RP-13	13.8	80

Note: [1]) not possible to determine

Table H.27: Series C(Phyll.Pub)-ST-RP; bar II

Test specimen [-]	f_v [N/mm^2]	Bamboo failure [%]
C(Phyll.Pub)-ST-RP-14	12.5	0
C(Phyll.Pub)-ST-RP-15	11.8	0
C(Phyll.Pub)-ST-RP-16	11.3	40
C(Phyll.Pub)-ST-RP-17	9.1	0
C(Phyll.Pub)-ST-RP-18	12.4	20
C(Phyll.Pub)-ST-RP-19	10.9	10
C(Phyll.Pub)-ST-RP-20	14.7	20
C(Phyll.Pub)-ST-RP-21	13.3	0
C(Phyll.Pub)-ST-RP-22	-[1]	0
C(Phyll.Pub)-ST-RP-23	14.6	10
C(Phyll.Pub)-ST-RP-24	14.5	20
C(Phyll.Pub)-ST-RP-25	12.1	0
C(Phyll.Pub)-ST-RP-26	12.4	40

Note: [1]) not possible to determine

Table H.28: Series C(Phyll.Pub)-ST-RP; bar III

Test specimen [-]	f_v [N/mm^2]	Bamboo failure [%]
C(Phyll.Pub)-ST-RP-27	11.8	40
C(Phyll.Pub)-ST-RP-28	10.8	-[1]
C(Phyll.Pub)-ST-RP-29	8.3	0
C(Phyll.Pub)-ST-RP-30	10.5	0
C(Phyll.Pub)-ST-RP-31	9.3	0
C(Phyll.Pub)-ST-RP-32	13.2	0
C(Phyll.Pub)-ST-RP-33	13.5	40
C(Phyll.Pub)-ST-RP-34	12.2	20
C(Phyll.Pub)-ST-RP-35	11.8	10
C(Phyll.Pub)-ST-RP-36	11.1	10
C(Phyll.Pub)-ST-RP-37	12.0	60
C(Phyll.Pub)-ST-RP-38	12.3	10
C(Phyll.Pub)-ST-RP-39	11.4	10

Note: [1]) not possible to determine

H.5.3 Statistical Results: Paired Samples T Test

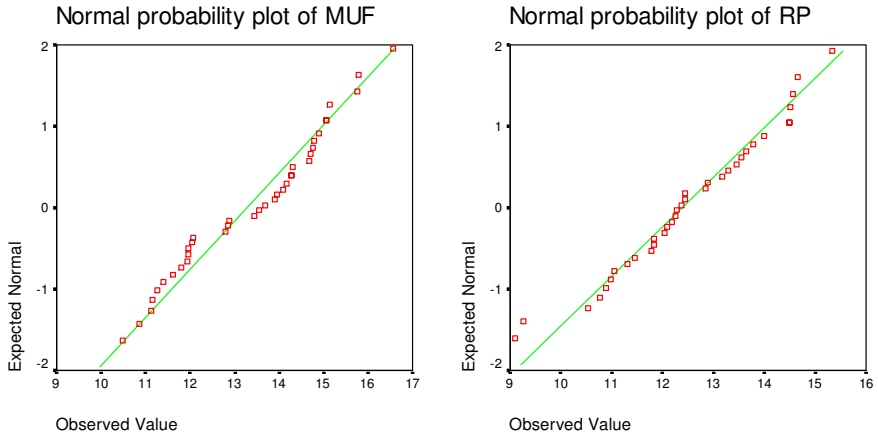

Figure H.59: Normal probability plots of MUF type specimens and RP type specimens

Table H.29: Results of tests of normality

SAMPLE	Kolmogorov-Smirnov[2]			Shapiro-Wilk		
	Statistic	df	Sig.	Statistic	df	Sig.
MUF	0.129	38	0.109	0.964	38	0.255
RP	0.079	36	0.200[1]	0.972	36	0.475

Note: [1]) this is a lower bound of the true significance; [2]) lilliefors Significance Correction

Table A.5: Results of independent samples t test

	Levene's Test for Equality of Variances		t-test for Equality of Means						
	F	Sig.	t	df	Sig. (2-tailed)	Mean Difference	Std. Error Difference	95% Confidence Interval of the Difference	
								Lower	Upper
Equal variances assumed	.798	.375	2.307	72	.024	.8970	.38890	.12178	1.67229
Equal variances not assumed			2.309	71.956	.024	.8970	.38858	.12241	1.67165

H.6 Bending Behavior of Laminated Bamboo Beams

H.6.1 Experimental Results: Four-Point Bending Test on Laminated Bamboo Beams

Table H.30: Properties of laminated bamboo beams (sample B)

Test specimen [-]	Failure mode [-]	M_u [kNm]	f_m [N/mm^2]	E_m [N/mm^2]	MC [%]	ρ_0 [kg/m^3]
B(Phyll.Pub)-BT-Preliminary Test[1]	Scarf-joint	21.0	64	7362	-[2]	-[2]
B(Phyll.Pub)-BT-01	Node	23.3	75	10374	8.5	601
B(Phyll.Pub)-BT-02	Scarf-joint	21.4	66	8959	8.4	612
B(Phyll.Pub)-BT-03	Scarf-joint	24.8	76	8563	8.2	624
B(Phyll.Pub)-BT-04	Scarf-joint	23.6	73	8246	8.2	618
B(Phyll.Pub)-BT-05	Node	24.2	74	6466	8.4	611
B(Phyll.Pub)-BT-06	Node	25.0	77	8528	8.2	617

Note: [1]) the loading speed used during the preliminary test (5 mm/min) differed from the other tests (20 mm/min);
[2]) not determined